Development of a continuous downstream process for microbial produced virus-like particle based Group A Streptococcus vaccine

THE UNIVERSITY of ADELAIDE

Lukas Gerstweiler

A thesis submitted for the degree of Doctor of Philosophy

School of Chemical Engineering and Advanced Materials

The University of Adelaide

Adelaide, Australia

April 2022

DEM LEBENDIGEN GEIST

Declaration

I certify that this work contains no material which has been accepted for the award of any other degree or diploma in any university of other tertiary institution to Lukas Gerstweiler and, to the best of my knowledge and belief, contains no material previously published or written by another person, except where due reference has been made in the text. In addition, I certify that no part of this work will, in the future, be used in a submission in my name, for any other degree or diploma in any university or other tertiary institution without the prior approval of the University of Adelaide and where applicable, any partner institution responsible for the joint-award of this degree.

I acknowledge that copyright of published works contained within this Thesis resides with the copyright holder(s) of those works.

I also give permission for the digital version of my Thesis to be made available on the web, via the University's digital research repository, the Library Search and through web search engines, unless permission has been granted by the University to restrict access for a period.

Name: Lukas Gerstweiler

Signature:

Date: 04.04.2022

Acknowledgments

First of all, I want to thank my parents Doris and Klaus for their extraordinary support throughout my entire life. I can’t think of better parents and without them I would not be where I am today.

Just as grateful, I am towards my supervisor Anton Middelberg who offered me the project of this thesis. Coming to a new country with absolutely no idea what will happen I am more than grateful to meet him. I want to thank you for the interesting topic that I really enjoyed, the support in every aspect, the happy meetings, and in particular the freedom and trust in my skills I received during my candidature.

Another big thanks go to my second supervisor Jingxiu Bi for her supportive and welcoming attitude. All her support outside of university really helped me to settle and contributed a lot to my fabulous experience here.

Furthermore, I want to thank Jagan Billakanti for his input and support during the second half of my project.

I also want to thank my group Annie, Bingyang, Shuang, Matt, Afshin, the students Iris, Linh, Vy, and Thrang as well as the whole School of Chemical Engineering and Advanced Materials for their company and the good times I had.

I further want to mention the importance of my family, friends, and relatives Felix, Eva, Sophia, Heike, Elfi, Paul, Heidi, Ralf, Thekla, Phillip, Ginnes, and everyone I met during my time in Australia. Thank you for every moment we had together and everything I did learn from you.

Finally, yet importantly, I want to thank my partner Julia for commencing the adventure of Australia together with me and her mental support during my candidature.

Summary

The current pandemic outlines the need for efficient and mass-produced vaccines to fight infectious diseases. Group A Streptococcus is a human pathogen causing hundreds of millions of infections every year and leading to over 500,000 deaths annually. Unfortunately, there is still no efficient vaccine developed today. A novel class of vaccines that can overcome some of the limitations of traditional vaccines are virus-like particles (VLPs) that can induce strong and long-lasting immune responses. However, caused by lengthy and complicated production routes they are also among the most expensive.

Microbially-expressed modular virus-like particles with inserted foreign antigens are a promising platform technology for rapid and low-cost vaccines but their current purification methods lack scale-ability and process performance. A main burden during processing is the formation of soluble aggregates and poor performance during chromatographic purification. Processing of viral capsomeres usually requires hard-to-scale unit operations and enzymatic treatment to remove DNA. The first half of my project, therefore, investigated the cause of the aggregate formation and investigated possible purification pathways. It was found that a main source of soluble aggregates during processing is DNA-capsomere aggregates, caused by the strong DNA affinity of viral capsomeres. This aggregation does not only lead to poor product quality during viral assembly but is also responsible for poor chromatographic performance as the large-size aggregates cannot enter the pores of the chromatographic resin and hinder the efficient removal of DNA. It was furthermore shown, that these DNA-capsomere interactions can be controlled by adjusting the ionic strength of the buffer system and high salt buffers can suppress DNA-capsomere interactions. Controlling DNA-capsomere interactions did not only lead to better product quality and improved DNA removal, but it also enables efficient chromatographic processing at elevated salt concentrations using salt-tolerant mixed-mode ion exchange resins.

The novel approach of processing viral capsomeres at elevated salt concentrations, suppressing DNA-capsomere interactions, with novel salt-tolerant mixes mode ion exchange resins led to the development of several integrated purification pathways, that were optimized using high-throughput binding studies. The optimized purification pathways were comparatively evaluated using a range of analytical techniques. After optimization, the preferred integrated purification pathway was capable of producing highly pure virus-like particles without any of the common hard-to-scale unit operations found in other described methods and showed outstanding process performance. The finding of these two studies are not only relevant for my specific virus-like particle but are also of high interest if other viral proteins are processed as the underlying DNA binding sites are conserved within many viruses. Furthermore, the finding can explain many challenges occurring during the processing of virus-like particles and viral proteins, that are described in the literature.

The second part of my studies focuses on the transition of the batch process to a continuous one. Continuous bioprocessing gains significant attention within the biopharmaceutical industry in recent years, as it promises faster, cheaper, and more consistent production. However, unlike other industries, continuous biomanufacturing is still in its infancy.

Research in this field mostly concentrates on antibody production and VLPs are not addressed yet. This project, therefore, aims to widen the research field of continuous biomanufacturing to virus-like particles, and an automated, continuous production route was developed. Based on the findings of the first part of my studies the first fully integrated and continuous purification pathway for virus-like particle vaccines was developed. The process showed a robust behaviour over a wide range of inlet stream concentrations and produced Group A Streptococcus virus-like particle vaccines of constantly high quality over the examined period.

A novel key concept is the integration of a flow-through step with multi-modal cation exchanger in a periodic counter-current chromatography (PCC) set-up, that allows seamless integration of the two-unit operations without buffer adjustment in between. The process also shows the possibility to remove the reducing agent DTT during column elution using chromatography, eradicating an additional buffer exchange unit operation before in-line viral assembly. A main challenge to solve was the development of a new control strategy for continuous periodic counter-current chromatography subject to unstable/fluctuating inlet stream concentrations. Current control strategies fail if the inlet stream concentration does not remain constant during column loading. The developed approach was modelled *in-silico,* using mechanistic models, and enables a more robust controlling of PCC processes than common approaches.

Apart from describing the first continuous purification pathway for virus-like particle vaccines, the described process might lay the fundamentals for continuous production for a wide range of biopharmaceuticals. The process can be easily adapted to other biopharmaceuticals as the process can be changed using different chromatographic resins and is not constructed around a specific affinity chromatographic step.

This project outlines the development of a continuous manufacturing process for microbially expressed VLP vaccines against Group A Streptococcus from scratch. It shows exemplarily the development and optimization of a batch process and the subsequent transition to a continuous and integrated process and therefore can serve as a blueprint for the development of continuous processes for biopharmaceuticals other than VLPs.

Table of Contents

Chapter 1

Introduction

This chapter introduces the overall research project and gives an outline of the thesis structure, content, aims, and objectives.

1.1 Background

Vaccination is one of the key tools to fight human infectious diseases and is an outstanding achievement of biomedical research and public health [1–3]. Smallpox was declared eradicated by the WHO in 1980 after global immunization [4]. Furthermore, the current global pandemic of COVID-19 illustrates the importance of efficient vaccines in the fight against infectious diseases. Traditional vaccines containing dead or inactivated viruses, or single key proteins, have been successfully developed against a wide variety of diseases such as measles, mumps, rubella, poliomyelitis diphtheria, tetanus, hepatitis A/B and can prevent morbidity and mortality up to 100% [1,5]. Yet, in 2019 more than 10 million people died globally because of communicable diseases outlining the threat of infectious diseases to human health.

Group A Streptococcus (GAS) is responsible for over 500,000 deaths and infects hundreds of millions every year, making it a major burden within our society [6]. Unfortunately, there is no commercial vaccine available yet, and the high number of genotypes and possible cross-reactions with the immune system challenges the development of efficient vaccines [7,8]. Due to lower access to healthcare mostly developing countries and low-income settings are affected by GAS and therefore an ideal vaccine candidate is not only highly efficient but can also be produced cheaply and at large scale.

Traditional vaccine production requires long culturing processes and complicated purification pathways. This makes production of vaccines expensive and also limits a possible reaction to sudden pandemic threats [9]. To overcome these problems of GAS vaccine development, new highly efficient vaccines and advanced manufacturing technologies have to be developed to provide cost-effective, highly efficient, and rapidly manufactured vaccines at a global scale.

Virus-like particles are a new and promising vaccine approach. They mimic the overall structure of the underlying virus, yet lack genetic material and are therefore non-infectious and safe to use. Caused by their native and highly repetitive structure they elicit a strong and long-lasting immune response. VLPs can also be used as a platform to present foreign antigens to the immune system, thus allowing the construction of vaccines against a wide variety of pathogens [10]. However, currently VLPs are among the most expensive class of vaccines due to their complicated and expensive production routine [11,12].

A possible low-cost platform technology for the production of VLP vaccines was developed by Middelberg et al. [13]. Based on murine polyomavirus major capsid protein VP1 with inserted antigen, immunogenic VLPs against different pathogens can be produced and a promising candidate against GAS has been developed. A main advantage is that VP1 can be rapidly expressed in *E. coli* making the production theoretically easy, rapid and cost-efficient. However, to achieve the full potential of this technology the purification pathway requires further development that allows full-scale ability. Additionally, further intensification of the production can be achieved by changing from batch to continuous manufacturing. State-of-the-art biomanufacturing is still heavily relying on batch-wise unit operations. Changing from batch to continuous manufacturing can lead to significant reductions in operational and investment costs and the field of continuous biomanufacturing gains increasing attention in recent years [14].

Recent research on continuous bioprocessing mainly investigates the processing of antibodies; other important biopharmaceuticals such as VLPs have been neglected. There is currently no research published on the continuous production of virus-like particles and in general integrated and continuous purification pathways for biopharmaceuticals are minimally examined and seldom described. Therefore, this research project, tries to widen the field of continuous biomanufacturing towards VLPs and explores continuous and integrated

production pathways for VLP vaccines based on murine polyomavirus major capsid protein VP1 with a Group A Streptococcus vaccine as a model construct.

1.2 Aims and Objectives

The overall aim of this Ph.D. project is to develop a continuous downstream process for the production of microbial-produced virus-like particle vaccines based on the murine polyomavirus-like particle vaccine platform. The process shall be scale-able, automated, integrated, and produce VLPs of high quality. Non-tagged VP1 capsomere with inserted J8 GAS antigen is used as a model construct to obtain VLP vaccines against Group A Streptococcus due to the significance of this pathogen. Although this project focuses on VLPs this thesis shall also provide a blueprint for the development of continuous processes for other biopharmaceuticals apart from antibodies.

As a first step, possible new purification pathways for non-affinity tagged VP1-J8 will be explored and a new integrated batch process will be developed that is fully scale-able and only utilizes unit operations that can be translated into continuous processes. Aggregation during processing and low chromatographic performance will be investigated in detail. Subsequently, this process will be further optimized using high-throughput approaches.

Once a suitable batch process is developed, this will be translated into a continuous and integrated process. A control strategy for process automation will be developed that considers concentration fluctuations during processing and the process robustness will be analyzed and examined.

1.3 Thesis outline

The thesis is structured into eight chapters, of which Chapter 3, 4, 5, 6, and 7 are presented as a publication. A short overview of each Chapter will be given in the following:

Chapter 1 Introduction. This chapter introduces the overall research project and gives an outline of the thesis structure, content, aims, and objectives.

Chapter 2 Literature Review. This chapter reviews the current literature and aims to give the reader a comprehensive overview of the topics relevant to this thesis. Virus-like particles, Group A Streptococcus, and current purification strategies are discussed. Furthermore, the murine polyomavirus-like particle vaccine platform is introduced.

Chapter 3 Continuous downstream bioprocessing for intensified manufacture of biopharmaceuticals and antibodies. This chapter provides an extensive review on continuous biomanufacturer and introduces different continuous concepts and completes the literature review of Chapter 2.

Chapter 4 Influence of DNA-VP1 aggregates on downstream processing. In this chapter, it is investigated how the control of DNA-VP1 interactions can influence the downstream processing of viral capsomeres. Multi-modal cation exchange resin was identified as a novel approach to process VP1 capsomeres at elevated salt concentrations, enabling the suppression of DNA-VP1 interactions and thus allowing for higher binding capacities. Furthermore, the influence of DNA-VP1 interactions on the formation of aggregates during assembly is investigated.

Chapter 5 Comparative evaluation of integrated downstream processes. Based on the findings of Chapter 4 several integrated downstream processes for VP1-J8 VLPs were developed. Optimal process conditions were explored using high-throughput studies. The processes were characterized in terms of purity and product quality and comparatively evaluated.

Chapter 6 Control strategy for PCC processes subject to fluctuating inlet stream concentrations. Integration of a flow-through chromatography step with a continuous PCC

process leads to fluctuating inlet stream concentrations, which hinders controlling of the PCC process. In this chapter a novel control strategy for PCC processes with fluctuating inlet stream concentrations is developed. The new approach was verified *in-silico* using mechanistic modelling as well as experimentally.

Chapter 7 Continuous downstream process for the production of VLP vaccines. In this chapter, a continuous, automated, and integrated downstream process for the production of VLP vaccines against Group A Streptococcus was developed. The process integrates the findings of the previous chapters. The robustness of the process was tested with different initial lysate concentrations and the product quality was determined over several hours of processing.

Chapter 8 Conclusion and future directions. This chapter sums up the findings of the previous chapters and gives an outlook of possible future research questions that can be addressed.

1.4 References

[1] S.W. Roush, T.V. Murphy, Historical comparisons of morbidity and mortality for vaccine-preventable diseases in the United States, JAMA 298 (2007) 2155–2163. https://doi.org/10.1001/jama.298.18.2155.

[2] Impact of Vaccines Universally Recommended for Children--United States, 1900-1998, JAMA: The Journal of the American Medical Association 281 (1999) 1482–1483. https://doi.org/10.1001/jama.281.16.1482.

[3] Ten Great Public Health Achievements—United States, 1900-1999, JAMA: The Journal of the American Medical Association 281 (1999) 1481. https://doi.org/10.1001/jama.281.16.1481.

[4] D.A. Henderson, The eradication of smallpox--an overview of the past, present, and future, Vaccine 29 Suppl 4 (2011) D7-9. https://doi.org/10.1016/j.vaccine.2011.06.080.

[5] W.G. van Panhuis, J. Grefenstette, S.Y. Jung, N.S. Chok, A. Cross, H. Eng, B.Y. Lee, V. Zadorozhny, S. Brown, D. Cummings, D.S. Burke, Contagious diseases in the United States from 1888 to the present, N. Engl. J. Med. 369 (2013) 2152–2158. https://doi.org/10.1056/NEJMms1215400.

[6] J.R. Carapetis, A.C. Steer, E.K. Mulholland, M. Weber, The global burden of group A streptococcal diseases, The Lancet Infectious Diseases 5 (2005) 685–694. https://doi.org/10.1016/S1473-3099(05)70267-X.

[7] WHO, Global health estimates 2019 summary table, deaths by cause, age and sex, by world bank income group 2000-2019, 2020. https://www.who.int/data/gho/data/themes/mortality-and-global-health-estimates/ghe-leading-causes-of-death (accessed 13 November 2021).

[8] S.A. Castro, H.C. Dorfmueller, A brief review on Group A Streptococcus pathogenesis and vaccine development, R. Soc. Open Sci. 8 (2021) 201991. https://doi.org/10.1098/rsos.201991.

[9] F. Krammer, R. Grabherr, Alternative influenza vaccines made by insect cells, Trends Mol. Med. 16 (2010) 313–320. https://doi.org/10.1016/j.molmed.2010.05.002.

[10] E.V.L. Grgacic, D.A. Anderson, Virus-like particles: passport to immune recognition, Methods 40 (2006) 60–65. https://doi.org/10.1016/j.ymeth.2006.07.018.

[11] F. Barra, U.L.R. Maggiore, G. Bogani, A. Ditto, M. Signorelli, F. Martinelli, V. Chiappa, D. Lorusso, F. Raspagliesi, S. Ferrero, New prophylactics human papilloma virus (HPV) vaccines against cervical cancer, J. Obstet. Gynaecol. 39 (2019) 1–10. https://doi.org/10.1080/01443615.2018.1493441.

[12] J.T. Schiller, M. Müller, Next generation prophylactic human papillomavirus vaccines, The Lancet Oncology 16 (2015) e217-e225. https://doi.org/10.1016/S1470-2045(14)71179-9.

[13] A.P.J. Middelberg, T. Rivera-Hernandez, N. Wibowo, L.H.L. Lua, Y. Fan, G. Magor, C. Chang, Y.P. Chuan, M.F. Good, M.R. Batzloff, A microbial platform for rapid and low-cost virus-like particle and capsomere vaccines, Vaccine 29 (2011) 7154–7162. https://doi.org/10.1016/j.vaccine.2011.05.075.

[14] J. Walther, R. Godawat, C. Hwang, Y. Abe, A. Sinclair, K. Konstantinov, The business impact of an integrated continuous biomanufacturing platform for recombinant protein production, J. Biotechnol. 213 (2015) 3–12. https://doi.org/10.1016/j.jbiotec.2015.05.010.

Chapter 2

Literature Review

This chapter reviews the current literature and aims to give the reader a comprehensive overview of the topics relevant to this thesis. Virus-like particles, Group A Streptococcus, and current purification strategies are discussed. Furthermore, the murine polyomavirus-like particle vaccine platform is introduced.

2.1 Virus-like Particle Based Vaccines

Virus-like particles are nano-sized structures mimicking the overall structure of their native virus [1]. They are formed by one or several viral structural proteins which can be expressed in various systems like bacteria, yeast or eukaryotic cell cultures. Although they are identical or closely related to intact viruses, they lack genomic material and are therefore non-infectious by design [2,3]. Due to their highly repetitive and native structure VLPs strongly stimulate B cells and induce a vigorous and enduring antibody response [4,5]. VLPs can be used as efficient vaccines against their underlying virus, and might even trigger stronger immune responses than a natural infection [6]. Native VLPs are used as vaccines against Human Papilloma Virus and commercialized under the name Cervarix® and Gardasil®.

VLPs can also be used as a platform to present covalent bound foreign antigens and thus form a completely new class of vaccines. As the foreign antigens are presented in a more "natural" virus pattern, a very strong immune response can be triggered without any adjuvant [7]. VLPs presenting foreign antigens are called chimeric or modular VLPs and have been heavily examined against pathogens such as HIV, HPV, poliovirus, Hepatitis, and others [8,9]. A main disadvantage of VLPs as vaccines is their complicated and laborious production route. Random aggregation, shear sensitivity, low recoveries, low binding capacities, the need for nuclease treatment, and hard-to-scale unit operations such as size exclusion chromatography and ultra-centrifugation make them comparably expensive [1,8]. A dose of HPV vaccine is priced over 300 US-Dollars and even the not-for-profit price (Global Alliance for vaccines and Immunization) of 4.50 US-Dollar is too high for the use in low-income countries [10–12].

2.2 Murine Polyomavirus VLP based Vaccine platform

A VLP vaccine platform that was specially designed to meet the need for rapidly-produced and low-cost VLP vaccines is the murine polyomavirus major capsid protein VP1 VLP

platform. Murine Polyomavirus-like particles are icosahedral formed particles, containing 72 major capsid protein VP1-pentamers, with an approximate size of 45 nm and a molecular mass of 15 300 kDa. The VP1-pentamers, called capsomeres, have a molecular mass of 212.5 kDa [13]. One main advantage of murine polyomavirus VLPs is that the capsomeres can be expressed unassembled in microbial expression systems. These unassembled capsomeres can then be purified and assembled into VLPs in a controlled environment *in-vitro* thereafter [14]. This paradigm follows other mass manufacturing approaches (e.g. for automobiles) where components are made and subjected to quality control and are then assembled into a complex structure. The capsomere as well as an assembled Murine Polyomavirus VLP are illustrated in Figure 2-1.

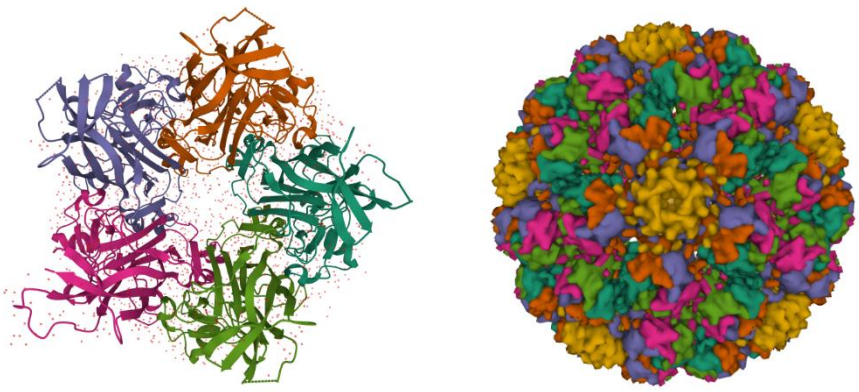

Figure 2-1Murine Polyomavirus capsomere (PDB-ID 5CPU) and assembled VLP (PDB-ID 1SIE).

The assembly/disassembly reaction can be easily controlled by changing the buffer system. While VLP assembly is triggered by Ca^{2+} ions, capsomeres are stabilized in the presence of chelating agents such as EDTA and a reducing environment [13–15]. Processing of unassembled capsomeres followed by *in-vitro* assembly into VLPs provide several advantages over simultaneous expression and assembly *in-vivo.* One point is that by

controlling the quality of the capsomeres before assembly and by controlling the assembly process directly, a better overall quality of the VLPs can be achieved. Another important point is, that this approach prevents the introduction of unknown and variable contaminants inside the VLPs, so-called internal contaminants, that get trapped inside the VLPs during *in-vivo* assembly. Removal of internal contaminants requires an additional dis- and re-assembly step during processing which impacts the overall process economics yet is not required for the murine polyomavirus VLP platform [14].

By fusing antigens with VP1, chimeric or modular VLPs can be produced that present foreign antigens in a highly immunogenic manner. A proof of concept was implemented for different antigens including Influenza, GAS, and Rotavirus and it was shown that modular VP1 VLPs induce strong immune responses [16–18]. Furthermore, the modular VP1-antigen capsomeres can be expressed and produced in microbial expression systems such as *E. coli*, and expression levels of gram-per litre have been achieved [19]. This reveals another benefit of this platform technology. Contrary to traditional egg or cell culture produced vaccines, which need between 11 and 20 weeks production time, VLP vaccines produced in microbes can be available within days, can be quickly modified to the circulating strain, and are furthermore cheap to produce [17]. Estimated costs for vaccines based on this technology using process economic tools are in the range of cents per dose for large-scale production, slashing the price of conventional vaccines by several hundred times [20].

2.3 Group A Streptococcus and J8 antigen

Streptococcus pyogenes also known as Group A Streptococcus is a gram-positive human pathogen, which can cause mild symptoms such as pharyngitis, but can also lead to serious and potential life-threatening diseases such as necrotizing fasciitis, acute rheumatic fever (ARF) and rheumatic heart disease (RHD). GAS is responsible for over 500,000 deaths and several hundred million infections per year, mainly threatening developing countries and

indigenous communities [21–23]. Currently, there is no vaccine commercially available. Thus, in 2015 not only the World Health Organization (WHO) decided to force the development of a GAS vaccine but also the Australian government decided to invest 35 million dollars [24,25].

The surface of GAS is coated with a major virulence factor called M-protein [26]. The M-protein, firstly described in 1927, acts as the primary antigen and as a serological marker [27,28]. Upon infection an individual produces type specific antibodies against the M-protein and develops subsequent protection against this serotype [29]. Therefore, the M-protein is an ideal target antigen for vaccine development and was extensively investigated as a target for vaccine development. However, there are certain drawbacks associated with using M-protein as a target antigen. First of all the M-protein has a hypervariable region on the N-terminus and with more than 200 known serotypes and thus it is challenging to find a vaccine that is effective against a broad range of GAS types [30]. Another even more important aspect concerns possible cross-reactions upon vaccination with M-protein as it can raise antibodies reacting with alpha-helical coiled human proteins, and an early study with partially purified M-protein induced the development of ARF in some volunteers, which subsequently led to the prohibition of GAS organisms and derivates for vaccines [31–33]. Although the decision made by the FDA was revoked in 2006, the induction of possible cross-reactive antibodies are a major concern that needs to be addressed during development of a GAS vaccines [34].

The M-protein consists of two polypeptide chains that form an alpha-helical coiled-coil structure on the surface of GAS and consists mainly of blocks of repeated amino acid sequences that can be split into four repeat regions A-D, as illustrated in figure 2-2 [35]. The C-terminal end is highly conserved with the sequence differing by less than 2% between different serotypes. At the N-terminus however, the M-protein becomes more variable with

an additional hypervariable nonhelical region of 11 amino acids adjunct to the A-repeat block that defines the biological activity of the molecule [35].

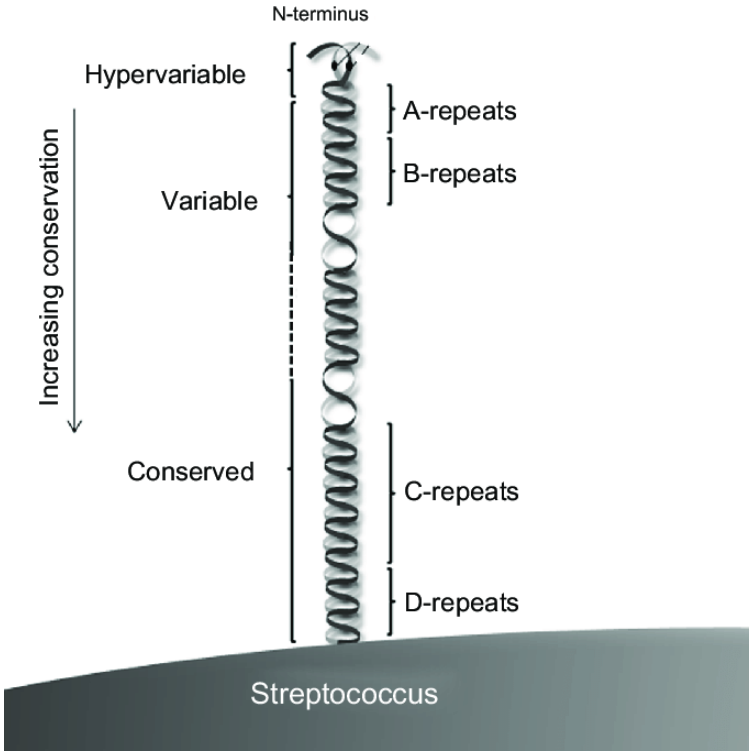

Figure 2-2 Schematic illustration of M-protein of Group A Streptococcus [36].

One approach to obtain a general vaccine against most serotypes is to induce antibodies against the conserved part of the M-protein. A promising target within the highly conserved C-terminus of the M-protein is epitope p145 having 20 amino acids length, as p145 antibodies were able to opsonize *streptococci* [37]. Hayman [38] has developed a chimeric peptide called J8, containing the minimal epitope J8i (12 amino acids) of p145 that is fused with flanking GCN4-peptides on each side to promote the native helical structure which is essential for efficiency [17]. This chimeric J8 peptide was able to stimulate the production of antibodies that opsonize GAS but do not induce potential human cross-reactions [38].

Modular VLP vaccines against GAS based on the murine polyomavirus platform can be obtained by fusing the chimeric peptide J8 with VP1. J8 peptide was inserted with flanking G4S linker at position 293 of VP1 resulting in the chimeric construct VP1-J8. The flanking linkers, allow for more space and promote the natural helical conformation of J8 [17]. After assembly of the VP1-J8 capsomeres into VLPs, the antigen J8 is presented in a highly repetitive manner on the surface of the VLP as shown in Figure 2-3. This modular GAS VLP vaccine has proven to be efficient in inducing a strong systemic and mucosal immune system response in mice, even without the addition of adjuvants [7,17].

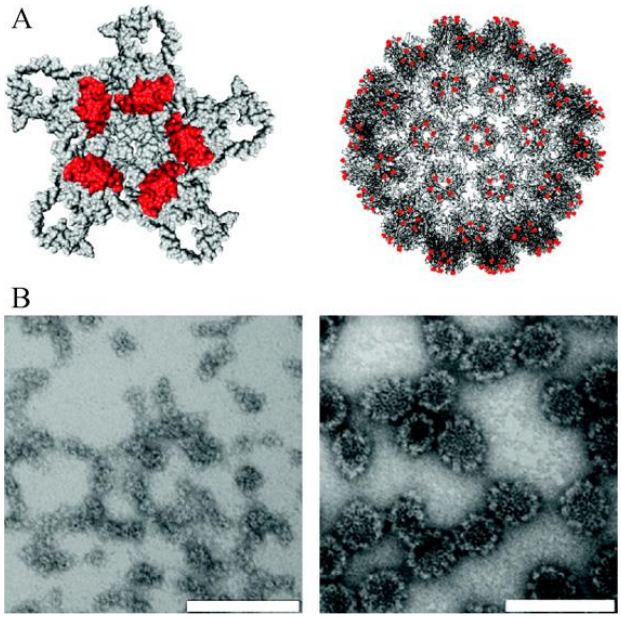

Figure 2-3 *Chimeric VP1 displaying Group A Streptococcus J8 peptide (J8-VP1). (A) Structural prediction for a J8-VP1 capsomere and virus-like particle (J8-VP1 VLP). J8 peptides (red) are presented on the surfaces of chimeric VP1 capsomere (left), which self-assemble into a VLP. (B) Transmission electron micrograph showing the self-assembly of J8-VP1 capsomeres (left) into J8-VP1 VLPs (right). Scale bar is 100 nm. From [17].*

2.4 Expression and Purification of Murine Polyomavirus Derived VLP Vaccines

The two main bioprocess manufacturing options for murine polyomavirus-based VLPs are shown in Figure 2-4, namely the *in-vivo* pathway in eukaryotic, yeast, and insect cells and the *in-vitro* pathway in prokaryotic cells. During the *in-vivo* pathway VP1 capsomeres assemble into VLPs inside the host cell and can therefore incorporate cellular contaminants internalised to their structure. Thus, a disassembly and reassembly step is essential during the purification process to remove these internal contaminants. In contrast, during the *in-vitro* pathway, VP1 capsomeres remain unassembled inside the cell and the actual assembly process occurs after the removal of impurities in a controlled environment. As the disassembly and reassembly step is no longer required, the *in-vitro* pathway is in general more stable and efficient [14].

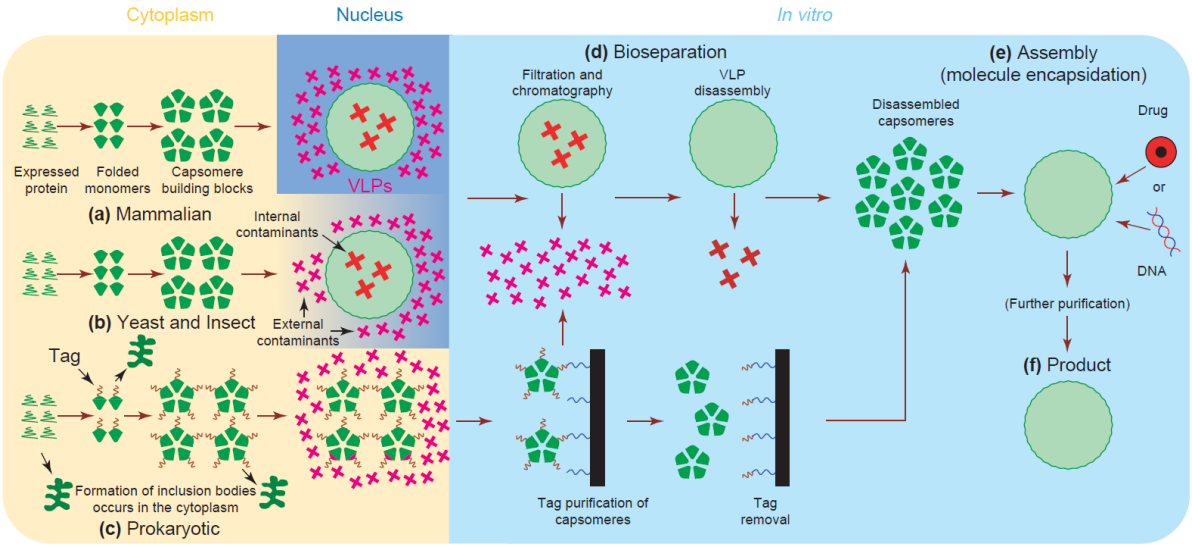

Figure 2-4 Different bioprocess production options for VLPs. During the in-vivo pathway (a) and (b) VLPs assemble inside of the cell, while in the prokaryotic expression system (c) capsomeres remain unassembled and can be assembled after purification in vitro [14].

In literature, modular VP1 protein such as VP1-J8 is expressed in a transformed *E. coli* Rosetta (DE3) with the pGEX-4T-1 plasmid as a cloning vector. Expression levels described in the literature are usually low but also gram-per-litre expression has been achieved, with the

highest described value being 1.63 g l^{-1} [39]. The optimal conditions for VP1 expression have not been discovered yet as the results are contrary to each other; for example, Ladd Effio et al. [39] measured the highest expression at 37 °C while Chuan et al. [40] at 26 °C. The highest described value has been achieved at pH 6, 37 °C, and a relatively low shaker speed. It is assumed that inducing stress during growth and expression, either by low pH or low oxygen levels, has a positive influence on soluble product titres.

For a convenient purification process of the expressed VP1 capsomeres, a GST affinity tag is usually inserted into the VP1-antigen sequence. After cell disruption and clarification, the GST-tagged capsomeres are captured on a GSTrap HP column, after which GST is cleaved with thrombin followed by size exclusion chromatography to remove aggregates and the GST-tag [40]. This purification pathway is used in nearly all publications concerning VP1 [41–43], although some add further steps like anion exchange chromatography to remove endotoxin and sterile filtration [17,41]. Endotoxins have been furthermore removed using Triton X-114 and Tobacco Etch Virus protease (TEVp) has been used as an alternative to thrombin for GST-tag cleavage [43,44].

Using affinity tags leads to several disadvantages during downstream processing such as multimerization effects, low recovery, a costly and inefficient chromatographic step, and a further enzymatic tag removal step. Still, GST-tag free purification procedures are rarely described [44]. Alternative pathways without affinity purification include selective salting out with sodium sulfate [45] or anion exchange chromatography followed by size exclusion chromatography [39]. Another challenge during purification of VLPs and viral capsomeres is the removal of DNA. Described protocols often remove DNA only incompletely and are usually dependent on utilizing enzymatic nuclease treatment to remove DNA, adding another layer of complexity and timely processing to the purification pathway [46,47].

The large molecular size of VP1, the need for conformational integrity, and the tendency to aggregate, further challenge purification. Slow diffusion and low pore accessibility can lead to low binding capacities and unfavourable buffer conditions can lead to instabilities [1,48].

Although purification of tagged and non-tagged VP1 capsomeres is possible with different techniques, described methods lack process performance, suffer from low recoveries, and are heavily dependent on hard-to-scale unit operations. Finding and integrating different unit operations into a fast, efficient, scale-able, and reliable purification process without massive product losses is the major current challenge in VLP/capsomeres purification; no efficient process neither in batch, nor in continuous mode, is described for VP1 capsomeres yet [1].

2.5 VP1 Process Development

To achieve the aim of this project and develop a continuous downstream process for VP1-J8 VLP vaccines against GAS, several challenges need to be solved. The current limitations for non-tagged VP1 constructs, as outlined in Chapter 2.4, need to be addressed to develop an efficient batch process first. Possible solutions for aggregation and low binding capacities can involve stabilizing buffer conditions and new chromatographic resins with favourable performance properties respectively. Another approach for process intensification is switching from batch to continuous manufacturing. Counter-current chromatography can help to overcome challenges with low binding capacities and solves the trade-off between resin utilization and productivity [49]. Other possible benefits of continuous processing are higher automatization, lower footprint, faster processing and thus less product degradation and less batch-to-batch variations.

There are multiple possible options to transfer a process from batch to continuous, depending on the required unit operations. Therefore, a detailed review of continuous biomanufacturing,

possible unit operations and challenges during continuous processing is provided as Chapter 3 in the form of a published and incorporated paper.

2.6 References

[1] C.L. Effio, J. Hubbuch, Next generation vaccines and vectors: Designing downstream processes for recombinant protein-based virus-like particles, Biotechnol. J. 10 (2015) 715–727. https://doi.org/10.1002/biot.201400392.

[2] J. Johnson, Structures of virus and virus-like particles, Current Opinion in Structural Biology 10 (2000) 229–235. https://doi.org/10.1016/S0959-440X(00)00073-7.

[3] P. Pushko, P. Pumpens, E. Grens, Development of virus-like particle technology from small highly symmetric to large complex virus-like particle structures, Intervirology 56 (2013) 141–165. https://doi.org/10.1159/000346773.

[4] K.M. Frietze, D.S. Peabody, B. Chackerian, Engineering virus-like particles as vaccine platforms, Curr. Opin. Virol. 18 (2016) 44–49. https://doi.org/10.1016/j.coviro.2016.03.001.

[5] F. Zabel, T.M. Kündig, M.F. Bachmann, Virus-induced humoral immunity: on how B cell responses are initiated, Curr. Opin. Virol. 3 (2013) 357–362. https://doi.org/10.1016/j.coviro.2013.05.004.

[6] M. Stanley, Immunobiology of HPV and HPV vaccines, Gynecol. Oncol. 109 (2008) S15-21. https://doi.org/10.1016/j.ygyno.2008.02.003.

[7] T. Rivera-Hernandez, J. Hartas, Y. Wu, Y.P. Chuan, L.H.L. Lua, M. Good, M.R. Batzloff, A.P.J. Middelberg, Self-adjuvanting modular virus-like particles for mucosal vaccination against group A streptococcus (GAS), Vaccine 31 (2013) 1950–1955. https://doi.org/10.1016/j.vaccine.2013.02.013.

[8] A. Roldão, M.C.M. Mellado, L.R. Castilho, M.J.T. Carrondo, P.M. Alves, Virus-like particles in vaccine development, Expert Rev. Vaccines 9 (2010) 1149–1176. https://doi.org/10.1586/erv.10.115.

[9] P. Pumpens, E. Grens, Artificial Genes for Chimeric Virus-Like Particles, in: Y. Khudyakov, H. Fields (Eds.), Artificial DNA, CRC Press, 2002.

[10] C.A. MacLennan, Vaccines for low-income countries, Semin. Immunol. 25 (2013) 114–123. https://doi.org/10.1016/j.smim.2013.05.004.

[11] C. Clendinen, Y. Zhang, R.N. Warburton, D.W. Light, Manufacturing costs of HPV vaccines for developing countries, Vaccine 34 (2016) 5984–5989. https://doi.org/10.1016/j.vaccine.2016.09.042.

[12] D.G. McNeil, Cancer vaccines get a price cut in poor nations, The New York Times 9 (2013).

[13] U. Schmidt, R. Rudolph, G. Bohm, Mechanism of Assembly of Recombinant Murine Polyomavirus-Like Particles, J. Virol. 74 (2000) 1658–1662. https://doi.org/10.1128/JVI.74.4.1658-1662.2000.

[14] L.K. Pattenden, A.P.J. Middelberg, M. Niebert, D.I. Lipin, Towards the preparative and large-scale precision manufacture of virus-like particles, Trends Biotechnol. 23 (2005) 523–529. https://doi.org/10.1016/j.tibtech.2005.07.011.

[15] Y.P. Chuan, Y.Y. Fan, L.H.L. Lua, A.P.J. Middelberg, Virus assembly occurs following a pH- or Ca2+-triggered switch in the thermodynamic attraction between structural protein capsomeres, J. R. Soc. Interface 7 (2010) 409–421. https://doi.org/10.1098/rsif.2009.0175.

[16] M.R. Anggraeni, N.K. Connors, Y. Wu, Y.P. Chuan, L.H.L. Lua, A.P.J. Middelberg, Sensitivity of immune response quality to influenza helix 190 antigen structure displayed

on a modular virus-like particle, Vaccine 31 (2013) 4428–4435. https://doi.org/10.1016/j.vaccine.2013.06.087.

[17] A.P.J. Middelberg, T. Rivera-Hernandez, N. Wibowo, L.H.L. Lua, Y. Fan, G. Magor, C. Chang, Y.P. Chuan, M.F. Good, M.R. Batzloff, A microbial platform for rapid and low-cost virus-like particle and capsomere vaccines, Vaccine 29 (2011) 7154–7162. https://doi.org/10.1016/j.vaccine.2011.05.075.

[18] A. Tekewe, Y. Fan, E. Tan, A.P.J. Middelberg, L.H.L. Lua, Integrated molecular and bioprocess engineering for bacterially produced immunogenic modular virus-like particle vaccine displaying 18 kDa rotavirus antigen, Biotechnol. Bioeng. 114 (2017) 397–406. https://doi.org/10.1002/bit.26068.

[19] M.W.O. Liew, A. Rajendran, A.P.J. Middelberg, Microbial production of virus-like particle vaccine protein at gram-per-litre levels, J. Biotechnol. 150 (2010) 224–231. https://doi.org/10.1016/j.jbiotec.2010.08.010.

[20] Y.P. Chuan, N. Wibowo, L.H. Lua, A.P.J. Middelberg, The economics of virus-like particle and capsomere vaccines, Biochemical Engineering Journal 90 (2014) 255–263. https://doi.org/10.1016/j.bej.2014.06.005.

[21] M.J. Walker, T.C. Barnett, J.D. McArthur, J.N. Cole, C.M. Gillen, A. Henningham, K.S. Sriprakash, M.L. Sanderson-Smith, V. Nizet, Disease manifestations and pathogenic mechanisms of Group A Streptococcus, Clin. Microbiol. Rev. 27 (2014) 264–301. https://doi.org/10.1128/CMR.00101-13.

[22] N. Bocking, C.-L. Matsumoto, K. Loewen, S. Teatero, A. Marchand-Austin, J. Gordon, N. Fittipaldi, A. McGeer, High Incidence of Invasive Group A Streptococcal Infections in Remote Indigenous Communities in Northwestern Ontario, Canada, Open Forum Infect. Dis. 4 (2017) ofw243. https://doi.org/10.1093/ofid/ofw243.

[23] P.J. May, A.C. Bowen, J.R. Carapetis, The inequitable burden of group A streptococcal diseases in Indigenous Australians, Med. J. Aust. 205 (2016) 201–203. https://doi.org/10.5694/mja16.00400.

[24] Andrew Steer, Status of vaccine research and development of vaccines for streptococcus pyogenes [Internet]. WHO Product Development for Vaccines Advisory Committee (PD-VAC) meeting – 2015, 2015. http://who.int/immunization/research/meetings_workshops/pdvac/en/.

[25] Ken Wyatt, 2019. http://www.health.gov.au/internet/ministers/publishing.nsf/Content/health-mediarel-yr2019-wyatt031.htm.

[26] V.A. Fischetti, Streptococcal M protein: molecular design and biological behavior, Clin. Microbiol. Rev. 2 (1989) 285–314. https://doi.org/10.1128/CMR.2.3.285.

[27] D. Metzgar, A. Zampolli, The M protein of group A Streptococcus is a key virulence factor and a clinically relevant strain identification marker, Virulence 2 (2011) 402–412. https://doi.org/10.4161/viru.2.5.16342.

[28] R.C. Lancefield, THE ANTIGENIC COMPLEX OF STREPTOCOCCUS HAEMOLYTICUS I. DEMONSTRATION OF A TYPE-SPECIFIC SUBSTANCE IN EXTRACTS OF STREPTOCOCCUS HAEMOLYTICUS, J. Exp. Med. 47 (1928) 91–103. https://doi.org/10.1084/jem.47.1.91.

[29] R.C. Lancefield, Current knowledge of type-specific M antigens of group A streptococci, J. Immunol. 89 (1962) 307–313.

[30] D.J. McMillan, P.-A. Drèze, T. Vu, D.E. Bessen, J. Guglielmini, A.C. Steer, J.R. Carapetis, L. van Melderen, K.S. Sriprakash, P.R. Smeesters, Updated model of group A Streptococcus M proteins based on a comprehensive worldwide study, Clin. Microbiol. Infect. 19 (2013) E222-9. https://doi.org/10.1111/1469-0691.12134.

[31] B.F. Massell, Rheumatic Fever Following Streptococcal Vaccination, JAMA: The Journal of the American Medical Association 207 (1969) 1115. https://doi.org/10.1001/jama.1969.03150190037007.

[32] FDA, Status of specific products; Group A Streptococcus 21 CFR 610.19, 1979.

[33] L. Guilherme, R. Ramasawmy, J. Kalil, Rheumatic fever and rheumatic heart disease: genetics and pathogenesis, Scand. J. Immunol. 66 (2007) 199–207. https://doi.org/10.1111/j.1365-3083.2007.01974.x.

[34] FDA, Revocation of status of specific product; Group A Streptococcus, 2005. https://www.federalregister.gov/documents/2005/12/02/05-23546/revocation-of-status-of-specific-products-group-a-streptococcus (accessed 23 March 2022).

[35] V.A. Fischetti, Streptococcal M Protein, Sci Am 264 (1991) 58–65. https://doi.org/10.1038/scientificamerican0691-58.

[36] D. Nitsche-Schmitz, A. Sharma, Challenges to developing effective streptococcal vaccines to prevent rheumatic fever and rheumatic heart disease, VDT (2014) 39. https://doi.org/10.2147/VDT.S45037.

[37] S. Pruksakorn, A. Galbraith, R.A. Houghten, M.F. Good, Conserved T and B cell epitopes on the M protein of group A streptococci. Induction of bactericidal antibodies, J. Immunol. 149 (1992) 2729–2735.

[38] W. Hayman, Mapping the minimal murine T cell and B cell epitopes within a peptide vaccine candidate from the conserved region of the M protein of group A streptococcus, International Immunology 9 (1997) 1723–1733. https://doi.org/10.1093/intimm/9.11.1723.

[39] C. Ladd Effio, P. Baumann, C. Weigel, P. Vormittag, A. Middelberg, J. Hubbuch, High-throughput process development of an alternative platform for the production of virus-

like particles in Escherichia coli, J. Biotechnol. 219 (2016) 7–19. https://doi.org/10.1016/j.jbiotec.2015.12.018.

[40] Y.P. Chuan, L.H.L. Lua, A.P.J. Middelberg, High-level expression of soluble viral structural protein in Escherichia coli, J. Biotechnol. 134 (2008) 64–71. https://doi.org/10.1016/j.jbiotec.2007.12.004.

[41] A. Seth, I.G. Kong, S.-H. Lee, J.-Y. Yang, Y.-S. Lee, Y. Kim, N. Wibowo, A.P.J. Middelberg, L.H.L. Lua, M.-N. Kweon, Modular virus-like particles for sublingual vaccination against group A streptococcus, Vaccine 34 (2016) 6472–6480. https://doi.org/10.1016/j.vaccine.2016.11.008.

[42] M.W. Liew, Y.P. Chuan, A.P. Middelberg, High-yield and scalable cell-free assembly of virus-like particles by dilution, Biochemical Engineering Journal 67 (2012) 88–96. https://doi.org/10.1016/j.bej.2012.05.007.

[43] N. Wibowo, Y.P. Chuan, L.H. Lua, A.P. Middelberg, Modular engineering of a microbially-produced viral capsomere vaccine for influenza, Chemical Engineering Science 103 (2013) 12–20. https://doi.org/10.1016/j.ces.2012.04.001.

[44] N.K. Connors, Y. Wu, L.H. Lua, A.P.J. Middelberg, Improved fusion tag cleavage strategies in the downstream processing of self-assembling virus-like particle vaccines, Food and Bioproducts Processing 92 (2014) 143–151. https://doi.org/10.1016/j.fbp.2013.08.012.

[45] N. Wibowo, Y. Wu, Y. Fan, J. Meers, L.H.L. Lua, A.P.J. Middelberg, Non-chromatographic preparation of a bacterially produced single-shot modular virus-like particle capsomere vaccine for avian influenza, Vaccine 33 (2015) 5960–5965. https://doi.org/10.1016/j.vaccine.2015.08.100.

[46] N. Hillebrandt, P. Vormittag, N. Bluthardt, A. Dietrich, J. Hubbuch, Integrated Process for Capture and Purification of Virus-Like Particles: Enhancing Process Performance by

Cross-Flow Filtration, Front. Bioeng. Biotechnol. 8 (2020) 489. https://doi.org/10.3389/fbioe.2020.00489.

[47] S.B. Carvalho, R.J.S. Silva, M.G. Moleirinho, B. Cunha, A.S. Moreira, A. Xenopoulos, P.M. Alves, M.J.T. Carrondo, C. Peixoto, Membrane-Based Approach for the Downstream Processing of Influenza Virus-Like Particles, Biotechnol. J. 14 (2019) e1800570. https://doi.org/10.1002/biot.201800570.

[48] L. Shi, G. Sanyal, A. Ni, Z. Luo, S. Doshna, B. Wang, T.L. Graham, N. Wang, D.B. Volkin, Stabilization of human papillomavirus virus-like particles by non-ionic surfactants, Journal of Pharmaceutical Sciences 94 (2005) 1538–1551. https://doi.org/10.1002/jps.20377.

[49] D. Baur, M. Angarita, T. Müller-Späth, M. Morbidelli, Optimal model-based design of the twin-column CaptureSMB process improves capacity utilization and productivity in protein A affinity capture, Biotechnol. J. 11 (2016) 135–145. https://doi.org/10.1002/biot.201500223.

Chapter 3

Continuous Downstream Bioprocessing for Intensified Manufacture of Biopharmaceuticals and Antibodies

This chapter provides an extensive review on continuous biomanufacturer and introduces different continuous concepts and completes the literature review of Chapter 2.

Statement of Authorship

Title of Paper	Continuous Downstream Bioprocessing for Intensified Manufacture of Biopharmaceuticals and Antibodies
Publication Status	published
Publication Details	Lukas Gerstweiler, Jingxiu Bi, Anton P.J. Middelberg, Continuous downstream bioprocessing for intensified manufacture of biopharmaceuticals and antibodies Chemical Engineering Science, Volume 231, 2021, 116272, ISSN 0009-2509 https://doi.org/10.1016/j.ces.2020.116272

Principal Author

Name of Principal Author (Candidate)	Lukas Gerstweiler		
Contribution to the Paper	Conceptualization, Writing – original draft, Writing – review & editing		
Overall percentage	80%		
Signature		Date	4.4.2022

Co-Author Contributions

By signing the Statement of Authorship. Each author certifies that:

I. The candidate's stated contribution to the publication is accurate (as detailed above)

II. Permission is granted for the candidate in include the publication in the thesis; and

III. The sum of all co-author contribution is equal to 100% less the candidate's stated contribution

Name of Co-Author	Jingxiu Bi		
Contribution to the Paper	Writing - review & editing, Supervision		
Signature		Date	31/03/2022

Name of Co-Author	**Anton P.J. Middelberg**		
Contribution to the Paper	Conceptualization, Writing - review & editing, Supervision		
Signature		Date	31 March 2022

Chemical Engineering Science 231 (2021) 116272

Contents lists available at ScienceDirect

Chemical Engineering Science

journal homepage: www.elsevier.com/locate/ces

Continuous downstream bioprocessing for intensified manufacture of biopharmaceuticals and antibodies

Lukas Gerstweiler, Jingxiu Bi, Anton P.J. Middelberg *

The University of Adelaide, School of Chemical Engineering and Advanced Materials, SA 5000, Australia

HIGHLIGHTS

- Continuous processing (CP) is delivering new efficiencies in biomanufacturing.
- The traditional focus on antibodies is being broadened to other biopharmaceuticals.
- CP can leap biomanufacturing into the 21stC cementing it as an advanced industry.
- A process systems approach to integrated continuous bioprocess design is required.
- Further research is urgently needed to accelerate this new paradigm.

ARTICLE INFO

Article history:
Received 23 May 2020
Received in revised form 12 October 2020
Accepted 2 November 2020
Available online 8 November 2020

Keywords:
Continuous processing
Antibody
Biopharmaceuticals
Continuous purification
Periodic counter current chromatography
Downstream process development
Process intensification

ABSTRACT

Continuous production delivers higher productivity and better quality than traditional batch-wise approaches. It intensifies production lowering capital cost and enables better control. Despite obvious advantages, continuous processing has not yet guided biomanufacturing to 21st Century Advanced Manufacturing status. Production relies primarily on batch-wise methods that have served the industry through its infancy. While great improvements have been achieved on the upstream side, downstream processing lacks development in continuous processing and is now the handbrake on modernisation. Nevertheless, there are hopeful advances. Research on continuous chromatographic purification for antibodies is maturing, and work has commenced on other unit operations and on process system integration. This exciting field of process intensification research is at a turning point, though considerably more research is needed. This review aims to summarize the latest developments and capabilities of continuous downstream processing applied in biopharmaceutical research and gives an overview of recent developments.

1. Introduction

With a predicted worldwide market of nearly 400 billion dollars in 2024, the biopharmaceutical market is one of the largest industrial sectors and has a tremendous positive impact on society (Mordor Intelligence, 2019). For a long time, the biopharmaceutical industry focused mainly on development of new and innovative therapies, but now, the intensification of the production process is becoming a focus of interest (Jacoby et al., 2015). Process intensification is defined as any chemical engineering development that leads to a substantially smaller, cleaner and more efficient technology with the aim to reduce the overall production costs for a given product (Stankiewicz and Moulijn, 2000). This shift is driven by various factors. One main driver is the increase in therapeutic competition due to expiring patents, with the introduction of biosimiliars to the market and next generation medicines pressuring

Abbreviations: AEX, Anion exchange; ATF, Alternating tangential flow filtration; ATPs, Aqueous two phase systems; BSA, Bovine serum albumin; CEX, Cation exchange; CF, Concentration factors; CFIR, Coiled ow inversion reactor; CHO, Chinese Hamster Ovary; COG, Cost of goods; CCC, Counter current chromatography; CCTC, Counter-current tangential chromatography; CPC, Centrifugal partition chromatography; EDFM, Electrodialysis with filtration membranes; FDA, Food and Drug Administration; GCSF, Granulocyte colony stimulating factor; HCP, Host cell protein; IgG, Immunoglobulin G; IC, Interconnected; IEX, Ion exchange; PAT, Process analytic technology; PCC, Periodic counter current; PEG, Polyethylene glycol; P-CAC, Preparative continuous annular chromatography; MSB, Mixer settler batteries; MCSGP, Multicolumn counter current solvent gradient purification; mAb, Monoclonal antibody; OCC, One-column continuous chromatography; PAT, Process analytic technologies; sCPC, Sequential centrifugal partition chromatography; SEC, Size Exclusion Chromatography; SMCC, Sequential multi-column chromatography; SPDF, Single pass diafiltration; SPTFF, Single pass tangential flow filtration; SMB, Simulated moving bed; TPP, Three-phase-partition; TFF, Tangential flow filtration; TMB, True moving bed; VLPs, Virus like particles.

* Corresponding author.
E-mail address: anton.middelberg@adelaide.edu.au (A.P.J. Middelberg).

https://doi.org/10.1016/j.ces.2020.116272
0009-2509/

lower production costs by more efficient processes. Another consideration is the requirement for more flexible production routes and equipment that can be used for multiple products, as more and more new, large-molecule drugs like vaccines, orphan drugs and personalized medicine are developed, that require only small volumes of product and a high flexibility of producers (Jacoby et al., 2015). Very recently Sanofi opened a new biologics manufacturing facility, in which continuous biologic production technology will reportedly be used, highlighting a potential turning point in this field (Sanofi, 2019).

Traditional large-scale manufacturing processes rely on large stainless-steel vessels and a batch-wise production, as this was the only way to achieve high productivity through large volumes while ensuring process safety. However, stainless steel plants are not only capital investment intensive, they also require long planning and construction times, and late modifications are costly, resulting in an inflexible and risky investment (Xenopoulos, 2015; Frank, 2018; Hummel et al., 2019). Single-use equipment was introduced as an alternative and is becoming universally accepted in the industry. This disposal technology enables high flexibility and lower investment cost, as it can be ordered on demand and is delivered pre-sterilized, making cleaning and cleaning validation unnecessary (Frank, 2018). Arguably, this simplification is achieved at the expense of sustainability at a time when social license is increasingly directed toward the circular economy.

Shifting from batch-wise to continuous production intensified other process industries and is a promising approach to shorten the production cycle, reduce facility footprint, increase equipment utilization, enable constant product quality, and therefore, lower the overall cost of goods (Woodcock, 2014; Konstantinov and Cooney, 2015; Hummel et al., 2019; Cataldo et al., 2020). This is particularly pertinent for sensitive molecules that degrade over time. One main source of degradation in bioprocessing is due to long holding times between the purification steps, in which enzymatic reactions or reactions with other impurities, oxygen etc. occur. Another source is long column residence times that can affect some proteins. Integrated continuous processes, in which holding times between the individual steps are eradicated and the overall average residence time is dramatically lowered, offer a pathway with less product loss (Vogel et al., 2012; Warikoo et al., 2012; Konstantinov and Cooney, 2015; Fisher et al., 2019).

The modern development of continuous perfusion reactors has increased productivity and product titres to a level where the downstream process is now the bottleneck of the production process (Kunert and Reinhart, 2016). As antibodies are by far the biggest market for biopharmaceuticals, recent research on continuous purification processes has largely focused on costly capturing of antibodies using protein A affinity chromatography, attempting to integrate this process with perfusion reactors to prepare a highly concentrated initial solution for further purification steps.

To obtain a fully integrated continuous process, and ultimately reduce the footprint and intensify the process, however, possible ways to integrate the individual unit operations as well as other continuous unit operations have to be developed and examined. Recent techniques made significant progress in enabling continuous processes. For example, single pass tangential flow filtration enables in-line buffer exchange and therefore a seamless integration of different unit operations. Alternative purification techniques as a substitute for chromatographic processes, which are inherently batch-wise and therefore usually semi continuous, like crystallization, precipitation and membrane technologies, are consistently becoming more advanced, opening up new purification pathways and process design strategies for continuous processing. Although there is a lack of research in this field, they are theoretically easier to transfer into a continuous process using tubular reactors and other standard formats.

A number of excellent reviews have been published on continuous purification of biopharmaceuticals, though mostly focused on specific aspects. A number of them address specific chromatographic processes (Steinebach et al., 2016b; Vogg et al., 2018), or only address antibodies (Somasundaram et al., 2018). Excellent overviews are given by (Jungbauer, 2013) and (Zydney, 2016), describing current and potential processes. As interest in this field is growing and more research on continuous purification strategies is being released, this review will provide an overview of the current status of continuous downstream processing technologies applied, not only using antibodies, but also other therapeutic proteins. A focus is placed on continuous processes that have proved the concept and highlight parameters such as productivity or purity to demonstrate the capabilities of these processes. A short and necessarily incomplete overview of recent publications, the targeted molecule and achieved process performances is given in Table 1 and is elaborated in subsequent sections.

Table 1. Overview of different continuous purification processes used for purification of biopharmaceuticals or proteins and some process parameters where applicable.

2. Continuous chromatographic unit operations

Chromatography remains the workhorse in bioseparation as commercial processes are heavily based on several chromatographic steps. Because of the natural batch-like process with different consecutive steps, transferring chromatography into a continuous process is a challenge, and needs creative approaches, often based on multi-column set-ups.

2.1. Periodic counter current chromatography

Periodic Counter Current (PCC) chromatography is so far the most developed continuous chromatography technique, containing of a minimum of 2 columns, for which several companies offer different commercial equipment set-ups. Besides the normal PCC design, several special approaches exist, such as sequential multi-column chromatography (SMCC) (Theoleyre, 2006; Ng et al., 2014; Girard et al., 2015), StepSMB (Grabski et al., 2014), CaptureSMB (Angarita et al., 2015) and BioSMB (Bisschops, 2014), differing in number of columns and column switching format. An overview of the current commercial available continuous chromatography systems has been recently provided (Somasundaram et al., 2018). Steinebach et al. (2016b) gives an excellent overview of different multi-column purification systems. Primarily used for capturing of antibodies using protein A affinity resins, the basic principle is relatively simple; a column is overloaded and the leaking flow through is used to load a second column. If the first column is completely loaded, the feed is directed to the second column and the leaking flow through is loaded on a third column. During the loading of the second and third column, the first column can be eluted and regenerated (Godawat et al., 2012; Mahajan et al., 2012). Multi-column PCC therefore usually outperforms batch-wise chromatography in terms of higher productivity and capacity utilization (Heeter and Liapis, 1995; Baur et al., 2016b, 2018) but is also lower in buffer consumption, has higher product concentration and requires smaller column volumes (Godawat et al., 2012; Mahajan et al., 2012; Angarita et al., 2015).

One obvious advantage of this system is that very high column loadings, approaching the static binding capacity limit, can be achieved. Furthermore, the residence time of the protein on the column can be decreased, leading to smaller required column sizes and less burden for sensitive molecules (Warikoo et al., 2012; Angarita et al., 2015). PCC can therefore overcome the dilemma of batch chromatography giving higher resin utilization for a

Table 1
Overview of different continuous purification processes used for purification of biopharmaceuticals or proteins and some process parameters where applicable.

Methods	Technology	Protein	Purity	Yield	Productivity	Reference
Extraction	packed differential contractors	IgG	84%	85%		Rosa et al. (2012)
	counter current mixer settler	IgG	99%	80%		Rosa et al. (2013)
	counter current mixer settler	IgG mAb	72%	95%		Eggersgluess et al. (2014)
	tubular separator	whey protein		90%		Vázquez-Villegas et al., 2011
	magnetic nano particle	A33 Fab	98%	70%		Fischer et al. (2013)
Precipitation	tubular reactor, TFF	mAbs	97%	95%		Burgstaller et al. (2019)
	CFIR	process impurities from IgG		90%	6–16 times higher	Kateja et al. (2016)
Virus inactivation	Flow through packed bed					Sencar et al. (2020)
	CFIR					David et al. (2019)
Refolding	CFIR	GCSF	84%		15 times higher	Sharma et al. (2016)
	4-Zone Simulated moving bed	Eddie fusion protein		100%	4.7 mg/lh	Wellhoefer et al. (2014)
Crystallization	air bubbled tubular reactor	lysozyme		68%	21 g/lh (0.72 g/h)	Neugebauer and Khinast (2015)
	oscillatory flow reactor	lysozyme		60%	3.8 g/lh	Yang et al. (2019)
	continuous stirred tank	mAb	96%	93%	6.4 g/lh	Hekmat et al. (2017)
Desalting/buffer exchange	counter current diafiltration	IgG		100%		Jabra et al. (2019)
	flow through chromatography	ScFV		99%	1.63 times higher	Walch and Jungbauer (2017)
Chromatography	8 column PCC (BIOSMB)	mAbs			50 g/lh	Gjoka et al. (2017)
	3 column CEX-PCC	GCSF			7.4 times higher	Kateja et al. (2017)
	3 column AEX-PCC	Lipase B	high	97%	12 g/lh	Brämer et al., 2018
	3 column IMAC-PCC	patchoulol synthase	98%	68%	1.1 g/lh	Brämer et al., 2019a
	2 column PCC (CaptureSMB)	mAbs		95%	44.8 g/lh	Sun et al. (2020)
	1 column continuous	mAbs	<55 ppm HCP		34 g/lh	Kamga et al. (2018)
	pH gradient 3-Zone SMB (HisTrap)	single chain Ab fragment	66%	91%	24 mg/lh	Martínez Cristancho and Seidel-Morgenstern, 2016
	SEC-SMB	influenca virus			3.8 times higher	Kröber et al., 2013
	4-Zone SEC-SMB refolding	Eddie fusion protein		100%	4.7 mg/lh	Wellhoefer et al. (2014)
	CCTC	mAbs		96%	140 g/lh	Fedorenko et al., 2020

specific yield, which in single-column formats can only be achieved by lowering the feed flow rate which itself reduces productivity (Baur et al., 2016a; Steinebach et al., 2016a). As shown in Eq. (1), the number of necessary columns N is based on the time needed to complete the different chromatographic steps (loading, washing, elution, regeneration, and equilibration) (Warikoo et al., 2012),

$$N > 2 + \frac{\tau_R C_f}{R_t K_S} \tag{1}$$

where τ_R is the elution-recover-regeneration time for one column, C_f the target concentration in the feed, R_t the target residence time and K_S the static or actual binding capacity. Reducing the total number of columns is generally favourable as it simplifies the process and also reduces the total number of valves, pumps, controlling devices etc. Most critical is therefore the loading time in relation to all other steps combined. In view of the fact that a small number of columns is favourable, it can be concluded from Eq. (1) that a long loading time, compared to the elution-recover-regeneration time, is beneficial. This can be achieved by either high column capacities or lower flow rates (Godawat et al., 2012; Angarita et al., 2015). A deeper theoretical description of the PCC process has been given elsewhere (Godawat et al., 2012).

While nearly all publications concerning PCC systems are focused on protein A capturing of monoclonal antibodies with reported productivities of $50 mg_{antibody} ml_{resin}^{-1} h^{-1}$ (Gjoka et al., 2017) the process itself is not limited to protein A affinity chromatography or affinity chromatography in general (Mahajan et al., 2012; Godawat et al., 2015; Gjoka et al., 2017; Somasundaram et al., 2018; Chiang et al., 2019). Few PCC processes other than protein A affinity chromatography have been described and reveal a high increase in productivity compared to batch processes. For example, Godawat et al. (2015) used a three column PCC with cation exchange (CEX) membranes as an intermediate step for mAbs. Recombinant proteins derived from *E. coli* have also been purified. Granulocyte colony stimulating factor (GCSF) has been purified by a 3-column CEX-PCC with 7.4-fold productivity increase (Kateja et al., 2017). *Candida antartica* lipase B purification by a 3-column AEX-PCC gave a 36% productivity increase (Brämer et al., 2018), and patchoulol synthase purification by a 3-column immobilized metal affinity PCC provided a 47% productivity increase (Brämer et al., 2019a). Productivity can be further increased by using disposable membrane columns as shown by Brämer et al. (2019b) using Sartobind® Q in a 4-column setup. Another benefit of the PCC system is that it can handle a constant feed flow if three or more columns are used.

If a semi continuous feed flow is sufficient, designs with less than 3 columns can be utilized, reducing investment costs. For example, 2-column PCC processes are investigated by Morbidelli et al. and commercially distributed by ChromaCon AG under the name CaptureSMB (Angarita et al., 2015; Baur et al., 2016a, 2019; Steinebach et al., 2016a; Feidl et al., 2020). During the process, the 2 columns are switched between an interconnected (IC) step and a batch step. During the interconnected step, the first column is loaded and the flow through is loaded onto the second column, then the feed is stopped and the columns are washed to remove impurities. Subsequently, during the batch step the first

column is eluted and regenerated, while the second column is loaded at a lower flow rate (Angarita et al., 2015). It has to be mentioned that the feed stream is processed semi-continuously as it is interrupted during washing and uses different flow rates between IC and batch step (Angarita et al., 2015). Another process with continuous and steady feed was developed with additional in-line feed during the interconnected wash step (Steinebach et al., 2016a; Karst et al., 2017). The process was used to purify antibodies from clarified CHO cell broth and showed better performance than batch production, e.g. 40% higher productivity (Baur et al., 2016a) and 2.5 times higher column capacity utilization (Steinebach et al., 2016a), which can be coupled with a continuous perfusion reactor (Karst et al., 2017). Reachable productivities are highly dependent on the feed concentration and model assisted predictions for twin column systems report values between 14 and $47 mg_{product} ml_{resin}^{-1} h^{-1}$ (Sun et al., 2020). The superior process is hard to judge as it is dependent on numerous variables such as resin utilization, productivity, buffer consumption, investment costs etc., but numerical simulations comparing the performance of batch, 2-/3- and 4-column PCC systems for antibody capturing showed that the 2-column PCC process is favourable for low ($c_{Feed} < 0.5$ mgml^{-1}) and high ($c_{Feed} > 5$ mgml^{-1}) feed concentrations, while 3-column PCC is favoured for medium feed concentrations (1.5 mgml^{-1} $< C_{Feed} <$ 2.5 mgml^{-1}) (Baur et al., 2016b). In general, using more columns in the loading zone lead to higher resin utilization, thus lead to better process performances. But as this benefit is also dependent on the feed concentration more columns are not necessary the most cost effective (Pagkaliwangan et al., 2019). Nonetheless, very few data are available to guide comparison of the different PCC processes, while productivity and resin utilization must also be accounted for, as well as investment costs, process complexity and development. Therefore, further research is required in this field to answer the question as to which process is favourable under certain conditions.

An interesting approach is the use of only 1 column coupled with a small hold tank to obtain a semi continuous capturing as described by (Kamga et al., 2018), who coupled a perfusion reactor with the developed one-column continuous chromatography (OCC) for continuous therapeutic antibody capturing using a protein A column. They obtained a productivity of $34 mg_{product} ml_{resin}^{-1} h^{-1}$ which is an increase of 72% compared to the productivity of $19.7 mg_{product} ml_{resin}^{-1} h^{-1}$ described by (Baur et al., 2016a) using the 2-column CaptureSMB process. By choosing very low flow rates, a high dynamic binding capacity could be achieved resulting in nearly 100% column capacity utilization. Another benefit of this method, is that it can be implemented with standard AKTAs and does not require investment in new equipment, which makes it economically strategic, particularly for academic research and smaller institutes with limited resources (Kamga et al., 2018).

2.2. Simulated moving bed chromatography

Simulated moving bed (SMB) is based on the fictional true moving bed (TMB) and imitates a counter current movement of the solid and liquid phase by valve switching (Aniceto and Silva, 2015). Conventional SMB processes consist of 4 zones as shown in Fig. 1, and are capable of splitting the feed stream in two elution streams, one containing the weaker adsorbed component and another the stronger adsorbed. The feed stream is applied between Zone II and III and loaded onto the column in Zone III. The stronger adsorbed component remains in the column longer, while the weaker adsorbed component travels faster through the column and can be collected between Zones III and IV, with another part of the product stream also loaded onto Zone IV. If the stronger adsorbed component reaches the end of Zone III, the columns are switched counter-clockwise and the former Zone III becomes Zone II. The eluent enters the system between Zone IV and I (opposite of the feed), and elutes the stronger adsorbed product in Zone I which can be collected between Zones I and II. However, new design approaches have been developed enabling more difficult separations, better performance, step gradients and tertiary separations (Beste and Arlt, 2002; Ströhlein et al., 2006; Wei et al., 2011; Kim et al., 2017).

An interesting concept for continuous purification is the 3-zone open loop SMB, which lacks Zone IV, comparing Fig. 1, and therefore does not recycle elution buffer but prevents cross contamination and enables new process designs with modulated solvent properties, for example the use of affinity and ion exchange (IEX) resins (Kessler et al., 2007; Martínez Cristancho and Seidel-Morgenstern, 2016; Fischer et al., 2018). An overview of the recent developments and process design is provided by Aniceto and Silva (2015), Seidel-Morgenstern et al. (2008) and Kim et al. (2017). However, SMB processes, particularly specially design configurations are equipment intensive and complicated to construct and therefore rarely described for the purification of biopharmaceuticals.

By modulating the solvent composition in different sections the process performance can be increased. For example, to improve IEX-SMB the salt concentration in Zones III and IV can be lowered and in Zones I and II can be raised. This so called salt gradient IEX-SMB was used to separate bovine serum albumin (BSA) and myoglobin (Houwing et al., 2002), lactoglobuline A and B (Wenkenborg et al., 2004) and IgG and lysozyme (Kessler et al., 2007). By modulating the zone composition, new purification strategies can be conducted as shown by Martínez Cristancho and Seidel-Morgenstern (2016), who purified histidine tagged single chain fragment antibodies from clarified cell broth using a three-zone pH-gradient SMB (HisTrap^{TM} HP columns) and obtained 11-times higher productivity ($24 mg_{product} l_{resin}^{-1} h^{-1}$) (Martínez Cristancho et al., 2013; Martínez Cristancho and Seidel-Morgenstern, 2016). It was also shown that influenza A virus particles can be continuously purified from cell culture by anion exchange monoliths with a 3-zone open loop SMB process, however, the productivity is nearly 50% lower compared to the batch process (Fischer et al., 2018). Nonetheless, this approach is highly interesting and should be further examined. The question arises, if a three-zone open loop SMB process with a modulated desorption zone has any benefits relative to a 3-column PCC process, as the processes are very similar, but the SMB process lacks the possibility to overload the first column and has therefore a lower resin utilization and is also more complex to construct. Further research should be done in this direction to establish the preferred approach.

Simulated moving bed processes are so far the only way of implementing Size Exclusion Chromatography (SEC) in a satisfactory continuous way. As biopharmaceutical proteins are often large molecules, or there is a need to separate aggregates or the need for a desalting process, the separation process can be seen as a pseudo binary mixture, for which size exclusion SMB is a suitable process. Influenza viruses could be separated from contaminating proteins, with a 3.8 times higher productivity in a three zone open loop SMB compared to a regular batch process (Kröber et al., 2013). Also plasmid DNA can be separated efficiently (Paredes et al., 2005). A quasi continuous design process with interrupted feed stream using only two size exclusion columns allowed the separation of adenovirus particles from clarified and concentrated cell broth. The process increased the productivity by six times and had a higher yield than the compared batch process (Nestola et al., 2014, 2015). Also, continuous desalting can be achieved by

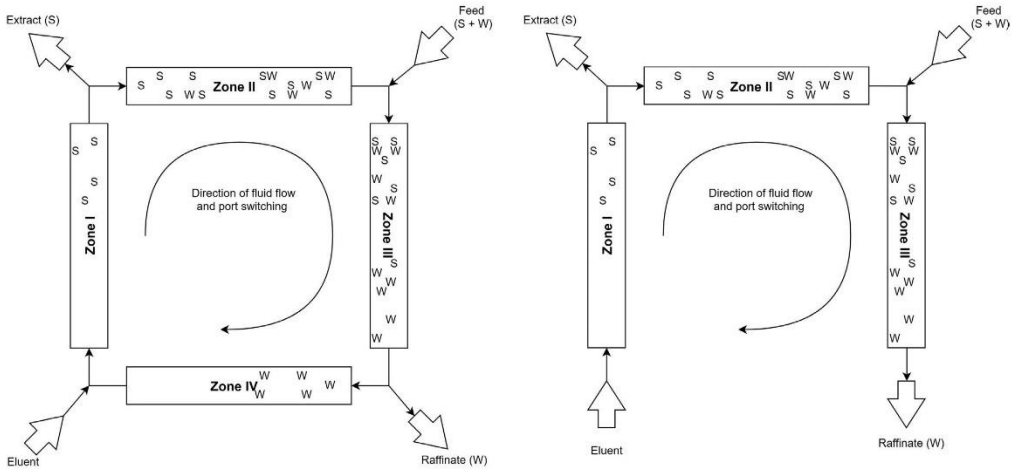

Fig. 1. Design of 4-Zone and 3-Zone Simulated moving bed processes. The stronger adsorbing component (S) remains longer on the column while the weaker adsorbing component (W) is travelling faster within the direction of the fluid flow. Zone IV is used to recycle the used buffer and is missing in the 3-Zone set up. The 3-Zone SMB process thus therefore has a higher buffer consumption but allows a broader range of process designs. The ports are switched periodically so that former Zone III becomes Zone II, former Zone II becomes Zone I, and so on.

a 3-column SMB, which was shown by (Hashimoto et al., 1988) who removed ammonium sulphate from a BSA solution. Simulated moving bed processes offer many advantages for continuous binary separations and therefore should be further examined in the production of biopharmaceuticals, especially the open loop three zone SMB seems to be suitable for biopharmaceuticals as the open loop design allow more separation techniques, no cross contamination and an easier process design.

2.3. Continuous flow-through chromatography

The most straight forward approach to obtain continuous chromatography is flow through or negative chromatography. By choosing appropriate conditions, the desired product shows no or minor interaction with the chromatographic resin and flows through the column, the impurities however are adsorbed to the column. Flow through chromatography by columns or membranes is widely used and described as a polishing step in different downstream processes (Godawat et al., 2015; Steinebach et al., 2017b). In an alternating twin column design, the first column can be washed and regenerated while the other one is used for the process, enabling a continuous process with a constant feed stream (Walch and Jungbauer, 2017). Transforming the process from batch to continuous is easy, as only minor adjustments such as a suitable column size and flow rate have to be made. Ichihara et al. (2018) proposed that antibodies and other proteins do neither bind to cation exchangers nor anion exchangers, and therefore can be purified by connected columns, if the pH and salt concentration are set correctly. This approach was used for polishing of antibodies after protein A capturing, obtaining high recoveries of more than 98% and sufficient removal of impurities (host cell protein (HCP), DNA, aggregates) (Ichihara et al., 2018; Yoshimoto et al., 2019). The process can be further intensified by adding an activated carbon column, which helps to remove HCP and DNA and requires no in-line pH adjustment or holding tanks (Ichihara et al., 2019). Of special interest is the process in combination with new porous resin materials that sterically hinder large molecules from accessing binding sites. Walch and Jungbauer (2017) showed a continuous desalting after refolding by combining a nano-porous cation and anion exchanger, which proteins could not access, and therefore removed salts but not proteins. This principle could also be used for the separation of very large biomolecules like virus like particles (VLPs) as new porous-bead resins like Capto Core™ have been developed. However, a satisfactory proof of concept has not been done so far. Although few publications address flow through chromatography only, it offers, especially in combination with new resins, many opportunities in continuous polishing and needs to be further evaluated. The straight forward process integration and scalability are two of the main reasons why this approach needs further attention.

Packed beds columns in flow through modus, are also a handy solution whenever defined reaction times are needed, due to the very narrow residence time distribution and fluid homogeneity over a broad design space inside those columns (Sencar et al., 2020b). Promising results were achieved for enzymatic digestion of IgG and virus inactivation under different conditions (Martins et al., 2019, 2020; Ulmer et al., 2019).

2.4. Further multi-column chromatographic concept designs

Besides the already mentioned processes, there are further continuous multi-column chromatographic processes, targeting special problems that are worth mentioning. The continuous multi-column counter current solvent gradient purification (MCSGP) process, shown in Fig. 2, is a process that combines SMB with a linear gradient elution, targeting the trade-off between purity and yield for centre-cut separation with overlapping peaks. The process adjusts the solvent conditions before every column in the tray by additional pumps and therefore enables a linear or step gradient over the process and furthermore enables internal recycling by having a recycle loop. Mostly used for continuous polishing steps on IEX resins, it can also be used as a capturing step (Müller-Späth et al., 2010a). The system contains 2, 3 or 6 columns, can be run continuously or semi-continuously, and the number of different molecules that can be separated depends on the number of used columns (Aumann and Morbidelli, 2007, 2008; Krättli et al.,

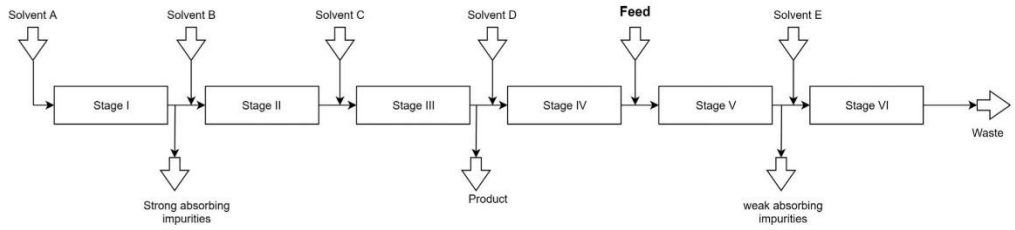

Fig. 2. Multicolumn counter current solvent gradient purification. In the open loop simulated moving bed process new solvent of different composition is added at every stage and thus a step gradient can be achieved over the process. Internal recycling loops can be introduced into the system to further improve the separation of hard-to-separate biomolecules.

2013; Steinebach et al., 2017a; Ulmer et al., 2019). Polishing of different charged isoforms of antibodies after protein A capture and the separation of a mixture of 4 model proteins (α-chymotrypsinogen, cytochrome *c*, lysozyme and avidin) were explored (Krättli et al., 2013; Steinebach et al., 2017a). Although higher yields and productivities for a given purity can be achieved, the MCSGP process does not always outperform the corresponding batch process in terms of productivity as finding the optimal process parameters is challenging (Aumann and Morbidelli, 2007; Müller-Späth et al., 2010b; Steinebach et al., 2017a; Vogg et al., 2019). As an example, for a given purity the purification of glucangon using a continuous 2-column MCSGP system achieved a 23% higher product recovery at a cost of 38% reduced productivity (de Luca et al., 2020). The process is therefore particularly suitable for polishing of high-value products, for which reducing product loss is more important than high productivity. Another approach is continuous counter-current tangential chromatography (CCTC) in which the resin is pumped in the form of a slurry through static mixers and hollow fibre membranes with a true counter current staging, as shown in Fig. 3. Each chromatographic step is represented by a number of mixers and membrane modules, enabling a counter-current flow. The process enables not only a continuous feeding but also a steady outlet stream with a constant product concentration which is unique compared to other multi column systems and opens new options for continuous process design (Napadensky et al., 2013; Dutta et al., 2015). Purification of antibodies from clarified CHO cell culture using protein A resins was shown with steady productivities of $140 g_{product} l_{resin}^{-1} h^{-1}$ and productivities up to $190 g_{product} l_{resin}^{-1}$ proposed as possible with this system. Also, post capture purification with mixed mode resins was demonstrated, achieving a magnitude higher productivity, showing that the process is capable of using different chromatographic resins. However, the process requires much higher amounts of buffer, nevertheless the buffer consumption is dependent on the counter-current stages per chromatographic step and can be decreased through further process design (Dutta et al., 2016, 2017; Fedorenko et al., 2020).

3. Continuous non-chromatographic approaches

Although chromatography remains the workhorse of biopharmaceutical purification, other approaches (e.g. extraction, precipitation, filtration and crystallization) can also be used for purification and are of high interest for integrated continuous processes, as enabling technologies for connecting unit operations, or as an alternative to chromatographic techniques if they are not applicable.

3.1. Continuous liquid-liquid extraction

Liquid-liquid extraction is a commonly-used process to extract and concentrate proteins or bioactive products (Oelmeier et al., 2011). Aqueous, two phase systems (ATPs) are the most common systems for liquid-liquid extraction, as organic solvent can denature the proteins and are therefore generally unsuitable for

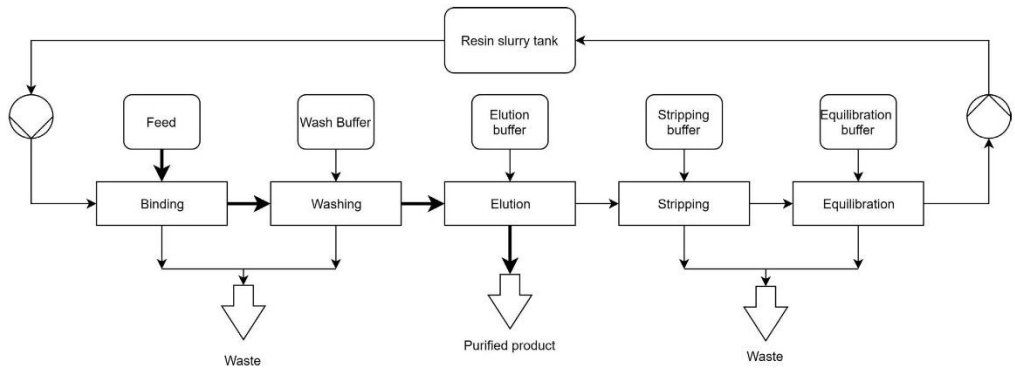

Fig. 3. Continuous counter-current tangential chromatography. The resin is recirculating as a slurry through the system. Every chromatographic step is represented by a number of mixers and membrane modules enabling the buffers to constantly flow round the resin. With this approach a constant and steady product stream can be achieved (Dutta et al., 2017).

biopharmaceuticals (Jungbauer, 2013). Different devices that can be separated into column contactors and mixer settle units are available for continuous processing of ATPs, each with their own advantages and disadvantages (Rosa et al., 2012; Espitia-Saloma et al., 2014). While the low interfacial tension and density difference of the phases allows fast phase mixing, phase separation remains the bottleneck for continuous ATPs extraction (Eggersgluess et al., 2014). Rosa et al. (2012) examined the performance of packed differential contractors for the continuous extraction of antibodies from a Chinese Hamster Ovary (CHO) cell supernatant with polyethylene glycol (PEG)-salt systems. For the construction of the process they chose the PEG rich phase as the dispersed phase as smaller droplets could be achieved. Furthermore, the dispersed phase should interact as little as possible with the packing surface to ensure an even flow. By determining the wetting properties of different metals and plastics, it was shown that plastics usually show a higher PEG rich phase interaction than steel. Regular stainless steel interacted the least and thus should be used as a packing material (Rosa et al., 2012). The same group reported impurity removal up to 99% and a yield of 80% using a 3-step process comprising a multi-stage extraction, back-extraction and washing for Immunoglobulin G (IgG) purification. This process was run in a continuous manner for several hours using standard counter-current mixer settler batteries (MSB) of 15 ml volume and flowrates of several hundred ml h^{-1}, which also enables a recycling of the used buffers (Rosa et al., 2013). Another study using only counter current extraction and no washing or back extraction achieved a purity of 46% for antibodies with 10 stages of cross-current mixer settler (Eggersgluess et al., 2014). High (78%) recovery of spiked IgG with cell supernatant was achieved with a 3-stage continuous mixer-settler configuration with recirculating loops (Espitia-Saloma et al., 2016). A further approach was the use of a tubular separator after an in-line mixer gaining product recovery up to 90% for whey protein extract as a model protein mixture (Vázquez-Villegas et al., 2011).

A possible advantage of ATPs is direct capturing from the supernatant or cell broth as ATPs are robust towards biomass, making a clarification step unnecessary (Rito-Palomares, 2004; Rosa et al., 2013). As an example C-phycocyanin was extracted continuously from crude extract in a coiled flow inversion reactor (CFIR) (Ruiz-Ruiz et al., 2019). However, as the physical principles of the partition behaviour remain unclear, the process development requires high experimental effort (Oelmeier et al., 2011; Torres-Acosta et al., 2019). Furthermore, sufficient purities can only be achieved with complicated multi-stage extractions, back extraction and washing, which negatively affects process economics. Thus, it is unlikely that continuous ATPs extraction of biopharmaceuticals will play an important role in the near future (González-Valdez et al., 2018). However, new developments in liquid-liquid extraction systems namely counter current chromatography (CCC) and centrifugal partition chromatography (CPC) addressing these issues and continuous separation modes have been developed, called sequential centrifugal partition chromatography (sCPC). Although these promising technologies are already used for plant derived pharmaceuticals applicability for biopharmaceuticals has yet to be examined (Hopmann et al., 2012; Oelmeier et al., 2012; Bojczuk et al., 2017; Morley and Minceva, 2019; Roehrer and Minceva, 2019).

Other extraction systems like three-phase-partition (TPP) systems and affinity enhanced ATPs have been developed in recent years. In TPP systems, a mixture of an alcohol and an aqueous solution forms two liquid layers and an intermediate layer with the desired precipitated product (Chew et al., 2019). Affinity-enhanced ATPs are systems with chemical modified polymers or alternative ligands, promising an increase and predictable selectivity of the systems (Azevedo et al., 2009). This opens up new possibilities for continuous separation as shown by Fischer et al. (2013) using functionalized magnetic nanoparticles in an aqueous micellar two-phase system to continuously separate antibody fragments from *E. coli* extract with purities above 98%.

3.2. Continuous precipitation

Precipitation offers an interesting approach for capturing of biopharmaceuticals, as it usually has a high yield of over 90% and is able to reduce process volume significantly in a single step. In contrast to crystallization, the influence of reaction time on the process outcome is insignificant (Hammerschmidt et al., 2014; Neugebauer and Khinast, 2015; van Alstine et al., 2018; Burgstaller et al., 2019). Hammerschmidt et al. (2014) examined the possibilities of precipitation in a continuous manner for the purification of antibodies and developed different processes. They compared a continuous process for mAbs using four precipitation steps (Caprylic acid, PEG, CaCl2 and cold ethanol) combined with a flow-through anion exchange (AEX) step and a standard chromatographic purification, and showed that the continuous process provides cost reduction at all scales. Continuous precipitation in a tubular reactor filled with static mixers produced the same results as a batch-wise precipitation in a stirred tank reactor (Hammerschmidt et al., 2015). It was shown that using continuous tangential flow filtration instead of centrifugation as a precipitate capture leads to similar results and even increases re-solubility (Hammerschmidt et al., 2016). Burgstaller et al. (2019) showed that the combination of a tubular reactor and tangential flow filtration enables constant mass flow with a steady product concentration. Furthermore, a second stage to their process was added, whereby the precipitate was washed with precipitation buffer continuously to further remove high-molecular-weight impurities, reporting an antibody purity level of 97%, while recovering 95% of the product. This combination of a tubular reactor linked to a continuous TFF system was also used for continuous IgG precipitation using $ZnCl_2$ instead of PEG as a precipitation agent. This approach lead to a lower viscosity compared to PEG precipitation, which positively affected filtration, and achieved yields of 70% (Dutra et al., 2020). Instead of feed and bleed tangential flow filtration to separate precipitated product, hollow fibre membranes were used in flow through mode to obtain an integrated continuous process without intermediate feed pumps and intervening hold steps, with mAb yields of 80% achieved (Li et al., 2019).

One major point that has to be considered when using tubular reactors, is the flow behaviour inside the channel. As low flow rates are usually used, a laminar flow regime can be assumed which leads to insufficient mixing and a broad residence-time distribution (Danckwerts, 1953, 1958). One solution to this problem is the use of static mixers inside the tubular reactor, which greatly increases radial mixing and uniformity of the reactant. However, it has been found that static mixers inside a tubular reactor trap small flocks of precipitate and accumulate them over time, causing insufficient mixing (Zelger et al., 2016). An alternative to a tubular reactor filled with static mixers is the coiled flow inversion reactor (CFIR). If a fluid flows through a helically-coiled tube the centrifugal forces, caused by the curvature of the tube, induce a secondary flow pattern, which forms Dean Vortices. These vortices induce mixing of the fluid inside the tube. In the CFIR, helically-coiled tubes are bent 90° several times, changing the direction of the centrifugal force inside of the tube and therefore inverting the flow in the tube. This inversion leads to a chaotic mixing of the liquid even at low Reynolds numbers and efficiently narrows the residence time distribution to be near plug flow (Saxena and Nigam, 1984; Kumar and Nigam, 2005; Mridha and Nigam, 2008). Kateja et al. (2016) showed a productivity increase of between 6 and 16 times, depending on the process, using a continuous CFIR for the

precipitation of process-related impurities from clarified cell culture supernatant containing monoclonal antibody (mAb). CFIR precipitation has also been integrated into a fully continuous process together with a cation exchange and a multi modal chromatography step to purify different antibodies from clarified CHO-cell supernatant (Kateja et al., 2018). It has furthermore been shown that CFIR reactors are suitable for other time-dependent reactions such as low-pH viral inactivation with inclusion into integrated continuous processes (David et al., 2019, 2020b, 2020a).

3.3. Continuous crystallization

Crystallization as a unit operation for biopharmaceuticals is proposed in the literature as an innovative alternative to chromatography in intermediate and polishing steps, and has been described for different products, such as therapeutic antibodies, aprotinin and other recombinant proteins (Peters et al., 2005; Takakura et al., 2006; Hebel et al., 2013; Smejkal et al., 2013; Hekmat et al., 2015). Protein crystals can be used as a way to store biopharmaceuticals as it protects the product from degradation, and is proposed as a better alternative in drug delivery (Basu et al., 2004; Peters et al., 2005). Yields of more than 85% and purities over 98% were achieved by using optimised batch stirred tanks (Hebel et al., 2013; Hekmat et al., 2015). The first continuous crystallization of protein was accomplished using a tubular reactor and lysozyme as a model protein (Neugebauer and Khinast, 2015). Air bubbles were introduced into a tubular reactor periodically to ensure a segmented flow, good mixing and a narrow residence time distribution despite laminar flow, required to ensure low shear forces. Three heating/cooling zones along the reactor were used to control the crystallization process. Although well-defined crystals with a narrow size distribution could be produced, there were only low process yields of 68% due to the limited residence time that could be achieved. Instead of using air bubbles to generate the desired flow behaviour, Yang et al. (2019a) used a continuous oscillatory flow reactor, which may also be beneficial for molecules that are sensitive to gas exposure. They suggested the use of the Reynolds-number to determine the process conditions for the scaling up from small scale batch shaking tube experiments to a continuous oscillating flow system. The applicability of oscillating reactors should be further examined, as they have well-defined mixing characteristics, are scalable and showed comparable results to stirred-tanks for refolding proteins (Smith, 2000; Lee et al., 2001). An alternative continuous reactor design was developed based on a stirred tank reactor and tested not only for lysozyme but also for full length monoclonal antibodies from a pre-treated clarified CHO cell culture supernatant (Hekmat et al., 2017). As shown in Fig. 4, the reactor is equipped with a cooled recirculating bypass system allowing two zones with different temperatures during the process to control the crystal formation. By placing the product removal on the bottom of the stirred tank reactor, only crystals reaching a certain size, and therefore sediment, are collected and discharged semi-continuously. It was demonstrated that it is possible to control crystal size and morphology in a continuous process with obtained yields of more than 90% and a doubled crystallization formation rate compared to batch wise processes, not only for lysozyme but also for monoclonal antibodies (Hekmat et al., 2017).

Ability to control nucleation, crystal growth, and formation of aggregates, coupled with a general lack of knowledge about protein crystallization, remain the major issues to be solved for the development of reliable continuous crystallization process. Incomplete mixing of the reaction solution can be considered as one of the main challenges that has to be addressed during the development of a continuous crystallization step, especially as the low shear forces of a laminar flow are desired. As the distribution of the molecules strongly affects the reaction kinetics, the agitation and flow pattern in a continuous reactor has a strong influence on crystallization processes and reliable strategies for up-scaling have to be developed (Danckwerts, 1958). Higher productivity continuous reactors also offer advantages for the introduction of new crystallization-promoting strategies including through the use of lasers, microwaves, magnetic and electric fields. These new modalities are conceivable as continuous reactors offer a larger surface-to-volume ratio of flow channels compared to conventional batch reactors (Li and Lakerveld, 2018).

3.4. Continuous protein refolding

Protein refolding is often a necessary step in bioprocessing for biopharmaceuticals expressed using the highly productive host cell *Escherichia coli*, if the product manifests as a solid inclusion body (Middelberg, 2002). With the advent of continuous flow cell-disruption systems (Tseng et al., 2019), continuous protein refolding takes on new potential.

Like crystallization, protein refolding is a time-dependent reaction. In tubular flow systems a well-mixed system with a narrow residence time distribution is required for a predictable and consistent continuous process (Danckwerts, 1958), while in batch chromatography systems there is some evidence that enhanced dispersion may actually be beneficial (Ding et al., 2008). Additionally, mixing in bulk liquid reactor systems strongly influences yield, with some evidence that the initial dispersion step is quite critical for both batch and oscillatory flow reactors (Lee et al., 2002).

In contrast to precipitation and crystallization, no insoluble material is desired to be formed during the process, and in fact the objective is to minimise non-productive protein aggregation (Buswell and Middelberg, 2002), allowing the use of a wide range of packed beds, like size exclusion columns, to optimise the flow systems and to achieve intensification also through matrix-enhanced refolding (Jungbauer et al., 2004; Langenhof et al., 2005; Machold et al., 2005; Basu and Leong, 2012). In general, during refolding the "correct" pathway competes with inter-molecular aggregation (Doglia et al., 2008; Ryś et al., 2015). In practical systems, one simple way to avoid adverse intermolecular interactions during protein refolding is to keep protein concentration low during the process, leading to large process volumes (Jungbauer and Kaar, 2007). For these systems a continuous process would be very beneficial in reducing the footprint and the overall cost of the process (Ferré et al., 2005; Schlegl et al., 2005b).

One of the earliest demonstrations of continuous protein refolding (Lanckriet and Middelberg, 2004) used a system known as preparative continuous annular chromatography (P-CAC), which relies on a mechanically moving bed. P-CAC was used to translate a batch SEC refolding process into a continuous one. As P-CAC shows a similar elution profile to batch, the translation is comparably simple and the resin loading can be increased by an order of magnitude, leading to lower buffer consumption and higher product concentrations, compared to the batch process. It was furthermore shown, that the aggregated fraction in a P-CAC system can be recycled to increase the yield significantly (Schlegl et al., 2005a). However, as P-CAC relies on a mechanically-rotating bed it is subject to some complexity in both design and operation.

An alternative approach is the use of size exclusion columns in a SMB set-up, which has been used for refolding of different proteins (Jungbauer et al., 2004). It could be shown that the SMB refolding process can be simulated with good agreement, from data obtained from batch processes, and the continuous process leads to an overall lower sample dilution compared to the batch process with SEC columns (Park et al., 2005; Saremirad et al., 2015). By using a 4-column 4-zone open loop SMB, Freydell et al. (2010) reported a

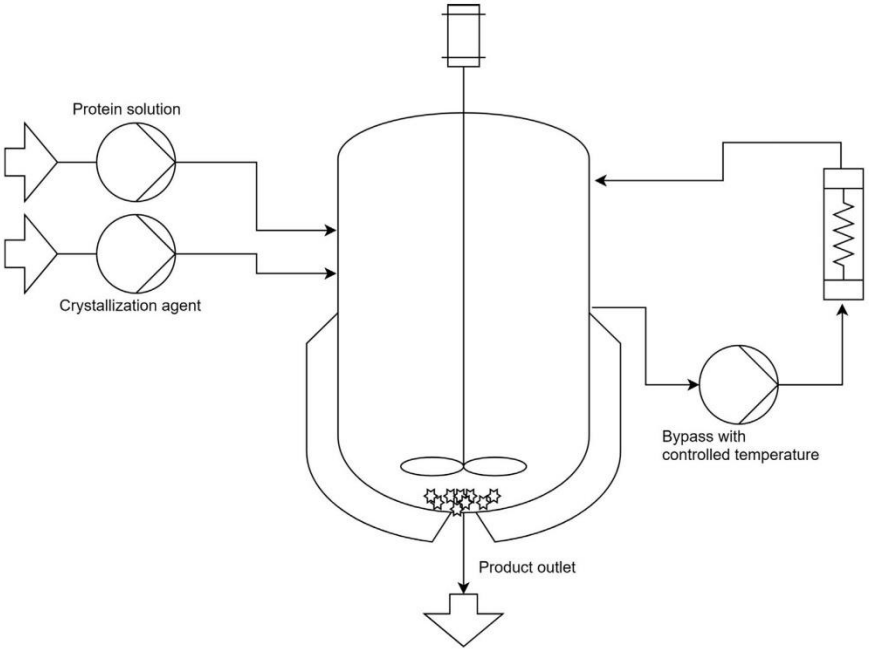

Fig. 4. Continuous stirred tank based crystallization reactor with cooled bypass to control the crystallization process. The temperature in the bypass and in the stir tank vessel can be controlled separately and optimised to nucleons forming and crystallization. If the crystals reach a minimum size, they sediment to the bottom of the vessel and can be harvested continuously. The minimum size of the crystals can be controlled by the agitation speed and geometrics of the stirred vessel (Hekmat et al., 2017).

53 times higher volumetric productivity with 90% less buffer consumption and a 4.5 times higher product concentration for refolding a protein expressed as inclusion bodies. If the SMB process is operated under isocratic conditions and the extraction phase contains the product of interest, the refolding/desorption buffer can be recycled by filtering it through a tangential flow filtration unit. This concept was shown by Wellhoefer et al. (2014) who combined two 4-Zoneclosed loop SMB, the first closed loop SMB for continuous refolding of inclusion bodies and the second for further purification of the auto-cleaved protein. High refolding buffer recycle of 99% was achieved and the overall combined process had a 180-fold higher productivity.

In other approaches a tubular reactor or a CFIR has been used. Both showed an increase in volumetric productivity over batch processes and the high volume to surface area also enabled accurate temperature control in large scale production (Pan et al., 2014; Sharma et al., 2016). Also, a continuous stirred tank reactor in combination with a tangential flow filtration was used to refold proteins in a continuous manner, however this set-up requires large and costly equipment (Schlegl et al., 2005b). Nevertheless, refolding by dialysis with ultrafiltration in some cases enables higher product concentration during refolding and is therefore particularly interesting (West et al., 1998; Yoshii et al., 2000; Zhao et al., 2014; Ryś et al., 2015). As new techniques for continuous filtration, described in Section 3.5 are developed, continuous refolding by ultrafiltration might be better enabled and should be further exploited.

Research on continuous refolding of therapeutic proteins seems to be under-represented in the literature, which might be because most complex therapeutic proteins are expressed in a soluble form. Two major design approaches have been studied. SEC-SMB systems show better process economics, while tubular reactors and CFIRs have a distinctively less-complex process design. Another possible reactor that has yet to be examined in detail for continuous refolding is the continuous oscillating reactor, although it has shown good performance for batch refolding (Lee et al., 2001). As continuous refolding could be an enabling technology for cheap *E. coli* derived biopharmaceuticals, especially as generics rise in importance, the capabilities of these systems and possible integration into continuous purification processes should be further explored.

3.5. Continuous filtration

As filtration enables separation based on molecular particle size, it is an important unit operation in the purification process of biopharmaceuticals and can be used for several different purposes. While microfiltration can be used to remove precipitates and other solids, protein solutions can be concentrated with ultrafiltration as a pre-treatment for further purification steps. Diafiltration is commonly used for buffer exchange between chromatographic steps, or to provide sufficient conditions for virus-like particle assembly, and as a formulation step while nanofiltration is used as a virus clearance step (Liew et al., 2012; Jungbauer, 2013; Rivera-Hernandez et al., 2013; Hekmat et al., 2017).

There are different ways to implement filter systems in a continuous manner within a process; an overview of different design strategies for filter systems is given by Jungbauer (2013). Dead-end filters can be easily integrated into the process in a parallel

manner, if one filter is blocked, the system switches to the next one and the blocked filter can be changed or washed, this however has no additional benefit despite a constant mass flow in the system. For insufficient separation or yield, several filter units can be connected into a cascade enabling higher purities and less buffer consumption due to a possible counter current flow. Cascades of filters can furthermore be used to separate complex mixtures into three product streams, each of them rich in another product of interest. So far, this has been applied to mixtures of oligosaccharides and insulin, but not for therapeutic proteins (Siew et al., 2013; Patil et al., 2015; Rizki et al., 2019). Burgstaller et al. (2019) used a standard tangential flow microfiltration with a recirculation loop to separate precipitated antibodies from cell broth, obtaining a constant mass flow. This was achieved using a constant feed rate and removal rate from the retention vessel, termed feed-and-bleed configuration. After 10 h of operating a steady state, constant mass flow was achieved. A very straight forward and promising method to implement continuous filtration is single pass tangential flow filtration (SPTFF). By increasing the filter area and contact time, the desired filtration can be achieved by only one passage, which also spares sensitive molecules as it requires only one pump pass and lower flow rates are used. In contrast to conventional tangential flow filtration (TFF), the product concentration and therefore the sieving coefficient change throughout the filter length (Arunkumar et al., 2018). SPTFF modules can be used as an inline concentrator, achieving concentration factors (CF) for bovine IgG solutions up to 25 times and product recoveries over 95% (Casey et al., 2011). This is of particular practical interest as it not only further reduces column loading times, but also to concentrates low titre cell culture harvest, avoiding large storage vessels (Arunkumar et al., 2017). Arunkumar et al. (2018) examined the retention and concentration behaviour of partially retained (lysozyme) and fully retained (mAb) proteins in SPTFF and compared it to normal TFF. The results indicate that the retention behaviour in SPTFF is complicated and cannot be described with models developed for TFF. Furthermore, an increase in pore size throughout the filter length leads to an increase in concentration behaviour. Several single pass tangential flow filtration modules can be combined with interim dilutions into a continuous single pass diafiltration (SPDF) process. The final concentration of a given component i can be described as

$$c_f^i = c_0^i \left(\frac{1}{X}\right)^n \tag{2}$$

where c_f^i is the final concentration of component i, c_0^i is the initial concentration,X is the dilution factor and n the number of stages. A process is therefore always a trade-off between system complexity (number of stages) and buffer consumption. Rucker-Pezzini et al. (2018) showed that a 3-stage SPDF can achieved buffer exchanges greater than 99.75% applied as a final step in a continuous mAb production, but with the trade-off of a distinctly higher buffer consumption compared to batch diafiltration. By installing a countercurrent system as shown in Fig. 5, the buffer consumption could be reduced significantly and impurity removal up to 99.9% was be achieved (Jabra et al., 2019). SPTFF seems to be a promising filtration technique for continuous downstream processing, especially due to its reduced process times and single pump pass, for large and sensitive biomolecules. In contrast to TFF with a recirculation loop, it does not require a minimal process volume and is therefore suitable for small-scale processes. But, there are still many questions to be answered, for example, retention and fouling behaviour has to be further examined and models must be developed, not only for mAb, but also for other biomolecules. Furthermore, the proposed positive influence on structural integrity must be proven and optimised, while a wider variety of filter membranes need to be developed (Jabra et al., 2019). In recent years an increasing number of functionalized membranes have been developed, combining classic chromatographic approaches like ion exchange chromatography with a convective flow pattern in a filter membrane, which ultimately leads to very high dynamic binding capacities.

Besides intensifying chromatography, functionalized membranes with a molecular weight cut-off open completely new design strategies. The unique combination of defined pore sizes and controllable surface properties enable the purification of biomolecules based on molecular size and charge selectivity in one step and external electric fields can further improve selectivity. As an alternative to a pressure-driven processes also electrodialysis cells can be used, called electrodialysis with filtration membranes (EDFM). Further research has to be done is this exciting new field which could lead filtration from a technique mostly used for buffer exchange and concentration to the key process during downstream processing. The simultaneous removal of aggregates and endotoxins in a polishing step or the direct processing of cell lysates are topics that could be addressed as well as continuous filter cascades for large scale purification systems. However, research in this area is still in its infancy and research on membrane design, purification capabilities and integration into continuous systems has to expand. Functionalized membranes with defined molecular weight cut-off can open a complete new research field and are as yet commercially unavailable (Bazinet and Firdaous, 2013; Henaux et al., 2019; Kadel et al., 2019).

4. Fully integrated processes and design considerations

The main objectives of continuous downstream processing are clearly an intensification of the process as well as a steady product quality for extended periods of time, with minimal product holdup in process. The full potential of continuity, however, can only be released if the full production is integrated into one robust and optimised continuous process. Only production lines in which all unit operations are integrated into one full continuous process offer the full advantages, such as: a completely closed process, which as a result does not require any special clean room housing for the machine; a short production time; no, or only small storage vessels and therefore a lower capital footprint, and; an extended operation duration and a reduced labour force. However, fully integrated processes are rarely described and usually use stirred tanks as holding vessels with buffer adjustments between the unit operations and are therefore not seamlessly integrated. The first published fully continuous production of recombinant antibodies was developed by Godawat et al. (2015) coupling a perfusion reactor with alternating tangential flow filtration (ATF) and two 4-column PCC processes (protein A capturing and CEX polishing) plus an AEX flow-through membrane, to obtain unformulated purified monoclonal antibody. They could achieve a steady product quality for more than 30 days operation and significantly decreased the equipment footprint and achieved more than 6 times higher productivity compared to batch processes. A similar set up was used by Gjoka et al. (2017) using two Cadence™ BioSMB (Sartorius) systems. They adapted a batch mAb purification platform for continuous operation and reported a several-folds increased productivity for protein A capturing, as well as for mixed-mode cation exchange chromatography, a 95% reduced resin volume and 44% less buffer consumption than the equivalent batch process (Gjoka et al., 2017). A reduction of the number of columns was shown by Steinebach et al. (2017b) by integrating a two column CaptureSMB process, a twin column MCSGP and a one-column flow-through polishing step into a fully integrated antibody production process, which results in a total of only 5 columns. The same group described a similar process in which a perfusion reactor was

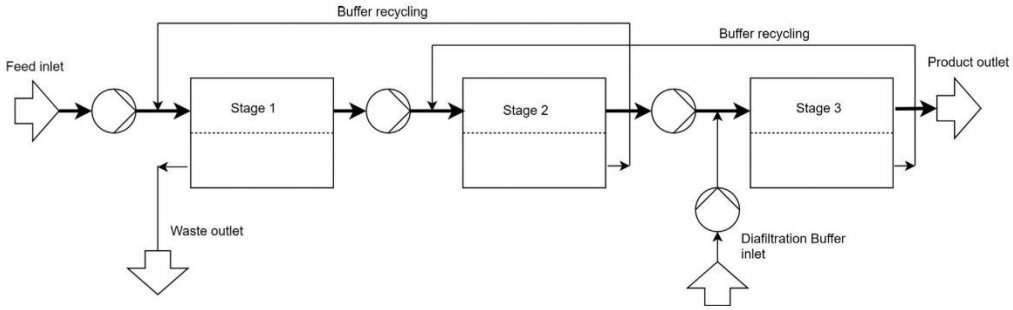

Fig. 5. Flow scheme of counter current single pass tangential flow diafiltration according to Jabra et al., (2019). In every stage a single pass tangential flow filtration occurs and the filtrate is recycled in the prior step by adding it to the feed stream in a counter-current manner. This set up does therefore only needs one inlet of fresh diafiltration buffer at the last stage and the buffer consumption can be reduced significantly.

coupled with a CaptureSMB process for continuous harvesting, followed by virus inactivation and a frontal analysis/flow through unit for final polishing (Feidl et al., 2020). A different process was used by Arnold et al. (2019), combining a 5-protein A column PCC capturing with a series of filters, membrane absorbers, a SPTFF and a SPDF to purify an antibody. Analysis of the cost of goods (COG) showed a cost reduction of 15% compared to commercial fed-batch facilities. In a fully continuous and automated downstream process run over 40 h it was recently shown that continuous production, compared to batch-wise production, does not affect the product quality negatively (David et al., 2020a).

It can be seen that a continuous downstream process can dramatically intensify the overall process, however it is a very challenging task to design such a process. The main advantage is thereby the integration of the different unit operations into one process and addressing the different buffer requirements during it. Often, downstream processes are developed from one step to the next one, until a working system is achieved and improvements are subsequently made by optimising each step, e.g. finding optimal binding conditions, flow rates etc. (Wheelwright, 1987). Design of experiment approaches using batch mode experiments can be used to develop efficient multi column chromatography processes (Utturkar et al., 2019). However, in order to design an optimal continuous process, a developed batch process cannot just be transferred by connecting the different continuous unit operations. Instead of focusing on optimal individual steps, the whole process must be seen as one; and efficiency of an individual step may be sacrificed for an overall better and easier process. Also, the slowest step will determine the throughput of the whole process. While the six classic heuristics for protein purification proposed by Scott Wheelwright e.g. 'the biggest step first', 'the most expensive step last' or 'keep it simple' are also true, specific characteristics have to be kept in mind (Wheelwright, 1987).

Chromatographic steps are challenging to integrate and are usually only semi-continuous. Therefore, alternative purification steps like crystallization, precipitation and filtration should be considered as a substitute. Buffer adjustments like pH and salt concentration should be always avoided between steps, ideally the outlet stream of one-unit operation can be directly used as a feed stream for the next unit operation. Flow through chromatography is a very straightforward and easy technique and by combining different resins in one train, high removals of impurities can be achieved as shown by Ichihara et al. (2018). A buffer can easily be changed during a chromatographic elution step and this can be used to prepare for the consecutive step. If an additional chromatographic step is required, instead of a salt gradient a pH shift might be suitable, or additives for crystallization and other reactions can be added (Schmidt et al., 2014).

A good example is the process developed by Kateja et al. (2017, 2018), used to purify antibodies and GCSF, consisting of a CFIR, that can be used for precipitation or protein refolding, followed by IEX-PCC and parallel IEX chromatography. The outlet streams are used as a feed stream of the consecutive step without any buffer adjustments and therefore the whole process was designed as an intensified process system, from the concept point onwards.

Finding an optimal process design, is however extremely challenging and time consuming and a trial-and-error approach might not find the optimal solution. Combining several unit operations and finding the overall best process conditions, keeping in mind the need for integration, might be impossible with only experimental methods. Model assisted process design will therefore play a crucial role in future, as it showed to accelerate and optimise development in the chemical industry and is widely used for smaller molecules. Mechanistic models, that are based on the physical fundamentals, are, in opposite to black-box models, predictive, even outside of their calibration range, do not require large amount of training data, and can be set up using small scale experiments. Therefore, they are ideally models for reliable process development. Such models have been developed for most unit operations, however, due to the complexity of some biologics grey-box models that combines data analytics and process understanding improve the accuracy (Hong et al., 2018). After characterizing different unit operations, digital twins can be created to predict different set-ups and find an overall optimal process in-silico, as shown by Nfor et al. (2013) for the optimization of batch chromatographic purification. Modelling all possible process designs with mechanistic models might be too complex to be practical, especially if many unit operations are considered. Speed-enhancing artificial neural networks coupled with mechanistic models has been shown able to optimise a multistep chromatographic purification and integrated processes. This is a very promising approach to find global optimums in processes with multiple unit operations, as is dramatically reduces the computational time (Pirrung et al., 2017, 2019). However, model based methods and total process descriptions are still seldom applied in the biopharmaceutical industry and in research, and further research has to be done as to how existing approaches can be adapted for continuous systems (Hong et al., 2018; Zobel-Roos et al., 2019).

5. Process analytical technology (PAT)

The FDA supports the implementation of continuous manufacturing processes which are defined as an integrated process of two or more unit operations, having a continuous inlet and outlet stream. Continuous systems are dynamic therefore critical process parameters must be controlled and kept in defined ranges (FDA, 2019). This is in particular challenging for bioprocessing as the inlet streams are often inconsistent and may vary over time. Also, resins can alter over extended run times, influencing overall process performance. Handling these inconsistencies requires advanced PAT and control strategies and can be considered as one of the main challenges that has to be solved to enable industrial implementation (Farid et al., 2014; Feidl et al., 2020). A deep understanding of the integrated process as well as of each unit operation is required to meet quality by design principles and to develop robust risk assessments (Elliott et al., 2013; FDA, 2019). Recently a possibility to model the residence time and mass flows inside an integrated continuous process was shown (Sencar et al., 2020a). Online monitoring of complex biological feed streams is complicated and the subject of current research. Deeper literature on this topic can be found elsewhere as complete discourse is beyond the scope of this current review (Read et al., 2010a, 2010b; Glassey et al., 2011; Rathore and Kapoor, 2015; Simon et al., 2015; Rüdt et al., 2017b; Holzberg et al., 2018). As continuous techniques evolve and further unit operations such as precipitation and crystallization are examined, appropriate PAT to monitor these systems has to be examined, and some recent development will be outlined.

Online spectroscopy such as UV-, near infrared-, and Raman spectroscopy has many advantages, as it enables real time monitoring, is non-destructive and comparably affordable (Esmonde-White et al., 2017; Kornecki and Strube, 2018). An overview of spectroscopy as a PAT technology in advanced downstream processing was published by Rüdt et al. (2017b). UV is widely used to determine protein concentration and can be used to dynamically control PCC systems by measuring the absorbance difference between column inlet and outlet. However, as impurities influence the absorbance this method is somewhat limited in complex and variant feed streams (Chmielowski et al., 2017). This limitation can be overcome by multi wavelength analysis combined with multivariate data analysis as shown by Rüdt et al. (2017a). As an alternative with better accuracy than UV, near infrared spectroscopy (NIR) was used to determine mAb concentrations and to control PCC capturing (Thakur et al., 2020). Raman spectroscopy can be used to monitor polymorphic transformation and was used to monitor continuous crystallization of carbamazepine and hence can be a powerful tool for biopharmaceuticals (Acevedo et al., 2018).

More information, such as product titre, charged variants and total protein content can be obtained by high-performance liquid chromatography (HPLC) within minutes (Fahrner and Blank, 1999; Escribà-Gelonch et al., 2018). At-line HPLC (Protein A, SEC) has been shown to be feasible to determine product titres, total protein concentration as well aggregate content before and after CaptureSMB processes. The data obtained was successfully used for model based control of the capturing process and to monitor performance during the process (Karst et al., 2017; Feidl et al., 2020). Continuous monitoring of charged variants at different stages of an integrated process by on-line HPLC was furthermore demonstrated (Patel et al., 2017). On-line HPLC is a very powerful tool, due to its easy implementation, commercial availability and a wide range of possible assays, however this comes at the cost of expensive equipment, data that is not truly provided in real time due to HPLC process time, and comparable high error-prone (Rüdt et al., 2017a).

Different in-line controlling of continuous precipitation has been examined, showing that conductivity sensors are more sensitive to monitoring buffer changes than pH sensors, mainly because of the possible buffering capacities (Zelger et al., 2016). They also compared in-line turbidity measurement and image processing and found that turbidity measurement is not a robust monitoring system due to high fluctuation of the signal and no quantitative resolution. Image processing on the other hand can characterize the precipitate into three different parameters (area, size and count) and can therefore be used to confirm the quality of the precipitate and is thus a possible monitoring system for future process control (Zelger et al., 2016). As image processing rapidly develops, this approach might also be applicable for continuous crystallization and suitability for batch crystallization has been proven (Borsos et al., 2017). Direct measurement of critical process parameters is often not possible, in this case soft sensors, that combine different available data to estimate process parameters, are a powerful way to obtain process data (Kornecki and Strube, 2018).

With many different tools available, the challenge is to identify the critical process parameter and control points, that have to be monitored within the integrated process. Another major challenge is how to use the obtained data to control the complex processes, taking into consideration feed variations and equipment altering. Digital twins and other model based control strategies will be the way to control these processes, as shown in some recent publications, but further research must be done in reliable and robust control strategies that take into account the many possible variations that can occur during the process (Nargund et al., 2019; Zobel-Roos et al., 2019; Feidl et al., 2020).

6. Conclusion and future outlook

More and more, research has been done on continuous downstream processing in recent years, addressing not only continuous affinity chromatography, but also other unit operations such as crystallization, precipitation and chromatographic polishing, incorporating the fact that every biopharmaceutical is different, and needs a unique purification process. Continuous production promises not only an overall cost reduction, but also faster production, higher productivity, less buffer consumption, a stable product quality and a lower footprint, while also offering greater flexibility for small-scale production. With a wider range of possible unit operations, it is now time for developing continuous processes for a variety of biopharmaceuticals and test different design strategies to find general platform technologies and design considerations. With integration as a key design criterion, we feel this process-system led approach to continuous biopharmaceutical processing will be a driver for future breakthroughs in advanced biomanufacturing. With new developed continuous processes research needs to focus on key challenges that hinder a broader application. Key areas that need to be addressed are process control and how to cope with unsteady product streams. Product titres may change over time and chromatographic unit operations produce product streams varying in concentration, which might influence subsequent unit operations and therefore require a continuous adaption. How can such a process be controlled? How to find the design space for a robust process? How can a continuous process line be validated and characterized? Which are critical control points that needs to be monitored and especially how can they be monitored? As there are only a few recent publications addressing these areas there is a big gap in knowledge (Feidl et al., 2020; Sencar et al., 2020a). Solving these problems will

require a deeper understanding of the underlying processes and is crucial to meet regulatory requirements, which can be considered as another major current challenge. Another big gap that needs to be addressed is the possibility to model continuous processes at different complexities. Reliable and easy to use models are required to analysis cost of goods at different scales. Deeper economic analysis is crucial for a broader acceptance in industry and only a few published works are available (Yang et al., 2019b; Cataldo et al., 2020). While simplified process models would help to set up and design continuous processes, more complex models of unit operations will help to find optimal design spaces, reduce start-up time to achieve steady-state, find strategies to scale-up, and may answer the question as to which combination of techniques is superior to any other. Model based approaches are particularly important as experiments are somewhat impractical due to the large number of possible process combinations and reaching even a pseudo steady state may take several hours. Model based approaches will also play a crucial role in future not only for process design, but also especially in process control. In-line data coupled with model predictive advanced control strategies are a possibility to implement quality by design and are necessary for reliable continuous processing. Those advanced control strategies and in-line sensors are yet to be developed. Nowadays a wide toolbox of mechanistic modelling, machine learning and grey-box models is available to cope with the complexity of biopharmaceuticals (Hong et al., 2018). For example, automated image and data processing coupled with a fluid dynamic description, could play a crucial role in the characterization of crystallization and precipitation processes.

Another area that should be tackled is the enormous process complexity that many of continuous processes have. Experts are rare and a wide acceptance can only be achieved if the processes are easy to set up and use, i.e. simple and robust. Despite a more user friendly experience less complex process-systems are often not only easier to control but also more robust. Keeping it simple and robust, with system design in mind from conception onwards, will be increasingly important for the future success and uptake of continuous bioprocessing.

CRediT authorship contribution statement

Lukas Gerstweiler: Conceptualization, Writing - original draft, Writing - review & editing. **Jingxiu Bi:** Writing - review & editing, Supervision. **Anton P.J. Middelberg:** Conceptualization, Writing - review & editing, Supervision.

Declaration of Competing Interest

The authors declare that they have no known competing financial interests or personal relationships that could have appeared to influence the work reported in this paper.

References

Acevedo, D., Yang, X., Mohammad, A., Pavurala, N., Wu, W.-L., O'Connor, T.F., Nagy, Z.K., Cruz, C.N., 2018. Raman spectroscopy for monitoring the continuous crystallization of carbamazepine. Org. Process Res. Dev. 22 (2), 156–165. https://doi.org/10.1021/acs.oprd.7b00322.

Angarita, M., Müller-Späth, T., Baur, D., Lievrouw, R., Lissens, G., Morbidelli, M., 2015. Twin-column CaptureSMB: a novel cyclic process for protein A affinity chromatography. J. Chromatogr. A 1389, 85–95. https://doi.org/10.1016/j.chroma.2015.02.046.

Aniceto, J.P.S., Silva, C.M., 2015. Simulated moving bed strategies and designs: from established systems to the latest developments. Sep. Purif. Rev. 44 (1), 41–73. https://doi.org/10.1080/15422119.2013.851087.

Arnold, L., Lee, K., Rucker-Pezzini, J., Lee, J.H., 2019. Implementation of fully integrated continuous antibody processing: effects on productivity and COGm. Biotechnol. J. 14 (2), e1800061. https://doi.org/10.1002/biot.201800061.

Arunkumar, A., Singh, N., Peck, M., Borys, M.C., Li, Z.J., 2017. Investigation of single-pass tangential flow filtration (SPTFF) as an inline concentration step for cell culture harvest. J. Membr. Sci. 524, 20–32. https://doi.org/10.1016/j.memsci.2016.11.007.

Arunkumar, A., Zhang, J., Singh, N., Ghose, S., Li, Z.J., 2018. Ultrafiltration behaviour of partially retained proteins and completely retained proteins using equally-staged single pass tangential flow filtration membranes. Biotechnol. Prog. 34 (5), 1137–1148. https://doi.org/10.1002/btpr.2671.

Aumann, L., Morbidelli, M., 2007. A continuous multicolumn countercurrent solvent gradient purification (MCSGP) process. Biotechnol. Bioeng. 98 (5), 1043–1055. https://doi.org/10.1002/bit.21527.

Aumann, L., Morbidelli, M., 2008. A semicontinuous 3-column countercurrent solvent gradient purification (MCSGP) process. Biotechnol. Bioeng. 99 (3), 728–733. https://doi.org/10.1002/bit.21585.

Azevedo, A.M., Rosa, P.A.J., Ferreira, I.F., Pisco, A.M.M.O., de Vries, J., Korporaal, R., Visser, T.J., Aires-Barros, M.R., 2009. Affinity-enhanced purification of human antibodies by aqueous two-phase extraction. Sep. Purif. Technol. 65 (1), 31–39. https://doi.org/10.1016/j.seppur.2008.03.006.

Basu, A., Leong, S.S.J., 2012. High productivity chromatography refolding process for Hepatitis B Virus X (HBx) protein guided by statistical design of experiment studies. J. Chromatogr. A 1223, 64–71. https://doi.org/10.1016/j.chroma.2011.12.037.

Basu, S.K., Govardhan, C.P., Jung, C.W., Margolin, A.L., 2004. Protein crystals for the delivery of biopharmaceuticals. Expert Opin. Biol. Ther. 4 (3), 301–317. https://doi.org/10.1517/14712598.4.3.301.

Baur, D., Angarita, M., Müller-Späth, T., Morbidelli, M., 2016a. Optimal model-based design of the twin-column CaptureSMB process improves capacity utilization and productivity in protein A affinity capture. Biotechnol. J. 11 (1), 135–145. https://doi.org/10.1002/biot.201500223.

Baur, D., Angarita, M., Müller-Späth, T., Steinebach, F., Morbidelli, M., 2016b. Comparison of batch and continuous multi-column protein A capture processes by optimal design. Biotechnol. J. 11 (7), 920–931. https://doi.org/10.1002/biot.201500481.

Baur, D., Angelo, J., Chollangi, S., Müller-Späth, T., Xu, X., Ghose, S., Li, Z.J., Morbidelli, M., 2019. Model-assisted process characterization and validation for a continuous two-column protein A capture process. Biotechnol. Bioeng. 116 (1), 87–98. https://doi.org/10.1002/bit.26849.

Baur, D., Angelo, J.M., Chollangi, S., Xu, X., Müller-Späth, T., Zhang, N., Ghose, S., Li, Z. J., Morbidelli, M., 2018. Model assisted comparison of Protein A resins and multi-column chromatography for capture processes. J. Biotechnol. 285, 64–73. https://doi.org/10.1016/j.jbiotec.2018.08.014.

Bazinet, L., Firdaous, L., 2013. Separation of bioactive peptides by membrane processes: technologies and devices. Recent Pat. Biotechnol. 7 (1), 9–27. https://doi.org/10.2174/1872208311307010003.

Beste, Y.A., Arlt, W., 2002. Side-stream simulated moving-bed chromatography for multicomponent separation. Chem. Eng. Technol. 25 (10), 956–962. https://doi.org/10.1002/1521-4125(20021008)25:10<956:AID-CEAT956>3.0.CO;2-7.

Bisschops, M., 2014. BioSMB Technology as an Enabler for a Fully Continuous Disposable Biomanufacturing Platform, in: Subramanian, G. (Ed.), Continuous Processing in Pharmaceutical Manufacturing, vol. 16. Wiley-VCH Verlag GmbH & Co. KGaA, Weinheim, Germany, pp. 35–52.

Bojczuk, M., Żyżelewicz, D., Hodurek, P., 2017. Centrifugal partition chromatography – a review of recent applications and some classic references. J. Sep. Sci. 40 (7), 1597–1609. https://doi.org/10.1002/jssc.201601221.

Borsos, Á., Szilágyi, B., Agachi, P.Ş., Nagy, Z.K., 2017. Real-time image processing based online feedback control system for cooling batch crystallization. Org. Process Res. Dev. 21 (4), 511–519. https://doi.org/10.1021/acs.oprd.6b00242.

Brämer, C., Ekramzadeh, K., Lammers, F., Scheper, T., Beutel, S., 2019a. Optimization of continuous purification of recombinant patchoulol synthase from Escherichia coli with membrane adsorbers. Biotechnol. Prog. e2812. https://doi.org/10.1002/btpr.2812.

Brämer, C., Lammers, F., Scheper, T., Beutel, S., 2019b. Development and testing of a 4-columns periodic counter-current chromatography system based on membrane adsorbers. Separations 6 (4), 55. https://doi.org/10.3390/separations6040055.

Brämer, C., Schreiber, S., Scheper, T., Beutel, S., 2018. Continuous purification of Candida antarctica lipase B using 3-membrane adsorber periodic counter-current chromatography. Eng. Life Sci. 18 (7), 414–424. https://doi.org/10.1002/elsc.201700159.

Burgstaller, D., Jungbauer, A., Satzer, P., 2019. Continuous integrated antibody precipitation with two-stage tangential flow microfiltration enables constant mass flow. Biotechnol. Bioeng. 116 (5), 1053–1065. https://doi.org/10.1002/bit.26922.

Buswell, A.M., Middelberg, A.P.J., 2002. Critical analysis of lysozyme refolding kinetics. Biotechnol. Prog. 18 (3), 470–475. https://doi.org/10.1021/bp0200189.

Casey, C., Gallos, T., Alekseev, Y., Ayturk, E., Pearl, S., 2011. Protein concentration with single-pass tangential flow filtration (SPTFF). J. Membr. Sci. 384 (1–2), 82–88. https://doi.org/10.1016/j.memsci.2011.09.004.

Cataldo, A.L., Burgstaller, D., Hribar, G., Jungbauer, A., Satzer, P., 2020. Economics and ecology: modelling of continuous primary recovery and capture scenarios for recombinant antibody production. J. Biotechnol. 308, 87–95. https://doi.org/10.1016/j.jbiotec.2019.12.001.

Chew, K.W., Ling, T.C., Show, P.L., 2019. Recent developments and applications of three-phase partitioning for the recovery of proteins. Sep. Purif. Rev. 48 (1), 52–64. https://doi.org/10.1080/15422119.2018.1427596.

Chiang, M.-J., Pagkaliwangan, M., Lute, S., Bolton, G., Brorson, K., Schofield, M., 2019. Validation and optimization of viral clearance in a downstream continuous chromatography setting. Biotechnol. Bioeng. https://doi.org/10.1002/bit.27023.
Chmielowski, R.A., Mathiasson, L., Blom, H., Go, D., Ehring, H., Khan, H., Li, H., Cutler, C., Lacki, K., Tugcu, N., Roush, D., 2017. Definition and dynamic control of a continuous chromatography process independent of cell culture titer and impurities. J. Chromatogr. A 1526, 58–69. https://doi.org/10.1016/j.chroma.2017.10.030.
Danckwerts, P.V., 1953. Continuous flow systems. Chem. Eng. Sci. 2 (1), 1–13. https://doi.org/10.1016/0009-2509(53)80001-1.
Danckwerts, P.V., 1958. The effect of incomplete mixing on homogeneous reactions. Chem. Eng. Sci. 8 (1–2), 93–102. https://doi.org/10.1016/0009-2509(58)80040-8.
David, L., Maiser, B., Lobedann, M., Schwan, P., Lasse, M., Ruppach, H., Schembecker, G., 2019. Virus study for continuous low pH viral inactivation inside a coiled flow inverter. Biotechnol. Bioeng. 116 (4), 857–869. https://doi.org/10.1002/bit.26872.
David, L., Schwan, P., Lobedann, M., Borchert, S.-O., Budde, B., Temming, M., Kuerschner, M., Alberti Aguilo, F.M., Baumarth, K., Thüte, T., Maiser, B., Blank, A., Kistler, V., Weber, N., Brandt, H., Poggel, M., Kaiser, K., Geisen, K., Oehme, F., Schembecker, G., 2020a. Side-by-side comparability of batch and continuous downstream for the production of monoclonal antibodies. Biotechnol. Bioeng. 117 (4), 1024–1036. https://doi.org/10.1002/bit.27267.
David, L., Waldschmidt, L.M., Lobedann, M., Schembecker, G., 2020b. Simulation of pH level distribution inside a coiled flow inverter for continuous low pH viral inactivation. Biotechnol. Bioeng. 117 (2), 429–437. https://doi.org/10.1002/bit.27201.
Ding, Y., He, L., Middelberg, A.P.J., 2008. Dispersion-enhanced chromatography refolding of denatured protein. Chem. Eng. Sci. 63 (17), 4333–4341. https://doi.org/10.1016/j.ces.2008.05.034.
Doglia, S.M., Ami, D., Natalello, A., Gatti-Lafranconi, P., Lotti, M., 2008. Fourier transform infrared spectroscopy analysis of the conformational quality of recombinant proteins within inclusion bodies. Biotechnol. J. 3 (2), 193–201. https://doi.org/10.1002/biot.200700238.
Dutra, G., Komuczki, D., Jungbauer, A., Satzer, P., 2020. Continuous capture of recombinant antibodies by ZnCl 2 precipitation without polyethylene glycol. Eng. Life Sci. 20 (7), 265–274. https://doi.org/10.1002/elsc.201900160.
Dutta, A.K., Fedorenko, D., Tan, J., Costanzo, J.A., Kahn, D.S., Zydney, A.L., Shinkazh, O., 2017. Continuous countercurrent tangential chromatography for mixed mode post-capture operations in monoclonal antibody purification. J. Chromatogr. A 1511, 37–44. https://doi.org/10.1016/j.chroma.2017.06.018.
Dutta, A.K., Tan, J., Napadensky, B., Zydney, A.L., Shinkazh, O., 2016. Performance optimization of continuous countercurrent tangential chromatography for antibody capture. Biotechnol. Prog. 32 (2), 430–439. https://doi.org/10.1002/btpr.2250.
Dutta, A.K., Tran, T., Napadensky, B., Teella, A., Brookhart, G., Ropp, P.A., Zhang, A.W., Tustian, A.D., Zydney, A.L., Shinkazh, O., 2015. Purification of monoclonal antibodies from clarified cell culture fluid using Protein A capture continuous countercurrent tangential chromatography. J. Biotechnol. 213, 54–64. https://doi.org/10.1016/j.jbiotec.2015.02.026.
Eggersgluess, J.K., Richter, M., Dieterle, M., Strube, J., 2014. Multi-stage aqueous two-phase extraction for the purification of monoclonal antibodies. Chem. Eng. Technol. 37 (4), 675–682. https://doi.org/10.1002/ceat.201300604.
Elliott, P., Billingham, S., Bi, J., Zhang, H., 2013. Quality by design for biopharmaceuticals: a historical review and guide for implementation. Pharmac. Bioprocess. 1 (1), 105–122. https://doi.org/10.4155/pbp.13.6.
Escribà-Gelonch, M., Shahbazali, E., Honing, M., Hessel, V., 2018. Quality-In(Process) Line (QuIProLi) process intensification for a micro-flow UV-photo synthesis enabled by online UHPLC analysis. Tetrahedron 74 (25), 3143–3151. https://doi.org/10.1016/j.tet.2018.02.016.
Esmonde-White, K.A., Cuellar, M., Uerpmann, C., Lenain, B., Lewis, I.R., 2017. Raman spectroscopy as a process analytical technology for pharmaceutical manufacturing and bioprocessing. Anal. Bioanal. Chem. 409 (3), 637–649. https://doi.org/10.1007/s00216-016-9824-1.
Espitia-Saloma, E., Vázquez-Villegas, P., Aguilar, O., Rito-Palomares, M., 2014. Continuous aqueous two-phase systems devices for the recovery of biological products. Food Bioprod. Process. 92 (2), 101–112. https://doi.org/10.1016/j.fbp.2013.05.006.
Espitia-Saloma, E., Vâzquez-Villegas, P., Rito-Palomares, M., Aguilar, O., 2016. An integrated practical implementation of continuous aqueous two-phase systems for the recovery of human IgG: from the microdevice to a multistage bench-scale mixer-settler device. Biotechnol. J. 11 (5), 708–716. https://doi.org/10.1002/biot.201400565.
Fahrner, R.L., Blank, G.S., 1999. Real-time control of antibody loading during protein A affinity chromatography using an on-line assay. J. Chromatogr. A 849 (1), 191–196. https://doi.org/10.1016/S0021-9673(99)00539-7.
Farid, S.S., Thompson, B., Davidson, A., 2014. Continuous bioprocessing: the real thing this time? 10(th) Annual bioProcessUK Conference, December 3–4, 2013, London, UK. mAbs 6 (6), 1357–1361. https://doi.org/10.4161/mabs.36151.
FDA, 2019. Quality Considerations for Continuous Manufacturing Guidance for Industry. URL: <https://www.fda.gov/media/121314/download>.
Fedorenko, D., Dutta, A.K., Tan, J., Walko, J., Brower, M., Pinto, N.D.S., Zydney, A.L., Shinkazh, O., 2020. Improved protein A resin for antibody capture in a continuous countercurrent tangential chromatography system. Biotechnol. Bioeng. 117 (3), 646–653. https://doi.org/10.1002/bit.27232.
Feidl, F., Vogg, S., Wolf, M., Podobnik, M., Ruggeri, C., Ulmer, N., Wälchli, R., Souquet, J., Broly, H., Butté, A., Morbidelli, M., 2020. Process-wide control and automation of an integrated continuous manufacturing platform for antibodies. Biotechnol. Bioeng. 117 (5), 1367–1380. https://doi.org/10.1002/bit.27296.
Ferré, H., Ruffet, E., Nielsen, L.-L.B., Nissen, M.H., Hobley, T.J., Thomas, O.R.T., Buus, S., 2005. A novel system for continuous protein refolding and on-line capture by expanded bed adsorption. Protein Sci.: Publ. Protein Soc. 14 (8), 2141–2153. https://doi.org/10.1110/ps.051396105.
Fischer, I., Hsu, C.-C., Gärtner, M., Müller, C., Overton, T.W., Thomas, O.R.T., Franzreb, M., 2013. Continuous protein purification using functionalized magnetic nanoparticles in aqueous micellar two-phase systems. J. Chromatogr. A 1305, 7–16. https://doi.org/10.1016/j.chroma.2013.06.011.
Fischer, L.M., Wolff, M.W., Reichl, U., 2018. Purification of cell culture-derived influenza A virus via continuous anion exchange chromatography on monoliths. Vaccine 36 (22), 3153–3160. https://doi.org/10.1016/j.vaccine.2017.06.086.
Fisher, A.C., Kamga, M.-H., Agarabi, C., Brorson, K., Lee, S.L., Yoon, S., 2019. The current scientific and regulatory landscape in advancing integrated continuous biopharmaceutical manufacturing. Trends Biotechnol. 37 (3), 253–267. https://doi.org/10.1016/j.tibtech.2018.08.008.
Frank, G.T., 2018. Transformation of biomanufacturing by single-use systems and technology. Curr. Opin. Chem. Eng. 22, 62–70. https://doi.org/10.1016/j.coche.2018.09.006.
Freydell, E.J., Bulsink, Y., van Hateren, S., van der Wielen, L., Eppink, M., Ottens, M., 2010. Size-exclusion simulated moving bed chromatographic protein refolding. Chem. Eng. Sci. 65 (16), 4701–4713. https://doi.org/10.1016/j.ces.2010.05.023.
Girard, V., Hilbold, N.-J., Candy, K.S., Pegon, L., Chahim, W., Rousset, F., Monchois, V., 2015. Large-scale monoclonal antibody purification by continuous chromatography, from process design to scale-up. J. Biotechnol. 213, 65–73. https://doi.org/10.1016/j.jbiotec.2015.04.026.
Gjoka, X., Gantier, R., Schofield, M., 2017. Transfer of a three step mAb chromatography process from batch to continuous: optimizing productivity to minimize consumable requirements. J. Biotechnol. 242, 11–18. https://doi.org/10.1016/j.jbiotec.2016.12.005.
Glassey, J., Gernaey, K.V., Clemens, C., Schulz, T.W., Oliveira, R., Striedner, G., Mandenius, C.-F., 2011. Process analytical technology (PAT) for biopharmaceuticals. Biotechnol. J. 6 (4), 369–377. https://doi.org/10.1002/biot.201000356.
Godawat, R., Brower, K., Jain, S., Konstantinov, K., Riske, F., Warikoo, V., 2012. Periodic counter-current chromatography—design and operational considerations for integrated and continuous purification of proteins. Biotechnol. J. 7 (12), 1496–1508. https://doi.org/10.1002/biot.201200068.
Godawat, R., Konstantinov, K., Rohani, M., Warikoo, V., 2015. End-to-end integrated fully continuous production of recombinant monoclonal antibodies. J. Biotechnol. 213, 13–19. https://doi.org/10.1016/j.jbiotec.2015.06.393.
González-Valdez, J., Mayolo-Deloisa, K., Rito-Palomares, M., 2018. Novel aspects and future trends in the use of aqueous two-phase systems as a bioengineering tool. J. Chem. Technol. Biotechnol. 93 (7), 1836–1844. https://doi.org/10.1002/jctb.5434.
Grabski, A., Zilberman, A., van Oosbree, T., Mierendorf, R., 2014. Bench top continuous chromatography: an enabling platform for highly productive mAb purification. Integrated Continuous Biomanufacturing Conference.
Hammerschmidt, N., Hintersteiner, B., Lingg, N., Jungbauer, A., 2015. Continuous precipitation of IgG from CHO cell culture supernatant in a tubular reactor. Biotechnol. J. 10 (8), 1196–1205. https://doi.org/10.1002/biot.201400608.
Hammerschmidt, N., Hobiger, S., Jungbauer, A., 2016. Continuous polyethylene glycol precipitation of recombinant antibodies: Sequential precipitation and resolubilization. Process Biochem. 51 (2), 325–332. https://doi.org/10.1016/j.procbio.2015.11.032.
Hammerschmidt, N., Tscheliessnig, A., Sommer, R., Helk, B., Jungbauer, A., 2014. Economics of recombinant antibody production processes at various scales: Industry-standard compared to continuous precipitation. Biotechnol. J. 9 (6), 766–775. https://doi.org/10.1002/biot.201300480.
Hashimoto, K., Adachi, S., Shirai, Y., 1988. Continuous desalting of proteins with a simulated moving-bed adsorber. Agric. Biol. Chem. 52 (9), 2161–2167. https://doi.org/10.1271/bbb1961.52.2161.
Hebel, D., Huber, S., Stanislawski, B., Hekmat, D., 2013. Stirred batch crystallization of a therapeutic antibody fragment. J. Biotechnol. 166 (4), 206–211. https://doi.org/10.1016/j.jbiotec.2013.05.010.
Heeter, G.A., Liapis, A.I., 1995. Perfusion chromatography: performance of periodic countercurrent column operation and its comparison with fixed-bed operation. J. Chromatogr. A 711 (1), 3–21. https://doi.org/10.1016/0021-9673(95)00013-D.
Hekmat, D., Breitschwerdt, P., Weuster-Botz, D., 2015. Purification of proteins from solutions containing residual host cell proteins via preparative crystallization. Biotechnol. Lett. 37 (9), 1791–1801. https://doi.org/10.1007/s10529-015-1866-5.
Hekmat, D., Huber, M., Lohse, C., den Eichen von, N., Weuster-Botz, D., 2017. Continuous crystallization of proteins in a stirred classified product removal tank with a tubular reactor in bypass. Cryst. Growth Des. 17 (8), 4162–4169. https://doi.org/10.1021/acs.cgd.7b00436.
Henaux, L., Thibodeau, J., Pilon, G., Gill, T., Marette, A., Bazinet, L., 2019. How charge and triple size-selective membrane separation of peptides from salmon protein hydrolysate orientate their biological response on glucose uptake. Int. J. Mol. Sci. 20 (8). https://doi.org/10.3390/ijms20081939.
Holzberg, T.R., Watson, V., Brown, S., Andar, A., Ge, X., Kostov, Y., Tolosa, L., Rao, G., 2018. Sensors for biomanufacturing process development: facilitating the shift

from batch to continuous manufacturing. Curr. Opin. Chem. Eng. 22, 115–127. https://doi.org/10.1016/j.coche.2018.09.008.
Hong, M.S., Severson, K.A., Jiang, M., Lu, A.E., Love, J.C., Braatz, R.D., 2018. Challenges and opportunities in biopharmaceutical manufacturing control. Comput. Chem. Eng. 110, 106–114. https://doi.org/10.1016/j.compchemeng.2017.12.007.
Hopmann, E., Goll, J., Minceva, M., 2012. Sequential centrifugal partition chromatography: a new continuous chromatographic technology. Chem. Eng. Technol. 35 (1), 72–82. https://doi.org/10.1002/ceat.201100266.
Houwing, J., van Hateren, S.H., Billiet, H.A.H., van der Wielen, L.A.M., 2002. Effect of salt gradients on the separation of dilute mixtures of proteins by ion-exchange in simulated moving beds. J. Chromatogr. A 952 (1–2), 85–98. https://doi.org/10.1016/S0021-9673(02)00091-2.
Hummel, J., Pagkaliwangan, M., Gjoka, X., Davidovits, T., Stock, R., Ransohoff, T., Gantier, R., Schofield, M., 2019. Modeling the downstream processing of monoclonal antibodies reveals cost advantages for continuous methods for a broad range of manufacturing scales. Biotechnol. J. 14 (2), e1700665. https://doi.org/10.1002/biot.201700665.
Ichihara, T., Ito, T., Gillespie, C., 2019. Polishing approach with fully connected flow-through purification for therapeutic monoclonal antibody. Eng. Life Sci. 19 (1), 31–36. https://doi.org/10.1002/elsc.201800123.
Ichihara, T., Ito, T., Kurisu, Y., Galipeau, K., Gillespie, C., 2018. Integrated flow-through purification for therapeutic monoclonal antibodies processing. mAbs 10 (2), 325–334. https://doi.org/10.1080/19420862.2017.1417717.
Jabra, M.G., Yehl, C.J., Zydney, A.L., 2019. Multistage continuous countercurrent diafiltration for formulation of monoclonal antibodies. Biotechnol. Prog. e2810. https://doi.org/10.1002/btpr.2810.
Jacoby, R., Heim, M., Pernenkil, L., Sabad, A., Harutunian, S., 2015. Advanced Biopharmaceutical Manufacturing: An Evolution Underway. Deloitte, May.
Jungbauer, A., 2013. Continuous downstream processing of biopharmaceuticals. Trends Biotechnol. 31 (8), 479–492. https://doi.org/10.1016/j.tibtech.2013.05.011.
Jungbauer, A., Kaar, W., 2007. Current status of technical protein refolding. J. Biotechnol. 128 (3), 587–596. https://doi.org/10.1016/j.jbiotec.2006.12.004.
Jungbauer, A., Kaar, W., Schlegl, R., 2004. Folding and refolding of proteins in chromatographic beds. Curr. Opin. Biotechnol. 15 (5), 487–494. https://doi.org/10.1016/j.copbio.2004.08.009.
Kadel, S., Pellerin, G., Thibodeau, J., Perreault, V., Lainé, C., Bazinet, L., 2019. How molecular weight cut-offs and physicochemical properties of polyether sulfone membranes affect peptide migration and selectivity during electrodialysis with filtration membranes. Membranes 9 (11). https://doi.org/10.3390/membranes9110153.
Kamga, M.-H., Cattaneo, M., Yoon, S., 2018. Integrated continuous biomanufacturing platform with ATF perfusion and one column chromatography operation for optimum resin utilization and productivity. Prep. Biochem. Biotech. 48 (5), 383–390. https://doi.org/10.1080/10826068.2018.1446151.
Karst, D.J., Steinebach, F., Soos, M., Morbidelli, M., 2017. Process performance and product quality in an integrated continuous antibody production process. Biotechnol. Bioeng. 114 (2), 298–307. https://doi.org/10.1002/bit.26069.
Kateja, N., Agarwal, H., Hebbi, V., Rathore, A.S., 2017. Integrated continuous processing of proteins expressed as inclusion bodies: GCSF as a case study. Biotechnol. Prog. 33 (4), 998–1009. https://doi.org/10.1002/btpr.2413.
Kateja, N., Agarwal, H., Saraswat, A., Bhat, M., Rathore, A.S., 2016. Continuous precipitation of process related impurities from clarified cell culture supernatant using a novel coiled flow inversion reactor (CFIR). Biotechnol. J. 11 (10), 1320–1331. https://doi.org/10.1002/biot.201600271.
Kateja, N., Kumar, D., Sethi, S., Rathore, A.S., 2018. Non-protein A purification platform for continuous processing of monoclonal antibody therapeutics. J. Chromatogr. A 1579, 60–72. https://doi.org/10.1016/j.chroma.2018.10.031.
Kessler, L.C., Gueorguieva, L., Rinas, U., Seidel-Morgenstern, A., 2007. Step gradients in 3-zone simulated moving bed chromatography. Application to the purification of antibodies and bone morphogenetic protein-2. J. Chromatogr. A 1176 (1–2), 69–78. https://doi.org/10.1016/j.chroma.2007.10.087.
Kim, K.-M., Lee, J.W., Kim, S., Santos da Silva, F.V., Seidel-Morgenstern, A., Lee, C.-H., 2017. Advanced operating strategies to extend the applications of simulated moving bed chromatography. Chem. Eng. Technol. 40 (12), 2163–2178. https://doi.org/10.1002/ceat.201700206.
Konstantinov, K.B., Cooney, C.L., 2015. White paper on continuous bioprocessing May 20–21 2014 continuous manufacturing symposium. J. Pharm. Sci. 104 (3), 813–820. https://doi.org/10.1002/jps.24268.
Kornecki, M., Strube, J., 2018. Process analytical technology for advanced process control in biologics manufacturing with the aid of macroscopic kinetic modeling. Bioengineering (Basel, Switzerland) 5 (1). https://doi.org/10.3390/bioengineering5010025.
Krättli, M., Müller-Späth, T., Morbidelli, M., 2013. Multifraction separation in countercurrent chromatography (MCSGP). Biotechnol. Bioeng. 110 (9), 2436–2444. https://doi.org/10.1002/bit.24901.
Kröber, T., Wolff, M.W., Hundt, B., Seidel-Morgenstern, A., Reichl, U., 2013. Continuous purification of influenza virus using simulated moving bed chromatography. J. Chromatogr. A 1307, 99–110. https://doi.org/10.1016/j.chroma.2013.07.081.
Kumar, V., Nigam, K.D.P., 2005. Numerical simulation of steady flow fields in coiled flow inverter. Int. J. Heat Mass Transf. 48 (23–24), 4811–4828. https://doi.org/10.1016/j.ijheatmasstransfer.2005.05.037.
Kunert, R., Reinhart, D., 2016. Advances in recombinant antibody manufacturing. Appl. Microbiol. Biotechnol. 100 (8), 3451–3461. https://doi.org/10.1007/s00253-016-7388-9.
Lanckriet, H., Middelberg, A.P.J., 2004. Continuous chromatographic protein refolding. J. Chromatogr. A 1022 (1–2), 103–113. https://doi.org/10.1016/j.chroma.2003.09.013.
Langenhof, M., Leong, S.S.J., Pattenden, L.K., Middelberg, A.P.J., 2005. Controlled oxidative protein refolding using an ion-exchange column. J. Chromatogr. A 1069 (2), 195–201. https://doi.org/10.1016/j.chroma.2005.01.063.
Lee, C.T., Buswell, A.M., Middelberg, A.P.J., 2002. The influence of mixing on lysozyme renaturation during refolding in an oscillatory flow and a stirred-tank reactor. Chem. Eng. Sci. 57 (10), 1679–1684. https://doi.org/10.1016/S0009-2509(02)00066-0.
Lee, C.T., Mackley, M.R., Stonestreet, P., Middelberg, A.P.J., 2001. Biotechnol. Lett. 23 (22), 1899–1901. https://doi.org/10.1023/A:1012734214751.
Li, F., Lakerveld, R., 2018. Electric-field-assisted protein crystallization in continuous flow. Cryst. Growth Des. 18 (5), 2964–2971. https://doi.org/10.1021/acs.cgd.8b00095.
Li, Z., Gu, Q., Coffman, J.L., Przybycien, T., Zydney, A.L., 2019. Continuous precipitation for monoclonal antibody capture using countercurrent washing by microfiltration. Biotechnol. Prog. 35 (6), e2886. https://doi.org/10.1002/btpr.2886.
Liew, M.W.O., Chuan, Y.P., Middelberg, A.P.J., 2012. Reactive diafiltration for assembly and formulation of virus-like particles. Biochem. Eng. J. 68, 120–128. https://doi.org/10.1016/j.bej.2012.07.009.
de Luca, C., Felletti, S., Lievore, G., Buratti, A., Vogg, S., Morbidelli, M., Cavazzini, A., Catani, M., Macis, M., Ricci, A., Cabri, W., 2020. From batch to continuous chromatographic purification of a therapeutic peptide through multicolumn countercurrent solvent gradient purification. J. Chromatogr. A 1625, 461304. https://doi.org/10.1016/j.chroma.2020.461304.
Theoleyre, M.A., 2006. Multicolumn Sequential Separation Process: WO US20090209736A1.
Machold, C., Schlegl, R., Buchinger, W., Jungbauer, A., 2005. Matrix assisted refolding of proteins by ion exchange chromatography. J. Biotechnol. 117 (1), 83–97. https://doi.org/10.1016/j.jbiotec.2005.01.004.
Mahajan, E., George, A., Wolk, B., 2012. Improving affinity chromatography resin efficiency using semi-continuous chromatography. J. Chromatogr. A 1227, 154–162. https://doi.org/10.1016/j.chroma.2011.12.106.
Martínez Cristancho, C.A., David, F., Franco-Lara, E., Seidel-Morgenstern, A., 2013. Discontinuous and continuous purification of single-chain antibody fragments using immobilized metal ion affinity chromatography. J. Biotechnol. 163 (2), 233–242. https://doi.org/10.1016/j.jbiotec.2012.08.022.
Martínez Cristancho, C.A., Seidel-Morgenstern, A., 2016. Purification of single-chain antibody fragments exploiting pH-gradients in simulated moving bed chromatography. J. Chromatogr. A 1434, 29–38. https://doi.org/10.1016/j.chroma.2016.01.001.
Martins, D.L., Sencar, J., Hammerschmidt, N., Flicker, A., Kindermann, J., Kreil, T.R., Jungbauer, A., 2020. Truly continuous low pH viral inactivation for biopharmaceutical process integration. Biotechnol. Bioeng. 117 (5), 1406–1417. https://doi.org/10.1002/bit.27292.
Martins, D.L., Sencar, J., Hammerschmidt, N., Tille, B., Kinderman, J., Kreil, T.R., Jungbauer, A., 2019. Continuous solvent/detergent virus inactivation using a packed-bed reactor. Biotechnol. J. 14 (8), e1800646. https://doi.org/10.1002/biot.201800646.
Middelberg, A.P.J., 2002. Preparative protein refolding. Trends Biotechnol. 20 (10), 437–443. https://doi.org/10.1016/S0167-7799(02)02047-4.
Mordor Intelligence, 2019. Biopharmaceuticals Market – Growth, Trends, and Forecast (2019–2024). Hyderabad, India.
Morley, R., Minceva, M., 2019. Operating mode and parameter selection in liquid-liquid chromatography. J. Chromatogr. A 460479. https://doi.org/10.1016/j.chroma.2019.460479.
Mridha, M., Nigam, K.D.P., 2008. Coiled flow inverter as an inline mixer. Chem. Eng. Sci. 63 (6), 1724–1732. https://doi.org/10.1016/j.ces.2007.10.028.
Müller-Späth, T., Aumann, L., Ströhlein, G., Kornmann, H., Valax, P., Delegrange, L., Charbaut, E., Baer, G., Lamproye, A., Jöhnck, M., Schulte, M., Morbidelli, M., 2010a. Two step capture and purification of IgG2 using multicolumn countercurrent solvent gradient purification (MCSGP). Biotechnol. Bioeng. 107 (6), 974–984. https://doi.org/10.1002/bit.22887.
Müller-Späth, T., Krättli, M., Aumann, L., Ströhlein, G., Morbidelli, M., 2010b. Increasing the activity of monoclonal antibody therapeutics by continuous chromatography (MCSGP). Biotechnol. Bioeng. 107 (4), 652–662. https://doi.org/10.1002/bit.22843.
Napadensky, B., Shinkazh, O., Teella, A., Zydney, A.L., 2013. Continuous countercurrent tangential chromatography for monoclonal antibody purification. Sep. Sci. Technol. 48 (9), 1289–1297. https://doi.org/10.1080/01496395.2013.767837.
Nargund, S., Guenther, K., Mauch, K., 2019. The move toward biopharma 4.0. Genetic Eng. Biotechnol. News 39 (6), 53–55. https://doi.org/10.1089/gen.39.06.18.
Nestola, P., Silva, R.J.S., Peixoto, C., Alves, P.M., Carrondo, M.J.T., Mota, J.P.B., 2014. Adenovirus purification by two-column, size-exclusion, simulated countercurrent chromatography. J. Chromatogr. A 1347, 111–121. https://doi.org/10.1016/j.chroma.2014.04.079.
Nestola, P., Silva, R.J.S., Peixoto, C., Alves, P.M., Carrondo, M.J.T., Mota, J.P.B., 2015. Robust design of adenovirus purification by two-column, simulated moving-bed, size-exclusion chromatography. J. Biotechnol. 213, 109–119. https://doi.org/10.1016/j.jbiotec.2015.01.030.

Neugebauer, P., Khinast, J.G., 2015. Continuous crystallization of proteins in a tubular plug-flow crystallizer. Cryst. Growth Des. 15 (3), 1089–1095. https://doi.org/10.1021/cg501359h.
Nfor, B.K., Ahamed, T., van Dedem, G.W.K., Verhaert, P.D.E.M., van der Wielen, L.A. M., Eppink, M.H.M., van de Sandt, E.J.A.X., Ottens, M., 2013. Model-based rational methodology for protein purification process synthesis. Chem. Eng. Sci. 89, 185–195. https://doi.org/10.1016/j.ces.2012.11.034.
Ng, C.K.S., Rousset, F., Valery, E., Bracewell, D.G., Sorensen, E., 2014. Design of high productivity sequential multi-column chromatography for antibody capture. Food Bioprod. Process. 92 (2), 233–241. https://doi.org/10.1016/j.fbp.2013.10.003.
Oelmeier, S.A., Dismer, F., Hubbuch, J., 2011. Application of an aqueous two-phase systems high-throughput screening method to evaluate mAb HCP separation. Biotechnol. Bioeng. 108 (1), 69–81. https://doi.org/10.1002/bit.22900.
Oelmeier, S.A., Ladd Effio, C., Hubbuch, J., 2012. High throughput screening based selection of phases for aqueous two-phase system-centrifugal partitioning chromatography of monoclonal antibodies. J. Chromatogr. A 1252, 104–114. https://doi.org/10.1016/j.chroma.2012.06.075.
Pagkaliwangan, M., Hummel, J., Gjoka, X., Bisschops, M., Schofield, M., 2019. Optimized continuous multicolumn chromatography enables increased productivities and cost savings by employing more columns. Biotechnol. J. 14 (2), e1800179. https://doi.org/10.1002/biot.201800179.
Pan, S., Zelger, M., Hahn, R., Jungbauer, A., 2014. Continuous protein refolding in a tubular reactor. Chem. Eng. Sci. 116, 763–772. https://doi.org/10.1016/j.ces.2014.06.002.
Paredes, G., Makart, S., Stadler, J., Mazzotti, M., 2005. Simulated moving bed operation for size exclusion plasmid purification. Chem. Eng. Technol. 28 (11), 1335–1345. https://doi.org/10.1002/ceat.200500119.
Park, B.-J., Lee, C.-H., Koo, Y.-M., 2005. Development of novel protein refolding using simulated moving bed chromatography. Korean J. Chem. Eng. 22 (3), 425–432. https://doi.org/10.1007/BF02719422.
Patel, B.A., Pinto, N.D.S., Gospodarek, A., Kilgore, B., Goswami, K., Napoli, W.N., Desai, J., Heo, J.H., Panzera, D., Pollard, D., Richardson, D., Brower, M., Richardson, D.D., 2017. On-line ion exchange liquid chromatography as a process analytical technology for monoclonal antibody characterization in continuous bioprocessing. Anal. Chem. 89 (21), 11357–11365. https://doi.org/10.1021/acs.analchem.7b02228.
Patil, N.V., Feng, X., Sewalt, J.J.W., Boom, R.M., Janssen, A.E.M., 2015. Separation of an inulin mixture using cascaded nanofiltration. Sep. Purif. Technol. 146, 261–267. https://doi.org/10.1016/j.seppur.2015.03.061.
Peters, J., Minuth, T., Schröder, W., 2005. Implementation of a crystallization step into the purification process of a recombinant protein. Protein Expr. Purif. 39 (1), 43–53. https://doi.org/10.1016/j.pep.2004.09.011.
Pirrung, S.M., Berends, C., Backx, A.H., van Beckhoven, R.F.W.C., Eppink, M.H.M., Ottens, M., 2019. Model-based optimization of integrated purification sequences for biopharmaceuticals. Chem. Eng. Sci.: X 3, 100025. https://doi.org/10.1016/j.cesx.2019.100025.
Pirrung, S.M., van der Wielen, L.A.M., van Beckhoven, R.F.W.C., van de Sandt, E.J.A.X., Eppink, M.H.M., Ottens, M., 2017. Optimization of biopharmaceutical downstream processes supported by mechanistic models and artificial neural networks. Biotechnol. Prog. 33 (3), 696–707. https://doi.org/10.1002/btpr.2435.
Rathore, A.S., Kapoor, G., 2015. Application of process analytical technology for downstream purification of biotherapeutics. J. Chem. Technol. Biotechnol. 90 (2), 228–236. https://doi.org/10.1002/jctb.4447.
Read, E.K., Park, J.T., Shah, R.B., Riley, B.S., Brorson, K.A., Rathore, A.S., 2010a. Process analytical technology (PAT) for biopharmaceutical products: Part I. concepts and applications. Biotechnol. Bioeng. 105 (2), 276–284. https://doi.org/10.1002/bit.22528.
Read, E.K., Shah, R.B., Riley, B.S., Park, J.T., Brorson, K.A., Rathore, A.S., 2010b. Process analytical technology (PAT) for biopharmaceutical products: Part II. Concepts and applications. Biotechnol. Bioeng. 105 (2), 285–295. https://doi.org/10.1002/bit.22529.
Rito-Palomares, M., 2004. Practical application of aqueous two-phase partition to process development for the recovery of biological products. J. Chromatogr., B: Anal. Technol. Biomed. Life Sci. 807 (1), 3–11. https://doi.org/10.1016/j.jchromb.2004.01.008.
Rivera-Hernandez, T., Hartas, J., Wu, Y., Chuan, Y.P., Lua, L.H.L., Good, M., Batzloff, M. R., Middelberg, A.P.J., 2013. Self-adjuvanting modular virus-like particles for mucosal vaccination against group A streptococcus (GAS). Vaccine 31 (15), 1950–1955. https://doi.org/10.1016/j.vaccine.2013.02.013.
Rizki, Z., Janssen, A.E.M., Boom, R.M., van der Padt, A., 2019. Oligosaccharides fractionation cascades with 3 outlet streams. Sep. Purif. Technol. 221, 183–194. https://doi.org/10.1016/j.seppur.2019.03.086.
Roehrer, S., Minceva, M., 2019. Evaluation of inter-apparatus separation method transferability in countercurrent chromatography and centrifugal partition chromatography. Separations 6 (3), 36. https://doi.org/10.3390/separations6030036.
Rosa, P.A.J., Azevedo, A.M., Sommerfeld, S., Bäcker, W., Aires-Barros, M.R., 2012. Continuous aqueous two-phase extraction of human antibodies using a packed column. J. Chromatogr., B: Anal. Technol. Biomed. Life Sci. 880 (1), 148–156. https://doi.org/10.1016/j.jchromb.2011.11.034.
Rosa, P.A.J., Azevedo, A.M., Sommerfeld, S., Mutter, M., Bäcker, W., Aires-Barros, M. R., 2013. Continuous purification of antibodies from cell culture supernatant with aqueous two-phase systems: from concept to process. Biotechnol. J. 8 (3), 352–362. https://doi.org/10.1002/biot.201200031.
Rucker-Pezzini, J., Arnold, L., Hill-Byrne, K., Sharp, T., Avazhanskiy, M., Forespring, C., 2018. Single pass diafiltration integrated into a fully continuous mAb purification process. Biotechnol. Bioeng. 115 (8), 1949–1957. https://doi.org/10.1002/bit.26708.
Rüdt, M., Brestrich, N., Rolinger, L., Hubbuch, J., 2017a. Real-time monitoring and control of the load phase of a protein A capture step. Biotechnol. Bioeng. 114 (2), 368–373. https://doi.org/10.1002/bit.26078.
Rüdt, M., Briskot, T., Hubbuch, J., 2017b. Advances in downstream processing of biologics – spectroscopy: an emerging process analytical technology. J. Chromatogr. A 1490, 2–9. https://doi.org/10.1016/j.chroma.2016.11.010.
Ruiz-Ruiz, F., López-Guajardo, E., Vázquez-Villegas, P., del Angel-Chong, M.E., Nigam, K.D.P., Willson, R.C., Rito-Palomares, M., 2019. Continuous aqueous two-phase extraction of microalgal C-phycocyanin using a coiled flow inverter. Chem. Eng. Process. – Process Intensification 142, 107554. https://doi.org/10.1016/j.cep.2019.107554.
Ryś, S., Muca, R., Kołodziej, M., Piątkowski, W., Dürauer, A., Jungbauer, A., Antos, D., 2015. Design and optimization of protein refolding with crossflow ultrafiltration. Chem. Eng. Sci. 130, 290–300. https://doi.org/10.1016/j.ces.2015.03.035.
Sanofi, 2019. Sanofi begins global digital enhancement manufacturing porject. URL: <http://www.news.sanofi.us/2019-10-15-Sanofi-opens-its-first-digitally-enabled-continuous-manufacturing-facility-ushers-in-next-generation-of-biotech-manufacturing#assets_all> (accessed 23 July 2020).
Saremirad, P., Wood, J.A., Zhang, Y., Ray, A.K., 2015. Oxidative protein refolding on size exclusion chromatography: from batch single-column to multi-column counter-current continuous processing. Chem. Eng. Sci. 138, 375–384. https://doi.org/10.1016/j.ces.2015.08.031.
Saxena, A.K., Nigam, K.D.P., 1984. Coiled configuration for flow inversion and its effect on residence time distribution. AIChE J. 30 (3), 363–368. https://doi.org/10.1002/aic.690300303.
Schlegl, R., Necina, R., Jungbauer, A., 2005a. Continuous matrix-assisted refolding of inclusion-body proteins: effect of recycling. Chem. Eng. Technol. 28 (11), 1375–1386. https://doi.org/10.1002/ceat.200500121.
Schlegl, R., Tscheliessnig, A., Necina, R., Wandl, R., Jungbauer, A., 2005b. Refolding of proteins in a CSTR. Chem. Eng. Sci. 60 (21), 5770–5780. https://doi.org/10.1016/j.ces.2005.04.086.
Schmidt, M., Hafner, M., Frech, C., 2014. Modeling of salt and pH gradient elution in ion-exchange chromatography. J. Sep. Sci. 37 (1–2), 5–13. https://doi.org/10.1002/jssc.201301007.
Seidel-Morgenstern, A., Keßler, L.C., Kaspereit, M., 2008. New developments in simulated moving bed chromatography. Chem. Eng. Technol. 31 (6), 826–837. https://doi.org/10.1002/ceat.200800081.
Sencar, J., Hammerschmidt, N., Jungbauer, A., 2020a. Modeling the residence time distribution of integrated continuous bioprocesses. Biotechnol. J. e2000008. https://doi.org/10.1002/biot.202000008.
Sencar, J., Hammerschmidt, N., Martins, D.L., Jungbauer, A., 2020b. A narrow residence time incubation reactor for continuous virus inactivation based on packed beds. New Biotechnol. 55, 98–107. https://doi.org/10.1016/j.nbt.2019.10.006.
Sharma, A.K., Agarwal, H., Pathak, M., Nigam, K.D.P., Rathore, A.S., 2016. Continuous refolding of a biotech therapeutic in a novel Coiled Flow Inverter Reactor. Chem. Eng. Sci. 140, 153–160. https://doi.org/10.1016/j.ces.2015.10.009.
Siew, W.E., Livingston, A.G., Ates, C., Merschaert, A., 2013. Continuous solute fractionation with membrane cascades – a high productivity alternative to diafiltration. Sep. Purif. Technol. 102, 1–14. https://doi.org/10.1016/j.seppur.2012.09.017.
Simon, L.L., Pataki, H., Marosi, G., Meemken, F., Hungerbühler, K., Baiker, A., Tummala, S., Glennon, B., Kuentz, M., Steele, G., Kramer, H.J.M., Rydzak, J.W., Chen, Z., Morris, J., Kjell, F., Singh, R., Gani, R., Gernaey, K.V., Louhi-Kultanen, M., O'Reilly, J., Sandler, N., Antikainen, O., Yliruusi, J., Frohberg, P., Ulrich, J., Braatz, R.D., Leyssens, T., von Stosch, M., Oliveira, R., Tan, R.B.H., Wu, H., Khan, M., O'Grady, Des, Pandey, A., Westra, R., Delle-Case, E., Pape, D., Angelosante, D., Maret, Y., Steiger, O., Lenner, M., Abbou-Oucherif, K., Nagy, Z.K., Litster, J.D., Kamaraju, V.K., Chiu, M.-S., 2015. Assessment of recent process analytical technology (PAT) trends: a multiauthor review. Org. Process Res. Dev. 19 (1), 3–62. https://doi.org/10.1021/op500261y.
Smejkal, B., Agrawal, N.J., Helk, B., Schulz, H., Giffard, M., Mechelke, M., Ortner, F., Heckmeier, P., Trout, B.L., Hekmat, D., 2013. Fast and scalable purification of a therapeutic full-length antibody based on process crystallization. Biotechnol. Bioeng. 110 (9), 2452–2461. https://doi.org/10.1002/bit.24908.
Smith, K.B., 2000. Scale-up of Oscillatory Flow Mixing (Doctoral thesis).
Somasundaram, B., Pleitt, K., Shave, E., Baker, K., Lua, L.H.L., 2018. Progression of continuous downstream processing of monoclonal antibodies: current trends and challenges. Biotechnol. Bioeng. 115 (12), 2893–2907. https://doi.org/10.1002/bit.26812.
Stankiewicz, A., Moulijn, J.A., 2000. Process intensification: transforming chemical engineering. Chem. Eng. Prog. 96, 22–33.
Steinebach, F., Angarita, M., Karst, D.J., Müller-Späth, T., Morbidelli, M., 2016a. Model based adaptive control of a continuous capture process for monoclonal antibodies production. J. Chromatogr. A 1444, 50–56. https://doi.org/10.1016/j.chroma.2016.03.014.
Steinebach, F., Müller-Späth, T., Morbidelli, M., 2016b. Continuous counter-current chromatography for capture and polishing steps in biopharmaceutical production. Biotechnol. J. 11 (9), 1126–1141. https://doi.org/10.1002/biot.201500354.

Steinebach, F., Ulmer, N., Decker, L., Aumann, L., Morbidelli, M., 2017a. Experimental design of a twin-column countercurrent gradient purification process. J. Chromatogr. A 1492, 19–26. https://doi.org/10.1016/j.chroma.2017.02.049.

Steinebach, F., Ulmer, N., Wolf, M., Decker, L., Schneider, V., Wälchli, R., Karst, D., Souquet, J., Morbidelli, M., 2017b. Design and operation of a continuous integrated monoclonal antibody production process. Biotechnol. Prog. 33 (5), 1303–1313. https://doi.org/10.1002/btpr.2522.

Ströhlein, G., Aumann, L., Mazzotti, M., Morbidelli, M., 2006. A continuous, counter-current multi-column chromatographic process incorporating modifier gradients for ternary separations. J. Chromatogr. A 1126 (1–2), 338–346. https://doi.org/10.1016/j.chroma.2006.05.011.

Sun, Y.-N., Shi, C., Zhang, Q.-L., Yao, S.-J., Slater, N.K.H., Lin, D.-Q., 2020. Model-based process development and evaluation of twin-column continuous capture processes with Protein A affinity resin. J. Chromatogr. A 1625, 461300. https://doi.org/10.1016/j.chroma.2020.461300.

Takakura, T., Ito, T., Yagi, S., Notsu, Y., Itakura, T., Nakamura, T., Inagaki, K., Esaki, N., Hoffman, R.M., Takimoto, A., 2006. High-level expression and bulk crystallization of recombinant L-methionine gamma-lyase, an anticancer agent. Appl. Microbiol. Biotechnol. 70 (2), 183–192. https://doi.org/10.1007/s00253-005-0038-2.

Thakur, G., Hebbi, V., Rathore, A.S., 2020. An NIR-based PAT approach for real-time control of loading in Protein A chromatography in continuous manufacturing of monoclonal antibodies. Biotechnol. Bioeng. 117 (3), 673–686. https://doi.org/10.1002/bit.27236.

Torres-Acosta, M.A., Mayolo-Deloisa, K., González-Valdez, J., Rito-Palomares, M., 2019. Aqueous two-phase systems at large scale: challenges and opportunities. Biotechnol. J. 14 (1), e1800117. https://doi.org/10.1002/biot.201800117.

Tseng, Y.-H., Mohanty, S.K., McLennan, J.D., Pease, L.F., 2019. Algal lipid extraction using confined impinging jet mixers. Chem. Eng. Sci.: X 1, 100002. https://doi.org/10.1016/j.cesx.2018.100002.

Ulmer, N., Ristanovic, D., Morbidelli, M., 2019. Process for continuous fab production by digestion of IgG. Biotechnol. J. 14 (10), e1800677. https://doi.org/10.1002/biot.201800677.

Utturkar, A., Gillette, K., Sun, C.-Y., Pagkaliwangan, M., Quesenberry, R., Schofield, M., 2019. A direct approach for process development using single column experiments results in predictable streamlined multi-column chromatography bioprocesses. Biotechnol. J. 14 (4). https://doi.org/10.1002/biot.201800243.

van Alstine, J.M., Jagschies, G., Łącki, K.M., 2018. Alternative separation methods: flocculation and precipitation. In: Biopharmaceutical Processing. Elsevier, pp. 221–239.

Vázquez-Villegas, P., Aguilar, O., Rito-Palomares, M., 2011. Study of biomolecules partition coefficients on a novel continuous separator using polymer-salt aqueous two-phase systems. Sep. Purif. Technol. 78 (1), 69–75. https://doi.org/10.1016/j.seppur.2011.01.023.

Vogel, J.H., Nguyen, H., Giovannini, R., Ignowski, J., Garger, S., Salgotra, A., Tom, J., 2012. A new large-scale manufacturing platform for complex biopharmaceuticals. Biotechnol. Bioeng. 109 (12), 3049–3058. https://doi.org/10.1002/bit.24578.

Vogg, S., Müller-Späth, T., Morbidelli, M., 2018. Current status and future challenges in continuous biochromatography. Curr. Opin. Chem. Eng. 22, 138–144. https://doi.org/10.1016/j.coche.2018.09.001.

Vogg, S., Ulmer, N., Souquet, J., Broly, H., Morbidelli, M., 2019. Experimental evaluation of the impact of intrinsic process parameters on the performance of a continuous chromatographic polishing unit (MCSGP). Biotechnol. J. 14 (7), e1800732. https://doi.org/10.1002/biot.201800732.

Walch, N., Jungbauer, A., 2017. Continuous desalting of refolded protein solution improves capturing in ion exchange chromatography: a seamless process. Biotechnol. J. 12 (6). https://doi.org/10.1002/biot.201700082.

Warikoo, V., Godawat, R., Brower, K., Jain, S., Cummings, D., Simons, E., Johnson, T., Walther, J., Yu, M., Wright, B., McLarty, J., Karey, K.P., Hwang, C., Zhou, W., Riske, F., Konstantinov, K., 2012. Integrated continuous production of recombinant therapeutic proteins. Biotechnol. Bioeng. 109 (12), 3018–3029. https://doi.org/10.1002/bit.24584.

Wei, F., Li, M., Huang, F., Chen, M., Jiang, H., Zhao, Y., 2011. A novel pseudo simulated moving bed with solvent gradient for ternary separations. J. Chromatogr. A 1218 (20), 2906–2911. https://doi.org/10.1016/j.chroma.2011.03.001.

Wellhoefer, M., Sprinzl, W., Hahn, R., Jungbauer, A., 2014. Continuous processing of recombinant proteins: integration of refolding and purification using simulated moving bed size-exclusion chromatography with buffer recycling. J. Chromatogr. A 1337, 48–56. https://doi.org/10.1016/j.chroma.2014.02.016.

Wenkenborg, K., Susanto, A., Frederiksen, S., Schmidt-Traub, H., 2004. Nicht-isokratische SMB-Trennung von Proteinen mittels Ionenaustauschchromatographie. Chem. Ing. Tech. 76 (6), 815–819. https://doi.org/10.1002/cite.200403355.

West, S.M., Chaudhuri, J.B., Howell, J.A., 1998. Improved protein refolding using hollow-fibre membrane dialysis. Biotechnol. Bioeng. 57 (5), 590–599. https://doi.org/10.1002/(SICI)1097-0290(19980305)57:5<590:AID-BIT11>3.0.CO;2-G.

Wheelwright, S.M., 1987. Designing downstream processes for large-scale protein purification. Nat. Biotechnol. 5 (8), 789–793. https://doi.org/10.1038/nbt0887-789.

Woodcock, J., 2014. Modernizing Pharmaceutical Manufacturing – Continuous Manufacturing as a Key Enabler. FDA, International Symposium on continuous manufacturing of Pharmaceuticals, Cambridge MA.

Xenopoulos, A., 2015. A new, integrated, continuous purification process template for monoclonal antibodies: process modeling and cost of goods studies. J. Biotechnol. 213, 42–53. https://doi.org/10.1016/j.jbiotec.2015.04.020.

Yang, H., Chen, W., Peczulis, P., Heng, J.Y.Y., 2019a. Development and workflow of a continuous protein crystallization process: a case of lysozyme. Cryst. Growth Des. 19 (2), 983–991. https://doi.org/10.1021/acs.cgd.8b01534.

Yang, O., Qadan, M., Ierapetritou, M., 2019b. Economic analysis of batch and continuous biopharmaceutical antibody production: a review. J. Pharm. Innov. 14, 1–19. https://doi.org/10.1007/s12247-018-09370-4.

Yoshii, H., Furuta, T., Yonehara, T., Ito, D., Linko, Y.Y., Linko, P., 2000. Refolding of denatured/reduced lysozyme at high concentration with diafiltration. Biosci. Biotechnol. Biochem. 64 (6), 1159–1165. https://doi.org/10.1271/bbb.64.1159.

Yoshimoto, N., Ichihara, T., Yamamoto, S., 2019. Connected flow-through chromatography processes as continuous downstream processing of proteins. MATEC Web Conf. 268, 1003. https://doi.org/10.1051/matecconf/201926801003.

Zelger, M., Pan, S., Jungbauer, A., Hahn, R., 2016. Real-time monitoring of protein precipitation in a tubular reactor for continuous bioprocessing. Process Biochem. 51 (10), 1610–1621. https://doi.org/10.1016/j.procbio.2016.06.018.

Zhao, D., Liu, Y., Wang, Y., Li, X., Wang, Q., Su, Z., 2014. Membrane combined with hydrophilic macromolecules enhances protein refolding at high concentration. Process Biochem. 49 (7), 1129–1134. https://doi.org/10.1016/j.procbio.2014.03.010.

Zobel-Roos, S., Schmidt, A., Mestmäcker, F., Mouellef, M., Huter, M., Uhlenbrock, L., Kornecki, M., Lohmann, L., Ditz, R., Strube, J., 2019. Accelerating biologics manufacturing by modeling or: is approval under the QbD and PAT approaches demanded by authorities acceptable without a digital-twin?. Processes 7 (2), 94. https://doi.org/10.3390/pr7020094.

Zydney, A.L., 2016. Continuous downstream processing for high value biological products: a review. Biotechnol. Bioeng. 113 (3), 465–475. https://doi.org/10.1002/bit.25695.

Chapter 4

Virus-like Particle Preparation is Improved by Control over Capsomere-DNA Interactions During Chromatographic Purification

In this chapter, it is investigated how the control of DNA-VP1 interactions can influence the downstream processing of viral capsomeres. Multi-modal cation exchange resin was identified as a novel approach to process VP1 capsomeres at elevated salt concentrations, enabling the suppression of DNA-VP1 interactions and thus allowing for higher binding capacities. Furthermore, the influence of DNA-VP1 interactions on the formation of aggregates during assembly is investigated.

Statement of Authorship

Title of Paper	Virus-like Particle Preparation is Improved by Control over Capsomere-DNA Interaction During Chromatographic Purification
Publication Status	published
Publication Details	Lukas Gerstweiler, Jingxiu Bi, Anton P.J. Middelberg, Virus-like Particle Preparation is Improved by Control over Capsomere-DNA Interaction During Chromatographic Purification, Biotechnology and Bioengineering, 2021 118:1688-1701 https://doi.org/10.1002/bit.27687.

Principal Author

Name of Principal Author (Candidate)	Lukas Gerstweiler		
Contribution to the Paper	Research idea, Conceptualization, performed study, experimental work, Writing - original draft, Writing - review & editing		
Overall percentage	80%		
Signature		Date	4.4.2022

Co-Author Contributions

By signing the Statement of Authorship. Each author certifies that:

IV. The candidate's stated contribution to the publication is accurate (as detailed above)

V. Permission is granted for the candidate in include the publication in the thesis; and

VI. The sum of all co-author contribution is equal to 100% less the candidate's stated contribution

Name of Co-Author	Jingxiu Bi		
Contribution to the Paper	Writing - review & editing, Conceptualization, Supervision		
Signature		Date	31/03/2022

Name of Co-Author	**Anton P.J. Middelberg**		
Contribution to the Paper	Conceptualization, Experimental design, Analysis, Writing - review & editing, Supervision		
Signature		Date	

31 March 2022

BIOTECHNOLOGY and BIOENGINEERING

VOLUME 118 NUMBER 4 APRIL, 2021

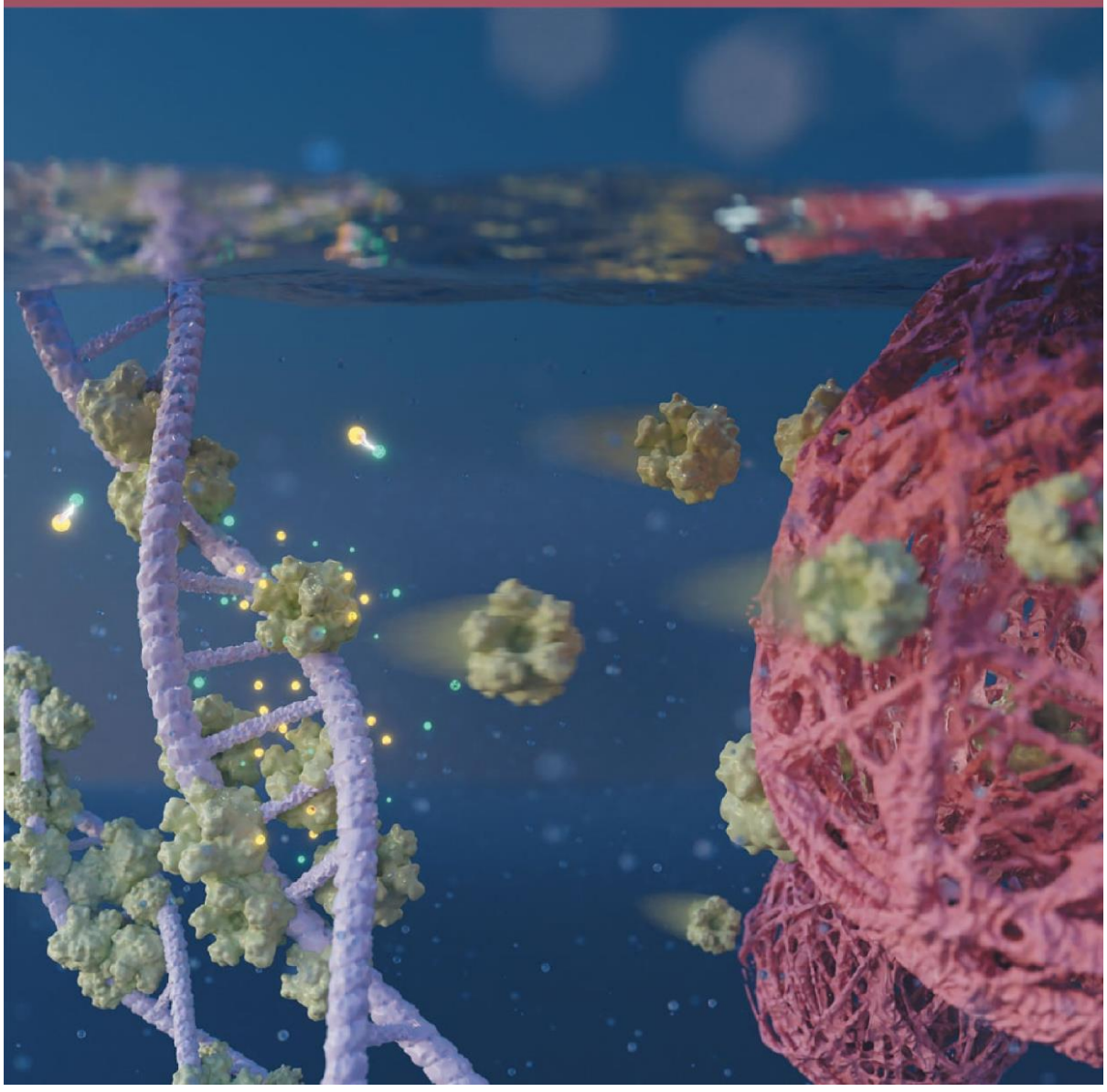

Received: 13 October 2020 | Revised: 9 December 2020 | Accepted: 12 January 2021

DOI: 10.1002/bit.27687

ARTICLE

BIOTECHNOLOGY BIOENGINEERING WILEY

Virus-like particle preparation is improved by control over capsomere-DNA interactions during chromatographic purification

Lukas Gerstweiler[1] | Jingxiu Bi[1] | Anton Peter Jacob Middelberg[2]

[1]School of Chemical Engineering and Advanced Materials, The University of Adelaide, Adelaide, South Australia, Australia

[2]Division of Research and Innovation, The University of Adelaide, Adelaide, South Australia, Australia

Correspodence
Anton Peter Jacob Middelberg, Division of Research and Innovation, The University of Adelaide, Adelaide, South Australia 5005, Australia.
Email: anton.middelberg@adelaide.edu.au

Abstract

Expression of viral capsomeres in bacterial systems and subsequent in vitro assembly into virus-like particles is a possible pathway for affordable future vaccines. However, purification is challenging as viral capsomeres show poor binding to chromatography media. In this study, the behavior of capsomeres in unfractionated bacterial lysate was compared with that for purified capsomeres, with or without added microbial DNA, to better understand reasons for poor bioprocess behavior. We show that aggregates or complexes form through the interaction between viral capsomeres and DNA, especially in bacterial lysates rich in contaminating DNA. The formation of these complexes prevents the target protein capsomeres from accessing the pores of chromatography media. We find that protein–DNA interactions can be modulated by controlling the ionic strength of the buffer and that at elevated ionic strengths the protein–DNA complexes dissociate. Capsomeres thus released show enhanced bind-elute behavior on salt-tolerant chromatography media. DNA could therefore be efficiently removed. We believe this is the first report of the use of an optimized salt concentration that dissociates capsomere–DNA complexes yet enables binding to salt-tolerant media. Post purification, assembly experiments indicate that DNA–protein interactions can play a negative role during in vitro assembly, as DNA–protein complexes could not be assembled into virus-like particles, but formed worm-like structures. This study reveals that the control over DNA–protein interaction is a critical consideration during downstream process development for viral vaccines.

KEYWORDS

aggregation, DNA–protein interaction, downstream processing, modular virus-like particles, multimodal chromatography

1 | INTRODUCTION

Virus-like-particles (VLPs) are self-assembled ensembles of viral structural proteins, having the same size and shape as the native virus. However, as they lack viral nucleic acids, they cannot replicate and are therefore noninfectious. VLPs are able to trigger a strong immune response, due to their highly repetitive immunogenic and native structure, making them promising candidates as vaccines (Al-Barwani et al., 2014; Bright et al., 2007; Donaldson et al., 2018; Effio & Hubbuch, 2015; Hume et al., 2019). Vaccines based on VLPs are commercially available against Hepatitis B (HBV), Hepatitis E (HEV), and human papillomavirus (HPV). VLPs are currently investigated as vaccines against a variety of viruses such as Influenza A (IAV), human Norovirus (HuNV), and Chikungunya virus (Donaldson et al., 2018; Frazer, 2004; VBI Vaccines Inc, 2018).

By manipulating the amino acid sequence of the structural proteins, VLPs can be modified to present foreign antigens. In this way, they can trigger immune responses against others than the underlying virus. These so called modular VLPs do expand the possible applications of VLPs. Through synthetic biology, unrelated antigens can be presented in an immunogenic context, allowing multivalent, and cross protective vaccines to be generated against all kind of targets. As computer-based simulation is developing, these three dimensional structures can be precisely modeled to predict and obtain the desired immunogenicity and stability of the modular VLP (Carter et al., 2016; Hume et al., 2019; Mobini et al., 2020; Zhang et al., 2015). Modular VLPs are examined as vaccines against pathogens like Group A Streptococcus (Seth et al., 2016), Influenza (Anggraeni et al., 2013), rotavirus (Tekewe et al., 2017), human papillomavirus (Zhai et al., 2017), and also against malaria (Pattinson et al., 2019), toxoplasmosis (Guo et al., 2019), cancer (Donaldson et al., 2017), diabetes (Cavelti-Weder et al., 2016), nicotine addiction (Cornuz et al., 2008), and others.

Although VLPs are extremely promising as next-generation vaccines, large scale production is still a challenge (Hume et al., 2019; Pattenden et al., 2005). Virus-like-particles can be produced by expressing viral structural protein in different host systems ranging from eukaryotics such as mammalian cells, yeast, and insect cells to prokaryotic cell systems. Despite the usual pros and cons of these systems, namely posttranslational modifications versus expression level and cost, the in vivo VLP self-assembly pathway always bears the risk of internal contaminations, like host cell DNA, RNA, and host cell protein (HCP) that co-assemble together with VLPs. Internal contaminations are hard to remove and can lead to batch to batch variations (Lua et al., 2014; Pattenden et al., 2005; Teunissen et al., 2013; Wu et al., 2010). The removal of internal contaminations requires an additional disassembling-reassembling step, including for the commercial HPV vaccine, making the overall process inefficient. Another pathway is the expression and purification of unassembled structural viral protein and a subsequent controlled in vitro assembly, eradicating the presence of internal contaminations and providing for enhanced process and product quality control (Pattenden et al., 2005).

Group A Streptococcus (GAS) is a human pathogen responsible for several million infections and more than 500,000 deaths every year (Carapetis et al., 2005). An efficient vaccine has yet not been developed and only two candidates are being evaluated in human trials (Vekemans et al., 2019). As GAS is mainly a severe health problem in developing countries, an ideal future vaccine does not only have to be efficacious but also should be very affordable, as still more than 700 million people worldwide are living in extreme poverty (The World Bank, 2018; Wibowo et al., 2013). In this study, a possible low-cost, future vaccine candidate, based on a modular polyoma virus-like-particle, was studied, that displays the J8 antigen from the GAS M-protein (Middelberg et al., 2011; Rivera-Hernandez et al., 2013).

The use of modified murine polyomavirus major capsid protein VP1 is a promising platform technology for fast, cheap, and efficient modular VLP vaccines. It can be expressed in gram-per-litre levels in *Escherichia coli*, and produced within days, rather than months as most vaccines nowadays, enabling possible costs of cents per dose and potential for a fast reaction on pandemic outbreaks (Chuan et al., 2014; Liew et al., 2010; Middelberg et al., 2011). VP1 and VP1-derived proteins are highly examined to study self-assembling processes and the use of VLPs as drug carriers and vaccines (Chuan et al., 2010; Li et al., 2003; Ou et al., 1999; Zhou et al., 2019). Like other viral proteins, the purification of VP1 capsomeres and VLPs presents challenges and no industrial scale process has yet been described (Buch et al., 2015; Gillock et al., 1997; Johne & Müller, 2004; Pattinson et al., 2019).

The main challenges during the purification of VP1 capsomeres and VLPs are low recoveries using chromatographic techniques (<40% on GSTrap™ HP affinity chromatography resins, 54% on CIMmultus™ QA monolith chromatography) and the formation of soluble aggregates during processing and assembling (Lipin et al., 2008; Zaveckas et al., 2018). Purification requires additional hard-to-scale unit operations, including size exclusion chromatography, enzymatic affinity tag removal or costly monoliths and membrane adsorbers (Ladd Effio, Hahn, et al., 2016; Lipin et al., 2008; Zaveckas et al., 2018). Also, DNA removal often requires additional enzymatic treatment (Simon et al., 2013). Aggregation and low recovery can influence each other as shown by Lipin et al. (2008), where low recovery on affinity chromatographic media could be attributed to the existence of aggregates unable to enter the pores of chromatographic resins. Several mechanisms are proposed in the literature to cause aggregation, such as polymerization by the used GST-tag, hydrophobic interactions, formation of disulfide bonds, and a competitive pathway during assembly. Furthermore, the stability is highly dependent on the inserted antigen (Abidin et al., 2015; Ding et al., 2010; Lipin et al., 2009; Tekewe et al., 2016). It could be shown that capsomere stability can be increased by the addition of non-ionic detergents, sorbitol, and polysorbate 20, and high-throughput methods have been developed to optimize buffer composition (Abidin et al., 2015; Mohr et al., 2013; Tekewe et al., 2015).

Although the strong DNA binding properties of VP1 are a well-known fact and described decades ago (Chang et al., 1993; Moreland et al., 1991), the influence on aggregation and chromatographic purification has never been examined in detail. This study therefore explores the influence of VP1's DNA affinity on aggregation, chromatographic purification, protein stability, and assembly. It is shown that VP1 aggregation (or complex formation), which hinders VP1 from accessing chromatography pores leading to poor binding capacities, can be caused by nonspecific DNA–protein complexation, which can be eliminated by increasing salt concentration. Also, efficient strategies for chromatographic capture and the removal of nucleic acids are developed to overcome the bottleneck of producing VP1 based virus-like-particles. Furthermore, it was shown, that VP1–DNA complexes cannot be assembled into VLPs as they form worm like structures during assembly. The findings in this study are of high importance for the production of VP1 based virus-like-particles and will help to develop cheap and reliable industrial purification protocols.

2 | MATERIALS AND METHODS

2.1 | Chemicals and buffers

Cultivation was done with terrific broth (TB) medium containing 12 g L^{-1} tryptone (Thermo Fisher Scientific), 24 g L^{-1} yeast extract (Thermo Fisher Scientific), 5 g L^{-1} glycerol (Chem-Supply), 2.31 g L^{-1} potassium dihydrogen phosphate (Chem-Supply), and 12.5 g L^{-1} dipotassium hydrogen phosphate (Chem-Supply). Chloramphenicol (Thermo Fisher Scientific) and ampicillin (Thermo Fisher Scientific) were added to final concentrations of 35 µg ml^{-1} and 100 µg ml^{-1}, respectively. Isopropyl β-D-1-thiogalactopyranoside (IPTG) for induction was obtained from Thermo Fisher Scientific. Saline for cell resuspension consisted of 9 g L^{-1} sodium chloride (Chem-Supply). Ultra-pure water was obtained with a Milli Q water (MQW) system and used for all experiments.

Lysis buffer comprised 40 mM Tris buffer, 2 mM EDTA, 5% w w^{-1} glycerol and 5 mM dithiothreitol (DTT) (all Chem-Supply) at pH 8. Lysis buffer without DTT was prepared as a five times stock and prior use was filtered (0.22 µm), vacuum degassed for 5 min and DTT was added. For chromatographic experiments, lysis buffer containing different concentrations of NaCl were used. VLP assembling buffer consisted of 0.5 M ammonium sulfate, 20 mM Tris, 1 mM calcium chloride, and 5% w w^{-1} glycerol (all Chem-Supply, Australia) at pH 7.4. Elution buffer at pH 12 was 40 mM Sodium hydrogen orthophosphate, 2 mM EDTA, 5% w w^{-1} glycerol, and 5 mM DTT. Lysis buffer with added NaCl (0–0.5 M NaCl) was used as running buffer for size exclusion experiments and polishing.

Sodium dodecyl sulfate (SDS) gel electrophoresis used 12% w v^{-1} self-casted acrylamide gels (per 10 ml: 2 ml MQW, 4 ml 30% w v^{-1} acrylamid/bis solution, 3.8 ml 1 M Tris pH 8.8, 0.1 ml 10% w w^{-1} SDS, 0.1 ml 10% w w^{-1} ammonium persulphate, 0.04 ml TEMED (all except Tris from BIO RAD Laboratories) with a 4% w v^{-1} stacking layer (per 2 ml: 1.4 ml MQW, 0.33 ml 30% w v^{-1} acrylamid/bis solution, 0.25 ml 1 M Tris pH 6.8, 0.02 ml 10% w w^{-1} SDS, 0.02 ml 10% w w^{-1} ammonium persulphate, 0.002 ml TEMED), using 5× loading buffer composed of 1.9 ml MQW, 0.6 ml 1 M Tris pH 6.8, 5 ml 50% w w^{-1} glycerol, 10 mg bromphenol blue (BIO RAD Laboratories), 2 ml 10% w w^{-1} SDS, 0.5 ml beta-mercaptoethanol (BIO RAD Laboratories), and 10× running buffer consisting of 30 g L^{-1} Tris, 144 g l^{-1} glycine (Chem-Supply, Australia), 10 g L^{-1} SDS, pH 8.3. Coomassie Brilliant Blue R-250 staining solution was obtained from BIO RAD Laboratories. A solution of 80% v v^{-1} MWQ, 10% v v^{-1} ethanol (Chem-Supply) and 10% v v^{-1} acetic acid (Chem-Supply, Australia) was used for destaining.

PEG-6000 was obtained by Chem-Supply, Australia. Lyophilized Unsheared *E. coli* DNA was obtained from Sigma (D4889) and dissolved in MQW.

2.2 | Instrumentation

A 5920R centrifuge (Eppendorf, Germany) was used for solid–liquid separation of cell harvest, removal of cell debris, and separation of precipitate. Cell disruption was done using a Scientz-IID Ultrasonic homogenizer (Ningbo Scientz Biotechnology) with a 6 mm diameter horn. Dynamic light scattering was conducted with a Zetasizer NanoZS (Malvern Panalytical/Spectric). Chromatographic experiments were done using an AKTApure® system equipped with a F9-R fraction collector (GE Healthcare Life Science). Superose™ 6 Increase, Capto™ Q, and Capto™ MMC columns were obtained from GE Healthcare Life Science. Absorbance at 595 nm for Bradford protein assay was measured on an ELx808 microplate absorbance reader (BioTek Instruments), UV spectrophotometry for DNA quantification was done on a 2300 Victor X5 multilabel reader (PerkinElmer). SDS Gels were run in a Mini-PROTEAN tetra cell (BIO RAD Laboratories).

2.3 | Plasmid construction, transformation, and host strain

The plasmid was constructed by the Protein Expression Facility of the University of Queensland. Group A Streptococcus antigen GCN4-J8 was inserted into Murine polyomavirus VP1 sequence (M34958) with flanking G4S linkers. The obtained gene VP1 GCN4 J8 was cloned into pETDuet-1 at multiple cloning site 2 (MCS2) at NdeI and PacI restriction site. The complete sequence was *MAPKRK SGVSKCETKCTKACPRPAPVPKLLIKGGMEVLDLVTGPDSVTEIEAFLNPRM GQPPTPESLTEGGQYYGWSRGINLATSDTEDSPGNNTLPTWSMAKLQLPM LNEDLTCDTLQMWEAVSVKTEVVGSGSLLDVHGFNKPTDTVNTKGISTPV EGSQYHVFAVGGEPLDLQGLVTDARTKYKEEGVVTIKTITKKDMVNKDQV LNPISKAKLDKDGMYPVEIWHPDPAKNENTRYFGNYTGGTTTPPVLQFTN TLTTVLLDENGVGPLCKGEGLYLSCVDIMGWRVTRGGGGSSQAEDKVKQS REAKKQVEKALKQLEDKVQAGGGGSYDVHHWRGLPRYFKITLRKRWVK NPYPMASLISSLFNNMLPQVQGQPMEGENTQVEEVRVYDGTEPVPGDPD MTRYVDRFGKTKTVFPGN** which was inserted in the plasmid as following: pT7-lacOp – pT7 – lacOp – VP1 – G4S linker – GCN4 J8 – G4S linker.

The sequence was verified using Abi BigDye Terminator 3.1. Sequencing, which was conducted by the Australian Genome Research Facility (AGRF).

VP1-J8 was transformed into Rosetta™ 2(DE3) Singles™ competent cells (Merck KGaA) via heat shock transformation using standard procedure. Plasmid DNA was mixed with the competent cells, incubated on ice for 5 min, heat shocked for 30 s at 42°C, followed by 2 min cooling on ice. Cells were then mixed with TOC medium and selected on agar plates containing 100 µg ml^{-1} ampicillin and 35 µg ml^{-1} chloramphenicol. A single colony was picked, grown on 50 ml TB medium in a 250 ml shake flask at 37°C. After an optical density OD_{600} of 0.5 AU was reached the cell suspension was mixed with glycerol to a total concentration of 25% w w^{-1} and stored in 100 µl aliquots at −80°C till further use.

2.4 | Protein expression

One 100 µl aliquot of transferred cells was thawed and poured into 50 ml of TB medium containing antibiotics, in a 250 ml shake flask, and grown overnight at 37°C at 200 rpm. Next morning 5 ml of the

overnight culture was transferred into 200 ml fresh TB medium in a 1 L shake flask and grown at 37°C and 200 rpm. After the optical density OD_{600} reached 0.5 AU product expression was started by adding IPTG to a final concentration of 0.1 mmol L^{-1} and lowering the temperature to 27°C. Product expression lasted 16 h, after which cells were harvested by centrifugation at 3200 g for 10 min at 4°C. The pellet was resuspended in 0.9% w w^{-1} saline and divided into 50 ml aliquots and centrifuged for 10 min at 20,130 *g* at 4°C to obtain 1 g pellets. The supernatant was withdrawn and the pellets where then stored at −80°C until further use.

2.5 | Purification of VP1-J8 protein

A 1 g pellet of *E. coli* was resuspended in 50 ml lysis buffer and sonicated for 15 min on ice, using 10 s bursts at 400 W followed by 40 s cool down phase. After sonication, the sample was centrifuged at 20,130 *g* for 30 min at 4°C to obtain clarified supernatant. The VP1-J8 was then precipitated using 3.5 g (7% w w^{-1}) PEG 6000 and 1.45 g NaCl (0.5 M final concentration). Suspension was gently mixed until the PEG and NaCl were dissolved and incubated on ice for 10 min to form precipitates. After centrifugation at 20,130 *g* at 4°C for 2 min, the supernatant was discharged and the pellet was gently washed three times with 5 ml MQW to remove all residual supernatant. The pellet was then resuspended in 20 ml running buffer containing 0.4 M NaCl. The solution was further purified by an anion exchange step (Capto™ Q) in flow through mode using a running buffer with 0.4 M NaCl at pH 8. A final polishing was achieved using size exclusion chromatography loading 0.5 ml sample on a Superose™ 6 increase column, collecting the peak eluting at 15 ml. If not stated otherwise, running buffer containing 0.4 M NaCl at pH 8 was used with a flowrate of 0.6 ml min^{-1}. Desalting was conducted using a 5 ml HiTrap™ Desalting column (GE Healtcare). All buffers and samples were cooled on ice throughout the whole process. The starting material used in the in following described experiments, are summarized in Table 1. SDS-PAGE analysis of the different purification steps are provided in the supplementary data.

2.6 | Cation exchange experiments on Capto™ MMC

Capto™ MMC was chosen as a cation exchanger as it provides, in contrast to Capto™ S, high binding over a broad range of salt concentrations. Elution is therefore usually done by pH shift. Samples were pre-purified by PEG precipitation as described, and the pellet after precipitation was dissolved in lysis buffer containing 0 M NaCl, at a protein concentration of 1.96 mg ml^{-1}. NaCl was added to a final concentration of 0.5 M NaCl to half of the sample. Lysis buffer containing either 0 M NaCl or 0.5 M NaCl was used as a running buffer and for equilibration. Sample was injected into a 2 ml sample loop and loaded to a 1 ml Capto™ MMC prepacked column at a flow rate of 0.33 ml min^{-1}. The elution was conducted using a 1 M NaCl sodium hydrogen orthophosphate buffer adjusted with NaOH to pH 12. Recovery was estimated by integrating the chromatograms at an absorbance of 280 nm and comparing peak areas of the flow through during loading and of elution peaks containing VP1-J8.

2.7 | Anion exchanger experiments on Capto™ Q

Sample pellets pre-purified by PEG precipitation as described were re-dissolved in lysis buffer at pH 8 either with 0.1 M NaCl or 0.4 M NaCl. Final protein concentration was adjusted to 0.54 mg ml^{-1}. Sample was used to fill a 100 µl sample loop. The pre packed 1 ml Capto™ Q column was equilibrated with the corresponding buffer and loaded at 0.33 ml min^{-1}, followed by a 1 M NaCl step elution, pH 8, at a flow rate of 1 ml min^{-1}.

2.8 | Assembling of virus-like particles

Purified VP1-J8 capsomeres as described were assembled into virus-like-particles by dialysis against assembling buffer for 24 h at 4°C as described previously (Middelberg et al., 2011). Capsomeres purified by multimodal cation exchange chromatography (Capto™ MMC) followed by SEC chromatography instead of anion exchange chromatography were also assembled into VLP's. The influence of DNA on assembly was examined by preparing VP1-J8 solutions with and without DNA before assembly. Host cell DNA free VP1-J8 obtained by AEX and SEC as described in Section 2.5 was desalted into lysis buffer pH 8 with 0.1 M NaCl or with 0.5 M NaCl and the concentration of VP1-J8 was adjusted to 0.2 mg ml^{-1}. DNA stock solution to a final concentration of 5 µg ml^{-1} was added to half of the sample. Obtained VLP's were examined by TEM.

2.9 | Protein analysis and SDS-PAGE

Protein concentration was measured using the Bradford Protein Assay (Bradford, 1976), following the standard protocol provided by

TABLE 1 Starting material used for the different experiments

Experiment	Starting material	Host cell DNA	DNA spiking
2.6 Cation exchange	Resolubilized PEG precipitate	Yes	No
2.7 Anion exchange	Resolubilized PEG precipitate	Yes	No
2.8 Assembly	Purified VP1-J8 (PEG + AEX + SEC)	No	Yes
2.11 SEC	Clarified lysate	Yes	No
2.12 Light Scattering	Purified VP1-J8 (PEG + AEX + SEC)	No	Yes

BioRad in 200 µl 96 well plates, with bovine serum albumin as a standard. BSA standard was prepared at different concentrations (0.05 mg ml^{-1}, 0.1 mg ml^{-1}, 0.2 mg ml^{-1} and, 0.4 mg ml^{-1}) and the concentration was verified measuring the A_{280} absorbance on a NanoDrop. All samples were measured in triplicates.

Self-casted gels as described were used for analysis. If not stated otherwise, 10 µl of sample was mixed with 2 µl of 5× loading buffer and heated at 100°C for 10 min before loading. A running buffer was used as described with a 200 V fixed current for the entire run. The gel was stained for 1 h with shaking, followed by 4 h destaining using an ethanol/acetic acid destaining buffer as described. Pictures were obtained on a ChemicDoc imaging system using standard configuration for Comassie Blue gels. Under reducing and denaturing conditions VP1-J8 is expected to be visible at a size of 46.4 kDa.

2.10 | DNA analysis

DNA quantification was conducted using Quant-iT™ High-Sensitivity dsDNA Assay Kit in a 96 well plate, following the manual. Fluorescence was measured at 485/530 nm and all samples were measured in duplicate. Preliminary tests showed that VP1–DNA interactions and aggregates had no influence on the result of the assay.

2.11 | Size-exclusion chromatography of VP1-J8 clarified supernatant at different NaCl concentrations by Superose™ 6 increase

SEC experiments were conducted to measure the elution volume of VP1-J8 capsomeres in crude clarified supernatant at different NaCl concentrations. The larger the molecule, the faster it elutes, therefore aggregates of VP1-J8 capsomeres can be measured in the supernatant. Crude clarified supernatant after cell disruption was obtained as described. The supernatant was split into 6 ml samples and NaCl was added to obtain final concentrations of 0 M, 0.1 M, 0.2 M, 0.3 M, 0.4 M, and 0.5 M. After gentle shaking until the salt was dissolved, the samples were stored on ice. A Superose™ 6 Increase 10/300 GL column was equilibrated for two column volumes with running buffer having the same NaCl concentration as the sample being examined. Samples were filtered (0.22 µm) and loaded into a 0.5 ml sample loop. Flow rate was 0.6 ml min^{-1}, samples were taken every 0.5 ml using the autosampler. Samples (10 µl) were then used for SDS-PAGE analysis.

2.12 | Dynamic light scattering of VP1-J8 capsomeres and VP1-J8–DNA complexes

To test whether the aggregation of VP1-J8 capsomeres was due to salt-induced precipitation or because of an affinity towards DNA, the hydrodynamic particle size of purified VP1-J8 was measured using dynamic light scattering as this technique allows determination of the hydrodynamic particle diameter at various controlled buffer compositions and is in particular sensitive towards aggregates. SEC could not be easily used because purified VP1-J8 capsomeres did bind to Superose™ 6 Increase and TSKgel® 3000/4000 size exclusion columns at low salt concentrations.

To assess the influences of DNA and NaCl on aggregation, VP1 capsomeres were purified as described. Running buffer for SEC polishing had a NaCl concentration of 0.5 M. The protein concentration of the purified sample was adjusted to 0.01 mg ml^{-1} and no residual DNA could be measured in the sample. The size distribution was measured using dynamic light scattering after which the sample was desalted into 0.1 M NaCl buffer. After desalting the DNA concentration increased to 0.09 ng µl^{-1} which might be residual DNA in the desalting column, contaminating the sample, or may not be a significant measurement noting the assay sensitivity is 0.2 ng µl^{-1}. The desalted sample was measured and to 1 ml of sample 100 µl of unsheared *E. coli* DNA solution (concentration 180 ng/µl) was added. After measurement of the light scattering NaCl was added to a final concentration of 1 M and the sample was incubated for 10 min before a subsequent measurements. As a reference, 100 µl of unsheared *E. coli* DNA solution in 1 ml of MQW was measured.

Samples were stored on ice until measurement. 1 ml of sample was equilibrated for 5 min to 20°C before starting the measurement. Each reported measurement is an average of 100 individual measurements. Analysis was done using the Zetasizer software by Malvern Technologies.

2.13 | Transmission electron microscope analysis

Samples measured via dynamic light scattering were also examined in a transmission electron microscope. Carbon coated square meshed grids (ProSciTec, standard A) were plasma cleaned for 15 s right before sample application. About 5 µl sample, diluted 1:10 with the corresponding buffer, was pipetted on the mesh and incubated for 5 min. After gently removing excess liquid with a tissue, the grid was washed twice with a drop of MQW to reduce salt crystals. The sample was subsequently stained for 2 min by negative staining using 2% w v^{-1} uranyl acetate. Transmission electron microscope (TEM) images were taken on a FEI Tecnai G2 Spirit equipped with an Olympus-SIS Veleta CCD camera at 120 kV voltage.

3 | RESULTS

3.1 | Molecular size distribution of VP1-J8 capsomeres in clarified supernatant at different salt concentrations using size exclusion chromatography

Purified VP1 capsomeres elute at a volume of 15 ml on a Superose™ 6 Increase 10/300 GL column (Ladd Effio, Baumann, et al., 2016). VP1-J8 capsomeres have a similar size to VP1 capsomeres (232 kDa vs. 212.3 kDa) and are therefore expected to elute at approximately

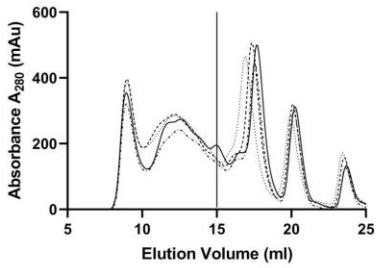

FIGURE 1 Size exclusion chromatogram of clarified supernatant containing VP1-J8 capsomeres at different NaCl concentrations of the sample. Running buffer had the same composition as the sample. Vertical line indicates the volume (15 ml) at which the capsomeres are expected to elute. (· · ·) 0.1 M NaCl, (- - -) 0.2 M NaCl, (- · - ·) 0.3 M NaCl, (—) 0.4 M NaCl

the same volume. Comparing the elution profile of clarified supernatant at different salt concentrations (Figure 1) no dedicated peak at 15 ml elution volume could be observed at salt concentrations of less than 0.3 M NaCl. However, using a salt concentration of 0.4 M NaCl a peak at 15 ml appeared, which was confirmed to be VP1-J8 by SDS-PAGE (Figure 2).

To measure the size distribution of VP1-J8 capsomeres and to verify the formation of aggregates, samples at different elution volumes from Superose™ 6 Increase were analyzed by SDS-PAGE (Figure 2). At salt concentrations lower than 0.3 M NaCl, the majority of VP1-J8 capsomeres were eluted at 9 ml (Figure 2a, 0 M NaCl), at 11 ml and 12 ml (Figure 2b, 0.1 M NaCl, and Figure 2c, 0.2 M NaCl), at 11 ml, 12 ml, and 14 ml (Figure 2d, 0.3 M NaCl). This result indicates the formation of VP1 complexes of several MDa size. In contrast, at salt concentrations above 0.3 M NaCl, capsomeres elute at the expected retention volume of ca. 15 ml (Figures 2e,f), indicating no or only minor extents of VP1 complexation.

3.2 | Particle size distribution of purified VP1-J8 capsomeres and VP1-J8–DNA complexes measured by dynamic light scattering (DLS)

Particle size distributions obtained by dynamic light scattering are shown in Figures 3 and 4. The particle size of purified VP1-J8 capsomeres in 0.5 M NaCl and 0.1 M NaCl buffer is nearly the same, at ca. 10 nm. At 0.1 M NaCl, a small amount of particles (< 5%) show a diameter of 20 nm. This is believed to be due to residual DNA in the desalting column that contaminated the sample, as verified by DNA content after desalting increasing from zero to 0.09 ng μl^{-1}. By adding unsheared DNA to VP1-J8 capsomeres, the signal changed drastically and particle diameters larger than 70 nm up to 1000 nm were measured. Unsheared *E. coli* DNA solution at 0 M NaCl, measured as a reference, showed a signal at around 20 nm diameter. The effect could also be reversed as shown in Figure 4. By adding sodium chloride to a final concentration of 1 M NaCl the aggregates broke up and the measured particle size of VP1-J8 plus DNA changed from > 90 nm to < 20 nm.

3.3 | TEM analysis of purified VP1-J8 capsomeres and VP1-J8–DNA complexes

Samples measured by DLS were also examined by TEM to confirm the DLS results. Purified VP1-J8 capsomeres are stable in 0.1 M NaCl and do not form aggregates (Figure 5a). After the addition of unsheared *E. coli* DNA irregular aggregates of different sizes are formed, as can been seen in Figure 5b. After subsequent addition of NaCl to a final concentration of 1 M, no aggregates could be observed, however very few spherical particles of 40–50 nm diameter could be seen (Figure 5c).

3.4 | Multimodal cation exchange chromatography on Capto™ MMC

Figure 6a shows the absorbance signal of the flow-through during loading. It can be seen, that loading resolubilized VP1-J8 (after PEG precipitation) in a lysis buffer containing 0.5 M NaCl leads to a significantly lower flow through signal (P1), indicating more VP1-J8 is binding on the column, compared with loading at 0 M NaCl (P2). The peak area of the flow through peak decreased from 5366.4 mAu s^{-1} when loaded at 0 M NaCl (P2) to 4791.7 mAu s^{-1} when loaded at 0.5 M NaCl (P1). The elution profile in Figure 6b shows two small elution peaks (P3.1 and P3.2), when loading was at 0 M NaCl, and only one large peak (P4), when loading was done at 0.5 M NaCl. Analyzing the peak areas of the elution peaks containing VP1-J8 showed a peak area of 527.8 mAu s^{-1} if loaded at 0.5 M NaCl (P4) and only 52.6 mAu s^{-1} if loaded at 0 M NaCl (P3.2). The elution peak area of 527.8 mAu s^{-1} approximates the difference in absorbance signals during loading (574.7 mAu s^{-1}) reasonably well, indicating, that the loaded material eluted completely at the chosen conditions and no material was permanently bound to the column. Therefore, it can be concluded that the binding on Capto™ MMC strongly increased and the recovery increased about 10 times.

The SDS-PAGE analysis of the process (Figure 7) revealed, that if loading was done at 0 M NaCl the majority of VP1-J8 did not bind to the column and remained in the flow through. In contrast, if loading was done at 0.5 M NaCl the majority of VP1-J8 did bind to the column. The first elution peak (P3.1), if loaded at 0 M NaCl, contained only trace amounts of protein, but did also contain DNA. Measured DNA concentration was 3 ng μl^{-1}. The second peak (P3.2) did contain some VP1-J8 at low concentrations and had a DNA content of 0.34 ng μl^{-1}. On the other hand, the whole elution peak after loading at 0.5 M NaCl (P4) did contain high amounts of VP1-J8 and low levels of DNA (0.46 ng μl^{-1}). The DNA concentration of the pre-purified sample was 110.6 ng μl^{-1}.

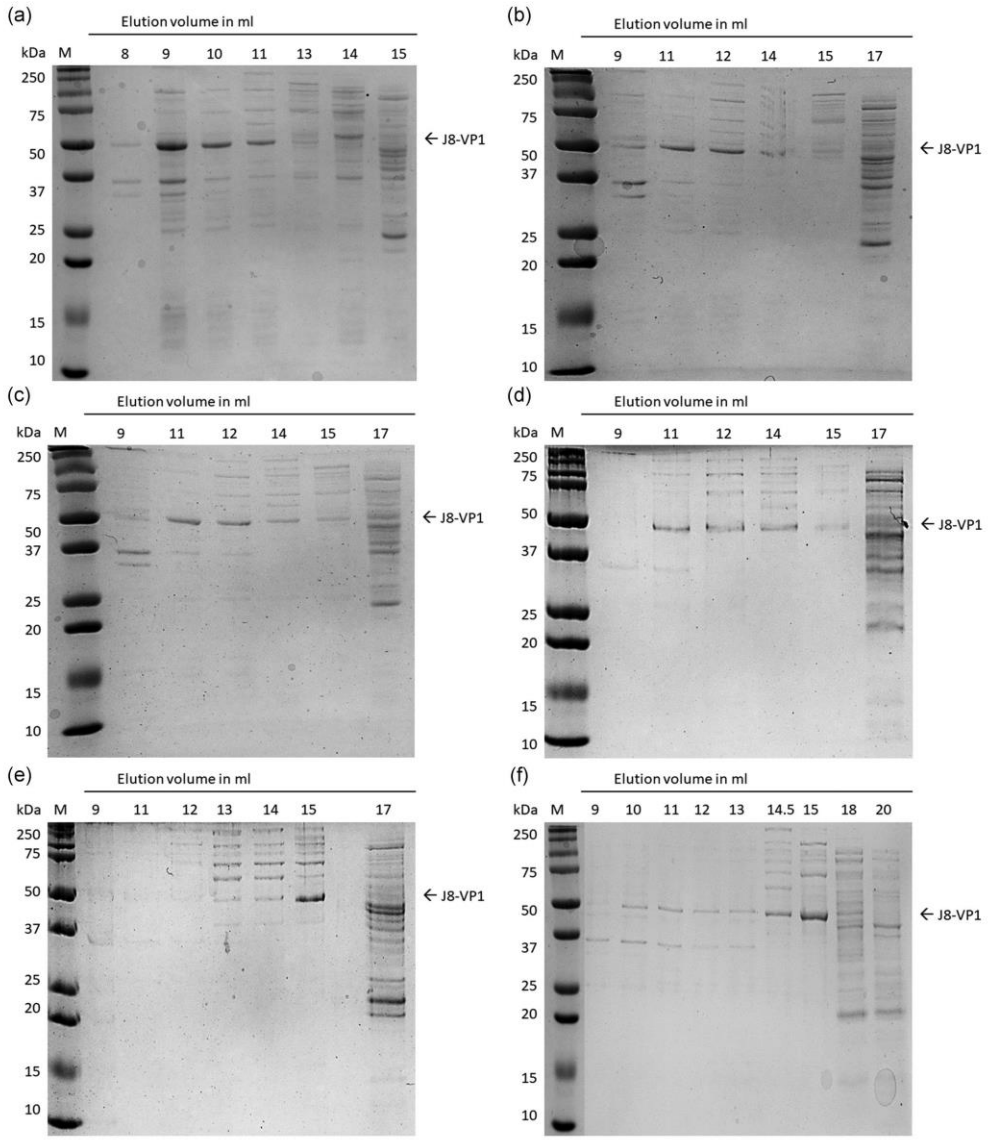

FIGURE 2 SDS-PAGE analysis of size exclusion fractions of clarified supernatant containing VP1-J8 at different salt concentrations and pH 8. (a) 0 M NaCl, (b) 0.1 M NaCl, (c) 0.2 M NaCl, (d) 0.3 M NaCl, (e) 0.4 M NaCl, (f) 0.5 M NaCl. SDS-PAGE, sodium dodecyl sulfate-polyacrylamide gel electrophoresis

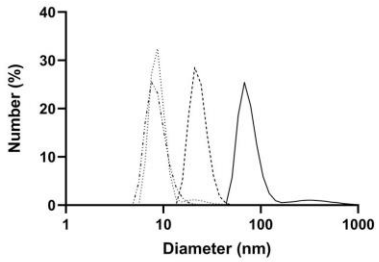

FIGURE 3 Size distribution of VP1-J8 capsomeres with and without DNA measured by dynamic light scattering at different buffer composition. (·····) VP1-J8 in 0.1 M NaCl, (-···-) VP1-J8 in 0.5 M NaCl, (- - -) DNA in 0 M NaCl (MQW), (—) VP1-J8 + DNA in 0.1 M NaCl

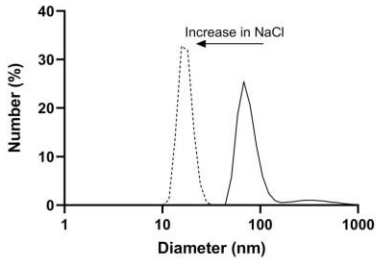

FIGURE 4 Size distribution of VP1-J8 capsomeres containing DNA, measured by dynamic light scattering, in 0.1 M NaCl (—) and after adding NaCl to a final concentration of 1 M NaCl (- - -)

3.5 | Anion exchange chromatography on Capto™ Q

Figure 8a,b shows chromatograms obtained for loading Capto™ Q at 0.1 M NaCl and 0.5 M NaCl, respectively. At low salt concentrations VP1-J8 binds to Capto™ Q, however the capacity is extremely low (< 0.2 mg ml^{-1}_{resin} at 2 min column residence time, data not shown). High overloading of the column does not result in significant increase of bound VP1-J8. Interestingly, elution experiments with a linear gradient reveal that the majority of VP1-J8 was eluted at the same salt concentration as it lost its affinity towards DNA (ca. 0.3 M NaCl) (chromatogram in supplementary data). If the loading was conducted at salt concentrations above 0.3 M NaCl, VP1-J8 remains in the flow through and DNA can be efficiently removed as it remains bound to the matrix. The DNA content of the pre-purified sample was 75 ng μl^{-1} and after flow through purification at 0.5 M NaCl loading condition, the DNA content was below the sensitivity of the DNA assay, with a measured value of 0.017 ng μl^{-1}. A comparison of the binding behavior on the two chromatographic matrixes is summarized in Table 2.

3.6 | Assembling of virus-like-particles

Both capsomeres obtained by anion exchanger and by multimodal cation exchanger could be assembled into virus-like-particles (determined by TEM, data not shown). Therefore, it can be assumed that the purification pathways do not alter protein integrity.

To test the influence of the presence of DNA on the assembling host cell DNA free VP1-J8 got spiked with DNA as described in Section 2.8 to obtain four samples (VP1-J8 with and without DNA in lysis buffer pH 8, at low and at high salt concentrations) were dialyzed against assembling buffer. TEM results are shown in Figure 9.

At initial NaCl concentrations of 0.5 M NaCl both samples without (Figure 9a) or with DNA (Figure 9b) assembled predominately into uniform capsid like structures around 45 nm in diameter. Also some smaller particles formed. The capsid like structures assembled without DNA showed a stronger internal staining compared with the one with DNA.

At low initial NaCl concentrations the protein–DNA complexes could not be assembled into capsid like structures (Figure 9c). Instead worm like structures of different sizes formed as well as small spherical particles less than 20 nm. On the other hand, if no DNA was present at low NaCl concentrations (Figure 9d), capsid like structures formed as well as smaller spherical particles of different size. Compared with the samples with higher initial NaCl, the samples with lower NaCl concentrations were less uniform.

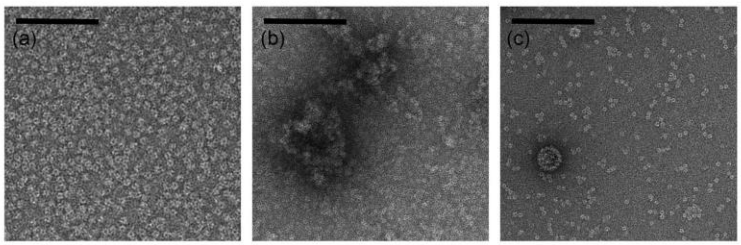

FIGURE 5 (a) Transmission electron microscope image of purified VP1-J8 capsomeres in 0.1 M NaCl buffer pH 8, containing no DNA. (b) Purified VP1-J8 capsomeres plus unsheared *E. coli* DNA in 0.1 M NaCl buffer pH 8. (c) The same sample as in (b) after the addition of NaCl to a final concentration of 1 M. The scale bar corresponds to 100 nm distance

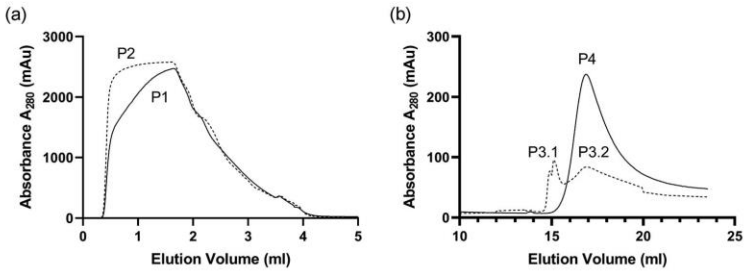

FIGURE 6 (a) Column loading. Absorbance at 280 nm obtained from the flowthrough while loading 2 ml of resolubilized VP1-J8 (after PEG precipitation) at NaCl concentrations of 0.5 M (—) or 0 M (- --) at pH = 8 onto a 1 ml multimodal weak cation exchanger (Capto™ MMC), loading started at 0 ml (b) Column eluting. Elution profile after loading resolubilized VP1-J8 (after PEG precipitation) at NaCl concentrations of 0.5 M (—) or 0 M (- - -) at pH = 8 onto a 1 ml multimodal weak cation exchanger (Capto™ MMC). Elution was obtained by applying a step gradient of 1 M NaCl phosphate buffer at pH 12 starting at 13.5 ml. The elution buffer had a different absorbance compared to the binding buffer, caused by the instability of DTT, resulting in a baseline shift towards the end of the chromatogram

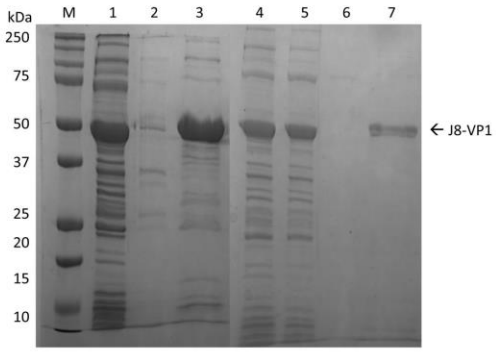

FIGURE 7 SDS-PAGE analysis of the bind and elute experiments of VP1-J8 onto Capto™ MMC (Figure 6). Lanes (1) and (4) correspond to the starting material used for loading at 0.5 M NaCl (lane 1) and 0 M NaCl (lane 4). (2) Flow through of loading at 0.5 M NaCl, (3) Elution after loading at 0.5 M NaCl, (5) Flow through of loading at 0 M NaCl, (6) First elution peak after loading at 0 M NaCl, (7) Second elution peak after loading at 0 M NaCl. SDS-PAGE, sodium dodecyl sulfate-polyacrylamide gel electrophoresis

4 | DISCUSSION

One of the major issues of purifying viral capsomeres and viral structures, either as a wild type or presenting a foreign antigen, is the poor binding onto chromatographic media and hence low recovery yields. That VP1 capsomeres in crude lysate form soluble aggregates of different size, is an observation that has already been made (Lipin et al., 2008). Different mechanisms have been suggested, for example polymerization because of the used GST tag or aggregation because of inserted hydrophobic antigens (Abidin et al., 2015; Lipin et al., 2008). These size exclusion experiments on GST-free nonpurified proteins show that nonpurified VP1-J8 forms aggregates below a NaCl concentration of 0.3 M. This can have various reasons, like salt dependent solubility, intermolecular attractions or the interaction with other molecules such as DNA. Polymerization because of affinity tags however, can be excluded as no affinity tag is used in these experiments.

Light scattering experiments of purified VP1-J8 revealed that purified VP1-J8 capsomeres are indeed stable at low salt concentrations and aggregates are formed due to an interaction with DNA. It could also be shown that this is a reversible interaction, as the aggregates disassociate if the salt concentration is raised, indicating that the DNA VP1-J8 interaction is a nonspecific electrostatic interaction. The slight increase of the measured hydrodynamic size of dissociated capsomeres compared to the starting material before the addition of DNA might be a result of overlapping signals of DNA and capsomeres, as dynamic light scattering is not capable of resolving multiple narrow species. However, as this technique is in particular sensitive towards larger particles it can be assumed no aggregates were present. The results were verified by TEM showing no aggregated VP1-J8 at low salt concentrations in the absence of DNA, and irregular shaped aggregates after the addition of DNA and the formed aggregates could be dissociated by applying a high salt concentration. Why some large, capsid-like aggregates could be observed at the TEM of capsomeres in high salt (Figure 5c) can only be speculated as there was no calcium in the solution, which is considered to be mandatory for self-assembling of VP1 capsomeres into well-formed virus-like-particles (Chuan et al., 2010; Schmidt et al., 2000). Maybe an increase of the hydrophobic attraction due to the high salt concentration and depleted DTT due to long exposure during processing, lead to a degree of capsomeres self-assembly, an effect that has also been observed in the past (Salunke et al., 1986). This process might be also mediated by "right sized" DNA fragments in the solution, supporting assembly, as a similar mechanism was proposed (Ou et al., 1999; Van Rosmalen et al., 2018).

To measure the influence of these aggregates on chromatographic purification, experiments with cation and anion exchangers

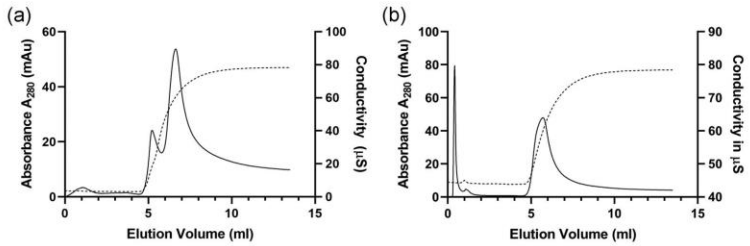

FIGURE 8 (a) Anion exchange chromatography elution of resolubilized VP1-J8 (after PEG precipitation) loaded on a 1 ml Capto™ Q column at 0.1 M NaCl, pH8. Only a minimal flow through can be observed and most of the protein, including VP1-J8 did bind to the column. VP1-J8 does elute in a first peak at 5 ml, followed by a peak of mostly impurities. (—) Absorbance A280, (- - -) Conductivity. (b) Anion exchange chromatography elution of resolubilized VP1-J8 (after PEG precipitation) loaded on a 1 ml Capto™ Q column at 0.5 M NaCl, pH8. VP1-J8 is not binding to the column and remains in the flow through that elutes at 0.5 ml. (—) Absorbance A280, (- - -) Conductivity

TABLE 2 Binding behavior of resolubilized (after PEG precipitation) VP1-J8 and DNA to a multimodal cation exchanger (Capto™ MMC) and a strong anion exchanger (Capto™ Q) at pH 8

	Capto™ MMC		Capto™ Q	
Loading buffer	VP1-J8 binding	DNA binding	VP1-J8 binding	DNA binding
pH 8 c(NaCl) < 0.3 M	Very low	Low	Very low	High
pH 8 c(NaCl) > 0.3 M	High	None	None	High

Note: At salt concentrations < 0.3 M NaCl VP1-J8 is binding to DNA and forming complexes.

were conducted. The assumption was that, in an aggregated form, the capsomeres cannot access the pores of chromatographic resin which typically have a diameter of roughly 40–80 nm, and therefore can only bind to the outer surface, leading to very low binding capacitates (J. Avallin et al., 2016). This assumption was proven as only minor amounts of VP1-J8 bound on multimodal cation exchanger columns (Capto™ MMC) when loaded at low salt concentrations. A pure cation exchanger like Capto™ S showed comparable low binding capacities at low salt concentrations (data not shown). Using a salt-tolerant cation exchanger (Capto™ MMC), which keeps a high binding capacity over a broad range of salt concentrations, it could be shown that the binding increased dramatically, and the majority of VP1-J8 protein was captured, if a salt concentration above the dissociation concentration was used. The enhanced binding leads to an increased recovery during the chromatographic purification. This can be explained by the fact that now non-aggregated capsomeres, having a size of 10–15 nm, could access the pores in the resin.

Another phenomenon was observed, namely that at low salt concentrations not only the capsomeres bound to a cation exchanger column, but also DNA. As DNA usually does not bind to a cation exchanger at pH 8, it likely bound to the capsomeres that were captured on the column, suggesting again the existence of DNA–protein complexes.

A purification method for viral capsomeres and viral capsids, proposed in the literature, is the use of strong anion-exchange membrane columns in bind and elute mode (Ladd Effio, Baumann, et al., 2016). Interestingly the capsomeres do bind to Capto Q resins, a strong anion exchanger, at the same pH value (pH 8) as they do bind to cation exchangers (Capto™ S, POROS™ HS, and Capto™ MMC). These experiments show that at low salt concentrations VP1-J8 binds to the column, however the capacity is extremely low, which again can be explained by poor accessibility to matrix pores, because of formed DNA–protein aggregates. The formation of aggregates also explains the comparably high reported capacities on membrane columns (Ladd Effio, Hahn, et al., 2016). Another interesting fact is that the capsomeres elute from anion exchangers at the same salt

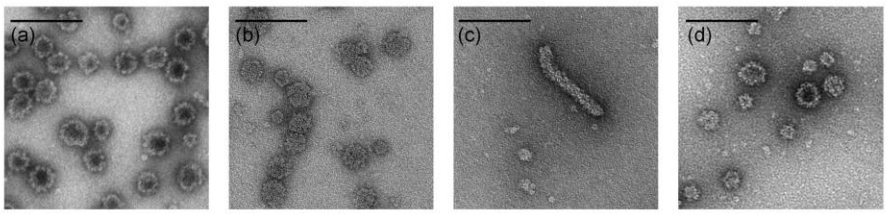

FIGURE 9 Assembly products of VP1 with and without DNA at different initial NaCl concentrations. Scale bar represents 100 nm. (a) 0.5 M NaCl no DNA. (b) 0.5 M NaCl plus DNA. (c) 0.1 M NaCl plus DNA. (d) 0.1 M NaCl no DNA

concentration as the DNA–protein aggregates dissociate, opening the question of the binding mechanism. Instead of actually binding onto the column proper, the VP1 capsomeres might actually bind to DNA, which then binds to the anion exchanger in a layer-by-layer process. This might be an explanation for the strange binding isotherms described for Sf9 insect cell-derived virus-like-particles, as the binding capacity would be dependent on the protein–DNA ratio (Ladd Effio, Hahn, et al., 2016).

Some DNA interactions with VP1 capsomere have been previously described. Early research found that VP1 capsomeres show a high affinity towards DNA, that this affinity is not sequence specific, and that VP1 capsomeres do elute from a DNA–cellulose column at salt concentrations between 0.3 and 0.4 M NaCl (Chang et al., 1993; Moreland et al., 1991). This is congruent with the observation that DNA–VP1-J8 complexes dissociate at NaCl concentrations above 0.3 M and also explains that the DNA–protein complexes can form with bacterial DNA or DNA of other sources. DNA–protein complex formation was also found by Štokrová et al. (1999) who showed that VP1 capsomeres coat circular DNA, as expected for viral packaging of nucleic acids in the native virus.

Another point is that the disassembly of polyomavirus results not only in free capsomeres but also in DNA–capsomere complexes (Brady et al., 1978). The reason why only some of the capsomeres form complexes, if viral capsids are dissembled, might be due the ratio of DNA to capsomeres, as there may have been insufficient DNA for all capsomeres to bind to.

The influence of DNA–capsomere interactions on production, stability, assembling, and purification of VP1 capsomeres has, however, been significantly underestimated. Especially if these capsomeres are produced in bacterial systems in an environment with excess DNA. Under such conditions it is highly likely that the majority of VP1 is bound to host-cell DNA, therefore forming large aggregates.

Assembling of capsomere–DNA complexes into VLPs was not possible in our experiments. Instead worm like aggregates of different sizes formed. These worm like aggregates do not form if the salt concentration is above the protein–DNA dissociation concentration and instead virus-like particle form, comparable to the assembly without DNA. The type and length of the present nucleic acid might play an important role on the shape and size of these aggregates (Ruiter et al., 2019) and comparable tubular aggregates can be found in the nucleus of infected cells (Erickson et al., 2012). Protein–DNA interactions therefore can be an explanation for at least some types of aggregates formed during assembly.

A recent study proposed that DNA can influence the assembly process beneficially, as less wrong size particles are formed (Van Rosmalen et al., 2018). This phenomenon however, could not be observed in our experiments as assembly products at high salt concentration, with or without DNA, showed well defined capsid like structures. Nevertheless, the presence of DNA seems to influence the assembly process and therefore the DNA–protein interaction needs to be tightly controlled to obtain reliable results. However, this topic still needs further investigation to understand the underlying mechanism.

Knowing that VP1 forms complexes with DNA at low salt concentrations, a few conclusions for purification can be made. At low salt concentrations VP1 or VP1 based vaccine candidates will bind onto conventional chromatographic media at low efficiency, as the complexes cannot enter the pores of the resin. An alternative is the use of membrane columns, monoliths or resins with large pores like POROS™ as shown in the literature (Ladd Effio, Baumann, et al., 2016). Another and preferable option is the use of conventional salt tolerant media like Capto™ MMC together with buffers having a salt concentration above the DNA–capsomere dissociation concentration, as they are widely available, cheap, and easy to scale. This approach leads to highly efficient binding and eradicates one of the main bottlenecks during purification.

DNA can only be efficiently removed if a salt concentration above the dissociation concentration is used during the process, as otherwise DNA and capsomeres will co-elute. Until complete removal of DNA, the capsomeres will be not stable in low salt concentration buffers. This is particularly important for alternative purification strategies like precipitation and extraction in which DNA is usually incompletely removed. The binding on anion exchangers might be mediated by DNA and therefore the ratio of DNA to VP1 in the lysate will affect the binding capacity and overall process behavior. It is furthermore not possible to assemble DNA–VP1 complexes into virus-like particles. Above the dissociating salt concentration, however, the presence of DNA seems not to affect the assembly negatively.

5 | CONCLUSION

Murine polyomavirus major capsid protein VP1 forms DNA–protein complexes of different sizes in buffers having low salt concentrations. It was shown that these aggregates have a significant impact on the bioprocessing of VP1 pentamers, as it was not possible to assemble these complexes into VLPs. Instead of spherical particles, tubular aggregates formed. Furthermore, the DNA–protein complexes lead to poor chromatographic recovery due to low pore accessibility. By increasing the salt concentration of the buffer above 0.3 M NaCl (pH 8) the DNA–protein complexes dissociate and uniform VLPs can be assembled even in the presence of DNA. The approach of processing VP1 in buffers having a NaCl concentration above the protein–DNA dissociation concentration dramatically improved the chromatographic binding behavior and the binding capacity increased by at least an order of magnitude. Those findings lead to the development of efficient purification strategies of VP1-J8, using salt tolerant multimodal cation exchanger, removing most of the host cell DNA and protein without significant product loss. Since DNA affinity is an inherent property of viral proteins, similar approaches are likely applicable for other viral proteins and will help to develop efficient bioprocessing strategies for viral proteins.

CONFLICT OF INTERESTS

The authors declare that there are no conflict of interests.

AUTHOR CONTRIBUTIONS

Lukas Gerstweiler conceived the original research idea, designed and performed the study, wrote the manuscript and carried out experimental work. Jingxiu Bi supervised the project and assisted with conceptualization and writing. Anton Middelberg supervised the project and contributed to conceptualization, experimental design and analysis, and writing. All authors reviewed and approved the manuscript.

DATA AVAILABILITY STATEMENT

The data that support the findings of this study are available from the corresponding author upon reasonable request.

ORCID

Lukas Gerstweiler https://orcid.org/0000-0002-2421-5503
Jingxiu Bi http://orcid.org/0000-0001-7056-8572
Anton Peter Jacob Middelberg http://orcid.org/0000-0001-5922-5704

REFERENCES

Abidin, R. S., Lua, L. H. L., Middelberg, A. P. J., & Sainsbury, F. (2015). Insert engineering and solubility screening improves recovery of virus-like particle subunits displaying hydrophobic epitopes. *Protein Science: A Publication of the Protein Society*, *24*(11), 1820–1828. https://doi.org/10.1002/pro.2775

Al-Barwani, F., Donaldson, B., Pelham, S. J., Young, S. L., & Ward, V. K. (2014). Antigen delivery by virus-like particles for immunotherapeutic vaccination. *Therapeutic Delivery*, *5*(11), 1223–1240. https://doi.org/10.4155/tde.14.74

Anggraeni, M. R., Connors, N. K., Wu, Y., Chuan, Y. P., Yap, P., Lua, L. H. L., & Middelberg, A. P. J. (2013). Sensitivity of immune response quality to influenza helix 190 antigen structure displayed on a modular virus-like particle. *Vaccine*, *31*(40), 4428–4435. https://doi.org/10.1016/j.vaccine.2013.06.087

Avallin, J., Nilsson, A., Asplund, M., Pettersson, N., Searle, T., & Jägersten, C. (2016). Columns upto 1600 mm in diameter packed with protein a chromatography medium using axial mechanical compression.

Bradford, M. M. (1976). A rapid and sensitive method for the quantitation of microgram quantities of protein utilizing the principle of protein-dye binding. *Analytical Biochemistry*, *72*(1-2), 248–254. https://doi.org/10.1016/0003-2697(76)90527-3

Brady, J. N., Winston, V. D., & Consigli, R. A. (1978). Characterization of a DNA-protein complex and capsomere subunits derived from polyoma virus by treatment with ethyleneglycol-bis-N,N'-tetraacetic acid and dithiothreitol. *Journal of Virology*, *27*, 193–204.

Bright, R. A., Carter, D. M., Daniluk, S., Toapanta, F. R., Ahmad, A., Gavrilov, V., & Ross, T. M. (2007). Influenza virus-like particles elicit broader immune responses than whole virion inactivated influenza virus or recombinant hemagglutinin. *Vaccine*, *25*(19), 3871–3878. https://doi.org/10.1016/j.vaccine.2007.01.106

Buch, M. H. C., Liaci, A. M., O'Hara, S. D., Garcea, R. L., Robert, L., Neu, U., & Stehle, T. (2015). Structural and functional analysis of murine polyomavirus capsid proteins establish the determinants of ligand recognition and pathogenicity. *PLoS Pathogens*, *11*(10), e1005104. https://doi.org/10.1371/journal.ppat.1005104

Carapetis, J. R., Steer, A. C., Mulholland, E. K., & Weber, M. (2005). The global burden of group A streptococcal diseases. *The Lancet Infectious Diseases*, *5*(11), 685–694. https://doi.org/10.1016/S1473-3099(05)70267-X

Carter, D. M., Darby, C. A., Lefoley, B. C., Crevar, C. J., Alefantis, T., Oomen, R., Anderson, S. F., Strugnell, T., Cortés-Garcia, G., Vogel, T. U., Parrington, M., Kleanthous, H., & Ross, T. M. (2016). Design and characterization of a computationally optimized broadly reactive hemagglutinin vaccine for H1N1 influenza viruses. *Journal of Virology*, *90*(9), 4720–4734. https://doi.org/10.1128/JVI.03152-15

Cavelti-Weder, C., Timper, K., Seelig, E., Keller, C., Osranek, M., Lässing, U., & Bachmann, M. F. (2016). Development of an interleukin-1β vaccine in patients with type 2 diabetes. *Molecular Therapy: The Journal of the American Society of Gene Therapy*, *24*(5), 1003–1012. https://doi.org/10.1038/mt.2015.227

Chang, D., Cai, X., & Consigli, R. A. (1993). Characterization of the DNA binding properties of polyomavirus capsid proteins. *Journal of Virology*, *67*(10), 6327–6331.

Chuan, Y. P., Yap, P., Fan, Y. Y., Lua, L. H. L., & Middelberg, A. P. J. (2010). Virus assembly occurs following a pH- or Ca2+-triggered switch in the thermodynamic attraction between structural protein capsomeres. *Journal of the Royal Society, Interface*, *7*(44), 409–421. https://doi.org/10.1098/rsif.2009.0175

Chuan, Y. P., Yap, P., Wibowo, N., Lua, L. H. L., Linda, H. L., & Middelberg, A. P. J. (2014). The economics of virus-like particle and capsomere vaccines. *Biochemical Engineering Journal*, *90*, 255–263. https://doi.org/10.1016/j.bej.2014.06.005

Cornuz, J., Zwahlen, S., Jungi, W. F., Osterwalder, J., Klingler, K., van Melle, G., & Cerny, T. (2008). A vaccine against nicotine for smoking cessation: A randomized controlled trial. *PLoS One*, *3*(6), e2547. https://doi.org/10.1371/journal.pone.0002547

Ding, Y., Chuan, Y. P., Yap, P.ang, He, L., & Middelberg, A. P. J. (2010). Modeling the competition between aggregation and self-assembly during virus-like particle processing. *Biotechnology and Bioengineering*, *107*(3), 550–560. https://doi.org/10.1002/bit.22821

Donaldson, B., Al-Barwani, F., Pelham, S. J., Young, K., Ward, V. K., & Young, S. L. (2017). Multi-target chimaeric VLP as a therapeutic vaccine in a model of colorectal cancer. *Journal for Immunotherapy of Cancer*, 5. https://doi.org/10.1186/s40425-017-0270-1

Donaldson, B., Lateef, Z., Walker, G. F., Young, S. L., & Ward, V. K. (2018). Virus-like particle vaccines: Immunology and formulation for clinical translation. *Expert Review of Vaccines*, *17*(9), 833–849. https://doi.org/10.1080/14760584.2018.1516552

Effio, C. L., & Hubbuch, J. (2015). Next generation vaccines and vectors: Designing downstream processes for recombinant protein-based virus-like particles. *Biotechnology Journal*, *10*(5), 715–727. https://doi.org/10.1002/biot.201400392

Erickson, K. D., Bouchet-Marquis, C., Heiser, K., Szomolanyi-Tsuda, E., Mishra, R., Lamothe, B., Garcea, R. L., & Robert, L. (2012). Virion assembly factories in the nucleus of polyomavirus-infected cells. *PLoS Pathogens*, *8*(4), e1002630. https://doi.org/10.1371/journal.ppat.1002630

Frazer, I. H. (2004). Prevention of cervical cancer through papillomavirus vaccination. *Nature Reviews Immunology*, *4*(1), 46–54. https://doi.org/10.1038/nri1260

Gillock, E. T., Rottinghaus, S., Chang, D., Cai, X., Smiley, S. A., An, K., & Consigli, R. A. (1997). Polyomavirus major capsid protein VP1 is capable of packaging cellular DNA when expressed in the baculovirus system. *Journal of Virology*, *71*(4), 2857–2865.

Guo, J., Zhou, A., Sun, X., Sha, W., Ai, K., Pan, G., & He, S. (2019). Immunogenicity of a virus-like-particle vaccine containing multiple antigenic epitopes of *Toxoplasma gondii* against acute and chronic toxoplasmosis in mice. *Frontiers in immunology*, *10*, 592. https://doi.org/10.3389/fimmu.2019.00592

Hume, H. K., Vidigal, J., Carrondo, M. J. T., Middelberg, A. P. J., Roldão, A., & Lua, L. H. L. (2019). Synthetic biology for bioengineering virus-like particle vaccines. *Biotechnology and Bioengineering*, *116*(4), 919–935. https://doi.org/10.1002/bit.26890

Johne, R., & Müller, H. (2004). Nuclear localization of avian polyomavirus structural protein VP1 is a prerequisite for the formation of virus-like particles. *Journal of Virology*, *78*(2), 930–937. https://doi.org/10.1128/JVI.78.2.930-937.2004

Ladd Effio, C., Baumann, P., Weigel, C., Vormittag, P., Middelberg, A., & Hubbuch, J. (2016). High-throughput process development of an alternative platform for the production of virus-like particles in *Escherichia coli*. *Journal of Biotechnology*, *219*, 7–19. https://doi.org/10.1016/j.jbiotec.2015.12.018

Ladd Effio, C., Hahn, T., Seiler, J., Oelmeier, S. A., Asen, I., Silberer, C., & Hubbuch, J. (2016). Modeling and simulation of anion-exchange membrane chromatography for purification of Sf9 insect cell-derived virus-like particles. *Journal of Chromatography A*, *1429*, 142–154. https://doi.org/10.1016/j.chroma.2015.12.006

Li, P. P., Naknanishi, A., Tran, M. A., Ishizu, K.-I., Kawano, M., Phillips, M., & Kasamatsu, H. (2003). Importance of Vp1 calcium-binding residues in assembly, cell entry, and nuclear entry of simian virus 40. *Journal of Virology*, *77*(13), 7527–7538. https://doi.org/10.1128/JVI.77.13.7527-7538.2003

Liew, M. W. O., Rajendran, A., & Middelberg, A. P. J. (2010). Microbial production of virus-like particle vaccine protein at gram-per-litre levels. *Journal of Biotechnology*, *150*(2), 224–231. https://doi.org/10.1016/j.jbiotec.2010.08.010

Lipin, D. I., Lua, L. H. L., & Middelberg, A. P. J. (2008). Quaternary size distribution of soluble aggregates of glutathione-S-transferase-purified viral protein as determined by asymmetrical flow field flow fractionation and dynamic light scattering. *Journal of Chromatography A*, *1190*(1-2), 204–214. https://doi.org/10.1016/j.chroma.2008.03.032

Lipin, D. I., Raj, A., Lua, L. H. L., & Middelberg, A. P. J. (2009). Affinity purification of viral protein having heterogeneous quaternary structure: Modeling the impact of soluble aggregates on chromatographic performance. *Journal of Chromatography A*, *1216*(30), 5696–5708. https://doi.org/10.1016/j.chroma.2009.05.082

Lua, L. H. L., Connors, N. K., Sainsbury, F., Chuan, Y. P., Yap, P., Wibowo, N., & Middelberg, A. P. J. (2014). Bioengineering virus-like particles as vaccines. *Biotechnology and Bioengineering*, *111*(3), 425–440. https://doi.org/10.1002/bit.25159

Middelberg, A. P. J., Rivera-Hernandez, T., Wibowo, N., Lua, L. H. L., Fan, Y., Magor, G., & Batzloff, M. R. (2011). A microbial platform for rapid and low-cost virus-like particle and capsomere vaccines. *Vaccine*, *29*(41), 7154–7162. https://doi.org/10.1016/j.vaccine.2011.05.075

Mobini, S., Chizari, M., Mafakher, L., Rismani, E., & Rismani, E. (2020). Computational design of a novel VLP-based vaccine for hepatitis B virus. *Frontiers in Immunology*, *11*, 2074. https://doi.org/10.3389/fimmu.2020.02074

Mohr, J., Chuan, Y. P., Yap, P., Wu, Y., Lua, L. H. L., & Middelberg, A. P. J. (2013). Virus-like particle formulation optimization by miniaturized high-throughput screening. *Methods*, *60*(3), 248–256. https://doi.org/10.1016/j.ymeth.2013.04.019

Moreland, R. B., Montross, L., & Garcea, R. L. (1991). Characterization of the DNA-binding properties of the polyomavirus capsid protein VP1. *Journal of Virology*, *65*(1168–1176), 1168–1176.

Ou, W. C., Wang, M., Fung, C. Y., Tsai, R. T., Chao, P. C., Hseu, T. H., & Chang, D. (1999). The major capsid protein, VP1, of human JC virus expressed in Escherichia coli is able to self-assemble into a capsid-like particle and deliver exogenous DNA into human kidney cells. *The Journal of General Virology*, *80*(Pt 1), 39–46. https://doi.org/10.1099/0022-1317-80-1-39

Pattenden, L. K., Middelberg, A. P. J., Niebert, M., & Lipin, D. I. (2005). Towards the preparative and large-scale precision manufacture of virus-like particles. *Trends in Biotechnology*, *23*(10), 523–529. https://doi.org/10.1016/j.tibtech.2005.07.011

Pattinson, D. J., Apte, S. H., Wibowo, N., Chuan, Y. P., Rivera-Hernandez, T., Groves, P. L., & Doolan, D. L. (2019). Chimeric murine polyomavirus virus-like particles induce plasmodium antigen-specific CD8+ T cell and antibody responses. *Frontiers in Cellular and Infection Microbiology*, *9*, 215. https://doi.org/10.3389/fcimb.2019.00215

Rivera-Hernandez, T., Hartas, J., Wu, Y., Chuan, Y. P., Lua, L. H. L., Good, M., & Middelberg, A. P. J. (2013). Self-adjuvanting modular virus-like particles for mucosal vaccination against group A streptococcus (GAS). *Vaccine*, *31*(15), 1950–1955. https://doi.org/10.1016/j.vaccine.2013.02.013

Ruiter, M. V., de van der Hee, R. M., Driessen, A. J. M., Keurhorst, E. D., Hamid, M., & Cornelissen, J. J. L. M. (2019). Polymorphic assembly of virus-capsid proteins around DNA and the cellular uptake of the resulting particles. *Journal of Controlled Release*, *307*, 342–354. https://doi.org/10.1016/j.jconrel.2019.06.019

Salunke, D. M., Caspar, D. L. D., & Garcea, R. L. (1986). Self-assembly of purified polyomavirus capsid protein VP1. *Cell*, *46*(6), 895–904. https://doi.org/10.1016/0092-8674(86)90071-1

Schmidt, U., Rudolph, R., & Bohm, G. (2000). Mechanism of assembly of recombinant murine polyomavirus-like particles. *Journal of Virology*, *74*(4), 1658–1662. https://doi.org/10.1128/JVI.74.4.1658-1662.2000

Seth, A., Kong, I. G., Lee, S.-H., Yang, J.-Y., Lee, Y.-S., Kim, Y., & Kweon, M.-N. (2016). Modular virus-like particles for sublingual vaccination against group A streptococcus. *Vaccine*, *34*(51), 6472–6480. https://doi.org/10.1016/j.vaccine.2016.11.008

Simon, C., Schaepe, S., Breunig, K., & Lilie, H. (2013). Production of polyomavirus-like particles in a Klgal80 knockout strain of the yeast Kluyveromyces lactis. *Preparative Biochemistry & Biotechnology*, *43*(2), 217–235. https://doi.org/10.1080/10826068.2012.750613

Štokrová, J., Palková, Z., Fischer, L., Richterová, Z., Korb, J., Griffin, B. E., & Forstová, J. (1999). Interactions of heterologous DNA with polyomavirus major structural protein, VP1. *FEBS Letters*, *445*(1), 119–125. https://doi.org/10.1016/S0014-5793(99)00003-4

Tekewe, A., Connors, N. K., Middelberg, A. P. J., & Lua, L. H. L. (2016). Design strategies to address the effect of hydrophobic epitope on stability and in vitro assembly of modular virus-like particle. *Protein Science: A Publication of the Protein Society*, *25*(8), 1507–1516. https://doi.org/10.1002/pro.2953

Tekewe, A., Connors, N. K., Sainsbury, F., Wibowo, N., Lua, L. H. L., Linda, H. L., & Middelberg, A. P. J. (2015). A rapid and simple screening method to identify conditions for enhanced stability of modular vaccine candidates. *Biochemical Engineering Journal*, *100*, 50–58. https://doi.org/10.1016/j.bej.2015.04.004

Tekewe, A., Fan, Y., Tan, E., Middelberg, A. P. J., & Lua, L. H. L. (2017). Integrated molecular and bioprocess engineering for bacterially produced immunogenic modular virus-like particle vaccine displaying 18 kDa rotavirus antigen. *Biotechnology and Bioengineering*, *114*(2), 397–406. https://doi.org/10.1002/bit.26068

Teunissen, E. A., de Raad, M., & Mastrobattista, E. (2013). Production and biomedical applications of virus-like particles derived from polyomaviruses. *Journal of Controlled Release*, *172*(1), 305–321. https://doi.org/10.1016/j.jconrel.2013.08.026

The World Bank (2018). Summary of chapter 1: Ending global poverty. Retrieved from http://pubdocs.worldbank.org/en/911401537279777945/PSPR2018-Ch1-Summary-EN.pdf

Van Rosmalen, M. G. M., Li, C., Zlotnick, A., Wuite, G. J. L., & Roos, W. H. (2018). Effect of dsDNA on the assembly pathway and mechanical strength of SV40 VP1 virus-like particles. *Biophysical Journal*, *115*(9), 1656–1665. https://doi.org/10.1016/j.bpj.2018.07.044

VBI Vaccines Inc. (2018). Immunogenicity and safety of Sci-B-Vac™ to Engerix-B® in adults ≥ 18 years old and superiority in adults ≥ 45 years old.: ClinicalTrials.gov Identifier: NCT03393754. *National Library of Medicine*. https://clinicaltrials.gov/ct2/show/NCT03393754

Vekemans, J., Gouvea-Reis, F., Kim, J. H., Excler, J.-L., Smeesters, P. R., O'Brien, K. L., & Kaslow, D. C. (2019). The path to group A *Streptococcus* vaccines: World Health Organization research and development technology roadmap and preferred product characteristics. *Clinical Infectious Diseases*, *69*(5), 877–883. https://doi.org/10.1093/cid/ciy1143

Wibowo, N., Chuan, Y. P., Lua, L. H. L., & Middelberg, A. P. J. (2013). Modular engineering of a microbially-produced viral capsomere vaccine for influenza. *Chemical Engineering Science*, *103*, 12–20. https://doi.org/10.1016/j.ces.2012.04.001

Wu, C.-Y., Yeh, Y.-C., Yang, Y.-C., Chou, C., Liu, M.-T., Wu, H.-S., & Hsiao, P.-W. (2010). Mammalian expression of virus-like particles for advanced mimicry of authentic influenza virus. *PLoS One*, *5*(3), e9784. https://doi.org/10.1371/journal.pone.0009784

Zaveckas, M., Goda, K., Ziogiene, D., & Gedvilaite, A. (2018). Purification of recombinant trichodysplasia spinulosa-associated polyomavirus VP1-derived virus-like particles using chromatographic techniques. *Journal of Chromatography B*, *1090*, 7–13. https://doi.org/10.1016/j.jchromb.2018.05.007

Zhai, L., Peabody, J., Pang, Y.-Y. S., Schiller, J., Chackerian, B., & Tumban, E. (2017). A novel candidate HPV vaccine: Ms2 phage VLP displaying a tandem HPV L2 peptide offers similar protection in mice to Gardasil-9. *Antiviral Research*, *147*, 116–123. https://doi.org/10.1016/j.antiviral.2017.09.012

Zhang, L., Lua, L. H. L., Middelberg, A. P. J., Sun, Y., & Connors, N. K. (2015). Biomolecular engineering of virus-like particles aided by computational chemistry methods. *Chemical Society Reviews*, *44*(23), 8608–8618. https://doi.org/10.1039/c5cs00526d

Zhou, X., Bai, H., Kataoka, M., Ito, M., Muramatsu, M., Suzuki, T., & Li, T.-C. (2019). Characterization of the self-assembly of New Jersey polyomavirus VP1 into virus-like particles and the virus seroprevalence in Japan. *Scientific Reports*, *9*(1), 13085. https://doi.org/10.1038/s41598-019-49541-y

SUPPORTING INFORMATION

Additional Supporting Information may be found online in the supporting information tab for this article.

How to cite this article: Gerstweiler, L, Bi, J, & Middelberg, A. P. J. Virus-like particle preparation is improved by control over capsomere-DNA interactions during chromatographic purification. *Biotechnology and Bioengineering*. 2021;118: 1688–1701. https://doi.org/10.1002/bit.27687

Chapter 5

Comparative Evaluation of Integrated Purification Pathways for Bacterial Modular Polyomavirus Major Capsid Protein VP1 to Produce Virus-Like Particles Using High Throughput Process Technologies

Based on the findings of Chapter 4 several integrated downstream processes for VP1-J8 VLPs were developed. Optimal process conditions were explored using high-throughput studies. The processes were characterized in terms of purity and product quality and comparatively evaluated.

Statement of Authorship

Title of Paper	Comparative evaluation of integrated purification pathways for bacterial modular polyomavirus major capsid protein VP1 to produce virus-like particles using high throughput process technologies
Publication Status	published
Publication Details	Lukas Gerstweiler, Jagan Billakanti, Jingxiu Bi, Anton P.J. Middelberg, Comparative evaluation of integrated purification pathways for bacterial modular polyomavirus major capsid protein VP1 to produce virus-like particles using high throughput process technologies, Journal of Chromatography A, Volume 1639, 2021 https://doi.org/10.1016/j.chroma.2021.461924

Principal Author

Name of Principal Author (Candidate)	Lukas Gerstweiler		
Contribution to the Paper	Conceptualization, Methodology, Investigation, Writing – original draft, Visualization		
Overall percentage	80%		
Signature		Date	4.4.2022

Co-Author Contributions

By signing the Statement of Authorship. Each author certifies that:

I. The candidate's stated contribution to the publication is accurate (as detailed above)

II. Permission is granted for the candidate in include the publication in the thesis; and

III. The sum of all co-author contribution is equal to 100% less the candidate's stated contribution

Name of Co-Author	Jagan Billakanti		
Contribution to the Paper	Conceptualization, Methodology, Writing – review & editing		
Signature		Date	31/3/22

Name of Co-Author	Jingxiu Bi		
Contribution to the Paper	Conceptualization, Resources, Writing – review & editing, Supervision		
Signature		Date	31/03/2022

Name of Co-Author	**Anton P.J. Middelberg**		
Contribution to the Paper	Conceptualization, Resources, Writing – review & editing, Supervision, Project administration		
Signature		Date	

30 March 2022

Journal of Chromatography A 1639 (2021) 461924

Contents lists available at ScienceDirect

Journal of Chromatography A

journal homepage: www.elsevier.com/locate/chroma

Comparative evaluation of integrated purification pathways for bacterial modular polyomavirus major capsid protein VP1 to produce virus-like particles using high throughput process technologies

Lukas Gerstweiler[a], Jagan Billakanti[b], Jingxiu Bi[a], Anton Middelberg[c,*]

[a] The University of Adelaide, School of Chemical Engineering and Advanced Materials, Adelaide, SA 5005, Australia
[b] Cytiva, Product and Application Specialist Downstream Design-In ANZ, Suite 547, Level 5, 7 Eden Park Drive, Macquarie Park, NSW 2113, Australia
[c] The University of Adelaide, Division of Research and Innovation, Adelaide, SA 5005, Australia

ARTICLE INFO

Article history:
Received 10 November 2020
Revised 11 January 2021
Accepted 16 January 2021
Available online 21 January 2021

Keywords:
Virus-like particles
Downstream processing
VP1
High-throughput development
Multi modal chromatography

ABSTRACT

Modular virus-like particles and capsomeres are potential vaccine candidates that can induce strong immune responses. There are many described protocols for the purification of microbially-produced viral protein in the literature, however, they suffer from inherent limitations in efficiency, scalability and overall process costs. In this study, we investigated alternative purification pathways to identify and optimise a suitable purification pathway to overcome some of the current challenges. Among the methods, the optimised purification strategy consists of an anion exchange step in flow through mode followed by a multi modal cation exchange step in bind and elute mode. This approach allows an integrated process without any buffer adjustment between the purification steps. The major contaminants like host cell proteins, DNA and aggregates can be efficiently removed by the optimised strategy, without the need for a size exclusion polishing chromatography step, which otherwise could complicate the process scalability and increase overall cost. High throughput process technology studies were conducted to optimise binding and elution conditions for multi modal cation exchanger, Capto™ MMC and strong anion exchanger Capto™ Q. A dynamic binding capacity of 14 mg ml^{-1} was achieved for Capto™ MMC resin. Samples derived from each purification process were thoroughly characterized by RP-HPLC, SEC-HPLC, SDS-PAGE and LC-ESI-MS/MS Mass Spectrometry analytical methods. Modular polyomavirus major capsid protein could be purified within hours using the optimised process achieving purities above 87% and above 96% with inclusion of an initial precipitation step. Purified capsid protein could be easily assembled *in-vitro* into well-defined virus-like particles by lowering pH with addition of calcium chloride to the eluate. High throughout studies allowed the screening of a vast design space within weeks, rather than months, and unveiled complicated binding behaviour for Capto™ MMC.

1. Introduction

The current outbreak of COVID-19 shows dramatically the threat of global pandemics and the need for potent vaccines that can be mass-manufactured efficiently. In a globally-mobile world pathogens such as corona virus, influenza virus, Ebola virus etc. can spread rapidly so keeping a local outbreak under control is challenging. Once emerged a sustainable control can only be achieved by mass vaccination as demonstrated for example for Polio and Measles [1–3]. An ideal vaccine candidate to do so is highly immunogenic, exceptionally safe and can be quickly mass produced. Another important point that is often neglected is the need for low production costs, thus enabling affordable to use in low income countries, which often suffer the most from infectious diseases and otherwise may function as a residual reservoir for global threat [4,5]. Conventional vaccines such as inactivated and attenuated viruses however, have a lengthy production time, expensive production costs and might be risky for people with immunodeficiency [6,7].

Promising future vaccine candidates that incorporate most of the desired properties are virus-like particles (VLPs). VLPs are self-assembled spherical particles of viral structural proteins, mimicking the overall appearance and structure of a native virus and due to a lack of genetic material are unable to replicate or infect, making them generally safe [8]. As the antigens are presented in a highly repetitive and native structure, VLPs induce a strong immunogenic response both humoral and cellular, even

* Corresponding author.
E-mail address: anton.middelberg@adelaide.edu.au (A. Middelberg).

https://doi.org/10.1016/j.chroma.2021.461924
0021-9673/

in the absence of any adjuvant [9]. The structural viral proteins can be amended to present foreign antigens on the surface of the VLP. These so called modular or chimeric VLPs widen the possible applications and enabled the development of vaccine platform technologies [10,11]. VLPs as vaccines are commercially available against human papilloma virus and hepatitis B/E virus (Cervarix®, Gardasil®, Cecolin®, Recombivax HB®, Energix-B®, Hecolin® etc.) and are heavily examined against many diverse pathogens including influenza A, Norovirus, Chikungunya virus, cytomegalovirus, rotavirus and Group A Streptococcus, to name a few [8,12–15]. However, the production and purification of existing commercial VLPs is challenging, making them comparatively expensive vaccines [11,16,17]. VLPs can be expressed in a variety of eukaryotic and prokaryotic systems, ranging from mammalian and insect cells to microbial, yeast and plant based systems [18]. Expression in eukaryotic cells leads to self-assembly of VLPs *in vivo*, which always bears the risk of co-assembled impurities such as host cell proteins and nucleic acids, therefore leading to product deviations that require a subsequent disassembly-reassembly step [19,20]. Another pathway is the expression in prokaryotic systems, which allow the purification of unassembled structural protein and a subsequent *in vitro* assembly in a controlled environment [20–22].

VLPs produced in a prokaryotic expression system are an exciting alternative due to their inherent advantages over eukaryotic ones in terms of speed and productivity, enabling possible costs of cents per vaccine dose [23–25]. China approved *E. coli* produced VLP vaccines Hecolin® and Cecolin® showing high efficiency and safety and providing proof of concept for *E. coli* produced VLP vaccines [26,27]. Several modular and non-modular VLPs based on a variety of structural viral protein such as hepatitis B core antigen (HBcAg), papilloma major capsid protein L1, bacteriophage Qβ, adeno-associated virus structural protein VP3 and polyomavirus major capsid protein VP1 have been produced in *E. coli* [24,25,28,29]. One of the most advanced approaches is the platform technology using modularized murine polyomavirus major capsid protein VP1 [10]. The viral protein can be expressed at grams per litre in *E. coli* giving VLPs able to induce a strong immune response against Group A Streptococcus, Influenza, Rotavirus, Plasmodium, and others [12,13,30–33]. However, described purification and production pathways for VP1, the related L1 and other microbial VLPs currently rely on hard-to-scale laboratory unit operations. Major issues during purification are the removal of DNA and aggregates and low binding on chromatographic resin caused by aggregates and the large size of capsomeres and VLPs [34–37]. Common practice is the use of affinity tags (GST, poly HIS, SUMO), which require a subsequent enzymatic cleavage and removal of the tag, leading to aggregation during long processing times and other process challenges, and subsequent preparative size exclusion chromatography (SEC) followed by dialysis to trigger assembly [10,34,38,39]. Other described pathways use furthermore various combinations of density gradient centrifugation, benzonase treatment, filtration, membrane columns, refolding of inclusion bodies and ammonium sulphate/PEG precipitation [27,34,35,40–42].

To overcome these challenges, we developed and optimised an integrated purification process using multi modal cation exchanger Capto^{TM} MMC as the main purification step. Multi modal ion exchange resin combines ion exchange with hydrophobic interaction and other modes, which lead to unique binding behaviour and high salt tolerance [43]. The salt tolerance of Capto^{TM} MMC enables processing at intermediate salt concentrations, which enables disaggregation of non-specific DNA-protein interactions, which otherwise hinder separation. The developed process produces well defined VLPs, removes aggregates, DNA and most host cell proteins, is designed for scale-up and does not require any buffer exchange during the optimized purification process, thus reducing overall process cost and time.

2. Material and methods

2.1. Buffers and chemicals

Milli-Q® water (MQW) was used for the preparation of all buffers. *E. coli* culture was grown in Terrific Broth (TB) medium (12 g l^{-1} tryptone (LP0042, Thermo Fisher Scientific, USA), 24 g l^{-1} yeast extract (P0021, Thermo Fisher Scientific, USA), 5 g l^{-1} Glycerol (GL010, ChemSupply, Australia), 2.31 g l^{-1} potassium dihydrogen phosphate (PO02600, ChemSupply Australia), 12.5 g l^{-1} dipotassium hydrogen phosphate (PA020. ChemSupply, Australia)), supplemented with 35 µg ml^{-1} chloramphenicol (GA0258, ChemSupply, Australia) and 100 µg ml^{-1} ampicillin (GA0283, ChemSupply, Australia). IPTG (15529019, Thermo Fisher Scientific. USA) and antibiotics were prepared in 1000x stock solutions and added before use. Sodium chloride (SL046, ChemSupply, Australia) solution, 9 g l^{-1}, was used as a washing saline.

Loading buffer (L buffer) consisted of 40mM buffer salt (Tris-hydrochloride (GB4431, ChemSupply, Australia) for pH 8 and 9, Glycine (GA007, ChemSupply, Australia) for pH 10 and sodium hydrogen orthophosphate (SL061, ChemSupply, Australia) for pH 11 and 12 buffer preparation) plus 2mM EDTA (EA023, ChemSupply, Australia), 5 % w w^{-1} glycerol, 5mM dithiothreitol (DTT) (DL131, ChemSupply, Australia) and 0–500 mM NaCl (SL046, ChemSupply, Australia). DTT and 1x SigmaFast^{TM} protease inhibitor (SA8820 Millipore Sigma, USA), which were added during cell lysis, were added freshly before use. Loading buffer was prepared from a 5x stock solution originally prepared, filtered (0.2 µm, KYL Scientific, Australia) and vacuum degassed before use. Calcium chloride (CA033, ChemSupply, Australia) was used to induce the assembly of VLPs.

TruPAGE^{TM} 4x LDS sample buffer (PCG3009) and 20x Tris-MOPS SDS express running buffer (PCG3003) were purchased from MilliporeSigma, USA. The 10x DTT sample reducer and 800x running oxidant (sodium bisulfite, 243973, Millipore Sigma, USA) reagents were freshly prepared before use. For staining of SDS-APGE gels a solution containing Coomassie Brilliant Blue R-250 (Bio-Rad Laboratories, USA), and for destaining a mixture of 10 % v v^{-1} ethanol (EA043, ChemSupply, Australia) and 10 % v v^{-1} acetic acid (AA009, ChemSupply, Australia) was used.

HPLC grade acetonitrile (LC1005) and Trifluoroacetic Acid (TFA) (TS181) were purchased from Chem-Supply, Australia

PEG-6000 (PL113, ChemSupply, Australia) was used for precipitation experiments.

2.2. Plasmid construction and protein expression

Group A Streptococcus antigen GCN4-J8 was inserted with flanking G4S linkers into murine polyomavirus major capsid protein VP1 sequence (M34958) and cloned into pETDuet-1 at multiple cloning site 2 (MCS2) at *NdeI* and *PacI* restriction sites. The plasmid was constructed by the Protein Expression Facility of the University of Queensland, Brisbane, Australia and the sequence was verified by the Australian Genome Research facility (AGRF), Brisbane, Australia.

Rosetta^{TM} 2(DE3) Singles^{TM} competent cells (Merck KGaA, Germany) were used as an expression system. The VP1-J8 plasmid was transformed by heat shock transformation. In brief, competent cells were mixed with plasmid DNA and incubated on ice for 5 min, followed by a heat shock at 42°C for 30 s and 2 min cooling on ice. Subsequently, they were diluted with TOC medium and inoculated on TB agar plates containing 100 µg ml^{-1} ampicillin and 35 µg ml^{-1} chloramphenicol. The Master Cell Bank (MCB) glycerol stocks were produced by growing a single colony at 37°C in 50 ml TB medium in a 250 ml shake flask until an optical density OD_{600} of 0.5 AU was reached and subsequent adding of glycerol to a fi-

nal concentration of 25 % w w^{-1}. Samples of 100 µl were collected and vials stored at -80°C until further use.

Cells were grown overnight in 50 ml of TB medium containing 35 µg ml^{-1} chloramphenicol and 100 µg ml^{-1} ampicillin in a 250 ml shake flask at 37°C and 200 rpm. A 5 ml sample of the overnight culture was transferred into a 200 ml of fresh TB medium in a 1 l shake flask and cells were grown under the same conditions till an OD_{600} of 0.5 AU was reached. Protein expression was induced by adding IPTG to a final concentration of 0.1 mmol and performed for 16 h at a reduced temperature of 27°C and 200 rpm. Cells were harvested by centrifugation in an A5920R centrifuge (Eppendorf, Germany) at 3200 g for 10 min at 4°C, resuspended in 0.9 % w w^{-1} saline and split into 50 ml aliquots. After centrifugation for 10 min at 20,130 g at 4°C the supernatant was discarded and the pellets were stored at -80°C until further process.

Clarified lysate was produced by resuspending approximately 1 g of cell pellet per 50 ml of L buffer pH 8, 0 M NaCl on ice. Cells were disrupted by ultrasonic homogenization using a Scientz-IID Ultrasonic homogeniser (Ningbo Scientz Biotechnology, China) equipped with a 6 mm diameter horn. The suspension was sonicated with 10 s bursts at 400 W followed by 40 s cool down on ice, for a total time of 15 min. Subsequently the lysed cell suspension was centrifuged for 45 min at 20130 g at 4°C to remove cell debris.

2.3. Characterisation

Expression was visualised by SDS-PAGE analysis under reducing and denaturing conditions using TruPAGE™ precast Gels 4-12 %, 10 × 10 cm 12-well (PCG2003, Millipore Sigma, USA), following the manufacturer's protocol. Total protein concentration of the samples was measured by Bradford protein assay and the amount of protein loaded on each well was normalised. Samples were prepared by mixing with 4X loading buffer prior heating for 10 min at 75°C. Gel electrophoresis carried out at 180 V fixed current was applied for separation until finished, followed by 1 h of staining and 4 h of destaining using the described buffers. Precision Plus Protein™ Standard (1610363, Bio-Rad, USA) was used as a protein marker.

Bradford Protein Assay for determination of total protein concentration used standard protocol as described by BioRad in 200 µl 96 well plates format [44]. As a reference bovine serum albumin was used. Concentration of the reference solutions was verified by A_{280} absorbance on a NanoDrop™ (Thermo Fisher Scientific, USA).

Quant-iT™ High-Sensitivity dsDNA Assay Kit (Q33232, Thermo Fisher Scientific, USA) was used for quantification of host cell DNA. Fluorescence at 485/530 nm was measured on a 2300 Victor X5 multilabel reader (PerkinElmer, US). The DNA content is given as $g_{DNA}\ g_{protein}{}^{-1}$, which is measured by Bradford.

VP1-J8 concentration was measured by RP-HPLC using a method described in the literature [45–47], on a Shimadzu UFLC-XR system (pump: LC-20AD-XR, autosampler: SIL-20AXR, diode array detector: SPD-M20A, column oven: CTO-20) with detection at 280 nm. A Vydac Protein C4 column 2.1 × 100 mm, 5 µm (214TP521) was used. Briefly, samples were mixed 1:4 with denaturing buffer (8 M guanidine (GE1914, ChemSupply, Australia), 50 mM DTT, 20 mM Tris pH 8) and incubated at 75°C for 10 min. Samples, 3 µl, were injected and separated by gradient elution with a water (Mobile Phase A, 0.5 % TFA) and acetonitrile (Mobile Phase B, 0.4 % TFA) system. The elution program was as following: 6 min gradient from 35 % B to 60 % B, 30 s gradient from 60 % B to 100 % B, 1 min 100 % B, 30 s from 100 % B to 35 % B and 4 min of 35 % B, giving a total analysis time of 12 min, at a flow rate of 1 ml min^{-1} and a column temperature of 60°C. As a reference purified VP1-J8 was used of which the concentration was determined by Bradford assay.

The same Shimadzu system was used for SEC-HPLC with a TSKgel G3000SW column (5 μm, 7.8 × 300 mm, Tosoh Corp.). 40 % v v^{-1} acetonitrile, 0.1 v v^{-1} TFA was used as a running buffer at a flow rate of 1 ml min^{-1} and 30°C column temperature. Samples received no pre-treatment except filtering through a 0.22 µm cellulose acetate filter (THCCH2213, Thermo Fisher Scientific, USA). The peak areas at A_{280} nm were analysed and categorized into high-molecular-weight impurities (HMWI) and low-molecular-weight (LMHI) impurities depending on if they elute before or after the VP1-J8 peak. An example chromatogram can be found in the appendix (figure A1).

Aggregates were quantified by SEC chromatography with a Superose® 6 Increase 10/300 GL (Cytiva, Sweden) with L buffer pH 8, 0.5 M NaCl as a running buffer and a flow rate of 0.6 ml min^{-1} on an ÄKTA pure system equipped with a sample pump (Cytiva, Sweden). Aggregates have been defined as the fraction remaining in the excluded volume of the Superose® 6 column. The identity as VP1-J8 aggregates was verified by SDS-PAGE. Absorbance was measured at 280 nm and 260 nm. Aggregates are expressed as the peak area in relation to the VP1-J8 peak area.

Liquid chromatography–electrospray ionisation tandem mass spectrometry (LC-ESI-MS/MS was used to analyse and identify the protein bands in the purified samples. Mass spectrometric analysis was performed at the Adelaide Proteomic Centre, University of Adelaide. In brief gel bands were destained and dried followed by in-gel reduction plus alkylation and subsequent trypsin digestion. Peptide separation was performed using a 75 μm ID C18 column (Acclaim PepMap100 C18 75 μm × 15 cm, Thermo-Fisher Scientific, USA). Raw MS/MS data was searched against the target sequence of VP1-J8 and *E. coli* entries present in the Swiss-Pro database in Proteome Discovery (v.2.4, Thermo-Fisher Scientific, USA). Full protocol can be found in appendix.

Transmission electron microscopy (TEM) was used to analyse VLPs. Samples of 5 µl were diluted 1:10 with MQW and pipetted on carbon coated square meshed grids (GSCU100C, ProSciTec, Australia) and incubated for 5 min. After removal of excess liquid, the sample was washed twice with MQW to reduce the formation of salt crystals. Negative staining was conducted for 2 min with 2 % w v^{-1} uranyl acetate. A FEI Tecnai G2 Spirit with an Olympus SIS Veleta CCD camera was used to obtain images at 120 kV voltage. Particle diameter was measured by counting pixels using GIMP 2.10.18.

2.4. High throughput process technology strategies applied for studying binding capacity of resins

Briefly, 96 well PreDictor® (Cytiva, Sweden) plates filled with 20 µl of Capto™ MMC or Capto™ Q were used for high throughput binding screening. The pH values 7.5, 8.0, 8.5 and 9.0 and NaCl concentrations from 0–500 mM were screened. L buffers at the desired pH values, containing 0 M NaCl, were prepared 6 times concentrated as well as 3 M NaCl solution and a VP1-J8 stock solution. The stock solutions were finally mixed in the PreDictor® plate wells to a total volume of 300 µl (50 µl 6x L buffer, 0-50 µl 3 M NaCl, 0-50 µl MQW, 200 µl VP1-stock solution or MQW for equilibration). The protocol followed standard procedure. Solutions in the PreDictor® plates were removed by 2 min centrifugation at 500 g. The wells were equilibrated 3 times with desired buffer (5 min shaking at 1200 rpm). After equilibration, buffer with VP1-J8 stock solution instead of MQW was added and shacked for 60 min at 1200 rpm. The bound VP1-J8 was calculated by measuring the concentration in the unbound samples by HPLC and subtract it from the initial VP1-J8 concentration for loading. The DNA concentration was measured as described and compared to the initial DNA concentration for loading. The experiments were automated using a Microlab® Nimbus4® automated liquid handler (Hamilton,

USA). The results presented here are an average of duplicates (experiments and samples).

VP1-J8 stock solution was prepared by adding PEG-6000 and NaCl to a final concentration of 7 % w v^{-1} and 0.5 M respectively to clarified lysate to precipitate the VP1-J8 out. After gently shaking and 10 min incubation on ice, the precipitated VP1-J8 was separated by centrifugation at 20,130 g for 10 min at 4°C. The pellet was washed several times with 5 ml MQW to remove PEG and salts. Thereafter the pellet was resolubilized in 15 ml L buffer containing no buffer salt (MQW, 5 % w w^{-1} glycerol, 5 mM DTT, 2 mM EDTA, 1x protease inhibitor) and the pH was readjusted to 8.25. Any undissolved residues were removed by centrifugation for 10 min at 20130 g, 4°C, and filtering through a 0.22 µm filter (16532 Minisart®, Sartorius, Germany).

2.5. High throughput elution study

To establish the optimal elution conditions elution studies on 96 well PreDictor® plates filled with 20 µl Capto™ MMC were performed. Elution buffers at pH values of 8, 9, 10, 11, 12 and NaCl concentrations of 0–2 M were examined. Pipetting was done with a Nimbus automated liquid handler (Hamilton, US). L buffers at different pH values were prepared 2 times concentrated, as well as a 4 M NaCl stock solution and mixed to a final volume of 200 µl inside the wells (100 µl 2x L buffer, 0-100 µl 4 M NaCl solution and 0-100 µl MQW). The VP1-J8 stock solution was prepared as described in the previous section, except precipitated VP1-J8 was resolubilized in L buffer pH 8, 0.5 M NaCl (40mM Tris, 5 % w w^{-1} glycerol, 5 mM DTT, 2 mM EDTA, 1x protease inhibitor). Predictor plates were equilibrated 3 times for 5 min at 1200 rpm with L buffer pH 8, 0.5 M NaCl and loaded 60 min at 1200 rpm with 200 µl of VP1-J8 stock solution. After loading the wells were washed 3 times at 1200 rpms for 5 min with L buffer pH 8, 0.5 M NaCl containing no DTT, to remove optical interfering substances like oxidized DTT and other impurities. Two elution steps were conducted in which the wells were filled with elution buffers, incubated for 5 min at 1200 rpm and centrifuged for 2 min at 500 g. The Absorbance A_{280} of the eluent solution was measured on a 2300 Victor X5 multilabel reader (PerkinElmer, US). The absorbances of both elution steps were added and normalized to the measured maximum. The results presented here are an average of duplicates (experiments and samples).

2.6. Dynamic binding capacity

The resin dynamic binding capacity at 10 % breakthrough (DBC_{10}) was measured at a flow rate of 0.33 ml min^{-1} on a 1 ml pre-packed Capto™ MMC column. VP1-J8 stock solution (VP1-J8 concentration: 2.13 mg_{VP1-J8} ml^{-1}) at pH 8.9, 0.35 M NaCl, prepared as described by PEG precipitation, was used and loaded onto the column. The flowthrough was collected in 2 ml fractions and the VP1-J8 contend determined by RP-HPLC. To verify the results and to test the influence of the starting impurity level or product concentration, purified sample by Capto™ MMC were diluted with L buffer pH 8 and readjusted to pH 8.9, 0.35 M NaCl (VP1-J8 concentration: 0.79 mg_{VP1-J8} ml^{-1}), fractions were analysed by Bradford assay.

2.7. Process integration and further polishing

Several possible purification pathways in which Capto™ MMC is incorporated have been examined as shown in Fig. 1 (pathway A to F). Pathway A and B started with PEG precipitation, followed by Capto™ MMC purification and an additional polishing step, either by SEC or by Capto™ Q. Pathway C and D also started with PEG precipitation, however, followed by Capto™ Q flow through chromatography and either SEC or Capto™ MMC was used as a third/polishing purification step. Pathway E combined Capto™ Q with Capto™ MMC without a PEG precipitation. Pathway F combined diafiltration with Capto™ MMC.

PEG precipitation was conducted as described in Section 2.4, except the precipitate was resolubilized in L buffer pH 8.9, 0.35 M NaCl. Under this condition VP1-J8 bound strongly to Capto™ MMC and basically did not bind to Capto™ Q. The salt concentration in the load material also minimizes DNA-protein interaction and therefore beneficially influenced the purification process by minimising product loss in the first step. Capto™ Q flow through experiments were done either with a custom-packed column containing 14 ml of resin (XK 16/20 Column, Cytiva, Sweden) or with a 1 ml pre-packed column on an ÄKTA pure system at flow rates of 1 ml min^{-1} or 0.33 ml min^{-1} respectively with L buffer pH 8.9, 0.35 M NaCl as a running buffer. Samples obtained from Capto™ Q flowthrough, PEG precipitation or clarified lysate were loaded on 1 ml Capto™ MMC with L buffer pH 8.9, 0.35 M NaCl at a flow rate of 0.33 ml min^{-1}. Elution from Capto™ MMC was achieved by applying a step gradient with L buffer pH 12, 0 M NaCl at 1 ml min^{-1}. In the case in which Capto™ Q flow through purification was performed after Capto™ MMC, the sample was diluted 1:4 with L buffer pH 8 and the pH and NaCl concentration were adjusted to 8.9 and 0.35 M respectively. A Superose®6 (Cytiva, Sweden) column was used for SEC polishing with L buffer pH 8, 0.5 M NaCl at a flow rate of 0.6 ml min^{-1}. For batch diafiltration 15 ml Amicon® Ultra-15 centrifugal filter units with a molecular weight cut-off of 100 kDa were used (UFC9100, MilliporeSigma, USA). A sample of 15 ml crude lysate (pH 8.9, 0.35 M NaCl) was centrifuged at 5000 g till the volume reached 2 ml. It was then diluted 1:1 with L buffer pH 8.9 0.35 M NaCl, and centrifuged till a volume of 2 ml. This step was repeated 5 times and it took about 8 h.

2.8. Virus-like particle assembly

Purified VP1-J8 capsomeres were assembled by adding calcium chloride directly into the protein solution, based on a method described by Liew et al. [46].

Purified VP1-J8 capsomeres were obtained as described in Table 1 pathway E. Clarified supernatant was purified on Capto™ Q in flow through mode (pH 8.9, 0.35 M NaCl) and without further buffer adjustment loaded onto a 1 ml Capto™ MMC column. After loading, the column was washed for 10 CV with washing buffer without DTT (20mM Tris, 5 % w w^{-1} glycerol, 1 mM EDTA, 0.35 M NaCl, pH 8.9) and step eluted with a sodium hydrogen orthophosphate buffer at pH 12 containing 1 M NaCl (20mM sodium hydrogen orthophosphate, 5 % w w^{-1} glycerol, 1 mM EDTA, 1 M NaCl, pH 12). The increased NaCl was chosen as it supports VLP assembly. The eluate was diluted with elution buffer to a VP1-J8 concentration of 0.6 mg ml^{-1} and pH adjusted to pH 7.2 with HCl. After pH adjustment 100 mM $CaCl_2$ stock solution was added to a final concentration of 3 mM $CaCl_2$ and subsequently incubated for 12h at room temperature. The solution was analysed by TEM as described in Section 2.3.

3. Results

3.1. High throughput binding studies

Figs. 2 and 3 show contour plots of the static binding of VP1-J8 on Capto™ Q and Capto™ MMC resins, respectively. Fig. 4 shows bound DNA on Capto™ Q expressed as percent of the loaded DNA. Values in the figures are rounded to the closest colour level. For Capto™ MMC initially 29.1 mg VP1-J8 per ml resin was loaded, and for Capto™ Q 53.5 mg VP1-J8 per ml resin. In general, VP1-J8 showed poor binding affinity towards Capto™ Q at all examined

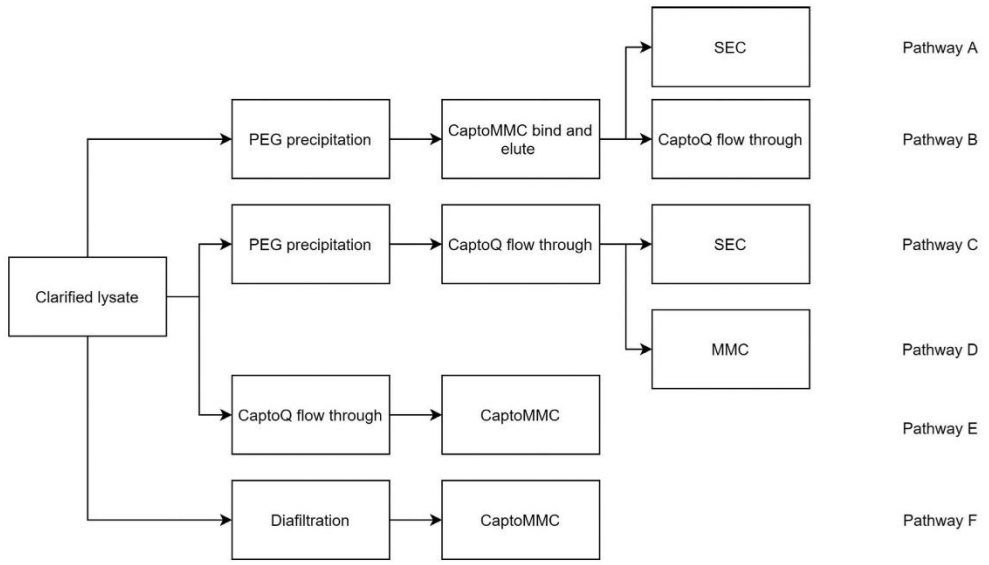

Fig. 1. Possible purification pathways examined in this research.

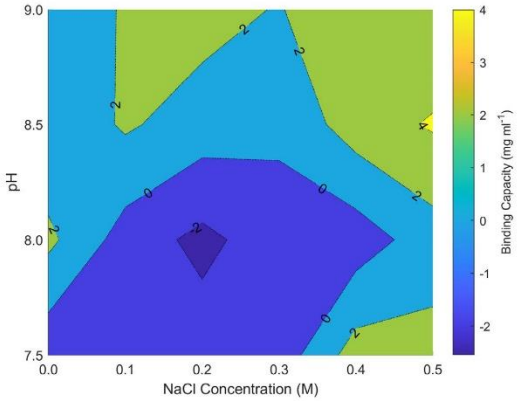

Fig. 2. Static binding of VP1-J8 on Capto™ Q measured with 20 µl PreDictor® plates in the range pH 7.5–9.0 and NaCl 0–0.5 M.

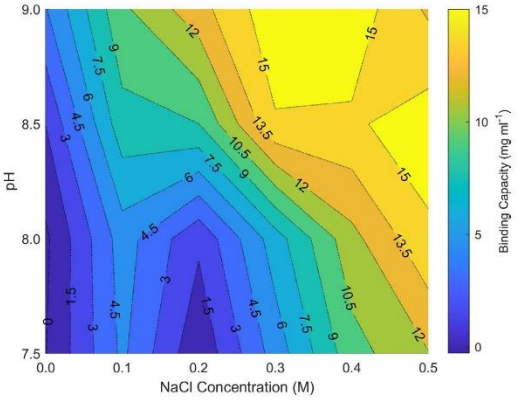

Fig. 3. Static binding of VP1-J8 on Capto™ MMC measured with 20 µl PreDictor® plates in the range pH 7.5–9.0 and NaCl 0–0.5 M.

conditions with a maximum measured binding capacity of 4.2 mg ml^{-1} at pH 8.5, 0.5 M NaCl and capacities ranging from -1.4 to 3.8 mg ml^{-1} at the other conditions. The negative value might be derived from measurement uncertainty, due to the high concentration of loaded material. Therefore, negative values should not be considered in this instance. The binding capacity slightly increased with increasing NaCl concentration. DNA binding on Capto™ Q was low if no NaCl was present in the buffer (< 5 % for pH 7.5–8.5, and 15 % at pH 9.0, 0 M NaCl in each case) and increased with increasing NaCl concentrations, eventually reaching an optimum at 0.3 M NaCl and decreased at higher NaCl concentrations. The highest DNA binding was measured at pH 7.5 at NaCl concentrations between 0.3 and 0.4 M, at which 38 % of the loaded DNA bound to the resin, as shown in Fig. 4.

In contrast, VP1-J8 showed a strong binding towards Capto™ MMC at elevated NaCl concentrations. The highest binding capacity was measured at pH 9, 0.3 M NaCl with 16.0 mg ml^{-1} and binding at 0 M NaCl was below 4 mg ml^{-1} at all pH values. There is a clear trend that VP1-J8 poorly binds to Capto™ MMC at low salt concentrations and starts binding with increasing NaCl concentrations. This effect is also pH dependent. While at pH 7.5, 0.4 M NaCl is required to obtain a binding capacity of 10 mg ml^{-1}, only 0.2 M NaCl is required at pH 9. The binding shows an optimum at a certain NaCl concentration and at higher NaCl binding decreases.

Table 1
Different examined purification pathways. HMWI: High molecular weight impurities LMWI: Low molecular weight impurities, Aggr: Aggregates, DNA: DNA content, NA: Not applicable if measurement was not expedient.

Pathway A	PEG precipitation	Capto™ MMC	SEC
	HMWI: NA, LMWI: NA, Aggr: NA, DNA: 29.7 µg mg^{-1}	HMWI: 17.9 %, LMWI: 2.7 %, Aggr: 0.6 %, DNA: 0.38 µg mg^{-1}	HMWI: 7.0 %, LMWI: 1.1 %, Aggr: 0 %, DNA: 0.04 µg mg^{-1}
Pathway B	PEG precipitation	Capto™ MMC	Capto™ Q
	HMWI: NA, LMWI: NA, Aggr: NA, DNA: 29.7 µg mg^{-1}	HMWI: 17.9 %, LMWI: 2.7 %, Aggr: 0.6 %, DNA: 0.38 µg mg^{-1}	HMWI: 4.2 %, LMWI: 2.8 %, Aggr: 0 %, DNA: 0.02 µg mg^{-1}
Pathway C	PEG precipitation	Capto™ Q	SEC
	HMWI: NA, LMWI: NA, Aggr: NA, DNA: 29.7 µg mg^{-1}	HMWI: 25.2 %, LMWI: 3.6 %, Aggr: 3.1 %, DNA: 0.04 µg mg^{-1}	HMWI: 18.1 %, LMWI: 1.5 %, Aggr: 0%, DNA: 0.01 µg mg^{-1}
Pathway D	PEG precipitation	Capto™ Q	Capto™ MMC
	HMWI: NA, LMWI: NA, Aggr: NA, DNA: 29.7 µg mg^{-1}	HMWI: 25.2 %, LMWI: 3.6 %, Aggr: 3.1 %, DNA: 0.04 µg mg^{-1}	HMWI: 2.1 %, LMWI: 1.5 %, Aggr: 0 %, DNA: 0.04 µg mg^{-1}
Pathway E	Capto™ Q	Capto™ MMC	
	HMWI: 42.7 %, LMWI: 22.9 %, Aggr: 2.8 %, DNA: 0.02 µg mg^{-1}	HMWI: 10.9 %, LMWI: 1.7 %, Aggr: 0 %, DNA: 0.004 µg mg^{-1}	
Pathway F	Diafiltration	Capto™ MMC	
	HMWI: 50.3 %, LMWI: 29.0 %, Aggr: NA, DNA: 23.61 µg mg^{-1}	HMWI: 50.0 %, LMWI: 1.1 %, Aggr: 14.6 %, DNA: 1.85 µg mg^{-1}	

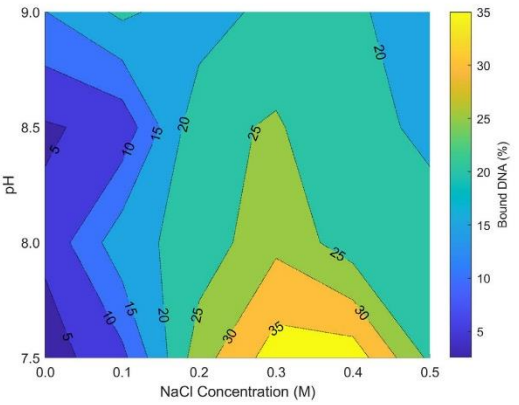

Fig. 4. Bound DNA on Capto™ Q during static binding studies with 20 µl PreDictor® plates in the range pH 7.5–9.0 and NaCl 0–0.5 M. Bound DNA is expressed as percentage of initial DNA loaded onto the resin.

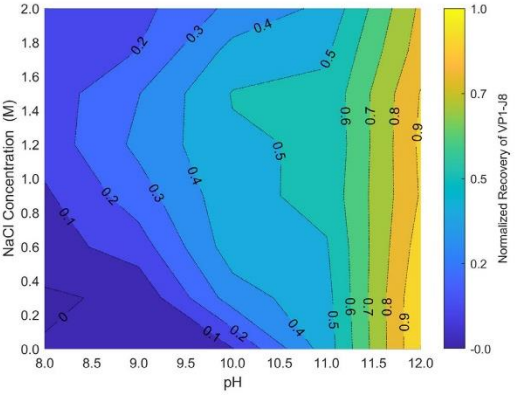

Fig. 5. Elution study of VP1-J8 from Capto™ MMC for a pH range from 8–12 and NaCl concentrations from 0–2 M. Cumulative recovery obtained from 2 consecutive steps normalized to the maximum.

For example, maximum binding at pH 9 is at 0.3 M NaCl (16.0 mg ml^{-1}) and at 0.5 M NaCl it decreased to 13.2 mg ml^{-1}.

3.2. High throughput elution studies

The best elution from Capto™ MMC was observed at pH 12, 0 M NaCl, and no elution was measured at pH values and NaCl concentrations below the loading condition (pH 8, 0.5 M NaCl). As can be seen as a general trend in Fig. 5, increasing NaCl concentration led to better elution with a maximum at around 1.2–1.4 M NaCl. At higher salt concentrations however, VP1-J8 elutes less. This trend is only true for pH values below 12, as at pH 12 the strongest elution is at 0 M NaCl. Increasing NaCl concentration led to lower elution, but still high, compared to other elution conditions tested. Rising pH supports elution gradually at all NaCl concentrations and showed a steep increase from pH 11 to 12.

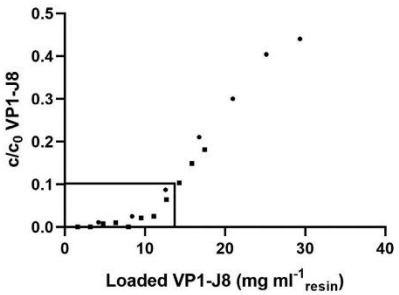

Fig. 6. Breakthrough curve of VP1-J8 on a 1 ml Capto™ MMC column at pH 8.9, 0.35 M NaCl at a flow rate of 1 ml min^{-1}. The marked square indicates a $DBC_{10\%}$. (•) VP1-J8 stock solution, obtained by PEG precipitation. (■) Purified VP1-J8.

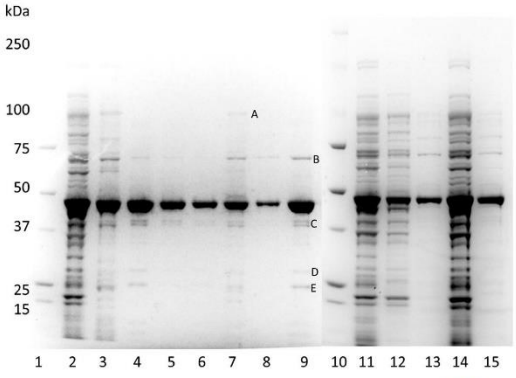

Fig. 7. SDS-PAGE analysis of purification pathways A-F as described in Fig. 1. (1 & 10) Marker, (2) clarified cell lysate, (3) resolubilized PEG precipitate (pathway A & B), (4) PEG followed by Capto™ MMC (pathway A & B), (5) SEC polishing (pathway A), (6) Capto™ Q polishing (pathway B), (7) PEG precipitation followed by Capto™ Q flow through (pathway C & D), (8) SEC polishing (pathway C), (9) Capto™ MMC polishing (pathway D), (11) clarified cell lysate, (12) Capto™ Q flow through of clarified cell lysate (pathway E), (13) Capto™ MMC polishing (pathway E), (14) retentate of diafiltration (pathway F), (15) Capto™ MMC polishing (pathway F). Protein identity of impurities A–E were analysed by LC-ESI-MS/MS Mass Spectrometry.

3.3. Dynamic binding capacity

As can be seen in Fig. 6, the purity and concentration of the starting material had a negligible influence on dynamic binding capacity. Both experiments showed a $DBC_{10\%}$ of around 14 mg ml_{resin}^{-1} at a residence time of 1 min for VP1-J8 on Capto™ MMC. The dynamic binding is comparable to high throughput results, but in this case slightly lower, to the static binding measured with high throughput binding studies in which a binding of 15-16 mg ml^{-1} was obtained for the chosen buffer conditions.

3.4. Process integration and further polishing

Although the binding of VP1-J8 on Capto™ MMC at a pH above 8 seems to be highly specific it was found that purification by Capto™ MMC alone does not result in a pure product.

The purity analysis of the different purification pathways is summarized in Table 1. The results of SDS-PAGE analysis are shown in Fig. 7. Purity analysis by size exclusion methods of the products obtained by PEG precipitation and diafiltration was not expedient as the impurity levels, in particular DNA levels, were too high and therefore distorted the results.

PEG precipitation followed by Capto™ MMC purification led to SEC purities of around 80 % and removed the majority of DNA. Very low levels of aggregates (0.6 %) could be measured, however the identity of the aggregates could not be verified as VP1-J8 aggregates. Both subsequent polishing steps, either by size exclusion chromatography or by flow through polishing on Capto™ Q further increased the purity to levels above 90 % and DNA levels below 0.04 µg $mg_{protein}^{-1}$. No aggregates could be detected after polishing.

PEG precipitation followed by Capto™ Q flow through purification lowered DNA levels to 0.04 µg $mg_{protein}^{-1}$, and achieved a SEC purity of around 70 %. Around 3.1 % VP1-J8 aggregates were present in the sample. Polishing by SEC led to the removal of aggregates, however HMWI remained high with 18.1 %. Polishing with Capto™ MMC removed aggregates and also removed most of the HMWI (HMWI: 2.1 %).

The combination of AEX flowthrough followed by Capto™ MMC purification, without a prior PEG precipitation step, showed similar results, with slightly higher impurities. After the flow through step the DNA level was very low, but VP1-J8 aggregates were present (2.8 % aggregates). HMWI (42.7 %) and LMWI (22.9 %) were higher than with a prior PEG precipitation step (HMWI: 25.2 %, LMWI: 3.6 %). The subsequent Capto™ MMC step strongly reduced HMWI and LMWI impurities to 10.9 % and 1.7 % respectively, and aggregates could not be detected. The remaining DNA content of 0.004 µg $mg_{protein}^{-1}$ was the lowest measured for all purification steps and is below the detection limit of the assay.

Diafiltration as an alternative first purification step resulted in insufficient outcomes. DNA levels could not be lowered in the diafiltration step and impurity levels remained high. Also the subsequent Capto™ MMC step showed poor performance and very high HMWI impurities of 50.0 % remained. Furthermore 14.6 % aggregates could be measured and DNA at a comparable very high level of 1.85 µg $mg_{protein}^{-1}$ was present. Nonetheless, the aggregates could not be identified by SDS-PAGE as VP1-J8 aggregates or any other protein and a comparison of the A_{260}/A_{280} ratio of 1.96 indicates that the measured aggregate fraction is in fact nucleic acid (data not shown).

SDS-PAGE analysis confirms the SEC-HPLC analysis. PEG precipitation, Capto™ Q and Capto™ MMC are possible unit operations to purify VP1-J8. PEG precipitation and Capto™ Q did not result in pure product (Fig. 7, line 3, 7, 12). In combination with Capto™ MMC the purity is very high. The Capto™ MMC step in particular showed a high specifity towards VP1-J8 and thus strongly increased the purity. This is especially evident for the purification after diafiltration (Fig. 7, line 14 & 15). The combination of Capto™ Q and Capto™ MMC lead to a product of high purity, with only faint bands of impurities visible (Fig. 7 lane 9 & 13, impurities A-E). These impurity bands could not be removedin our experiments and become visible if the SDS gel was overloaded. However, the pathway without prior PEG precipitation showed slightly higher impurities for proteins > 50 kDa (Fig. 7, lane 13) and lower impurities for proteins < 50 kDa. Impurity A has a molecular weight of around 90 kDa, impurity B of around 70 kDa, impurity C shows a double band at around 40 kDa and impurity D & E has a molecular weight of 25 & 20 kDa, respectively. Protein identification by comparing protein fingerprints of the impurity bands via LC-ESI-MS/MS as described in Section 2.3 against *E.coli* proteins and VP1-J8 revealed that impurities C, D and E showed the highest coverage with VP1-J8. Impurity C had a coverage of 69 %, impurity D of 57 % and impurity E of 59 %. Known *E. coli* proteins showed a significantly lower coverage. As impurities C, D and E have a lower molecule weight as native VP1-J8 but showed a high fingerprint coverage of VP1-J8, it can be concluded that impurities C, D and E

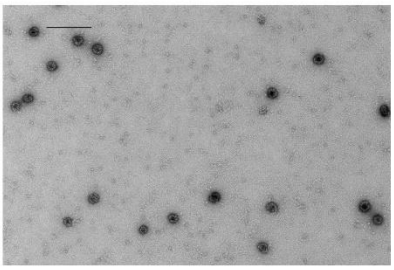

Fig. 8. TEM image of VLPs assembled by lowering the pH to 7.2 and adding calcium chloride to the eluate obtained from pathway E. Scale bar represents 200 nm.

are truncation products of VP1-J8. Unfortunately, Impurities A and B showed no signal in LC-ESI-MS/MS at all and therefore could not be identified (below detection limit).

3.5. VLP assembly

As can be seen in Fig. 8 the capsomeres from pathway E (Fig. 1) could be successfully assembled into capsid like structures by solely lowering the pH and adding calcium chloride. The measured diameters of the particles ranged from 42 nm to 52 nm. Apart from capsid like structures also unassembled capsomeres were visible on the TEM images but no spherical aggregates between 15 and 30 nm.

4. Discussion

At a pH range from 7.5 to 9.0 VP1-J8 capsomeres showed static binding capacities between ~1.4 to 3.8 mg ml_{resin}^{-1} on Capto^{TM} Q. Keeping in mind that at the high concentration used in these tests, 1 % error in the concentration determination corresponds to around 0.5 mg ml_{resin}^{-1} difference in binding capacity it can be concluded, that VP1-J8 capsomeres do not effectively bind Capto^{TM} Q. This result is unexpected given the fact that VP1-J8 has a theoretical isoelectric point of 6.57 and should therefore have an overall negative charge and expected to bind to strong anion exchangers for selected buffer systems. It is also contrary to reports in the literature in which VP1 capsomeres have been captured on Sartobind® Q membranes at pH 8 having the same ligand [41]. The slightly increased binding at elevated NaCl concentrations, can be explained by non-specific hydrophobic interactions. In contrast, VP1-J8 does bind strongly towards Capto^{TM} MMC, a mixed mode cation exchanger, at the examined pH range for elevated NaCl concentrations but with only low levels at low salt concentrations. For a given NaCl concentration (e.g. 0.3 M NaCl) the binding capacity actually increases with increasing pH. This behaviour is somewhat strange, and a plausible explanation would be that hydrophobic interactions are the predominant binding mechanism between Capto^{TM} MMC and VP1-J8. However, that would also mean that VP1-J8 binding increases with increasing salt concentrations [48]. As the binding capacity decreases again at high salt concentrations (see Fig. 3 pH 9, 0.5 M NaCl) this explanation seems to be untrue. Furthermore, the measured optimal salt concentrations (0.3-0.5 M NaCl) are far below reported concentrations in which hydrophobic effects play a dominant role at mixed mode cation exchangers [48]. The elution experiments strengthen the assumption that the binding mechanism is in fact an electrostatic binding. At salt concentrations down to 0 M NaCl VP1-J8 does not elute from Capto^{TM} MMC, which is contrary to the observations made during binding studies, in which VP1-J8 does poorly bind at this condition. If hydrophobic interactions are responsible for the binding it would be expected to show some elution at very low salt concentrations which cannot be observed [48]. The elution behaviour with a maximum elution at salt concentrations around 1.4 M NaCl and lower elution at higher salt concentrations shows that hydrophobic effects only play a dominant role at very high salt concentrations. Increasing the pH beneficially affects the elution as expected and as described by the manufacturer [49]. At a high pH value of 12 binding strongly decreased at all salt concentrations having the highest elution at 0 M NaCl. This might be explained by that fact that ionic binding occurs at a charged patch, rather than by the overall net charge of the protein. A possible binding site is the exposed N-terminal DNA binding site of VP1, which is rich in arginine and lysine, having pKa's of 12.48 and 10.53, respectively [50].

Assuming that the binding is predominantly caused by localised electrostatic interactions, the binding behaviour still opens questions. Comparing the binding of VP1-J8 on Capto^{TM} MMC with the binding of DNA onto Capto^{TM} Q the similarities are obvious. As shown in literature DNA binds to anion exchangers such Capto^{TM} Q especially well at low ionic strengths [51]. However, at low ionic strengths neither DNA on Capto^{TM} Q nor VP1-J8 on Capto^{TM} MMC bind properly on the resin and binding increased with increasing NaCl concentrations; a phenomenon between the two types of interactions are evident. We could show that VP1-J8 is forming soluble DNA-protein aggregates at low ionic strengths, caused by the strong DNA binding site on VP1 subunits, which effectively hinders VP1-J8 of accessing the pores of chromatographic resin and thus lead to very low binding capacities at low ionic strengths (results submitted to publication). At salt concentrations having an optimum binding (0.3–0.4 M NaCl) the ionic strength leads to dissociation of DNA-protein complexes, but due to the salt tolerance of Capto^{TM} MMC, only minimally affect the overall binding capacity. This effect explains the divergence between binding and eluting at low ionic strengths, the overall binding behaviour and also explains why DNA cannot be properly removed on Capto^{TM} Q at low ionic strengths. Combing the data, it can be concluded that processing of VP1-J8 requires a NaCl above 0.3 M NaCl. Optimal loading conditions on Capto^{TM} MMC are NaCl concentrations between 0.3 and 0.4 at pH values above 8.5 and for DNA removal on Capto^{TM} Q a pH of 7.5 should be chosen, but also higher pH values are applicable. Preferable elution conditions are at pH 12 at low ionic strengths, but NaCl can be added in concentrations up to 2 M with only minimal negative effects on elution.

The optimal elution conditions at a pH of 12 are generally considered as very harsh and should be avoided in protein processing as proteins at very high pH values might degenerate over time due to micro chemical changes. These reactions are favoured by long exposure time and high temperatures [52]. However, such harsh conditions are only used for a few minutes during elution and could be neutralized immediately. Therefore, it can be assumed that the degeneration is minimal. This is also supported by the fact that the acquired capsomeres show no abnormal behaviour compared to capsomeres obtained without a high pH elution step (e.g. pathway C, data not shown). Alternatively, as many other mixed mode ligands than Capto^{TM} MMC exist, a broad screening likely will find a ligand with enhanced elution at lower pH values [53].

The measured dynamic binding capacity was nearly independent from product concentration and product purity. Thus, a Capto^{TM} MMC purification step can be used at every step during purification without any negative impact on the performance. Although, the measured $DBC_{10\%}$ of 14 mg ml^{-1} is significantly lower than reported DBCs for e.g. BSA on Capto^{TM} MMC (30 mg ml^{-1}) [54], the capacity is comparable to highly overloaded affinity ligands (GSTrap HP, 22 mg ml^{-1}) [37] and far higher than reported dynamic binding capacities of 5.7 mg mL^{-1} for human B19 parvovirus-like particles on Sartobind® Q [55].

The obtained design space allows the construction of several purification pathways, of which a few have been examined. As expected, a three-step purification (pathway A–D) with capturing by selective precipitation leads to higher purities compared to a two-step purification (pathway E & F). Surprisingly, VP1-J8 aggregates seem not bind to Capto™ MMC as can be clearly seen in pathway E and D. This is unexpected as usually, even after an affinity purification step, aggregates are present and must be subsequently separated by SEC [56]. Steric hindrance of the aggregates might be an explanation; another rational could be that the binding site might be inaccessible in aggregated form. Although the mechanism is unknown, purification by Capto™ MMC eradicates the need for a size exclusion step, which is an expensive purification step.

Selective precipitation is a valuable process for lab scale purification, however, the scale-up raises issues, as the resolubilisation of the precipitate is challenging at large scale, especially if captured by centrifugation, which compresses the pellet and therefore hinders the resolubilisation [57]. Diafiltration, although widely used in industry for initial purification of VLPs, was impractical as an alternative to precipitation as it showed low removal of impurities, lead to aggregation of the product and proved to be very time consuming. Tangential flow filtration might increase the performance but was not tested. The two-step purification pathway (pathway E), without PEG precipitation, consisting of a Capto™ Q flow through step followed by a Capto™ MMC bind and elute step, showed similar process characteristics as pathway D. Aggregates and DNA are completely removed and SEC-HPLC purities close to 90 % are achieved. Furthermore, less truncation product could be identified, which might be a result of the faster processing compared to the three-step pathway. If higher purities are required, new multi modal size exclusion resins such as Capto™ Core™ might be a promising approach that yet has to be tested.

Using a flow through step on as an initial purification step is rather unusual, but in our process has the advantages of a direct subsequent loading onto Capto™ MMC without any buffer adjustment and therefore eradicates a unit operation. It also reduces the impurity level to a point at which the Capto™ MMC loading step can be controlled by the UV signal, which is impossible if crude lysate is loaded. This comes, however, at the cost of higher resin costs, as more resin is needed compared to a flow through polishing step. The eluate obtained from Capto™ MMC can be directly assembled into well-formed VLPs by just lowering the pH and adding calcium ions to the solution; no aggregates or miss formed VLPs could be identified. As expected a small amount of capsomeres remained unassembled, an effect already described in the literature, which is negatively correlated to the concentration during assembly [58]. A higher initial concentration can be easily achieved as VP1-J8 is eluted highly concentrated, which will lead to higher recoveries during assembly. Although the overall product recovery has not been evaluated, the process shows no intrinsic product loss and therefore likely has a very high recovery. Compared to other described processes in the literature for the production of viral capsomeres and VLPs our process has several advantages and address some of the common bottlenecks like benzonase treatment for DNA removal, removal of affinity tags, protein refolding, density gradient centrifugation, the use of SEC, multiple buffer exchanges, or the use of low capacity membrane columns [34,35,41,59]. Furthermore, the process is fully scalable, easy to integrate and rapid, as the purification is completed in less than 3 hours. The obtained VLPs are also already highly concentrated in PBS buffer containing only VLPs, capsomeres, EDTA, glycerol and NaCl at a physiological pH value, thus formulation can be achieved by solely diluting it to the required concentration.

Several VP1-J8 truncation products could be identified on SDS-PAGE analysis at purified samples. Although it was not possible to identify impurities A and B, it is likely that they are chaperones that bound to VP1-J8. Having a size of around 70 kDa, impurity B is probably the prokaryotic hsp70 chaperone DnaK, which was shown to copurify with VP1 [60] and impurity A is hsp90 which interacts with hsp70 [61]. Another possibility is the formation of inter-polypeptide aggregates of VP1-J8 and VP1-J8 truncation products during SDS sample preparation by partial reoxidation [62]. The double band on SDS-PAGE gels at 43 & 40 kDa have already been described in literature and occur due to auto digestion of VP1, as VP1 has an intrinsic serine protease activity [63]. As SEC-HPLC still reveals a near uniform capsomere peak we conclude, that partially digested VP1-J8 still remains in pentameric form together with intact VP1-J8 monomers and therefore are impossible to remove. The formation of truncation products of viral protein during the expression in *E. coli* has also been reported for adeno associated viral protein VP3 and might therefore also be a result of *E. coli* proteases [28]. Further research needs to be undertaken to minimize the formation of these digestion products, and how to remove the bound chaperons, but using protease inhibitors throughout the whole process instead of only during cell disruption, run at reduced temperature and addition of ATP to remove chaperones will likely solve the issue.

5. Conclusion

In this study we developed a robust and theoretically fully scalable, highly efficient process for the production of modular murine polyomavirus major structural protein VP1-J8 capsomeres and modular VLPs using high-throughput process development tools. Purification by mixed mode cation exchanger at pH values above 8 showed a highly specific binding and dynamic binding of 14 mg ml_{resin}^{-1} was achieved under the optimised conditions. The developed two step purification pathway, consisting of an anion exchange flow through step followed by a bind and elute step on a multimodal cation exchanger, requires no buffer adjustment during processing and is thus incomparably simple and fast. The developed process removes the majority of host cell protein, aggregates and DNA, without any of the common bottleneck unit operations in other described VLP production pathways. VLPs in PBS buffer can be obtained by simply adding calcium ions to the final eluate and lowering the pH to 7.2. This straightforward process, requiring only three integrated unit operations might lay the baseline for future cost effective, large scale production of microbial produced modular VLP vaccine candidates.

Declaration of Competing Interest

The authors declare that they have no known competing financial interests or personal relationships that could have appeared to influence the work reported in this paper.

CRediT authorship contribution statement

Lukas Gerstweiler: Conceptualization, Methodology, Investigation, Writing - original draft, Visualization. **Jagan Billakanti:** Conceptualization, Methodology, Writing - review & editing. **Jingxiu Bi:** Conceptualization, Resources, Writing - review & editing, Supervision. **Anton Middelberg:** Conceptualization, Resources, Writing - review & editing, Supervision, Project administration.

Acknowledgment

The authors thank Ms Ruth Wang for technical support for LC-ESI-MS/MS and the Protein Expression Facility of the University of Queensland, Brisbane, Australia for plasmid construction.

Supplementary materials

Supplementary material associated with this article can be found, in the online version, at doi:10.1016/j.chroma.2021.461924.

References

[1] S.L. Cochi, L. Hegg, A. Kaur, C. Pandak, H. Jafari, The global polio eradication initiative: progress, lessons learned, and polio legacy transition planning, Health Affairs 35 (2016) 277–283, doi:10.1377/hlthaff.2015.1104.

[2] WHO, Measels fact sheet, 2019. https://www.who.int/news-room/fact-sheets/detail/measles (accessed 16 September 2020).

[3] G. Yamey, M. Schäferhoff, R. Hatchett, M. Pate, F. Zhao, K.K. McDade, Ensuring global access to COVID-19 vaccines, Lancet 395 (2020) 1405–1406, doi:10.1016/S0140-6736(20)30763-7.

[4] M. Rahi, A. Sharma, Mass vaccination against COVID-19 may require replays of the polio vaccination drives, EClinicalMedicine 25 (2020) 100501, doi:10.1016/j.eclinm.2020.100501.

[5] S. Luby, R. Arthur, Risk and response to biological catastrophe in lower income countries, Curr. Top. Microbiol. Immunol. 424 (2019) 85–105, doi:10.1007/82_2019_162.

[6] T.R. Doel, FMD vaccines, Virus Res. 91 (2003) 81–99, doi:10.1016/s0168-1702(02)00261-7.

[7] F. Krammer, R. Grabherr, Alternative influenza vaccines made by insect cells, Trends Mol. Med. 16 (2010) 313–320, doi:10.1016/j.molmed.2010.05.002.

[8] B. Donaldson, Z. Lateef, G.F. Walker, S.L. Young, V.K. Ward, Virus-like particle vaccines: immunology and formulation for clinical translation, Expert Rev. Vaccines 17 (2018) 833–849, doi:10.1080/14760584.2018.1516552.

[9] M.A. Stanley, Human papillomavirus vaccines, Rev. Med. Virol. 16 (2006) 139–149, doi:10.1002/rmv.498.

[10] A.P.J. Middelberg, T. Rivera-Hernandez, N. Wibowo, L.H.L. Lua, Y. Fan, G. Magor, C. Chang, Y.P. Chuan, M.F. Good, M.R. Batzloff, A microbial platform for rapid and low-cost virus-like particle and capsomere vaccines, Vaccine 29 (2011) 7154–7162, doi:10.1016/j.vaccine.2011.05.075.

[11] H.K. Hume, J. Vidigal, M.J.T. Carrondo, A.P.J. Middelberg, A. Roldão, L.H.L. Lua, Synthetic biology for bioengineering virus-like particle vaccines, Biotechnol. Bioeng. 116 (2019) 919–935, doi:10.1002/bit.26890.

[12] A. Tekewe, Y. Fan, E. Tan, A.P.J. Middelberg, L.H.L. Lua, Integrated molecular and bioprocess engineering for bacterially produced immunogenic modular virus-like particle vaccine displaying 18 kDa rotavirus antigen, Biotechnol. Bioeng. 114 (2017) 397–406, doi:10.1002/bit.26068.

[13] A. Seth, I.G. Kong, S.-H. Lee, J.-Y. Yang, Y.-S. Lee, Y. Kim, N. Wibowo, A.P.J. Middelberg, L.H.L. Lua, M.-N. Kweon, Modular virus-like particles for sublingual vaccination against group A streptococcus, Vaccine 34 (2016) 6472–6480, doi:10.1016/j.vaccine.2016.11.008.

[14] T. Rivera-Hernandez, J. Hartas, Y. Wu, Y.P. Chuan, L.H.L. Lua, M. Good, M.R. Batzloff, A.P.J. Middelberg, Self-adjuvanting modular virus-like particles for mucosal vaccination against group A streptococcus (GAS), Vaccine 31 (2013) 1950–1955, doi:10.1016/j.vaccine.2013.02.013.

[15] M.R. Anggraeni, N.K. Connors, Y. Wu, Y.P. Chuan, L.H.L. Lua, A.P.J. Middelberg, Sensitivity of immune response quality to influenza helix 190 antigen structure displayed on a modular virus-like particle, Vaccine 31 (2013) 4428–4435, doi:10.1016/j.vaccine.2013.06.087.

[16] C.L. Effio, J. Hubbuch, Next generation vaccines and vectors: designing downstream processes for recombinant protein-based virus-like particles, Biotechnol. J. 10 (2015) 715–727, doi:10.1002/biot.201400392.

[17] V. Qendri, J.A. Bogaards, J. Berkhof, Pricing of HPV vaccines in European tender-based settings, Eur. J. Health Econ. 20 (2019) 271–280, doi:10.1007/s10198-018-0996-9.

[18] A. Zeltins, Construction and characterization of virus-like particles: a review, Mol. Biotechnol. 53 (2013) 92–107, doi:10.1007/s12033-012-9598-4.

[19] D.I. Lipin, Y.P. Chuan, L.H.L. Lua, A.P.J. Middelberg, Encapsulation of DNA and non-viral protein changes the structure of murine polyomavirus virus-like particles, Arch. Virol. 153 (2008) 2027–2039, doi:10.1007/s00705-008-0220-9.

[20] L.K. Pattenden, A.P.J. Middelberg, M. Niebert, D.I. Lipin, Towards the preparative and large-scale precision manufacture of virus-like particles, Trends Biotechnol. 23 (2005) 523–529, doi:10.1016/j.tibtech.2005.07.011.

[21] Y.P. Chuan, Y.Y. Fan, L.H.L. Lua, A.P.J. Middelberg, Virus assembly occurs following a pH- or Ca2+-triggered switch in the thermodynamic attraction between structural protein capsomeres, J. R. Soc. Interface 7 (2010) 409–421, doi:10.1098/rsif.2009.0175.

[22] L.H.L. Lua, N.K. Connors, F. Sainsbury, Y.P. Chuan, N. Wibowo, A.P.J. Middelberg, Bioengineering virus-like particles as vaccines, Biotechnol. Bioeng. 111 (2014) 425–440, doi:10.1002/bit.25159.

[23] Y.P. Chuan, N. Wibowo, L.H.L. Lua, A.P.J. Middelberg, The economics of virus-like particle and capsomere vaccines, Biochem. Eng. J. 90 (2014) 255–263, doi:10.1016/j.bej.2014.06.005.

[24] A. Roldão, M.C.M. Mellado, L.R. Castilho, M.J.T. Carrondo, P.M. Alves, Virus-like particles in vaccine development, Expert Rev. Vaccines 9 (2010) 1149–1176, doi:10.1586/erv.10.115.

[25] X. Huang, X. Wang, J. Zhang, N. Xia, Q. Zhao, *Escherichia coli*-derived virus-like particles in vaccine development, NPJ Vaccines 2 (2017) 3, doi:10.1038/s41541-017-0006-8.

[26] WHO, Weekly epidemiological record: No. 29, 2014, 89, 321-336, 2014. https://www.who.int/vaccine_safety/committee/reports/wer8929.pdf (accessed 17 September 2020).

[27] Y.-M. Hu, S.-J. Huang, K. Chu, T. Wu, Z.-Z. Wang, C.-L. Yang, J.-P. Cai, H.-M. Jiang, Y.-J. Wang, M. Guo, X.-H. Liu, H.-J. Huang, F.-C. Zhu, J. Zhang, N.-S. Xia, Safety of an *Escherichia coli*-expressed bivalent human papillomavirus (types 16 and 18) L1 virus-like particle vaccine: an open-label phase I clinical trial, Hum. Vaccin. Immunother. 10 (2014) 469–475, doi:10.4161/hv.26846.

[28] D.T. Le, M.T. Radukic, K.M. Müller, Adeno-associated virus capsid protein expression in *Escherichia coli* and chemically defined capsid assembly, Sci. Rep. 9 (2019) 18631, doi:10.1038/s41598-019-54928-y.

[29] Y. Zhang, S. Yin, B. Zhang, J. Bi, Y. Liu, Z. Su, HBc-based virus-like particle assembly from inclusion bodies using 2-methyl-2, 4-pentanediol, Process Biochem. 89 (2020) 233–237, doi:10.1016/j.procbio.2019.10.031.

[30] D.J. Pattinson, S.H. Apte, N. Wibowo, Y.P. Chuan, T. Rivera-Hernandez, P.L. Groves, L.H. Lua, A.P.J. Middelberg, D.L. Doolan, Chimeric murine polyomavirus virus-like particles induce plasmodium antigen-specific $CD8^+$ T cell and antibody responses, Front. Cell. Infect. Microbiol. 9 (2019) 215, doi:10.3389/fcimb.2019.00215.

[31] M.W.O. Liew, A. Rajendran, A.P.J. Middelberg, Microbial production of virus-like particle vaccine protein at gram-per-litre levels, J. Biotechnol. 150 (2010) 224–231, doi:10.1016/j.jbiotec.2010.08.010.

[32] J. Waneesorn, N. Wibowo, J. Bingham, A.P.J. Middelberg, L.H.L. Lua, Structural-based designed modular capsomere comprising HA1 for low-cost poultry influenza vaccination, Vaccine 36 (2016) 3064–3071, doi:10.1016/j.vaccine.2016.11.058.

[33] N. Wibowo, F.K. Hughes, E.J. Fairmaid, L.H.L. Lua, L.E. Brown, A.P.J. Middelberg, Protective efficacy of a bacterially produced modular capsomere presenting M2e from influenza: extending the potential of broadly cross-protecting epitopes, Vaccine 32 (2014) 3651–3655, doi:10.1016/j.vaccine.2014.04.062.

[34] N. Roos, B. Breiner, L. Preuss, H. Lilie, K. Hipp, H. Herrmann, T. Horn, R. Biener, T. Iftner, C. Simon, Optimized production strategy of the major capsid protein HPV 16L1 non-assembly variant in *E. coli*, Protein Expr. Purif. 175 (2020) 105690, doi:10.1016/j.pep.2020.105690.

[35] N. Hillebrandt, P. Vormittag, N. Bluthardt, A. Dietrich, J. Hubbuch, Integrated process for capture and purification of virus-like particles: enhancing process performance by cross-flow filtration, Front. Bioeng. Biotechnol. 8 (2020) 489, doi:10.3389/fbioe.2020.00489.

[36] J.C. Cook, J.G. Joyce, H.A. George, L.D. Schultz, W.M. Hurni, K.U. Jansen, R.W. Hepler, C. Ip, R.S. Lowe, P.M. Keller, E.D. Lehman, Purification of virus-like particles of recombinant human papillomavirus type 11 major capsid protein L1 from *Saccharomyces cerevisiae*, Protein Expr. Purif. 17 (1999) 477–484, doi:10.1006/prep.1999.1155.

[37] D.I. Lipin, L.H.L. Lua, A.P.J. Middelberg, Quaternary size distribution of soluble aggregates of glutathione-S-transferase-purified viral protein as determined by asymmetrical flow field flow fractionation and dynamic light scattering, J. Chromatogr. A 1190 (2008) 204–214, doi:10.1016/j.chroma.2008.03.032.

[38] N.K. Connors, Y. Wu, L.H.L. Lua, A.P.J. Middelberg, Improved fusion tag cleavage strategies in the downstream processing of self-assembling virus-like particle vaccines, Food Bioprod. Process. 92 (2014) 143–151, doi:10.1016/j.fbp.2013.08.012.

[39] A. Tekewe, N.K. Connors, F. Sainsbury, N. Wibowo, L.H.L. Lua, A.P.J. Middelberg, A rapid and simple screening method to identify conditions for enhanced stability of modular vaccine candidates, Biochem. Eng. J. 100 (2015) 50–58, doi:10.1016/j.bej.2015.04.004.

[40] J. Hirsch, B.W. Faber, J.E. Crowe, B. Verstrepen, G. Cornelissen, *E. coli* production process yields stable dengue 1 virus-sized particles (VSPs), Vaccine 38 (2020) 3305–3312, doi:10.1016/j.vaccine.2020.03.003.

[41] C. Ladd Effio, P. Baumann, C. Weigel, P. Vormittag, A. Middelberg, J. Hubbuch, High-throughput process development of an alternative platform for the production of virus-like particles in *Escherichia coli*, J. Biotechnol. 219 (2016) 7–19, doi:10.1016/j.jbiotec.2015.12.018.

[42] A. Tekewe, Virus-like particle and capsomere vaccines against rotavirus, 2016.

[43] W.K. Chung, A.S. Freed, M.A. Holstein, S.A. McCallum, S.M. Cramer, Evaluation of protein adsorption and preferred binding regions in multimodal chromatography using NMR, Proc. Natl. Acad. Sci. U. S. A. 107 (2010) 16811–16816, doi:10.1073/pnas.1002347107.

[44] M.M. Bradford, A rapid and sensitive method for the quantitation of microgram quantities of protein utilizing the principle of protein-dye binding, Anal. Biochem. 72 (1976) 248–254, doi:10.1016/0003-2697(76)90527-3.

[45] C. Ladd Effio, L. Wenger, O. Ötes, S.A. Oelmeier, R. Kneusel, J. Hubbuch, Downstream processing of virus-like particles: single-stage and multi-stage aqueous two-phase extraction, J. Chromatogr. A 1383 (2015) 35–46, doi:10.1016/j.chroma.2015.01.007.

[46] M.W.O. Liew, Y.P. Chuan, A.P.J. Middelberg, High-yield and scalable cell-free assembly of virus-like particles by dilution, Biochem. Eng. J. 67 (2012) 88–96, doi:10.1016/j.bej.2012.05.007.

[47] Y. Yuan, E. Shane, C.N. Oliver, Reversed-phase high-performance liquid chromatography of virus-like particles, J. Chromatogr. A 816 (1998) 21–28, doi:10.1016/S0021-9673(98)00065-X.

[48] B.K. Nfor, M. Noverraz, S. Chilamkurthi, P.D.E.M. Verhaert, L.A.M. van der Wielen, M. Ottens, High-throughput isotherm determination and thermodynamic modeling of protein adsorption on mixed mode adsorbents, J. Chromatogr. A 1217 (2010) 6829–6850, doi:10.1016/j.chroma.2010.07.069.

[49] Cytiva, Uppsala, Sweden, Instructions 11003505 AF - Capto™ MMC, 2018. https://cdn.cytivalifesciences.com/dmm3bwsv3/AssetStream.aspx?mediaformatid=10061&destinationid=10016&assetid=13701 (accessed 25 january 2021).
[50] D. Chang, X. Cai, R.A. Consigli, Characterization of the DNA binding properties of polyomavirus capsid protein, J. Virol. 67 (1993) 6327–6331, doi:10.1128/jvi.67.10.6327-6331.1993.
[51] C. Tarmann, A. Jungbauer, Adsorption of plasmid DNA on anion exchange chromatography media, J. Sep. Sci. 31 (2008) 2605–2618, doi:10.1002/jssc.200700654.
[52] M. Friedman, M.R. Gumbmann, P.M. Masters, Protein-alkali reactions: chemistry, toxicology, and nutritional consequences, Adv. Exp. Med. Biol. 177 (1984) 367–412, doi:10.1007/978-1-4684-4790-3_18.
[53] G. Zhao, X.-Y. Dong, Y. Sun, Ligands for mixed-mode protein chromatography: principles, characteristics and design, J. Biotechnol. 144 (2009) 3–11, doi:10.1016/j.jbiotec.2009.04.009.
[54] Cytiva, Uppsala, Sweden, Data File 11-0035-45 AA, 2005. https://www.cytivalifesciences.co.jp/newsletter/downstream/pdf/11003545aa.pdf (accessed 25 January 2021)
[55] C. Ladd Effio, T. Hahn, J. Seiler, S.A. Oelmeier, I. Asen, C. Silberer, L. Villain, J. Hubbuch, Modeling and simulation of anion-exchange membrane chromatography for purification of Sf9 insect cell-derived virus-like particles, J. Chromatogr. A 1429 (2016) 142–154, doi:10.1016/j.chroma.2015.12.006.
[56] D.I. Lipin, A. Raj, L.H.L. Lua, A.P.J. Middelberg, Affinity purification of viral protein having heterogeneous quaternary structure: modeling the impact of soluble aggregates on chromatographic performance, J. Chromatogr. A 1216 (2009) 5696–5708, doi:10.1016/j.chroma.2009.05.082.
[57] N. Hammerschmidt, S. Hobiger, A. Jungbauer, Continuous polyethylene glycol precipitation of recombinant antibodies: sequential precipitation and resolubilization, Process Biochem. 51 (2016) 325–332, doi:10.1016/j.procbio.2015.11.032.
[58] Y. Ding, Y.P. Chuan, L. He, A.P.J. Middelberg, Modeling the competition between aggregation and self-assembly during virus-like particle processing, Biotechnol. Bioeng. 107 (2010) 550–560, doi:10.1002/bit.22821.
[59] X.S. Chen, G. Casini, S.C. Harrison, R.L. Garcea, Papillomavirus capsid protein expression in *Escherichia coli*: purification and assembly of HPV11 and HPV16 L1, J. Mol. Biol. 307 (2001) 173–182, doi:10.1006/jmbi.2000.4464.
[60] L.R. Chromy, J.M. Pipas, R.L. Garcea, Chaperone-mediated in vitro assembly of polyomavirus capsids, Proc. Natl. Acad. Sci. U. S. A. 100 (2003) 10477–10482, doi:10.1073/pnas.1832245100.
[61] O. Genest, S. Wickner, S.M. Doyle, Hsp90 and Hsp70 chaperones: collaborators in protein remodeling, J. Biol. Chem. 294 (2019) 2109–2120, doi:10.1074/jbc.REV118.002806.
[62] R. Westermeier, Frequently made mistakes in electrophoresis, Proteomics 7 (Suppl 1) (2007) 60–63, doi:10.1002/pmic.200790077.
[63] J.H. Bowen, V. Chlumecky, P. D'Obrenan, J.S. Colter, Evidence that polyoma polypeptide VP1 is a serine protease, Virology 135 (1984) 551–554, doi:10.1016/0042-6822(84)90210-1.

Chapter 6

Control Strategy for Multi-Continuous Periodic Counter Current Chromatography Subject to Fluctuating Inlet Stream Concentration

Integration of a flow-through chromatography step with a continuous PCC process leads to fluctuating inlet stream concentrations, which hinders controlling of the PCC process. In this chapter a novel control strategy for PCC processes with fluctuating inlet stream concentrations is developed. The new approach was verified *in-silico* using mechanistic modelling as well as experimentally.

Statement of Authorship

Title of Paper	Control Strategy for Multi-Column Continuous Periodic Counter Current Chromatography Subject to Fluctuating Inlet Stream Concentration
Publication Status	published
Publication Details	Lukas Gerstweiler, Jagan Billakanti, Jingxiu Bi, Anton P.J. Middelberg, Control Strategy for Multi-Column Continuous Periodic Counter Current Chromatography Subject to Fluctuating Inlet Stream Concentration. Journal of Chromatography A. Volume 1667, 2022 https://doi.org/10.1016/j.chroma.2022.462884

Principal Author

Name of Principal Author (Candidate)	Lukas Gerstweiler		
Contribution to the Paper	Conceptualization, Methodology, Investigation, Writing – original draft, Visualization		
Overall percentage	80%		
Signature		Date	4.4.2022

Co-Author Contributions

By signing the Statement of Authorship. Each author certifies that:

I. The candidate's stated contribution to the publication is accurate (as detailed above)

II. Permission is granted for the candidate in include the publication in the thesis; and

III. The sum of all co-author contribution is equal to 100% less the candidate's stated contribution

Name of Co-Author	Jagan Billakanti		
Contribution to the Paper	Conceptualization, Methodology, Writing – review & editing		
Signature		Date	31/3/22

Name of Co-Author	Jingxiu Bi		
Contribution to the Paper	Conceptualization, Resources, Writing – review & editing, Supervision		
Signature		Date	31/03/2022

Name of Co-Author	**Anton P.J. Middelberg**		
Contribution to the Paper	Conceptualization, Resources, Writing – review & editing, Supervision, Project administration		
Signature		Date	30 March 2022

Journal of Chromatography A 1667 (2022) 462884

Contents lists available at ScienceDirect

Journal of Chromatography A

journal homepage: www.elsevier.com/locate/chroma

Control strategy for multi-column continuous periodic counter current chromatography subject to fluctuating inlet stream concentration

Lukas Gerstweiler[a,*], Jagan Billakanti[b], Jingxiu Bi[c], Anton P.J. Middelberg[c]

[a] School of Chemical Engineering and Advanced Material, The University of Adelaide, Adelaide, South Australia 5000, Australia
[b] Global Life Sciences Solutions Australia Pty Ltd, Level 11, 32 Phillip St, Parramatta, New South Wales 2150, Australia
[c] Division of Research and Innovation, The University of Adelaide, Adelaide 5000, Australia

ARTICLE INFO

Article history:
Received 10 November 2021
Revised 1 February 2022
Accepted 5 February 2022
Available online 6 February 2022

Keywords:
Periodic counter current chromatography
Continuous downstream processing
Controlling
Fluctuating concentration
Process integration

ABSTRACT

Fluctuations of the inlet feed stream concentration are a challenge in controlling continuous multi-column counter current chromatography systems with standard methods. We propose a new control strategy based on calculated product column breakthrough from UV sensor signals by neglecting an impurity baseline and instead using the impurity to product ratio. This calculation is independent of the inlet feed concentration. *In-silico* simulation showed that the proposed method can calculate the product column breakthrough perfectly even with fluctuating and highly unstable inlet feed concentration during a loading cycle. Applying the proposed method to control a three column periodic counter current chromatography process with fluctuating inlet feed concentration resulted in constant column loading in each cycle, while using the standard method failed to do so. Unavoidable band broadening caused by diffusion and dispersion has been identified as an inherent limiting factor for accurate calculation of column breakthrough comparing inlet and outlet UV signals. The proposed advanced calculations increase the robustness of periodic counter current chromatography and extend the capability to process unstable inlet streams.

1. Introduction

The global pandemic of COVID-19 highlighted the need for quick, large-scale manufacture of biopharmaceuticals such as vaccines, to meet the enormous worldwide demand. There is interest in moving biomanufacturing from batch to continuous production to lower the footprint, lower batch-to batch variations and to obtain a higher degree of automatization [1]. Traditional unit operations like precipitation, crystallization and extraction have been applied to continuous purification of biopharmaceuticals and described in the literature [2–4]. Chromatographic approaches remain the workhorse in described integrated continuous processes [5–8]. Multi-column continuous periodic counter current chromatography (PCC) with a solid stationary phase in bind-and-elute mode was widely used and examined. The basic principle of a PCC process is, that 3 or more columns are connected in series and loaded continuously. Column 1 is overloaded and the flow through is loaded onto column 2. After loading of column 1 is completed, the feed stream is then directed onto column 2 and the flow through is loaded onto column 3. The process continues thereafter. While loading is in progress for columns 2 and 3, the fully loaded column 1 undergoes column wash, elution and regeneration cycles to make this column available again for continuous feed material loading when column 2 is fully loaded [9]. This resulted in a cyclic process, which not only allowed for uninterrupted continuous loading, washing, elution and CIP, but also intensified the process by enabling a higher productivity and a better resin capacity utilization than traditional batch chromatography [10]. Different PCC set-ups are commercially available ranging from 2 column systems to the classic 3 and 4 column systems (3C-PCC, 4C-PCC), or systems with more columns [11]. These PCC systems were mostly utilized for protein-A affinity chromatography as an initial capturing step, but are suitable for all other chromatography steps such as intermediate ion exchange purification and polishing [5,12,13]. Although the transition from batch chromatography to a PCC process is theoretically quite straight forward, column overloading might change the separation performance caused by displacement of bound product, protein-protein interactions and elution peak broadening and distortion [14–18]. Another main challenge for designing such a process is to determine when the column loading is completed and when column switching needs to occur. Early column switching will result in an underutilizing of column and late switching will lead to product loss. There is a trade-off between yield and resin utilization [19]. For 100% $w w^{-1}$ yield the maximum load per col-

* Corresponding author.
E-mail address: Lukas.gerstweiler@adelaide.edu.au (L. Gerstweiler).

https://doi.org/10.1016/j.chroma.2022.462884
0021-9673/

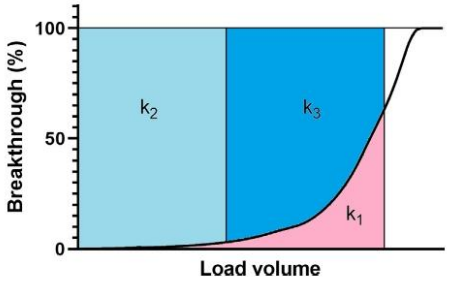

Fig. 1. Definition of areas around the breakthrough curve to visualize column overloading in a PCC process. The area k1 represents the flow through that is subsequently captured on column 2, k2 is the dynamic binding capacity for a given breakthrough level (here 5% ww^{-1}) and k3 is the possible increase in column utilization that can be achieved through overloading the column. The sum of k2 and k3 represent the total captured product on the column.

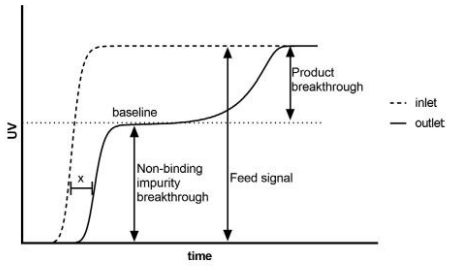

Fig. 2. Schematic representation of column breakthrough during PCC loading. (–) UV signal at the column inlet (UVinlet). (–) UV signal at the column outlet (UVoutlet). Baseline represent the UV signal caused by non-binding impurities; x is the delay caused by column dead volume.

umn can be derived from the area under the breakthrough curve, as shown in Fig. 1. The area k_1 underneath the breakthrough curve represents the breakthrough which is loaded onto the subsequent column and must be smaller than the rectangular area k_2, which represents the dynamic binding capacity of a column. In this model k_3 is the increase in column utilization, which can be obtained with the PCC process [9,19]. As the sum of k_2 and k_3 equals the total loaded product at a given breakthrough, the breakthrough can be used as a controlling signal to determine the column switching frequency to obtain an accurate constant loading for every cycle. The control strategy developed for ÄKTA PCC systems by Cytiva (formerly known as GE Healthcare) calculates the breakthrough or control signal ΔUV at a given time t as following:

$$\Delta UV^t = 100 * \frac{UV^t_{Breakthrough} - baseline}{UV^{t-x}_{Sample} - baseline} \quad (1)$$

With $UV_{Breakthrough}$ as the column outlet UV signal and UV_{Sample} as the column inlet UV signal. The UV_{Sample} signal is used from a previous time step $(t - x)$, to compensate for the time delay caused by the void volume. The constant x is calculated based on the column volume and the flowrate. The baseline is derived from the UV signal from non-binding impurities at the beginning of column loading as shown in Fig. 2 and is fixed for the whole cycle [20,21]. This so called *Dynamic Control* adjusts the baseline after every cycle and has been shown to automatically control PCC processes with different inlet concentrations, two alternating inlet concentrations and also slowly changing inlet concentrations if the amount of impurities remain constant [21–25]. Variable inlet streams have been identified as a main challenge to deal with in integrated continuous processes [1]. Chromatographic approaches produce highly variable outlet streams and also feed streams obtained from fermentation might fluctuate over time and thus it is challenging to process such outlet streams. Although the challenge of varying inlet stream concentration during column loading is well known, no research addressed the issue of how to cope with highly unstable inlet feed streams that change concentration multiple times. A recent publication describes a method to regulate loading time if the concentration changes once, using a previous cycle learning scheme [19], in which the elution peak area was measured and compared to a set point. In case of a deviation the subsequent loading time was either increased or decreased to adjust to the changed conditions. In this study, we show a possibility to control PCC loading and achieve constant column loading in every cycle, even with highly unstable inlet feed concentration, that fluctuates multiple times during each cycle.

2. Hypothesis and proposed calculation

2.1. Description of the problem

In affinity like bind-and-elute chromatography it can be assumed the inlet concentration c_{inlet} consists of a non-binding $c_{non-binding}$ impurity and binding product $c_{binding}$.

$$c_{inlet} = c_{binding} + c_{non-binding} \triangleq UV_{inlet} \quad (2)$$

The outlet concentration c_{outlet} can be expressed as a function of the breakthrough B

$$c_{outlet}(B) = c_{non-binding} + c_{binding} * B \triangleq UV_{outlet} \quad (3)$$

where B corresponds to the breakthrough level of the binding product component e.g. $B = 0$ at 0% MM^{-1} breakthrough of the binding component, $B = 0.5$ at 50% MM^{-1} breakthrough and so on.

The column breakthrough of the binding component in percent can therefore be derived from B as following

$$\%breakthrough = 100 * B \quad (4)$$

Under ideal conditions with no product breakthrough $(B = 0)$ the baseline corresponds to non-binding impurities as shown in Fig. 2 and is fixed for the cycle

$$baseline = c^0_{non-binding} \quad (5)$$

With the exponent 0 in $c^0_{non-binding}$ indicating the concentration at time $t = 0$.

The impurity level I is defined as the percentage of $c_{non-binding}$ of the total inlet concentration c_{inlet} and can be derived from the UV signals if $B = 0$

$$I = \frac{c_{non-binding}}{c_{inlet}} \triangleq \frac{UV_{outlet}}{UV_{inlet}} \quad (6)$$

Changes in the inlet concentration can be expressed as a function by introducing factor k

$$c_{inlet}\ (k_1, k_2) = c^0_{inlet} * k = c^0_{non-binding} * k_1 + c^0_{binding} * k_2 \quad (7)$$

With k_1 and k_2 corresponding to the change of non-binding impurities and binding product, respectively.

Furthermore, it is assumed that the ratio of non-binding impurities to binding product remains constant, (e.g. diluting the inlet with buffer, flow through chromatography), which leads to

$$k_1 = k_2 = k \quad (8)$$

Formula 7 can therefore be expressed as

$$c_{inlet}\ (k) = c^0_{inlet} * k = c^0_{non-binding} * k + c^0_{binding} * k \quad (9)$$

Combined formula (3) and (9), the outlet can be expressed as:

$$c_{outlet}(k,B) = c^0_{non-binding} * k + c^0_{binding} * k * B = (c^0_{non-binding} + c^0_{binding} * B) * k \quad (10)$$

Combining formula (1) and (10), the signal ΔUV can then be expressed as a function of k and B representing the behaviour for changing inlet concentration and breakthrough level:

$$\Delta UV(k,B) = \frac{(c^0_{non-binding} + c^0_{binding} * B) * k - baseline}{(c^0_{non-binding} + c^0_{binding}) * k - baseline} * 100 \quad (11)$$

With the baseline as the initial impurities

$$\Delta UV(k,B) = \frac{(c^0_{non-binding} + c^0_{binding} * B) * k - c^0_{non-binding}}{(c^0_{non_{binding}} + c^0_{binding}) * k - c^0_{non-binding}} * 100 \quad (12)$$

2.2. Proposed strategy

We propose as an alternative to calculate a control signal ΔC which neglects the baseline at a given time point t

$$\Delta C^t = \frac{UV^t_{Breakthrough}}{UV^{t-x}_{Sample}} * 100 \quad (13)$$

With $t - x$ compensates the void volume of the column.

ΔC can be expressed as a function of breakthrough B and a concentration factor k combining formula 2, 3 and 9

$$\Delta C(k,B) = \frac{(c^0_{non-binding} + c^0_{binding} * B) * k}{(c^0_{non-binding} + c^0_{binding}) * k} * 100 \quad (14)$$

The concentration factor k cancels itself out of the equation so that the signal is independent of the concentration

$$\Delta C(k,B) = \frac{c^0_{non-binding} + c^0_{binding} * B}{c^0_{non-binding} + c^0_{binding}} * 100 \quad (15)$$

This formula can be rearranged as following (derivation in appendix)

$$B = \frac{\frac{\Delta C}{100} - \frac{c^0_{non-binding}}{c^0_{non-binding} + c^0_{binding}}}{1 - \frac{c^0_{non-binding}}{c^0_{non-binding} + c^0_{binding}}} \quad (16)$$

Combining formula 2 and 6 the impurity level I can be expressed as

$$I = \frac{c^0_{non-binding}}{c^0_{non-binding} + c^0_{binding}} \quad (17)$$

This can then be inserted in formula 16 and combined with formula 4 to

$$\%breakthrough = B * 100 = \frac{\frac{\Delta C}{100} - I}{1 - I} * 100 \quad (18)$$

The impurity level can be derived from the UV signals at the beginning of the breakthrough, similar to the baseline, as shown in Eq. (6) and remains constant for the entire process. ΔC at the timepoint t can be obtained from the UV signals according to formula 13. Therefore, the control signal ΔC can be used to predict the column breakthrough independently from the inlet concentration and can thus be used to control column loading based on product breakthrough.

3. Material and methods

3.1. Influence of inlet concentration changes on control signals

To examine the influence of changes in the concentration of the inlet stream on ΔUV and the control signal ΔC, both signals were calculated for changing inlet concentrations and various breakthrough levels according to Eqs. (12) and (15), respectively.

An example Matlab code can be found in the Appendix A.

3.2. Simulation of chromatographic column breakthrough with fluctuating inlet stream and examination of peak broadening

A simple model consisting of an inlet, a stirred tank and a chromatographic column was modeled to simulate column breakthroughs with fluctuating inlet streams. The fluctuation inlet profile was achieved by a repeated inlet sequence of low concentration -> high concentration -> low concentration, followed by no feeding, into the stirred tank. The chromatographic column is then subsequently loaded from the stirred tank at a reduced flow rate to obtain a closed mass balance. The impurity level I was set to 0.8. The idea of this set-up is to mimic an integrated process of a flow through chromatography followed by a PCC bind-and-elute step as shown in Fig. 3.

A quasi-stationary lumped rate model with pores, in which mass transfer happens only by binding and a lumped film diffusion, was chosen to represent the chromatographic column due to its simplicity and wide use in modeling of protein chromatography [26–28], with a classic Langmuir binding as a binding model [29]. Model parameters are adapted from literature to represent a reasonable affinity like behaviour of protein purification with a long breakthrough and are summarized in Table 1.

In the first simulation band broadening due to column dispersion and film diffusion was neglected for impurities (dispersion = 0 m²/s, pore diffusion = 1 m/s) to show the influence of this parameters on the calculated signals ΔUV and ΔC. The different control signals were calculated in accordance with Eqs. (1) and (13) and ΔC was transferred in percent with Eq. (18). The average impurity concentration was set as a baseline for calculations.

To further examine the influence of band broadening on the control signals, a non-binding rectangular inlet signal was modeled incorporating column dispersion and film diffusion and analyzed.

An example code can be found in the Appendix B.

3.3. Software

Mechanistic modeling was conducted using the open source software "Chromatography Analysis and Design Toolkit (CADET)" version 4.1.0 (https://cadet.github.io/) [30]. Coding and calculations were done in Python 3.8 (Anaconda Inc., USA) and Matlab R2019b (MathWorks Inc., USA). Prism 9 (GraphPad Software, USA) was used for visualization.

3.4. Experimental control of integrated process

Two experiments were conducted to compare two different approaches. An integrated continuous process developed by our group for the production of virus-like particles based on murine polyomavirus major capsid protein VP1 platform, consisting of flow through chromatography, followed by a capturing in bind and elute mode was used experimentally [31,32]. In brief, murine polyomavirus major capsid protein VP1 with inserted antigen J8 was expressed in *E.coli* (Rosetta™ 2(DE3), Merck, Germany), lyzed by ultrasonication, centrifuged twice and filtered through 0.45 µm filter (Minisart®, Sartorius, Germany) to obtained clarified cell lysate

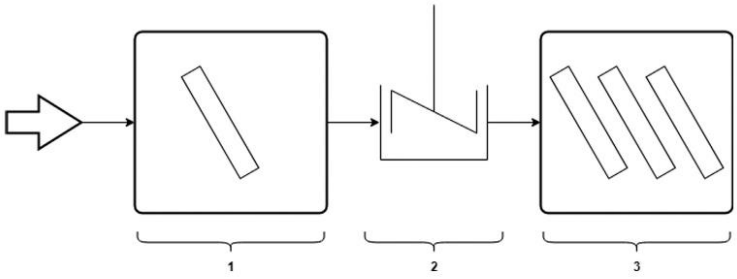

Fig. 3. Experimental set up. The clarified supernatant was first purified in multiple cycle flow through step (1) and collected in a stirred tank (2). The collected flow through was then processed in a 3 column PCC process in bind and elute mode (3). Both ÄKTAs were run parallel to obtain a continuous process.

Table 1
Model parameter used to model column breakthrough with varying inlet stream concentration.

Inlet									
Phase 1	conc. binding	1.00E-06	mol/m^3	conc. non-binding	4.00E-06	mol/m^3	flowrate	1	ml/min
Phase 2	conc. binding	3.00E-06	mol/m^3	conc. non-binding	1.20E-05	mol/m^3	flowrate	1	ml/min
Phase 3	conc. binding	1.00E-06	mol/m^3	conc. non-binding	4.00E-06	mol/m^3	flowrate	1	ml/min
Phase 4	conc. binding	0.00E+00	mol/m^3	conc. non-binding	0	mol/m^3	flowrate	0	ml/min
Stirred tank									
initial volume		2.00E-05	m^3						
initial conc. binding		2.20E-06	mol/m^3	initial conc. Non-binding	8.80E-06	mol/m^3			
Column									
Model		Lumped rate with pores							
Binding		Langmuir							
Flowrate		1	ml/min						
Length		0.025	m						
Radius		3.75E-03	m						
Dispersion		5.00E-07	m^2/s	[35]					
Porosity		0.36		[36]					
Particle porosity		0.9		[36]					
Particle radius		7.50E-05	m						
Film diffusion		2.00E-06	m/s	[37]					
K_A/K_D		2.00E+08		[38]					
Q_{max}		1.00E-03	mol/m^3						

for further processing. Multiple cycle flow-through chromatography was conducted on an ÄKTA™ Avant with a prepacked 5 ml Capto™ Q column. The flowthrough was collected in a 50 ml stirred tank, which was used as a continuous feed for an ÄKTA™ 3C-PCC equipped with three Capto™ MMC columns (column volume 1 ml, Cytiva, Sweden). The process is illustrated in Fig. 3. The flow rate during loading for the 3C-PCC was 0.5 ml/min and the cycle time of the flow through process, consisting of loading, regeneration and equilibration was set to an overall output of 0.5 ml/min. For the first run the classic dynamic control calculating ΔUV as described by Cytiva was used for process control, in which the baseline is adjusted after every cycle [22]. Column switching was triggered as soon as ΔUV reached 60% MM^{-1}. The second run used ΔC to calculated the breakthrough by neglecting the baseline (formula (13)) and used this signal to control the column switching. Column switching was triggered as soon as the signal ΔC reached 93.5% MM^{-1}. The impurity level I to transfer the control signal into a percentual breakthrough was obtained by the first breakthrough after 5 min and had the value 0.84. According to formula 18 this corresponds to a product column breakthrough of 60% MM^{-1}. This is similar to obtaining the baseline to calculate ΔUV for which the breakthrough signal after 5 min is set as a baseline. To compare the performance, the elution peak areas were calculated by integrating the UV_{280} signal over time to estimate the actual amount of bound product per cycle.

4. Results

4.1. Influence of concentration change on control signal ΔUV

The influence of a changing inlet concentration on the control signal ΔUV and ΔC is plotted in Fig. 4. As shown in Fig. 4 (C) and (D), the control signal ΔC does not change if the inlet concentration changes. This is true for all impurities levels as well as for all breakthrough levels. On the other hand, the use of an impurity baseline in calculating ΔUV leads to an extremely sensitive signal (Fig. 4 (A) and (B)). Slight deviations in the inlet concentration have a massive impact on the resulting ΔUV signal. For example, an increase of only 5% MM^{-1} of the inlet concentration results in a calculated ΔUV of 30% MM^{-1} if there are 90% MM^{-1} impurities in the sample and 0% MM^{-1} breakthrough is assumed. Similarly, a decrease of 5% MM^{-1} changes ΔUV to an illogical value of -90% MM^{-1} for the same conditions. A further reduction in the inlet concentration shows asymptotic behaviour towards $\pm\infty$ and eventually flips to values of $\Delta UV > 100\%$ MM^{-1}. The vertical asymptote is dependent on the impurity level and the position equals the impurity level (e.g. the asymptote of an impurity level of 10% MM^{-1} will be reached at a 10% MM^{-1} decrease in the inlet concentration). Different breakthrough levels (Fig. 4 (C)) do not influence the overall trend. The percentile change is smaller for higher breakthrough levels and results in a stable signal at

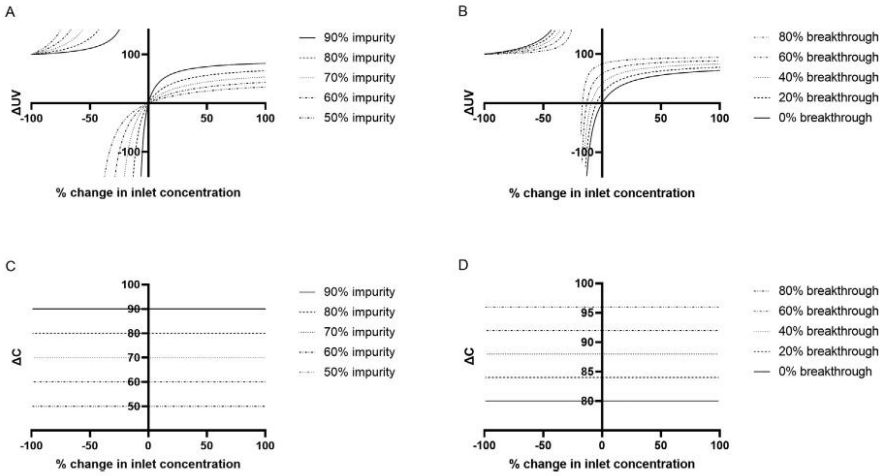

Fig. 4. Change of control signal ΔUV as a function of change of inlet concentration. (A) Classic approach with initial impurity level as baseline at various impurity levels, with 0% w w^{-1} breakthrough. (B) Classic approach with initial impurity of 80% w w^{-1} as baseline at different breakthroughs (C) Neglecting baseline at various impurity levels, with 0% w w^{-1} breakthrough. (D) Neglecting baseline with initial impurity of 80% w w^{-1} at different breakthroughs.

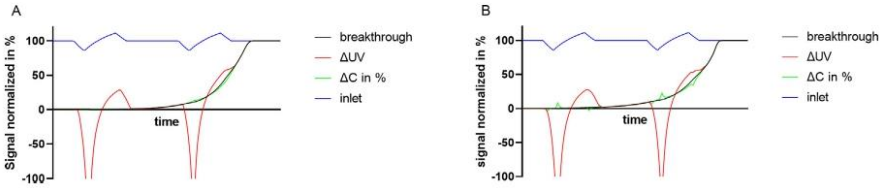

Fig. 5. Simulated column breakthrough of the binding part during loading and the corresponding control signal ΔUV with or without a baseline, normalized in percent. In (A) diffusion caused by dispersion and film diffusion was neglected for the non-binding part, while in (B) the non-binding parameter has the same values for dispersion and film diffusion as the binding part.

100% MM^{-1} breakthrough (not shown in graph). In general, the higher the impurities, the more sensitive is the signal.

4.2. Simulation of chromatographic column breakthrough with fluctuating inlet stream and examination of peak broadening

During the modeled set-up, the inlet stream concentration fluctuated ≤15% MM^{-1} around the average concentration. As can be clearly seen in Fig. 5 (A), changes in the inlet concentration result in strong changes of ΔUV and the signal only partially follows the actual breakthrough. The control signal decreases to illogical values below 0% MM^{-1} twice. It also overestimates the actual breakthrough as high values of 30% MM^{-1} can be observed, even though the actual breakthrough of the binding product is below 5% MM^{-1}. On the other hand, the breakthrough calculated from ΔC matches the actual breakthrough perfectly. This corresponds to the theoretical behaviour of the signals described Section 4.1. In the more realistic simulation in which band broadening caused by column dispersion and film diffusion is included (Fig. 5 (B)), the overall trend remains the same and opposed to the classic signal ΔUV, ΔC represents the actual breakthrough appropriately and can be used to control a process with fluctuating inlet concentration. Small sharp spikes in the signal can be observed (Fig. 5 (B), green line), whenever the inlet concentration fluctuates. This effect is clearer in Fig. 6 which demonstrates the simulation of a non-binding rectangular inlet pulse. After passing the column, the former rectangular shaped pulse becomes a bell-shaped peak, with a broader base and a lower maximum concentration. As nothing binds to the column, a constant ΔC of 100% MM^{-1} would be expected, which is not the case. At the edges of the outlet peak, ΔC shows sharp spikes and is above 100% MM^{-1}. In the middle of the

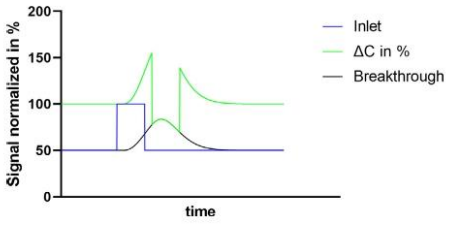

Fig. 6. Simulated column breakthrough and corresponding control signal ΔC in % w w^{-1} of a rectangular non-binding inlet impulse. Blue shows the normalized concentration at the column inlet, black shows the concentration at the column outlet. Green represents ΔC in % w w^{-1} calculated from the inlet and outlet signal. Formatted: Font: Not Italic Formatted: Font: Not Italic Captions. (For interpretation of the references to colour in this figure legend, the reader is referred to the web version of this article.)

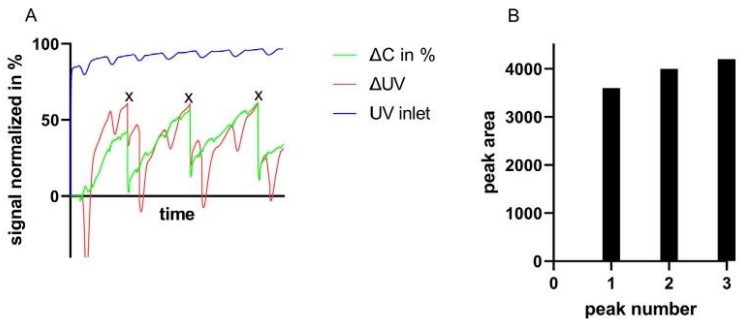

Fig. 7. (A) Chromatogram of a 3 column PCC experiment with fluctuating inlet stream (blue) controlled by the classic dynamic control using ΔUV (in red) and baseline adjustment after each column switching. (x) indicates when column switching was triggered. The ΔUV signal is directly obtained from the ÄKTA system, while ΔC is calculated from the raw data. (B) Elution peak area obtained by peak integration at 280 nm for the corresponding elution steps. (For interpretation of the references to colour in this figure legend, the reader is referred to the web version of this article.)

peak, ΔC shows values below 100% MM^{-1} and follows the actual breakthrough. Band broadening can therefore influence the calculated ΔUV and ΔC.

4.3. Experimental control of integrated process

The chromatogram of an experiment in which the ÄKTA PCC is controlled with the classic dynamic control using ΔUV as a control signal is shown in Fig. 7 (A), and the measured elution peak areas of the corresponding elution peaks are plotted in Fig. 7 (B). The inlet concentration fluctuates between 5 and 10% MM^{-1} and shows a slight overall increase over the entire run. The ΔUV signal obtained directly from the ÄKTA system fluctuates strongly, and also shows negative values at some points. These fluctuations can be dramatically in both directions, for example there is a rapid drop of a calculated breakthrough from 50% MM^{-1} to $<$ 0% MM^{-1} in the second loading cycle or an increase from 30% to 50% MM^{-1} in the third cycle. Overall, the signal seems to follow an increasing trend during loading, and changes in the inlet signal lead to strong variations in the signal in both directions. The calculated ΔC from the raw data as a comparison shows a steady increase in the breakthrough during each loading cycle and has only slight variation whenever the inlet concentration fluctuates. It does also noticeably differ from the ΔUV breakthrough signal when column switching was triggered. While ΔUV shows a product breakthrough of 60% MM^{-1} whenever column switching was triggered, ΔC calculated a product breakthrough of 43% MM^{-1}, 57% MM^{-1} and 61% MM^{-1}, respectively. Importantly, the elution peak areas of the experiment are not consistent and increase from 3600 to 4000 to 4200 mAU min^{-1} showing the same trend as the calculated ΔC indicates.

Fig. 8 shows the chromatogram of a similar run controlled by ΔC. The inlet stream concentration fluctuates between 5 and 10% MM^{-1} and slightly dips towards the middle of the run. The control signal ΔC from the ÄKTA system transferred into the actual breakthrough with formula (18) shows a steady increase from 0% MM^{-1} to ca. 60% MM^{-1} at which column switching is triggered. There are only minor spikes whenever there is a sudden change in the inlet concentration and an oscillation at the end of the third loading, which was caused by an air bubble in the pump. The ΔUV signal calculated from the raw data on the other hand is never in a reasonable range between 0 and 100% MM^{-1} and flips several times from negative to positive values above 100% MM^{-1} and vice versa (shown in Fig. 8(A), red line). The elution peak areas are very consistent for every loading cycle and differ less than 2% mAU min^{-1} mAU^{-1} min from their average.

5. Discussion

The classic way of calculating the breakthrough in a PCC process using ΔUV in which a baseline is subtracted works perfectly if the concentration of the inlet stream remains constant within a loading cycle. This has been shown multiple times in literature [9,23,24,33]. As demonstrated already small changes in the inlet concentration can have a massive impact on the resulting signal. This effect is distinct for a high non-binding impurity level. The PCC processes are often used for initial capturing of protein from cell supernatant or clarified cell lysate with very high levels of non-binding impurities and therefore this is a real threat in real-time applications. An increase in the inlet concentration leads to an increase in the resulting ΔUV, overestimating the breakthrough and therefore triggers an early column switching. As a consequence, the resin dynamic binding capacity utilization will decrease, however no product will be lost. A decrease in the inlet concentration can have a more severe impact as it results in a lower or even negative ΔUV and therefore underestimates the breakthrough. Thus, column switching will be delayed or not triggered at all, which results in product loss due to overloading. Further decreases in the inlet concentration will flip the signal ΔUV to values above 100% MM^{-1} as the vertical asymptote is crossed. As this will always trigger column switching this can lead to a very early interruption of the loading cycle. In contrary in our study, using ΔC as a control signal solves this issue, as it is independent of inlet feed concentration. The *in-silico* simulations showed that ΔC opposed to ΔUV, can be used to perfectly calculate the column breakthrough from the UV inlet and UV outlet signals for changing inlet concentrations, as long as column dispersion is neglected. In real set-ups there is always dispersion of the signal and thus the signal ΔC will show spikes in the signal whenever inlet concentration changes quickly. The simulated non-binding rectangular inlet impulse elucidated this effect. At the edges the control signal is above 100% MM^{-1}, while inside the peak the signal is below 100% MM^{-1}. This is a logical consequence caused by dispersion, the concentration outside of the former shape is higher than before and inside the former shape the concentration is lower. This explains the spikes that can be observed in the simulation with column dispersion and diffusion (Fig. 5 (B)) and is an unavoidable effect if the inlet concentration changes. Due to dispersion the outlet signal will never perfectly fit the inlet signal and flaws the calculation. This was particularly critical at the edges of signals and might be negligible for rather slow changes in the concentration. Sudden changes will result in spikes in the control signal, which might trigger column switching.

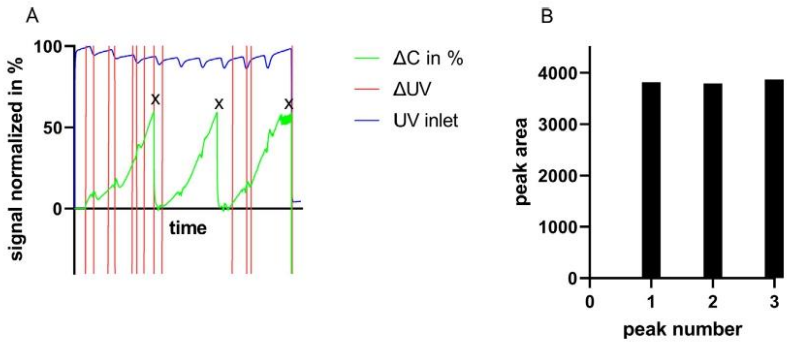

Fig. 8. (A) Chromatogram of a 3 column PCC experiment with fluctuating inlet stream (blue) controlled with ΔC (in green) as a control signal. (x) indicates when column switching was triggered. The ΔC signal is directly obtained from the ÄKTA system and translated in % $w w^{-1}$, while ΔUV is calculated from the raw data. (B) Elution peak area obtained by peak integration at 280 nm for the corresponding elution steps. (For interpretation of the references to colour in this figure legend, the reader is referred to the web version of this article.)

The experiments verified the findings of *in-silico* simulations. Controlling a periodic counter current chromatography process with the classic ΔUV approach led to inconsistent loading. As the inlet concentration slightly increased during the experiment, the actual breakthrough was overestimated and column switching was triggered early (see Section 4.1). Interestingly, this can be clearly seen in the ΔC signal calculated from raw data. Given a slight increase of the inlet feed concentration over time it would have been expected that the elution peak areas decrease in the subsequent cycles, caused by the breakthrough overestimation. This was not the case and can be explained by the sensitivity of ΔUV to concentration fluctuations. The fluctuations of the inlet stream concentration led to massively fluctuating ΔUV signals and column switching therefore occurred rather randomly than in a controlled manner. It is also worth noting that depending on when and how exactly the concentration changed, experiments often failed completely. The use of ΔC enables the control of a PCC process even if the inlet concentration fluctuated or changed over time and led to very consistent loading results. Calculating ΔUV from the raw data showed the typical problem of this signal. It did not represent the breakthrough and would have triggered column switching several times at wrong time points. A process with changing inlet concentration would be impossible to control. Another problem that is circumvented by neglecting a baseline is to determine when exactly the baseline has to be set. In a highly unstable signal, the breakthrough curve never reaches a stable plateau as shown in Fig. 2 and therefore inevitably leads to a baseline that does not represent the impurity content, as the absolute impurity content is dependent on the concentration. In contrast, the impurity level I is independent on the concentration and can be determined at the beginning of the process as long as no product breakthrough occurs. Band broadening caused by dispersion and diffusion does also limit ΔC and also every other method that is based on comparing inlet to outlet signals. New concepts need to be developed to control such a process, for example signal smoothing or inclusion of a dispersion term can help to account for this issue. Another potential solution is the integration of a stirred tank, as shown in the experiments, that can help to level out changes in the concentration to a controllable degree, albeit with added complexity. Another limitation of the proposed strategy is, that the calculations are only valid if the ratio of non-binding impurities to binding product remains constant, as obtained e.g. by dilution, flow through chromatography or elution from a prior chromatography step. If both non-binding impurities and binding product concentrations in the inlet feed stream change independently, and the ratio of binding product to non-binding impurities changes, the proposed strategy might fail. Non-product specific signals such as UV absorbance cannot distinguish between product and impurity and if the feed concentration as well as the ratio of product/impurities change alternative approaches need to be developed that are not based on UV signals alone. Recently, Raman and UV spectroscopy in combination with Partial-Least-Squares models and Convolutional Neural Networks have been examined to predict mAb concentration in column effluent, which seems to be a promising approach for defined products [34].

6. Conclusion

The proposed way of calculating the column breakthrough from inlet and outlet UV data is not influenced by the changes in the inlet concentration. Therefore, it extends the control of PCC process from only constant feed streams to feed streams with fluctuating concentration. This not only increases the robustness of controlling column loading in general, but also enables the control of integrated processes, which often show unsteady product streams and varying concentrations. It can be easily adapted in commercial PCC systems as no hardware adaption is needed and application is also not limited to the use of UV sensors. Although in theory even rapid changes in the concentration should not alter the control signal, peak broadening caused by dispersion and diffusion is an inherent characteristic that can flaw the control signal and strategies to limit the slope of concentration changes need to be developed to obtain a useable signal in integrated continuous processes. The new control strategy presented in this work has the potential to provide for enhanced PCC control in real-world applications where process inlet fluctuations occur.

Funding

This research did not receive any specific grant from funding agencies in the public, commercial, or not-for-profit sectors.

Declaration of Competing Interest

The Authors declare that they have no known competing financial interest or personal relationships that could have appeared to influence the work reported in this paper.

CRediT authorship contribution statement

Lukas Gerstweiler: Conceptualization, Methodology, Software, Formal analysis, Visualization, Investigation, Writing – original draft. **Jagan Billakanti:** Conceptualization, Methodology, Writing – review & editing. **Jingxiu Bi:** Conceptualization, Resources, Supervision, Writing – review & editing. **Anton P.J. Middelberg:** Conceptualization, Resources, Supervision, Writing – review & editing, Project administration.

Acknowledgments

The authors acknowledge the work of the modeling and simulation department at the Forschungszentrum Jülich for developing CADET and providing their help.

Supplementary materials

Supplementary material associated with this article can be found, in the online version, at doi:10.1016/j.chroma.2022.462884.

References

[1] L. Gerstweiler, J. Bi, A.P. Middelberg, Continuous downstream bioprocessing for intensified manufacture of biopharmaceuticals and antibodies, Chem. Eng. Sci. 231 (2021) 116272, doi:10.1016/j.ces.2020.116272.
[2] Z. Li, Q. Gu, J.L. Coffman, T. Przybycien, A.L. Zydney, Continuous precipitation for monoclonal antibody capture using countercurrent washing by microfiltration, Biotechnol. Prog. 35 (2019) e2886, doi:10.1002/btpr.2886.
[3] D. Hekmat, M. Huber, C. Lohse, N. von den Eichen, D. Weuster-Botz, Continuous crystallization of proteins in a stirred classified product removal tank with a tubular reactor in bypass, Cryst. Growth Des. 17 (2017) 4162–4169, doi:10.1021/acs.cgd.7b00436.
[4] P.A.J. Rosa, A.M. Azevedo, S. Sommerfeld, M. Mutter, W. Bäcker, M.R. Aires-Barros, Continuous purification of antibodies from cell culture supernatant with aqueous two-phase systems: from concept to process, Biotechnol. J. 8 (2013) 352–362, doi:10.1002/biot.201200031.
[5] R. Godawat, K. Konstantinov, M. Rohani, V. Warikoo, End-to-end integrated fully continuous production of recombinant monoclonal antibodies, J. Biotechnol. 213 (2015) 13–19, doi:10.1016/j.jbiotec.2015.06.393.
[6] L. Arnold, K. Lee, J. Rucker-Pezzini, J.H. Lee, Implementation of fully integrated continuous antibody processing: effects on productivity and COGm, Biotechnol. J. 14 (2019) e1800061, doi:10.1002/biot.201800061.
[7] N. Kateja, D. Kumar, S. Sethi, A.S. Rathore, Non-protein A purification platform for continuous processing of monoclonal antibody therapeutics, J. Chromatogr. A 1579 (2018) 60–72, doi:10.1016/j.chroma.2018.10.031.
[8] F. Feidl, S. Vogg, M. Wolf, M. Podobnik, C. Ruggeri, N. Ulmer, R. Wälchli, J. Souquet, H. Broly, A. Butté, M. Morbidelli, Process-wide control and automation of an integrated continuous manufacturing platform for antibodies, Biotechnol. Bioeng. 117 (2020) 1367–1380, doi:10.1002/bit.27296.
[9] R. Godawat, K. Brower, S. Jain, K. Konstantinov, F. Riske, V. Warikoo, Periodic counter-current chromatography-design and operational considerations for integrated and continuous purification of proteins, Biotechnol. J. 7 (2012) 1496–1508, doi:10.1002/biot.201200068.
[10] D. Baur, M. Angarita, T. Müller-Späth, F. Steinebach, M. Morbidelli, Comparison of batch and continuous multi-column protein A capture processes by optimal design, Biotechnol. J. 11 (2016) 920–931, doi:10.1002/biot.201500481.
[11] B. Somasundaram, K. Pleitt, E. Shave, K. Baker, L.H.L. Lua, Progression of continuous downstream processing of monoclonal antibodies: current trends and challenges, Biotechnol. Bioeng. 115 (2018) 2893–2907, doi:10.1002/bit.26812.
[12] X. Gjoka, R. Gantier, M. Schofield, Transfer of a three step mAb chromatography process from batch to continuous: optimizing productivity to minimize consumable requirements, J. Biotechnol. 242 (2017) 11–18, doi:10.1016/j.jbiotec.2016.12.005.
[13] C. Brämer, K. Ekramzadeh, F. Lammers, T. Scheper, S. Beutel, Optimization of continuous purification of recombinant patchoulol synthase from Escherichia coli with membrane adsorbers, Biotechnol. Prog. (2019) e2812, doi:10.1002/btpr.2812.
[14] A. Brown, J. Bill, T. Tully, A. Radhamohan, C. Dowd, Overloading ion-exchange membranes as a purification step for monoclonal antibodies, Biotechnol. Appl. Biochem. 56 (2010) 59–70, doi:10.1042/BA20090369.
[15] K. Veeraragavan, A. Bernier, E. Braendli, Sample displacement mode chromatography: purification of proteins by use of a high-performance anion-exchange column, J. Chromatogr. A 541 (1991) 207–220, doi:10.1016/S0021-9673(01)95993-X.
[16] A. Creasy, J. Lomino, G. Carta, Gradient elution behavior of proteins in hydrophobic interaction chromatography with a U-shaped retention factor curve under overloaded conditions, J. Chromatogr. A 1578 (2018) 28–34, doi:10.1016/j.chroma.2018.10.003.
[17] J.M. Mollerup, A review of the thermodynamics of protein association to ligands, protein adsorption, and adsorption isotherms, Chem. Eng. Technol. 31 (2008) 864–874, doi:10.1002/ceat.200800082.
[18] M.F. Wahab, J.K. Anderson, M. Abdelrady, C.A. Lucy, Peak distortion effects in analytical ion chromatography, Anal. Chem. 86 (2014) 559–566, doi:10.1021/ac402624a.
[19] A. Löfgren, J. Gomis-Fons, N. Andersson, B. Nilsson, L. Berghard, C.L. Hägglund, An integrated continuous downstream process with real-time control: a case study with periodic countercurrent chromatography and continuous virus inactivation, Biotechnol. Bioeng. 118 (2021) 1664–1676, doi:10.1002/bit.27681.
[20] Bangtsson, Estrada, Lacki, Skoglar (2012). *Method in a chromatography system.* (US Patent No.: US20120091063A1)
[21] R.A. Chmielowski, L. Mathiasson, H. Blom, D. Go, H. Ehring, H. Khan, H. Li, C. Cutler, K. Lacki, N. Tugcu, D. Roush, Definition and dynamic control of a continuous chromatography process independent of cell culture titer and impurities, J. Chromatogr. A 1526 (2017) 58–69, doi:10.1016/j.chroma.2017.10.030.
[22] Cytiva, (2020). *The use of dynamic control in continuous chromatography. (Application note: CY15112-10Jul20-AN)* https://cdn.cytivalifesciences.com/dmm3bwsv3/AssetStream.aspx?mediaformatid=10061&destinationid=10016&assetid=30271
[23] J.P. Mendes, R.J.S. Silva, M. Berg, L. Mathiasson, C. Peixoto, P.M. Alves, M.J.T. Carrondo, Oncolytic virus purification with periodic counter-current chromatography, Biotechnol. Bioeng. (2021), doi:10.1002/bit.27779.
[24] V. Warikoo, R. Godawat, K. Brower, S. Jain, D. Cummings, E. Simons, T. Johnson, J. Walther, M. Yu, B. Wright, J. McLarty, K.P. Karey, C. Hwang, W. Zhou, F. Riske, K. Konstantinov, Integrated continuous production of recombinant therapeutic proteins, Biotechnol. Bioeng. 109 (2012) 3018–3029, doi:10.1002/bit.24584.
[25] C. Brämer, L. Tünnermann, A. Gonzalez Salcedo, O.W. Reif, D. Solle, T. Scheper, S. Beutel, Membrane adsorber for the fast purification of a monoclonal antibody using protein a chromatography, Membranes 9 (2019) (Basel), doi:10.3390/membranes9120159.
[26] A. Felinger, G. Guiochon, Comparison of the kinetic models of linear chromatography, Chromatographia 60 (2004), doi:10.1365/s10337-004-0288-7.
[27] F. Steinebach, M. Angarita, D.J. Karst, T. Müller-Späth, M. Morbidelli, Model based adaptive control of a continuous capture process for monoclonal antibodies production, J. Chromatogr. A 1444 (2016) 50–56, doi:10.1016/j.chroma.2016.03.014.
[28] D. Baur, M. Angarita, T. Müller-Späth, M. Morbidelli, Optimal model-based design of the twin-column CaptureSMB process improves capacity utilization and productivity in protein A affinity capture, Biotechnol. J. 11 (2016) 135–145, doi:10.1002/biot.201500223.
[29] I. Langmuir, The adsorption of gases on plane surfaces of glass, mica and platinum, J. Am. Chem. Soc. 40 (1918) 1361–1403, doi:10.1021/ja02242a004.
[30] S. Leweke, E. Von Lieres, Chromatography analysis and design toolkit (CADET), Comput. Chem. Eng. 113 (2018) 274–294, doi:10.1016/j.compchemeng.2018.02.025.
[31] L. Gerstweiler, J. Bi, A.P.J. Middelberg, Virus-like particle preparation is improved by control over capsomere-DNA interactions during chromatographic purification, Biotechnol. Bioeng. 118 (2021) 1707–1720, doi:10.1002/bit.27687.
[32] L. Gerstweiler, J. Billakanti, J. Bi, A. Middelberg, Comparative evaluation of integrated purification pathways for bacterial modular polyomavirus major capsid protein VP1 to produce virus-like particles using high throughput process technologies, J. Chromatogr. A 1639 (2021) 461924, doi:10.1016/j.chroma.2021.461924.
[33] C. Brämer, S. Schreiber, T. Scheper, S. Beutel, Continuous purification of Candida antarctica lipase B using 3-membrane adsorber periodic counter-current chromatography, Eng. Life Sci. 18 (2018) 414–424, doi:10.1002/elsc.201700159.
[34] L. Rolinger, M. Rüdt, J. Hubbuch, Comparison of UV- and Raman-based monitoring of the protein a load phase and evaluation of data fusion by PLS models and CNNs, Biotechnol. Bioeng. 118 (2021) 4255–4268, doi:10.1002/bit.27894.
[35] B. Guélat, R. Khalaf, M. Lattuada, M. Costioli, M. Morbidelli, Protein adsorption on ion exchange resins and monoclonal antibody charge variant modulation, J. Chromatogr. A 1447 (2016) 82–91, doi:10.1016/j.chroma.2016.04.018.
[36] S.M. Pirrung, D. Parruca da Cruz, A.T. Hanke, C. Berends, R.F.W.C. Van Beckhoven, M.H.M. Eppink, M. Ottens, Chromatographic parameter determination for complex biological feedstocks, Biotechnol. Prog. 34 (2018) 1006–1018, doi:10.1002/btpr.2642.
[37] G. Wang, T. Briskot, T. Hahn, P. Baumann, J. Hubbuch, Estimation of adsorption isotherm and mass transfer parameters in protein chromatography using artificial neural networks, J. Chromatogr. A 1487 (2017) 211–217, doi:10.1016/j.chroma.2017.01.068.
[38] R.A. Latour, The Langmuir isotherm: a commonly applied but misleading approach for the analysis of protein adsorption behavior, J. Biomed. Mater. Res. A 103 (2015) 949–958, doi:10.1002/jbm.a.35235.

Chapter 7

An Integrated and Continuous Downstream Process for Microbial Virus-Like Particle Vaccine Biomanufacture

In this chapter, a continuous, automated, and integrated downstream process for the production of VLP vaccines against Group A Streptococcus was developed. The process integrates the findings of the previous chapters. The robustness of the process was tested with different initial lysate concentrations and the product quality was determined over several hours of processing.

Statement of Authorship

Title of Paper	An integrated and Continuous Downstream Process for Microbial Virus-Like Particle Vaccine Biomanufacture
Publication Status	Submitted to Biotechnology and Bioengineering
Publication Details	

Principal Author

Name of Principal Author (Candidate)	Lukas Gerstweiler		
Contribution to the Paper	Conceptualization, Methodology, Investigation, Writing – original draft, Visualization		
Overall percentage	80%		
Signature		Date	4.4.2022

Co-Author Contributions

By signing the Statement of Authorship. Each author certifies that:

I. The candidate's stated contribution to the publication is accurate (as detailed above)

II. Permission is granted for the candidate in include the publication in the thesis; and

III. The sum of all co-author contribution is equal to 100% less the candidate's stated contribution

Name of Co-Author	Jagan Billakanti		
Contribution to the Paper	Conceptualization, Methodology, Writing – review & editing		
Signature		Date	31/3/22

Name of Co-Author	Jingxiu Bi		
Contribution to the Paper	Conceptualization, Resources, Writing – review & editing, Supervision		
Signature		Date	31/03/2022

Name of Co-Author	**Anton P.J. Middelberg**		
Contribution to the Paper	Conceptualization, Resources, Writing – review & editing, Supervision, Project administration		
Signature		Date	30 March 2022

7.1 Abstract

In this study, we present the first integrated and continuous downstream process for the production of microbial virus-like particle vaccines. Modular murine polyomavirus major capsid VP1 with integrated J8 antigen was used as a model virus-like particle vaccine. The integrated continuous downstream process starts with crude cell lysate and consists of a flow through chromatography step followed by periodic counter current chromatography (PCC) (bind-elute) using salt tolerant mixed-mode resin and a subsequent in-line assembly. The automated process showed a robust behaviour over different inlet feed concentrations ranging from 1.0 mg ml^{-1} to 3.2 mg ml^{-1} with only minimal adjustments needed, and produced continuously high-quality virus-like particles, free of nucleic acids, with constant purity over extended periods of time. The average size remained constant between 44.8 ± 2.3 nm and 47.2 ± 2.9 nm comparable to literature. The process had an overall product recovery of 88.6% and a process productivity up to 2.56 mg h^{-1} ml_{resin}^{-1} in the PCC step, depending on the inlet concentration. Integrating a flow through step with a subsequent PCC step allowed streamlined processing, showing a possible continuous pathway for a wide range of products of interest.

7.2 Introduction

Viral structural proteins can self-assemble into particles that correspond to the overall appearance of native viruses, yet lacking genetic material. These so called virus-like particles (VLPs) are therefore unable to replicate and thus are considered non-pathogenic [1]. Due to their native capsid structure, VLPs can induce strong humoral and cellular immune responses without the need for adjuvants, making them powerful candidates for future vaccines [2–4]. Another key benefit of VLPs as vaccine candidates is the possibility to insert foreign antigens to construct vaccine candidates against all types of diseases while the underlying VLP construct remains the same. VLPs are therefore extensively examined as vaccine candidates

against pathogens such as Influenza, Rotavirus, Group A Streptococcus and others, and also are commercial products against human papillomavirus, malaria and hepatitis B/E [3,5–7].A disadvantage however, are the rather high costs of VLPs caused by complicated production and purification processes [8–10]. Downstream processing is often based on size exclusion chromatography and ultra-centrifugation that might face challenges in large-scale set-ups [8,11]. Another challenge are low binding capacities during chromatography in bind-and-elute mode [8].

To overcome some of the production challenges and to intensify the production of VLP vaccines, platform technologies have been developed that allow the production of a variety of VLPs while only requiring minimal adjustments of the underlying production process [12]. One possible pathway is to produce VLPs and antigens separately and subsequently attach them either by conjugation or by tag coupling approaches [13]. Another pathway is genetic fusion in which the antigen is genetically inserted into the viral structural protein with subsequent protein expression as one construct [14,15]. An advanced platform technology for VLP vaccines involves the use of murine poliomavirus major capsid protein VP1 with inserted antigen [12]. VLP vaccines based on this platform showed promising results in animal studies for pathogens such as Influenza, Group A Streptococcus and Rotavirus [6,16,17]. The capsomeres can be expressed unassembled in gram-per-litre concentration in *E.coli* and a highly efficient, scalable and integrated purification and production pathways have been developed [18,19].

Continuous bio-processing promises process intensification due to higher automation, increased equipment utilization and a reduced facility footprint, and furthermore leads to constant product quality and less batch-to-batch variation. A review on current developments of continuous bio-manufacturing has been recently published [20]. Despite its promises, continuous processing is not widely utilized within bio-pharmaceutical processing yet, but

gains more and more attention within scientific and industrial communities. Most research focuses on the transition of existing batch unit operations to continuous ones. Strategies such as periodic counter-current chromatography (PCC), multi-column solvent gradient purification (MCSGP) and simulated moving bed (SMB) for chromatography, counter-current mixer settlers for extraction, coiled-flow inverter and tubular reactors for precipitation and single-pass tangential flow filtration for filtration have been developed and described in the literature [21–28]. Integrated continuous processes however are seldom described and usually focus on antibody purification. For example 29 [29] coupled two PCC (protein A and CEX) steps with a flow through step, while 30 [30] integrated a PCC process with MCSGP and a flow through polishing to purify antibodies. As far as we are aware, an integrated continuous production pathway for VLPs formed by self-assembly *ex vivo* has not been developed or described.

To further extend the field of continuous bio-processing we developed and here report an automated continuous and integrated purification process for microbially-expressed VLP vaccines based on an integrated production pathway developed by our group [19]. The process couples a flow through Capto^{TM} Q chromatography step followed by a bind-elute multi modal (Capto^{TM} MMC) PCC process with subsequent in-line assembly of VLPs. It has been previously shown that non purified VP1 capsomeres form soluble aggregates with microbial DNA at low buffer salt concentrations, hindering purification [31]. In batch processing, the use of salt-tolerant mixed-mode resins with a previous flow through step allows processing at elevated salt concentrations, which suppress VP1-DNA aggregation, and therefore leads to better recovery. The salt-tolerant mixed-mode resin furthermore allows an integration of the two unit operations without buffer adjustment in between and enables a wide design space [19,31]. The continuous process described in this paper, developed by building on these batch studies produces VLPs of a constant good quality, removes DNA and

most contaminants, is scalable and can act as a platform technology for the development for new continuous production pathways of vaccines and biopharmaceuticals other than monoclonal antibodies.

7.3 Materials and Methods

7.3.1 Protein Expression and Sample Preparation

Murine polyomavirus major capsid protein VP1 with inserted Group A Streptococcus antigen J8 was constructed and expressed as described in our earlier paper [19]. In brief GCN4-J8 was inserted with flanking G4S linkers into VP1 and cloned into pETDuet-1 and transformed by heat shock transformation into Rosetta^{TM} 2(DE3) Singles^{TM} competent cells (Merck KGaA, Germany) and stored as 25% glycerol stocks. Cell stock was grown overnight in Terrific Broth (TB) medium (12 g l^{-1} tryptone (LP0042, Thermo Fisher Scientific, USA), 24 g l^{-1} yeast extract (P0021, Thermo Fisher Scientific, USA), 5 g l^{-1} Glycerol (GL010, ChemSupply, Australia), 2.31 g l^{-1} potassium dihydrogen phosphate (PO02600, ChemSupply, Australia) and 12.5 g l^{-1} dipotassium hydrogen phosphate (PA020, ChemSupply, Australia)) with 35 µg ml^{-1} chloramphenicol (GA0258, ChemSupply, Australia) and 100 µg ml^{-1} ampicillin (GA0283, ChemSupply, Australia)) at 37°C and 200 rpm, 1 l shake flask, 200 ml medium. Next morning overnight culture was diluted 1:40 into fresh TB media and grown in 1 l shake flasks each containing 200 ml of fermentation broth at 37°C and 200 rpm. After reaching an optical density OD_{600} of 0.5, the temperature was reduced to 27°C and protein expression was induced by IPTG (15529019, Thermo Fisher Scientific, USA) addition to a final concentration of 0.1 mM After 16 h expression, the cells were harvested by centrifugation, cell paste was washed once with 0.9% w w^{-1} sodium chloride (SL046, ChemSupply, Australia) and stored at -80°C in 50 ml aliquots until subsequent use.

To obtain clarified cell lysate, cells were resuspended in lysis buffer (20 mM Tris-hydrochloride (GB4431, ChemSupply, Australia), 1 mM EDTA (EA023, ChemSupply, Australia), 5% w w^{-1} glycerol, 5 mM dithiothreitol (DTT) (DL131, ChemSupply, Australia), pH 8.9) with 1x SigmaFast™ protease inhibitor (SA8820 Millipore Sigma, USA), lysed by ultrasonication (Scientz-IID, China), centrifuged twice for 30 min at 20130 g, 4°C (A5920R centrifuge, Eppendorf, Germany) and filtered (0.45 µm, Minisart®, Sartorius, Germany). After filtration NaCl was added to a final concentration of 0.35 M and diluted with lysis buffer pH 8.9 containing 0.35 M NaCl as needed. Clarified lysate was stored on ice during processing.

7.3.2 In Process Analytics

Total protein concentration was measured using the Bradford assay at 595 nm (BioRad Laboratories, USA) in 96-well plates (200 µl) with bovine serum albumin (BSA) as a standard. BSA standard concentration was verified by A_{280} absorbance on a NanoDrop™ (Thermo Fisher Scientific, USA).

Host cell DNA was measured with the Quant-iT™ broad range dsDNA Assay Kit (Q33130, Thermo Fisher Scientific, USA), with fluorescence (485/530 nm) measured on a 2300 Victor X5 multilabel reader (PerkinElmer, USA)

RP-HPLC was used to determine VP1-J8 concentration as previously described [19]. In brief samples were combined 1:4 with a denaturing buffer (8 M guanidine (GE1914, ChemSupply, Australia), 50 mM DTT, 20 mM Tris pH 8) and heated for 10 min at 75 °C. A gradient elution with water, containing 0.5% TFA (Buffer A) (TS181, ChemSupply, Australia), and acetonitrile (LC1005, ChemSupply, Australia), containing 0.4% TFA (Buffer B), was used to separate the sample (3 µl) on a Vydac Protein C4 column 2.1x100 mm, 5 µm (214TP521), at a flow of 1 ml min^{-1} and 60 °C column temperature. The elution program was as following: 6

min gradient from 35 % B to 60 % B, 30 s gradient from 60 % B to 100 % B, 1 min 100 % B, 30 s from 100 % B to 35 % B and 4 min of 35 % B [19].A Shimadzu UFLC-XR system (pump: LC-20AD-XR, autosampler: SIL-20AXR, diode array detector: SPD-M20A, column oven: CTO-20) with detection at 280 nm was used for HPLC experiments.

Size and shape of VLPs were examined under transmission electron microscopy (TEM). Samples (10 µl) were diluted 1:10 with MilliQ water. A drop of 5 µl was put on plasma cleaned carbon coated square meshed grids (GSCU100C, ProSciTec, Australia) and incubated at room temperature for 5 min. The sample was removed with blotting paper and the grid was washed twice with water before stained with 2 % w v^{-1} uranyl acetate for 2 min. Images were taken with a FEI Tecnai G2 Spirit with an Olympus SIS Veleta CCD camera at 120 kV voltage. Sizes were measured by counting pixels with GIMP 2.10.18. The pixel size has been calibrated

Reducing SDS-PAGE was conducted with TruPAGE^{TM} precast Gels 12 %, 10 x 8 cm 12-well (PCG2010, Millipore Sigma, USA) following the manufacturer's recommendations. Equal volumes of samples (6 µl) were used for all runs with Precision Plus Protein^{TM} Standard (1610363, Bio-Rad, USA) as a size standard.

Dynamic light scattering (DLS) was conducted on a Zetasizer NanoZS(Malvern Panalytical, UK). Samples of 500 µl, equilibrated at 20 degrees Celsius for 5 min were measured. Each measurement is the average of 100 measurements of 1 sample. The refractive index of the dispersant was assumed to be 1.33 with a viscosity of 1.02 cp [32]. As a fitting algorithm non-negative constrained least squares (NNLS) fitting algorithm was used.

7.3.3 Flow Through Chromatography

Continuous flow through chromatography was conducted in repeating cycles of flow through chromatography starting with clarified cell lysate of different total protein concentrations as described on a 5 ml prepacked HiTrap™ Capto™ Q column (Cytiva, Sweden) on an AKTA™ AVANT™ system (Cytiva, Sweden). One cycle consisted of following steps: 1.2 CV equilibration (lysis buffer pH 8.9 containing 0.35 M NaCl) at 5 ml min^{-1}, followed by sample loading til 90% of $DBC_{1\%}$ at 2 ml min^{-1} and a subsequent post loading wash with equilibration buffer (1 CV). This was followed by a wash cycle of 2 CV H_2O (10 ml min^{-1}), 17 CV 1 M NaOH in reverse flow (5ml min^{-1}), 2 CV of H_2O (10 ml min^{-1}) and 5 CV equilibration (5 ml min^{-1}). The maximum loading volume was dependent on the clarified lysate concentration determined during the first cycle. The maximum loading volume was set as a loading volume for subsequent processing. To minimise dilution the flowthrough peak was collected as shown in Appendix A1. Recovery was determined in a separate experiment for 10 cycles with clarified lysate having a total protein concentration of 3 mg ml^{-1} as a starting material, as this was the highest concentration used in the experiments.

7.3.4 Periodic Counter Current Chromatography

Continuous periodic counter current chromatography in a 3C-PCC set up was performed on an AKTA™ PCC™ system (Cytiva, Sweden) with 1 ml prepacked HiTrap™ Capto™ MMC columns. The collected flowthrough from the previous Capto™ Q chromatography run, which was collected in a stirred vessel (50 ml bottle on ice, 50 rpm, 20 mm stirring bar), was used without any further adjustment for bind-elute processing. To determine the design space, breakthrough curves at flowrates of 1 ml min^{-1} (1 min contact time), 0.5 ml min^{-1} (2 min contact time) and 0.25 ml min^{-1} (4 min contact time) were measured at a VP1-J8 concentration of 0.71 mg ml^{-1} and the maximum possible overloading calculated, according

to the area under the breakthrough curve method [23,33]. The maximum overloading can be defined as being when the integral of the breakthrough curve equals the dynamic binding capacity. For the actual continuous processing the switching times of the PCC process were controlled based on the dynamic UV control method developed by Cytiva [34] using column inlet UV absorbance and the column outlet UV absorbance of the first column in a connected set-up to calculate the column breakthrough. However, we found that the proposed method with ΔUV as a controlling signal is error prone if the inlet feed concentration is not constant, which is a result of the integrated process; therefore, loading to approximately 70% breakthrough was controlled with a new approach developed by our group [35].A cycle of the PCC process consists of following phases: Loading at a flowrate between 0.4-0.8 ml min^{-1} til breakthrough level triggered; Post loading wash of 2 CV at 1 ml min^{-1}; Washing with 5 CV at 1 ml min^{-1} with equilibration buffer containing no DTT (lysis buffer pH 8.9 containing 0.35 M NaCl); Elution with 20 CV of elution buffer (40mM di sodium hydrogen phosphate (SA026, ChemSupply, Australia), 1 M NaCl, 5% w w^{-1} glycerol, 1mM EDTA) at 1 ml min^{-1}; Cleaning with 1 M sodium hydroxide (SA178, ChemSupply, Australia) for 15 CV at 1 ml min^{-1}; Washing with water for 5 CV at 1 ml min^{-1}, and; Re-equilibration for with equilibration buffer for 5 CV at 1 ml min^{-1}. Recovery was measured in a separate experiment with a loading material containing 0.32 mg ml^{-1} VP1-J8 at a flow rate of 0.45 ml min^{-1}.

7.3.5 Assembly of VLPs

The elution of the PCC process was collected in a 50 ml stirred vessel (20 mm stirring bar, 50 rpm). The vessel was prefilled with approximately 10 ml of elution buffer, containing no product, to submerge the sensor. As described in Section 2.4 the elution buffer does not contain stabilizing DTT, which supresses VLP assembly. This approach to change the buffer system during elution allowed the removal of DTT without a dedicated buffer exchange step

[19]. The pH value in the vessel was controlled at a value of pH 7.2. This was implemented with a BioFlo® 320 control panel (Eppendorf, Germany) with 1 % v v^{-1} HCl, 1 M NaCl, 5% w w^{-1} glycerol as an acid solution and 0.2 M NaOH, 1 M NaCl, 5% w w^{-1} glycerol as a base solution. The pH adjusted VP1-J8 solution was continuously used as inlet A on an AKTA™ Go system (Cytiva, Sweden) and mixed 9:1 in-line with assembly trigger solution (30 mM calcium chloride (CA033, ChemSupply, Australia), 1 M NaCl, 5% w w^{-1} glycerol). After dilution and neutralizing remaining EDTA this achieves a final calcium ion concentration of 2 mM. The outlet was fractionated every 5 ml and incubated for 24 h before storage at -80 °C.

7.3.6 Process Integration and Experimental Set-Up

Figure 7-1 shows an overall flow chart of the VLP purification process; a picture of the whole set-up can be found in the Appendix (A2). The three-unit operations used in this workflow – Capto™ Q in flow through chromatography, Capto™ MMC PCC in bind-elute chromatography and in-line assembly of VLPs - were coupled with surge vessels (50 ml glass bottles with 20 mm magnetic stirring bar, (Schott AG, Germany)) at 50 rpm. The overall footprint of the whole downstream processing set-up was approximately 4 m of laboratory bench space for up to 7.56 mg h^{-1} overall productivity (2.52 mg h^{-1} ml_{resin}^{-1} at the PCC step). A 5 ml HiTrap Capto™ Q and 3 x 1 ml Capto™ MMC columns were used. The surge vessels as well as the clarified cell lysate were constantly flushed with nitrogen to prevent undesired protein oxidation. To show the robustness of the process, experiments with 3 different initial total protein concentrations of clarified cell lysate (1.0 mg ml^{-1},2.2 mg ml^{-1} and 3.2 mg ml^{-1}) were conducted. The only process parameters that were changed were flow rates of the PCC process and assembly process to match the output of the flow through step. Each experiment was run between 10 and 12 h. The process parameters are summarized in Table 7-1.

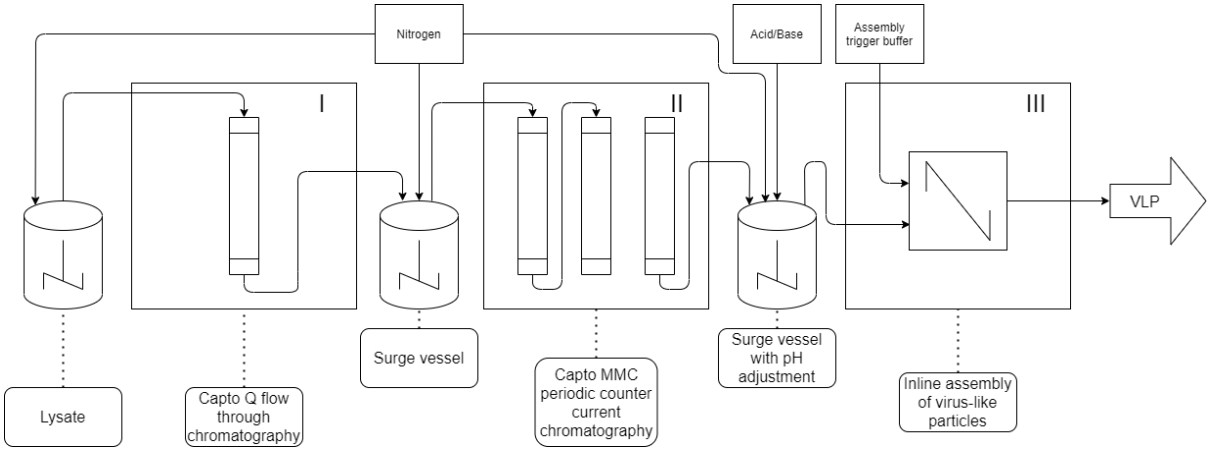

Figure 7-1 Flow chart of continuous process for the production of microbial VLPs consisting of three integrated unit operations. The clarified lysate containing viral capsomeres is first purified on Capto^{TM} Q in flow through mode (I, ÄKTA^{TM} AVANT^{TM}) and collected in a surge vessel. The collected flow through is then continuously loaded on Capto^{TM} MMC columns in a continuous periodic counter current chromatography process (II, ÄKTA^{TM} PCC^{TM}). The elution containing purified capsomeres is collected in a surge vessel and pH adjusted, after which it is mixed in-line with assembly trigger buffer (III, ÄKTA^{TM} GO^{TM}) to initiate assembly of VLPs. Pre-assembly the solutions are fumigated with nitrogen to prevent oxidation.

Table 7-1 Process parameter of conducted experiments.

	Experiment 1	Experiment 2	Experiment 3
Total protein concentration (mg mL^{-1})	1	2.2	3.2
DNA concentration (µg ml^{-1})	54.4	94.2	154
VP1 concentration (mg ml^{-1})	0.14	0.32	0.41
Loading flow through per cycle (ml)	25	17	14
PCC loading flow rate (ml min^{-1})	0.7	0.5	0.45
VLP Assembly flow rate (ml min^{-1})	0.22	0.2	0.2

7.4 Results and Discussion

7.4.1 Breakthrough Experiments and PCC design

Breakthrough experiments performed to determine process design space of the PCC process are illustrated in Figure 7-2. The breakthrough curve obtained for a flow rate of 0.25 ml min^{-1} (4 min residence time) demonstrated as expected a sigmoidal shape. However, in contrast, the breakthrough curve at 1 ml min^{-1} resembled more a logarithmic function. The curve for 0.5 ml min^{-1} describes a shape between the two aforementioned curves. This behaviour can be explained by the large size of VP1-J8 of 232 kDa and the resulting mass transfer limitations. This effect has been well described for other large biomolecules elsewhere in the literature [36–38]. The $DBC_{10\%}$ values decreased from 16.6 mg ml^{-1} to 13.3 mg ml^{-1} to 9.9 mg ml^{-1} with increasing flow rates of 0.25 ml min^{-1}, 0.5 ml min^{-1} and 1.0 ml min^{-1}, respectively. Similarly, the maximum column breakthrough until the column became overloaded in a PCC process decreased from 98% to 80% to 69%. The chosen trigger breakthrough level of 70 % for column switching ensured robust processing without significant product loss for the investigated flow rates between 0.25 ml min^{-1} and 1 ml min^{-1}. Lower flow rates would result in unreasonably long cycle times while higher flowrates bear the risk of product loss in the flow through. Recently it was shown that optimal process conditions in continuous twin column processes can be found at relatively low column residence times of between 1 and 2 min and column breakthroughs between 50% and 80% for low and medium product concentrations (< 5 mg ml^{-1}). This is however, highly dependent on the type of resin used and the desired product concentration in the feed stream, and it is thus hard to generalize [39].

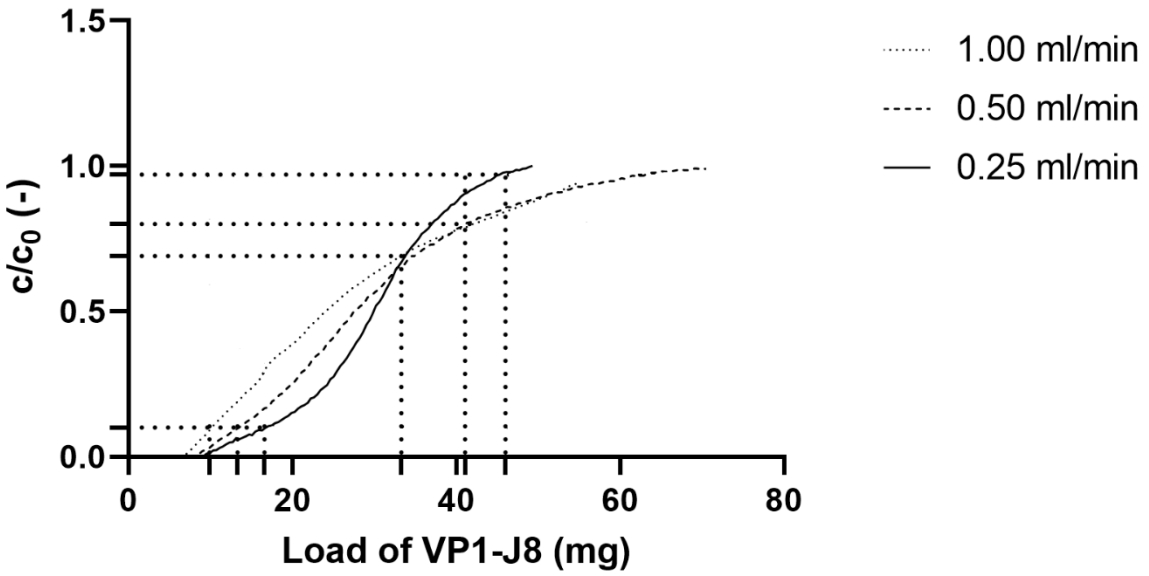

Figure 7-2 Breakthrough curves for VP1-J8 loading onto a 1 ml prepacked Capto™ MMC column at different flow rates. Maximum overloading for PCC processes based on the area under the curve method are highlighted with dotted lines, as well as $DBC_{10\%}$ as a reference for batch production.

7.4.2 Evaluating Integrated Process Performance

During the flowthrough chromatography step, a total of 60.3 ± 1.8 mg VP1 was applied to the Capto™ Q column and 60.0 ± 1.2 mg could be recovered, resulting in a recovery of 99.5 % for this step. This high recovery is expected as the product is not binding to the resin and thus losses are expected to be minimal. For the PCC step in bind-elute mode, out of 31.0 ± 0.62 mg VP1 applied on Capto™ MMC, 27.6 ± 1.38 mg (89.0 %) was recovered in the elution pool and approximately 0.73 ± 0.12 mg (2.4%) remained in the flow through. The product loss in the flow-through probably corresponds to aggregated VP1-J8 capsomeres, as we have recently shown that VP1-J8 aggregates do not bind to Capto™ MMC and remain in the flow-through [19]. The remaining 8.4% is either strongly bound to the matrix or non-eluted with selected conditions or stripped in the washing step with 1 M NaOH. A longer elution time

might help to further increase the recovery at the cost of a lower product concentration. Assembly into VLPs is triggered solely by the addition of assembly trigger buffer and therefore a 100% recovery for the assembly step is assumed. This results in an overall process recovery of 88.6 %, with a high product purity and quality as described in detail in Section 3.3. This is comparable to another process for HBCaAg VLPS achieving 86% recovery [40] and is significantly higher than other described batch processes for the production of VLPs that reported recoveries between 31% and 76% [40–43].

A chromatogram from the 3 column PCC unit operation of the third experiment having an initial total protein concentration of 3.2 mg ml^{-1} is shown in Figure 7-3. As can be seen the concentration of the inlet stream obtained from the surge vessel after Capto^{TM} Q flow through chromatography fluctuates slightly, caused by the cyclic nature of the prior flow through unit operation. The control strategy developed for unsteady inlet feed concentrations, reliably triggered column switching [35].

Figure 7-4 shows the VP1-8 concentration in the surge vessel after PCC processing, in which the pH value is adjusted (see Figure 7-1). The VP1-J8 concentration increases in the first 400 – 600 min before it reaches a stable level. This equilibration time is a result of prefilling the surge vessel with buffer, containing no product, to submerge the pH sensor. Although column switching in the PCC system is triggered at 70% product breakthrough and at a constant elution volume in all experiments, the VP1-J8 concentration equilibrates at different values in each experiment. As can be seen in Figure 7-4 the VP1-J8 concentration in the surge vessel equilibrates at concentrations of 0.43 mg ml^{-1}, 0.53 mg ml^{-1} and 0.70 mg ml^{-1} for initial total protein concentrations of the lysate of 1.0 mg ml^{-1}, 2.2 mg ml^{-1} and 3.2 mg ml^{-1} respectively. Thus, a higher product concentration in the inlet feed stream also translates to a higher product concentration in outlet stream if elution volume and column breakthrough remain constant. This can be explained by a non-constant bimding capacity in the concentration

range used in these experiments. The VP1-J8 concentration in the inlet feed of the PCC was only between 0.12 mg ml^{-1} (experiment 1) and 0.37 mg ml^{-1} (experiment 3) and assuming a Langmuir-like binding behaviour literature suggests a high dependence of the product concentration on the binding capacity in low concentration ranges [44,45]. If a constant product concentration in the surge vessel is desired, the elution volume could be controlled. Namely the elution volume could be decreased at low product concentrations or increased at higher product concentrations to obtain the same average product concentration.

Interestingly an increase in initial feed stream concentration does not translate linear increase in the overall productivity of the process. Doubling the initial protein concentration from 1 mg ml^{-1} to 2.2 mg ml^{-1} (experiment 1 to experiment 2) only increased the overall productivity after assembly by 12%, from 5.1 mg h^{-1} to 5.7 mg h^{-1} (1.7 mg h^{-1} ml_{resin}^{-1}, 1.9 mg h^{-1} ml_{resin}^{-1} in the PCC step). A further increase of the inlet concentration of 45% to 3.2 mg ml^{-1} (3. Experiment) increased the overall productivity by 32% to 7.56 mg h^{-1} (2.52 mg h^{-1} ml_{resin}^{-1} in the PCC step). This can be explained by the interplay of several effects. A main effect is that decreasing the inlet stream concentration enables longer cycles of the flow through chromatography step, which increases the volumetric throughput hence increasing the loading flow rate of the PCC step (see Table 1) compensating the lower product concentration. While the loading flow rate of the PCC step during experiment 1 (1 mg ml^{-1}) was 0.7 ml min^{-1} the flow rate was 0.5 ml min^{-1} in experiment 2 (2.2 mg ml^{-1}) and 0.45 ml min^{-1} in experiment 3 (3.2 mg ml^{-1}) (See Table 1).

Notably, the relationship between feed concentration and throughput of the flow through step is also not linear. Firstly, the time needed to regenerate the column (washing and equilibration) can be considered to be independent of the loading time and therefore leads to a non-linear relationship. Secondly, similar to the binding capacity of Capto™ MMC the binding capacity of the flow through step on Capto™ Q does also increase with increasing

inlet concentration. The amount of DNA that could be removed per flow-through cycle increased from 272 µg ml_{resin}^{-1} to 330 µg ml_{resin}^{-1} to 431 µg ml_{resin}^{-1}, thus leading to higher productivity of the flow through step and by extension the overall process.

Although higher concentrations in the starting material generally increase overall productivity, precise prediction of the extent of this increase is complicated as lower concentrations allow higher flowrates, but also change the binding capacities of the resins. In particular, the binding capacities seem to have a tremendous effect on the productivity, which also has been recently described for continuous 2 column processes in general [39]. A further in-depth analysis of the interplay of different process parameters and the influence of the feed stream concentration needs to be conducted, and optimal ratios of resin volumes of the flow through step to the PCC step in bind and elute need to be found. This might challenge upscaling as a rational selection of the required column volumes is currently not possible. The dependence of the performance on the feed concentration might limit a designed process to a certain concentration range which negatively affects the flexibility of the set-up. Recent developments in mechanistic modelling and the construction of so-called digital twins, might be a powerful tool for decision making, but needs to be extended to integrated processes.

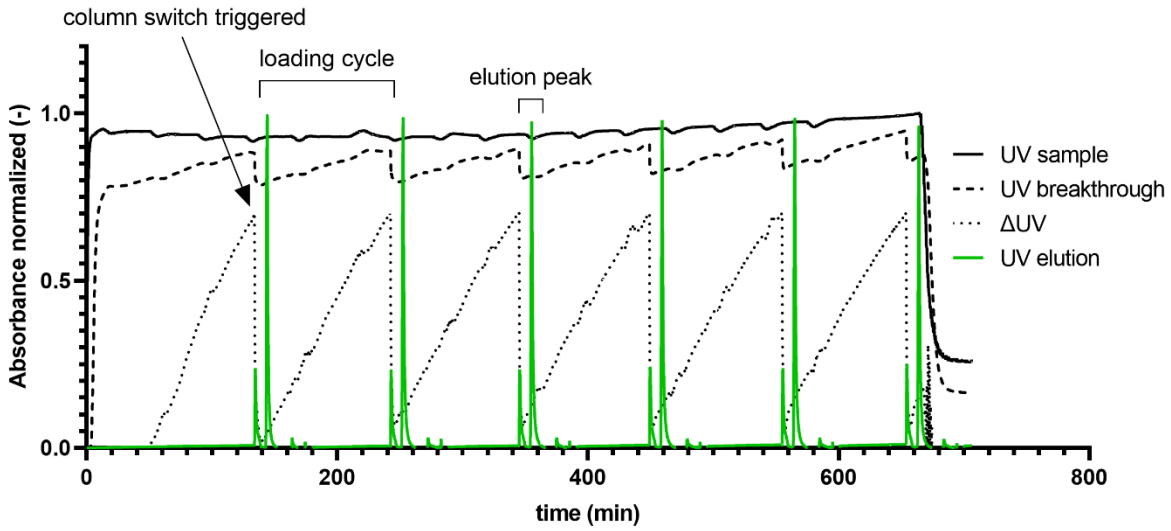

Figure 7-3 Chromatogram of continuous periodic counter current chromatography in bind and elute mode integrated with a prior flow through step. Starting material had an initial total protein concentration of 3.2 mg ml^{-1}. Shown are the UV sample signal (output of flow through chromatography), UV breakthrough profile of the overloaded column, the calculated column product breakthrough (ΔUV) and UV elution step signals. The smaller peak previous of the elution peak is a signal caused by the post loading wash step, and is not eluted but collected on the second column. Values normalized to 1 (UV sample and UV breakthrough to maximum UV sample value, UV elution to maximum UV elution, ΔUV divided by 100).

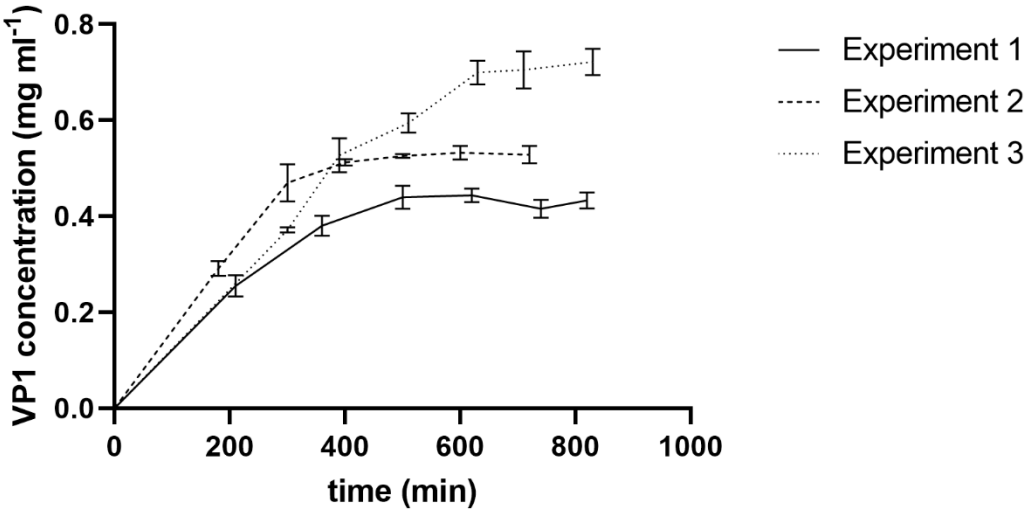

Figure 7-4 VP1-J8 concentration in surge vessel after PCC processing but before assembly. Runs were conducted with initial protein concentrations of 1 mg ml^{-1} (Experiment 1), 2.2 mg ml^{-1} (Experiment 2) and 3.2 mg ml^{-1} (Experiment 3).

7.4.3 Integrated Process Product Quality

TEM images of VLPs collected at different time points at the outlet of the process are presented in Figure 7-5 and size analysis by counting pixels from TEM and analysis by DLS are presented in Figure 7-6. The optimised process produced highly uniform VLPs with a mean diameter of the samples, measured by counting pixels, ranging between 44.8 ± 2.3 nm and 47.2 ± 2.9 nm for all 3 different initial protein concentrations over the entire experiments; no trend in the size could be observed. There are no aggregates visible in the samples, however all images show non-assembled capsomeres similar to batch processing in our recent publication and other published work [19,46]. Also, there is no apparent difference in the quality of VLPs produced at the beginning of the process compared to VLPs produced towards the end of the process (Figure 7-5).

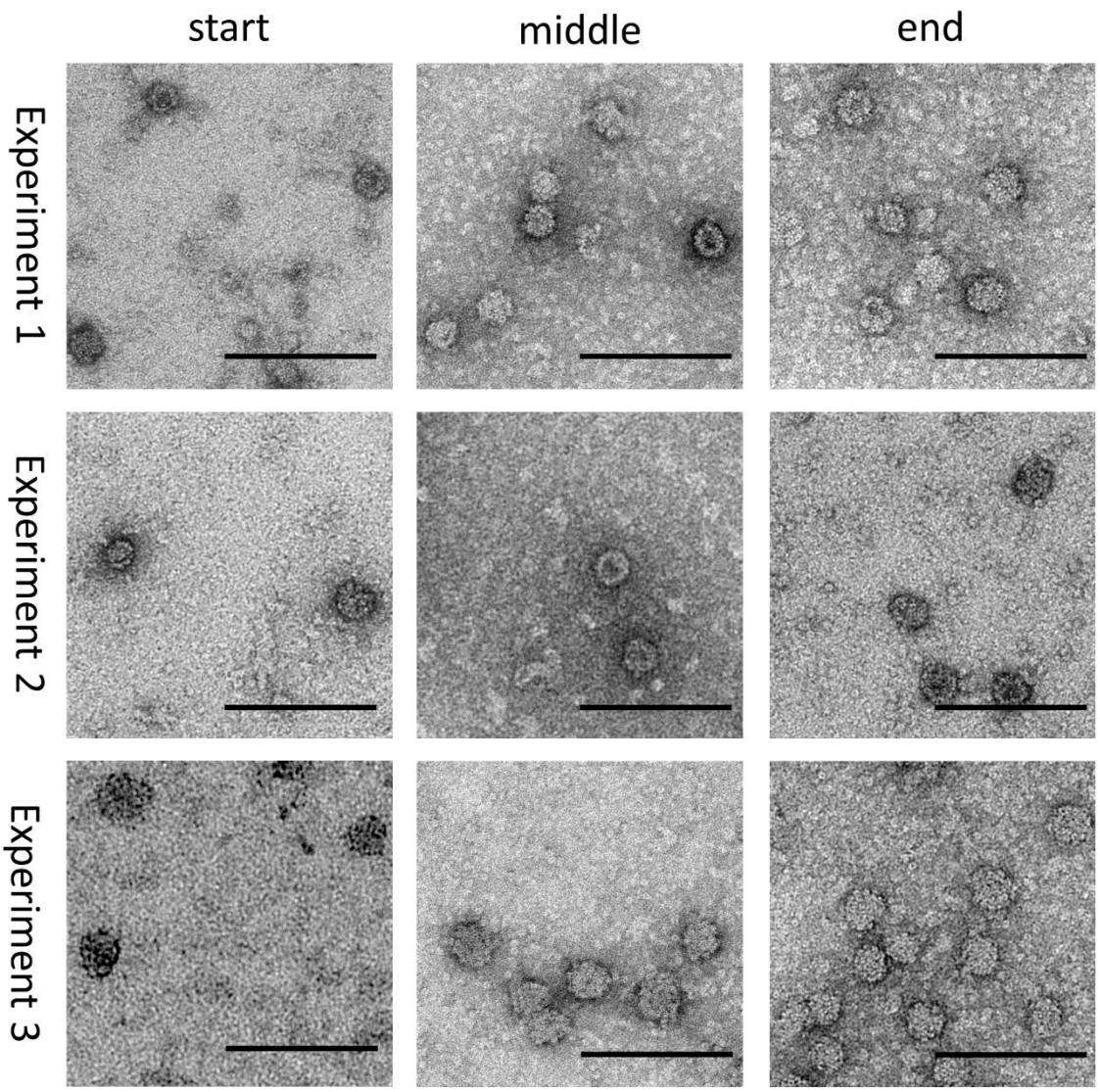

Figure 7-5 *TEM images of VLPs obtained at different times during continuous processing. Scale bar represents 200 nm.*

Examining the assembly products using DLS shows a similar result. The intensity weighted mean hydrodynamic size (Z-average) for samples taken during the experiments is shown in Figure 7-6. All three experiments show nearly steady Z-averages of the VLPs between 46.6 nm and 53.0 nm during the entire process (except the second sample of the first experiment which shows a Z-average of only 43.4 nm, which we cannot explain), slightly higher than by

counting pixels. This difference is likely a consequence of parameters used in DLS analysis and/or the effect of preparation of samples for TEM. It is well known that DLS is measuring the average hydrodynamic diameter which is dependent on ionic strength, temperature and buffer composition.

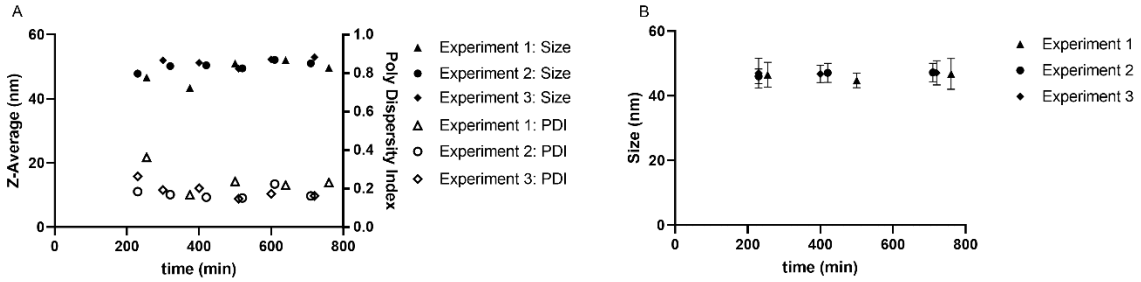

Figure 7-6 Variation of VLP diameter (measured by DLS (A) and TEM (B)) with process time. Runs were conducted with initial protein concentrations of 1 mg ml^{-1} (Experiment 1), 2.2 mg ml^{-1} (Experiment 2) and 3.2 mg ml^{-1} (Experiment 3).

There is a slight upward trend in the Z-average diameters as the first samples of each experiment have Z-averages of 46.6 nm, 47.8 nm and 48.0 nm, respectively. While samples taken later in the process show Z-averages slightly above 50 nm. The upward trend in DLS size, that cannot be observed by counting pixels, might be caused by the higher proportion of unassembled capsomeres compared to assembled VLPs in the early process, caused by low VP1-J8 concentrations of 0.26 mg ml^{-1}, 0.29 mg ml^{-1} and 0.37 mg ml^{-1}. It was shown in literature, that during assembly of VP1 around 0.02 mg ml^{-1} capsomeres remain unassembled and therefore a lower overall VP1-J8 capsomere concentration negatively influences the ratio of unassembled capsomeres to assembled VLPs [47]. The PDI remains relatively stable during the experiments, but is slightly higher at the beginning of each experiment. This again can be explained by the low concentration of the sample and the consequential higher unassembled capsomere content. The average PDI of experiment 1 to experiment 3 are 0.243

± 0.064, 0.174 ± 0.025 and 0.190 ± 0.037 respectively. Which are within acceptable limits, although experiment 1 is slightly elevated [48]. The slightly higher PDI of experiment 1 might be also explained by the lower concentration, but it can also be a random error and requires further investigation.

Both measured sizes of approximately 47 nm by counting pixels on TEM and a Z-average slightly above 50 nm matches well with reported sizes in literature of a murine poliomavirus VLPs, that reports a Z-average of 52.0 nm and TEM sizes up to 48 nm [32].

The instruments, and process conditions used for assembly of VLPs could be improved further to achieve enhanced VLP yield and by reducing the level of non-assembled capsomeres. Knowing the complexity of *in-vitro* VLP assembly, finding optimal assembly conditions is challenging and requires the consideration of suitable pH, ionic strength/salt type and temperature conditions [49]. As the capsomeres have the same protein composition as the VLPs, we do not anticipate that these represent a product contaminant *per se*. Our previous work has demonstrated that capsomeres invoke a similar quality of immune response to that of VLPs, albeit at a lower level in the absence of adjuvant [50].

SDS-PAGE analysis (Figure 7-7) shows a good purity with some contaminations of VP1-J8 after purification with Capto^{TM} Q and Capto^{TM} MMC. Samples taken at the different times during experiment 2 (Figure 7-7 lane 3-5) show no difference in the purity, however sample concentration at the beginning of the process is too low, to show impurities. Also, comparing purities of the three experiments (Figure 7-7 lane 5-7), each taken towards the end of the process, reveals no apparent difference in the purity. In one of our recent publications we could show, that the low molecular weight impurities are mainly VP1-J8 truncation products, that were hard to remove, even with further purification. The overall purity equals to the purity obtained in batch processes [19].

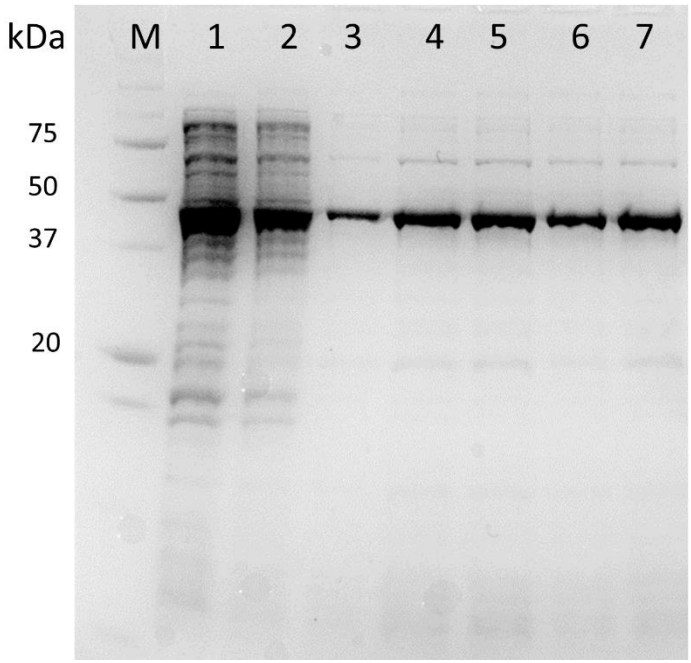

Figure 7-7 SDS-PAGE analysis of the process. M: protein marker; (1) Crude lysate from Experiment 2; (2) After flow through chromatography purification on Capto^{TM} Q from Experiment 2; (3) After PCC step on Capto^{TM} MMC from Eexperiment 2, start of the process; (4) After PCC step on Capto^{TM} MMC from Experiment 2, middle of the process; (5) After PCC step on Capto^{TM} MMC from Experiment 2, end of the process; (6) After PCC step on Capto^{TM} MMC from Experiment 1, end of the process; (7) After PCC on Capto^{TM} MMC from Experiment 3, end of the process.

Similarly, the DNA concentration of all samples was measured to be between 0.7 and 1.7 ng ml^{-1} at VP1-J8 concentrations between 0.43 and 0.7 mg ml^{-1} and remains stable during the experiments (Figure 7-8). Given the fact that the sensitivity level of the assay is 2 ng ml^{-1} it can be assumed the samples are effectively DNA free. As vaccines are given at very low dose of for example only 20 µg protein per dose, DNA levels are expected to be at least a 3 magnitudes lower than permitted levels [51,52].

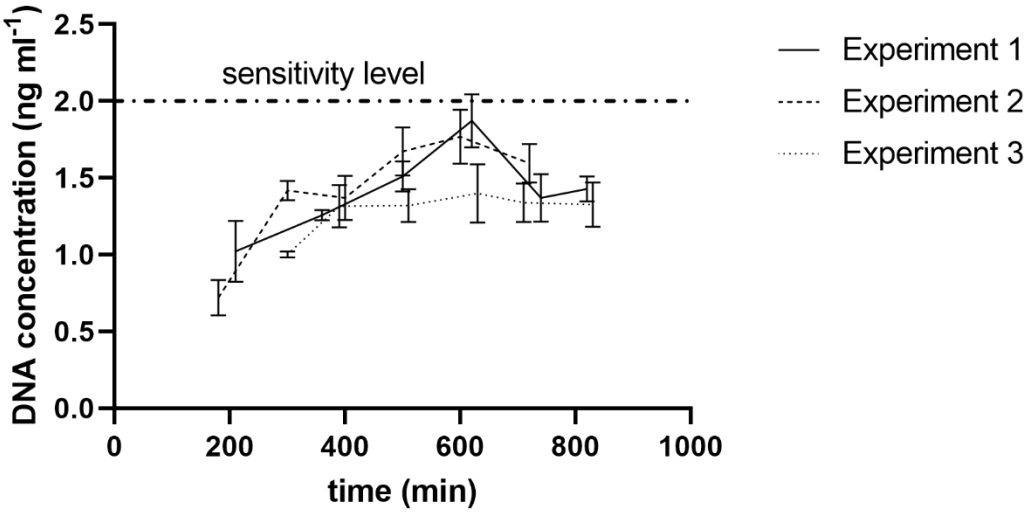

Figure 7-8 Variation in DNA concentration during VLP processing. Runs were conducted with initial protein concentrations of 1 mg ml^{-1} (Experiment 1), 2.2 mg ml^{-1} (Experiment 2) and 3.2 mg ml^{-1} (Experiment 3).

Based on these outcomes, it is evident that that the described process can produce constantly high quality VLP vaccines continuously over the examined duration of at least 10h. The product quality is in this work independent of the feed concentration, but the overall productivity increases with increased feed concentrations.

Integrating a flow through chromatography step with a subsequent PCC bind-elute process using salt tolerant mixed mode chromatography resins (Capto^{TM} MMC) is a powerful approach for continuous biomanufacturing of VLP vaccines. The biggest advantage is that it enables a streamlined process without any intermediate buffer adjustment between the two unit-operations and therefore theoretically enables a seamless integration without any holding vessel. Like in the previously developed batch process, this set-up also allows impurities to be reduced to a level that enables UV based control of the column loading and a buffer exchange during elution that enables the removal of stabilizing DTT without a dedicated buffer exchange step [19].

The process fulfils several proposed benefits of continuous processing. Once set-up the entire process runs automatically and no user interference is required. As sown in Figure 7-2 applying continuous PCC instead of batch-wise bind-and-elute, allows for much higher column loading, without product loss, and therefore solves the trade-off between column utilization and productivity. Furthermore, this leads to smaller required columns and a decrease in buffer consumption compared to batch processing. The overall footprint is only 4 m bench space as only minimal hold-up vessels are needed between the unit operations. The footprint would also not increase much if the process is scaled-up by increasing resin volumes. Continuous processing also decreases the mean residence time of the product as holding times between unit operations are minimal and do not vary between batch-to-batch. This can lead to a better product quality and less quality variations compared to batch processing. It is well known that long processing and hold-up times can lead to product loss caused by aggregation and proteolytic degradation and our previous study indicates that a quick processing is beneficial for the quality of VP1 [19,53–55].Furthermore, a higher product output can be achieved by solely running the process for a longer time.

We believe that this set-up can be used as a template for continuous processing of many biologics other than VLPs and viral capsomeres. Although the performance of this process using other entities than VP1-J8 has not been tested the combination of a flow through step with a bind and elute PCC is not product specific. There is also room for adapting the process by changing resins and the substitution of the assembly unit operation with a final flow through polishing. This will likely allow the processing of a wide variety of biologics.

7.5 Conclusion

Here we report for the first time an integrated and continuous downstream process for the production of VLP vaccines. Coupling a flow through step with a bind and elute PCC process allows for a streamlined process without buffer adjustment between the unit operations.

Buffer exchange during elution prepared for a direct VLP assembly by adding calcium ions and pH adjustment thereafter. The process showed a robust behaviour towards different inlet concentrations and was capable of producing VLPs of constant high product quality continuously with an outstanding product recovery of 86% and an overall output of up to 7.56 mg h^{-1} with only 8 ml of chromatography resin used in the entire process, and a productivity of the PCC process of 2.52 mg h^{-1} ml_{resin}^{-1}. Furthermore, the entire process can be assembled on 4 m of lab space, which will only minimally increase if larger column volumes are used, as only minimal holding vessels are required. This clearly shows the dramatically reduced footprint that continuous processing can achieve.

Finding the optimal design space for highest productivity is challenging as different inlet concentrations lead to changes in the binding capacity and flowrates; and further research needs to be done on how to optimize the described process. As the combination of a flow through step with a subsequent PCC step using mixed mode resins allows for a wide design space and is not product specific, we believe that the described process can be easily adapted as a template for the development of continuous processing of VLPs and other biopharmaceuticals.

7.6 References

[1] B. Donaldson, Z. Lateef, G.F. Walker, S.L. Young, V.K. Ward, Virus-like particle vaccines: immunology and formulation for clinical translation, Expert Rev. Vaccines 17 (2018) 833–849. https://doi.org/10.1080/14760584.2018.1516552.

[2] M.A. Stanley, Human papillomavirus vaccines, Rev. Med. Virol. 16 (2006) 139–149. https://doi.org/10.1002/rmv.498.

[3] T. Rivera-Hernandez, J. Hartas, Y. Wu, Y.P. Chuan, L.H.L. Lua, M. Good, M.R. Batzloff, A.P.J. Middelberg, Self-adjuvanting modular virus-like particles for mucosal vaccination against group A streptococcus (GAS), Vaccine 31 (2013) 1950–1955. https://doi.org/10.1016/j.vaccine.2013.02.013.

[4] L.K. Pattenden, A.P.J. Middelberg, M. Niebert, D.I. Lipin, Towards the preparative and large-scale precision manufacture of virus-like particles, Trends Biotechnol. 23 (2005) 523–529. https://doi.org/10.1016/j.tibtech.2005.07.011.

[5] M.B. Laurens, RTS,S/AS01 vaccine (Mosquirix™): an overview, Hum. Vaccin. Immunother. 16 (2020) 480–489. https://doi.org/10.1080/21645515.2019.1669415.

[6] M.R. Anggraeni, N.K. Connors, Y. Wu, Y.P. Chuan, L.H.L. Lua, A.P.J. Middelberg, Sensitivity of immune response quality to influenza helix 190 antigen structure displayed on a modular virus-like particle, Vaccine 31 (2013) 4428–4435. https://doi.org/10.1016/j.vaccine.2013.06.087.

[7] S. Nooraei, H. Bahrulolum, Z.S. Hoseini, C. Katalani, A. Hajizade, A.J. Easton, G. Ahmadian, Virus-like particles: preparation, immunogenicity and their roles as nanovaccines and drug nanocarriers, J. Nanobiotechnology 19 (2021) 59. https://doi.org/10.1186/s12951-021-00806-7.

[8] C.L. Effio, J. Hubbuch, Next generation vaccines and vectors: Designing downstream processes for recombinant protein-based virus-like particles, Biotechnol. J. 10 (2015) 715–727. https://doi.org/10.1002/biot.201400392.

[9] H.K. Hume, J. Vidigal, M.J.T. Carrondo, A.P.J. Middelberg, A. Roldão, L.H.L. Lua, Synthetic biology for bioengineering virus-like particle vaccines, Biotechnol. Bioeng. 116 (2019) 919–935. https://doi.org/10.1002/bit.26890.

[10] V. Qendri, J.A. Bogaards, J. Berkhof, Pricing of HPV vaccines in European tender-based settings, Eur. J. Health Econ. 20 (2019) 271–280. https://doi.org/10.1007/s10198-018-0996-9.

[11] S. Tayyab, S. Qamar, M. Islam, Size exclusion chromatography and size exclusion HPLC of proteins, Biochemical Education 19 (1991) 149–152. https://doi.org/10.1016/0307-4412(91)90060-L.

[12] A.P.J. Middelberg, T. Rivera-Hernandez, N. Wibowo, L.H.L. Lua, Y. Fan, G. Magor, C. Chang, Y.P. Chuan, M.F. Good, M.R. Batzloff, A microbial platform for rapid and low-cost virus-like particle and capsomere vaccines, Vaccine 29 (2011) 7154–7162. https://doi.org/10.1016/j.vaccine.2011.05.075.

[13] K.D. Brune, D.B. Leneghan, I.J. Brian, A.S. Ishizuka, M.F. Bachmann, S.J. Draper, S. Biswas, M. Howarth, Plug-and-Display: decoration of Virus-Like Particles via isopeptide bonds for modular immunization, Sci. Rep. 6 (2016) 19234. https://doi.org/10.1038/srep19234.

[14] B.E. Clarke, S.E. Newton, A.R. Carroll, M.J. Francis, G. Appleyard, A.D. Syred, P.E. Highfield, D.J. Rowlands, F. Brown, Improved immunogenicity of a peptide epitope after fusion to hepatitis B core protein, Nature 330 (1987) 381–384. https://doi.org/10.1038/330381a0.

[15] K.E. Sapsford, W.R. Algar, L. Berti, K.B. Gemmill, B.J. Casey, E. Oh, M.H. Stewart, I.L. Medintz, Functionalizing nanoparticles with biological molecules: developing chemistries that facilitate nanotechnology, Chem. Rev. 113 (2013) 1904–2074. https://doi.org/10.1021/cr300143v.

[16] A. Seth, I.G. Kong, S.-H. Lee, J.-Y. Yang, Y.-S. Lee, Y. Kim, N. Wibowo, A.P.J. Middelberg, L.H.L. Lua, M.-N. Kweon, Modular virus-like particles for sublingual vaccination against group A streptococcus, Vaccine 34 (2016) 6472–6480. https://doi.org/10.1016/j.vaccine.2016.11.008.

[17] A. Tekewe, Y. Fan, E. Tan, A.P.J. Middelberg, L.H.L. Lua, Integrated molecular and bioprocess engineering for bacterially produced immunogenic modular virus-like particle vaccine displaying 18 kDa rotavirus antigen, Biotechnol. Bioeng. 114 (2017) 397–406. https://doi.org/10.1002/bit.26068.

[18] M.W.O. Liew, A. Rajendran, A.P.J. Middelberg, Microbial production of virus-like particle vaccine protein at gram-per-litre levels, J. Biotechnol. 150 (2010) 224–231. https://doi.org/10.1016/j.jbiotec.2010.08.010.

[19] L. Gerstweiler, J. Billakanti, J. Bi, A. Middelberg, Comparative evaluation of integrated purification pathways for bacterial modular polyomavirus major capsid protein VP1 to produce virus-like particles using high throughput process technologies, J. Chromatogr. A 1639 (2021) 461924. https://doi.org/10.1016/j.chroma.2021.461924.

[20] L. Gerstweiler, J. Bi, A.P.J. Middelberg, Continuous downstream bioprocessing for intensified manufacture of biopharmaceuticals and antibodies, Chemical Engineering Science 231 (2021) 116272. https://doi.org/10.1016/j.ces.2020.116272.

[21] T. Kröber, M.W. Wolff, B. Hundt, A. Seidel-Morgenstern, U. Reichl, Continuous purification of influenza virus using simulated moving bed chromatography, J. Chromatogr. A 1307 (2013) 99–110. https://doi.org/10.1016/j.chroma.2013.07.081.

[22] Y.-N. Sun, C. Shi, Q.-L. Zhang, S.-J. Yao, N.K. Slater, D.-Q. Lin, Model-based process development and evaluation of twin-column continuous capture processes with Protein A affinity resin, J. Chromatogr. A 1625 (2020) 461300. https://doi.org/10.1016/j.chroma.2020.461300.

[23] R. Godawat, K. Brower, S. Jain, K. Konstantinov, F. Riske, V. Warikoo, Periodic counter-current chromatography -- design and operational considerations for integrated and continuous purification of proteins, Biotechnol. J. 7 (2012) 1496–1508. https://doi.org/10.1002/biot.201200068.

[24] C.A. Martínez Cristancho, A. Seidel-Morgenstern, Purification of single-chain antibody fragments exploiting pH-gradients in simulated moving bed chromatography, J. Chromatogr. A 1434 (2016) 29–38. https://doi.org/10.1016/j.chroma.2016.01.001.

[25] P.A.J. Rosa, A.M. Azevedo, S. Sommerfeld, M. Mutter, W. Bäcker, M.R. Aires-Barros, Continuous purification of antibodies from cell culture supernatant with aqueous two-phase systems: from concept to process, Biotechnol. J. 8 (2013) 352–362. https://doi.org/10.1002/biot.201200031.

[26] N. Kateja, H. Agarwal, A. Saraswat, M. Bhat, A.S. Rathore, Continuous precipitation of process related impurities from clarified cell culture supernatant using a novel coiled flow inversion reactor (CFIR), Biotechnol. J. 11 (2016) 1320–1331. https://doi.org/10.1002/biot.201600271.

[27] D. Burgstaller, A. Jungbauer, P. Satzer, Continuous integrated antibody precipitation with two-stage tangential flow microfiltration enables constant mass flow, Biotechnol. Bioeng. 116 (2019) 1053–1065. https://doi.org/10.1002/bit.26922.

[28] A. Arunkumar, J. Zhang, N. Singh, S. Ghose, Z.J. Li, Ultrafiltration behaviour of partially retained proteins and completely retained proteins using equally-staged single

pass tangential flow filtration membranes, Biotechnol. Prog. 34 (2018) 1137–1148. https://doi.org/10.1002/btpr.2671.

[29] R. Godawat, K. Konstantinov, M. Rohani, V. Warikoo, End-to-end integrated fully continuous production of recombinant monoclonal antibodies, J. Biotechnol. 213 (2015) 13–19. https://doi.org/10.1016/j.jbiotec.2015.06.393.

[30] F. Steinebach, N. Ulmer, M. Wolf, L. Decker, V. Schneider, R. Wälchli, D. Karst, J. Souquet, M. Morbidelli, Design and operation of a continuous integrated monoclonal antibody production process, Biotechnol. Prog. 33 (2017) 1303–1313. https://doi.org/10.1002/btpr.2522.

[31] L. Gerstweiler, J. Bi, A.P.J. Middelberg, Virus-like particle preparation is improved by control over capsomere-DNA interactions during chromatographic purification, Biotechnol. Bioeng. 118 (2021) 1707–1720. https://doi.org/10.1002/bit.27687.

[32] Y.P. Chuan, Y.Y. Fan, L. Lua, A.P.J. Middelberg, Quantitative analysis of virus-like particle size and distribution by field-flow fractionation, Biotechnol. Bioeng. 99 (2008) 1425–1433. https://doi.org/10.1002/bit.21710.

[33] A. Löfgren, J. Gomis-Fons, N. Andersson, B. Nilsson, L. Berghard, C. Lagerquist Hägglund, An integrated continuous downstream process with real-time control: A case study with periodic countercurrent chromatography and continuous virus inactivation, Biotechnol. Bioeng. 118 (2021) 1664–1676. https://doi.org/10.1002/bit.27681.

[34] Bangtsson, Estrada, Lacki, Skoglar, Method in chromatography system (2012).

[35] L. Gerstweiler, J. Billakanti, J. Bi, A.P.J. Middelberg, Control strategy for multi-column continuous periodic counter current chromatography subject to fluctuating inlet stream concentration, J. Chromatogr. A 1667 (2022) 462884. https://doi.org/10.1016/j.chroma.2022.462884.

[36] C.K.S. Ng, H. Osuna-Sanchez, E. Valéry, E. Sørensen, D.G. Bracewell, Design of high productivity antibody capture by protein A chromatography using an integrated experimental and modeling approach, J. Chromatogr. B Analyt. Technol. Biomed. Life Sci. 899 (2012) 116–126. https://doi.org/10.1016/j.jchromb.2012.05.010.

[37] K. Swinnen, A. Krul, I. van Goidsenhoven, N. van Tichelt, A. Roosen, K. van Houdt, Performance comparison of protein A affinity resins for the purification of monoclonal antibodies, J. Chromatogr. B Analyt. Technol. Biomed. Life Sci. 848 (2007) 97–107. https://doi.org/10.1016/j.jchromb.2006.04.050.

[38] R. Hahn, P. Bauerhansl, K. Shimahara, C. Wizniewski, A. Tscheliessnig, A. Jungbauer, Comparison of protein A affinity sorbents II. Mass transfer properties, J. Chromatogr. A 1093 (2005) 98–110. https://doi.org/10.1016/j.chroma.2005.07.050.

[39] Y.-N. Sun, C. Shi, Q.-L. Zhang, N.K.H. Slater, A. Jungbauer, S.-J. Yao, D.-Q. Lin, Comparison of Protein A affinity resins for twin-column continuous capture processes: Process performance and resin characteristics, J. Chromatogr. A 1654 (2021) 462454. https://doi.org/10.1016/j.chroma.2021.462454.

[40] N. Hillebrandt, P. Vormittag, N. Bluthardt, A. Dietrich, J. Hubbuch, Integrated Process for Capture and Purification of Virus-Like Particles: Enhancing Process Performance by Cross-Flow Filtration, Front. Bioeng. Biotechnol. 8 (2020) 489. https://doi.org/10.3389/fbioe.2020.00489.

[41] C. Ladd Effio, L. Wenger, O. Ötes, S.A. Oelmeier, R. Kneusel, J. Hubbuch, Downstream processing of virus-like particles: single-stage and multi-stage aqueous two-phase extraction, J. Chromatogr. A 1383 (2015) 35–46. https://doi.org/10.1016/j.chroma.2015.01.007.

[42] S.B. Carvalho, R.J.S. Silva, M.G. Moleirinho, B. Cunha, A.S. Moreira, A. Xenopoulos, P.M. Alves, M.J.T. Carrondo, C. Peixoto, Membrane-Based Approach for the

Downstream Processing of Influenza Virus-Like Particles, Biotechnol. J. 14 (2019) e1800570. https://doi.org/10.1002/biot.201800570.

[43] D. Zhao, B. Sun, H. Jiang, S. Sun, F.T. Kong, Y. Ma, L. Jiang, L. Bai, X. Chen, P. Yang, C. Liu, Y. Xu, W. Su, W. Kong, F. Xu, C. Jiang, Enterovirus71 virus-like particles produced from insect cells and purified by multistep chromatography elicit strong humoral immune responses in mice, J. Appl. Microbiol. 119 (2015) 1196–1205. https://doi.org/10.1111/jam.12922.

[44] R.A. Latour, The Langmuir isotherm: a commonly applied but misleading approach for the analysis of protein adsorption behavior, J. Biomed. Mater. Res. A 103 (2015) 949–958. https://doi.org/10.1002/jbm.a.35235.

[45] M. Yu, Y. Li, S. Zhang, X. Li, Y. Yang, Y. Chen, G. Ma, Z. Su, Improving stability of virus-like particles by ion-exchange chromatographic supports with large pore size: advantages of gigaporous media beyond enhanced binding capacity, J. Chromatogr. A 1331 (2014) 69–79. https://doi.org/10.1016/j.chroma.2014.01.027.

[46] Y.P. Chuan, Y.Y. Fan, L.H.L. Lua, A.P.J. Middelberg, Virus assembly occurs following a pH- or Ca2+-triggered switch in the thermodynamic attraction between structural protein capsomeres, J. R. Soc. Interface 7 (2010) 409–421. https://doi.org/10.1098/rsif.2009.0175.

[47] Y. Ding, Y.P. Chuan, L. He, A.P.J. Middelberg, Modeling the competition between aggregation and self-assembly during virus-like particle processing, Biotechnol. Bioeng. 107 (2010) 550–560. https://doi.org/10.1002/bit.22821.

[48] M. Danaei, M. Dehghankhold, S. Ataei, F. Hasanzadeh Davarani, R. Javanmard, A. Dokhani, S. Khorasani, M.R. Mozafari, Impact of Particle Size and Polydispersity Index on the Clinical Applications of Lipidic Nanocarrier Systems, Pharmaceutics 10 (2018). https://doi.org/10.3390/pharmaceutics10020057.

[49] D.T. Le, K.M. Müller, In Vitro Assembly of Virus-Like Particles and Their Applications, Life (Basel) 11 (2021). https://doi.org/10.3390/life11040334.

[50] N. Wibowo, Y.P. Chuan, L.H. Lua, A.P. Middelberg, Modular engineering of a microbially-produced viral capsomere vaccine for influenza, Chemical Engineering Science 103 (2013) 12–20. https://doi.org/10.1016/j.ces.2012.04.001.

[51] Australian Government, Gardasil 9, 2022. https://immunisationhandbook.health.gov.au/vaccines/gardasil-9 (accessed 27 March 2022).

[52] WHO, Recommendations for the evaluation of animal cell cultures as substrates for the manufacture of biological medicinal products and for the characterization of cell banks (2010).

[53] FDA, Quality Considerations for Continuous Manufacturing Guidance for Industry, 2019. https://www.fda.gov/media/121314/download.

[54] V. Joshi, T. Shivach, V. Kumar, N. Yadav, A. Rathore, Avoiding antibody aggregation during processing: establishing hold times, Biotechnol. J. 9 (2014) 1195–1205. https://doi.org/10.1002/biot.201400052.

[55] B.J. Ryan, G.T. Henehan, Overview of approaches to preventing and avoiding proteolysis during expression and purification of proteins, Curr. Protoc. Protein Sci. Chapter 5 (2013) Unit5.25. https://doi.org/10.1002/0471140864.ps0525s71.

Chapter 8

Conclusions and Future Research Directions

This chapter sums up the findings of the previous chapters and gives an outlook of possible future research questions that can be addressed.

8.1 Conclusions

VP1 tends to aggregate during downstream processing and hence low recoveries, poor binding and quality issues are common in previously described processes. In this research, it was shown that VP1 aggregation can mainly be explained by the strong affinity of VP1 towards DNA, and that is possible to control this interaction via the ionic strength of the buffer (Chapter 4). This finding can explain many observed challenges during the purification and assembly of VP1. Control of DNA-VP1 interaction led to the development of a highly efficient downstream process based on a multi-modal cation exchanger, that allowed processing at elevated salt concentrations (Chapter 5). Optimization using high-throughput studies further deepened process understanding. The developed process for GAS VLP vaccines outperforms other described processes in most relevant aspects. Not only high-quality VLPs were obtained, but the process also removed aggregates, most impurities, is fully scale-able and integrated, and does not require costly unit operations or slow enzymatic treatments. This research shows that a solid understanding of underlying principles is necessary for the development of highly-efficient and robust processes.

Based on these findings the first fully-continuous and automated set-up for the production of VLP vaccines was developed (Chapter 7). The process was capable of continuously producing VLPs of constant product quality over the examined time period and showed robust behaviour towards variation of inlet feed concentrations. A key concept is the integration of a flow-through chromatography step with a periodic counter-current chromatography step using multi-modal ion exchangers. This novel approach allows seamless processing without buffer adjustment. The set-up demonstrates furthermore the possibility of removing unwanted reducing agents during bind and elution chromatography, which eradicates the need for a dedicated buffer exchange unit operation during viral assembly. Demonstrating these novel key principles expands the field of continuous

bioprocessing, and might help to develop new continuous bioprocesses for biopharmaceuticals other than VLPs, as the resins and conditions can be easily adapted, and are not limited to VP1 VLPs.

Concentration fluctuations during processing lead to the failure of standard controlling principles of PCC chromatography. This is a well know hurdle and is described as a key challenge to solve for continuous bioprocessing. The newly developed method (Chapter 6) can be easily adapted with standard PCC equipment using the same UV sensors and allows precise control of the loading phase during PCC chromatography, even with highly-unstable inlet feed stream concentrations and increases the robustness of PCC chromatography in general. Mechanistic modelling has been shown to be a powerful tool for testing and developing new approaches *in-silico*, as dispersion effects could be identified as a limiting factor for precise control with a rapidly-fluctuating inlet stream. The underlying principle of this new approach is not limited to UV control of PCC chromatography, but can also be adapted to other sensors that compare inlet and outlet column signals.

This thesis demonstrates the development of a continuous purification pathway for a novel therapeutic protein, namely a virus-like particle vaccine against Group A *Streptococcus*. It starts with general process development for batch processing and shows the translation into a fully integrated continuous process. Fundamental questions, such as the influence of DNA-capsomere interactions on processing, as well as the development of new algorithmic process control strategies for integrated PCC processes, have been addressed. This research can therefore be used as a possible blueprint on how to develop a continuous process for a novel therapeutic protein, starting from scratch, where no existing process is available.

8.2 Future Research

The research conducted in the project opens several further research questions that are worth exploring. While many problems and curiosities popped up during my research, not all of them are relevant and therefore only some of them are outlined.

The developed continuous process is obviously only a starting point and the robustness of the process needs to be further evaluated. Can the process be used as a platform process for VP1 capsomeres with different antigen and other VLPs? Probably, as the key concept of processing at high salt concentrations to supress DNA-capsomere interaction is not antigen specific. The DNA binding properties are in fact preserved within class of *Papovaviricetes*, and therefore it is likely that the process can be used with minimal adjustment for VP1 with other antigens and even other viral capsomeres. This is, however, something that needs further investigation and the performance of mixed-mode resins needs to be evaluated.

The combination of a flow-through step followed by a capturing step is a powerful design concept for continuous processing, as it allows for a streamlined processing without buffer adjustment. There are a wide variety of resins available and even new mixed mode flow-through resins have been developed, combining size exclusion with internal binding sites. The concept might be therefore applied to other biomolecules. The process could even be altered in a way that the flow-through step is changed to some kind of matrix assisted tubular reactor for enzymatic or chemical reactions (immobilized enzymes or catalysts) with an integrated affinity capturing to specifically remove product or unwanted by-products in a continuous recirculation loop. For example, this could be applied for the synthesis of mRNA or other biomolecules.

The strong binding of capsomeres with microbial DNA, causing aggregates and thus hindering purification, is a major problem, which was addressed in this research by

increasing the salt concentration during processing. An obvious explanation for this high affinity is that it helps to incorporate genetic material into the virus particle, and there are also suggestions in literature that “right-sized” DNA can actually enhance viral assembly. However, VLPs used for vaccination using chimeric designs do not require any genetic material inside the particle. The findings of Chapter 4 indicate that DNA binding is not necessary for viral assembly, and in fact can lead to incorrectly assembled products in the presence of microbial DNA. Instead of supressing the DNA-capsomere interaction during processing, it might be worth to explore if it is possible to redesign VP1 without DNA binding sites. This should theoretically lead to a platform capsomere that will show less or no aggregation and thus has a better processability. Yet, should still be able to be assembled into high-quality VLPs. This approach, if proven, would solve many challenges and can be furthermore used to study the influence of DNA-capsomere interaction on viral assembly, in detail.

The developed process control algorithmic approach described in Chapter 6 is a simple method that can be used to control a PCC process in the presence of fluctuating inlet stream concentrations. However, this is only true if the ratio of product to impurities remains constant. Another limitation relates to column dispersion effects that can lead to unstable control signals, particularly if the inlet stream concentration changes rapidly. As unstable feed streams are still a challenge in biomanufacturing this area should be further explored. Changing product to impurities ratios cannot be addressed with non-molecule specific sensors such as UV absorbance at a single wavelength. Raman spectroscopy and multiwavelength analysis have shown to be useful techniques in determining molecule concentrations in complex mixtures and it is therefore worth to explore if these techniques could be used to predict the impurity and/or product content. Maybe there are certain marker molecules that can be used to predict host cell protein and other impurities, although they are

a mixture by themselves. Dispersion effects can be accounted for by implementing some type of smoothing algorithm that needs to be developed. This could be either a moving average of the inlet feed stream or an actual calculation of the dispersion of the signal.

Chapter 7 describes another limitation of controlling column loading based on product breakthrough, which is the dependence of the dynamic binding capacity on the product concentration. This limits the use of breakthrough data for process control, as a certain breakthrough level does not necessarily correspond to an equal loading amount if the feed concentration changes. How such effects can be accounted for during process control is an exciting research field that needs to be explored. A possible solution involves model-based control strategies in which the process is modelled *in-silico* and on-line data is used to calibrate the model and find optimal process parameters. This can be further extended to unstable feed streams and high-quality models need to be developed and verified. Usually mechanistic models, based on physiochemical equations, are used for *in-silico* modelling. However, biomolecules are complex and isotherms/transport equations can be very complex, or else over-simplify the problem, and thus lack accuracy. The question arises as to what extent statistical approaches such artificial intelligence and neural networks can be applied to either simplify the models or improve them. Which phenomena actually need to be described with physiochemical equations and which are better described using statistical approaches? Another important aspect is how column fouling and variations of the column quality can be addressed in model-based approaches and what other process data can be used to support controlling of the process.

There is room for considerable optimization during continuous processing, and finding the optimal flow rate and column volumes for the highest efficiency is basically impossible experimentally. Findings from Chapter 7 show that the performance of one unit operation can influence the subsequent unit operation in an integrated process. This might challenge scale-

up and needs to be further investigated. Describing and modelling an entire integrated process is still a mostly unexplored field for which suitable methods need to be developed that can account for the enormous complexity. This is also a necessity to translate continuous processing from a mostly research-focused field to an industry-accepted method and to answer the key question; under which circumstances is a continuous process superior to a batch process?

In conclusion, the field of continuous biomanufacturing needs considerable further research to deliver the promises of continuous processing and enable 24/7 production of vaccines and biopharmaceuticals.

Appendix

9.1 Appendix Chapter 4

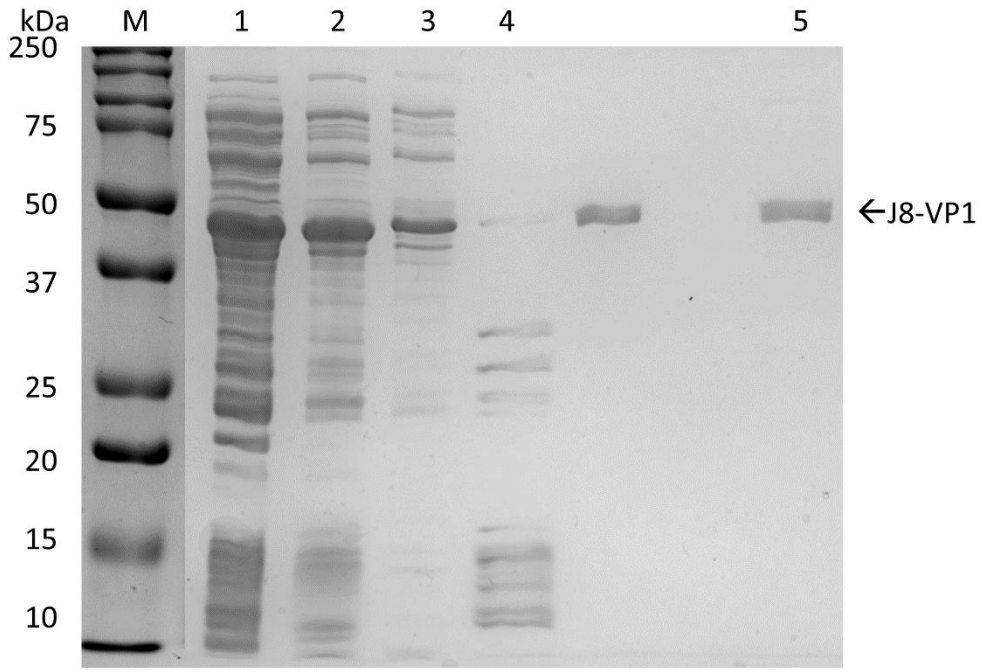

Figure A4-1 SDS-PAGE analysis of the different purification steps. Lanes as in Table A4-2.

Table A4-2 Description of SDS-PAGE in Figure A4-1 and DNA content of the samples.

Lane	Purification	DNA
1	Lysate	
2	After PEG precipitation	75.5 ng/µl
3	PEG plus AEX flow through	Non detectable (<0.02 ng/µl)
4	AEX wash	
5	SEC polishing	Non detectable (<0.02 ng/µl)

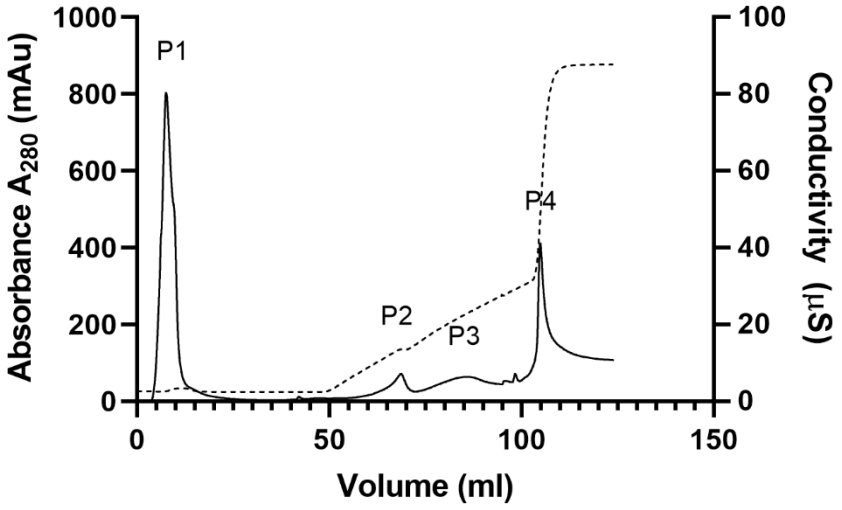

Figure A4-3 Chromatogram of 5 ml crude clarified lysate on 6 ml Capto^{TM} Q, Loading and washing with buffer A (20 mM Tris, pH 8, 0 M NaCl, 5 mM DTT, 2 mM EDTA, 5% Glycerol). Elution with gradient of buffer A and buffer B (20 mM Tris, pH 8, 1 M NaCl, 5 mM DTT, 2 mM EDTA, 5% Glycerol). (P1) flow through during loading, (P2), (P3) and (P4) elution peaks.

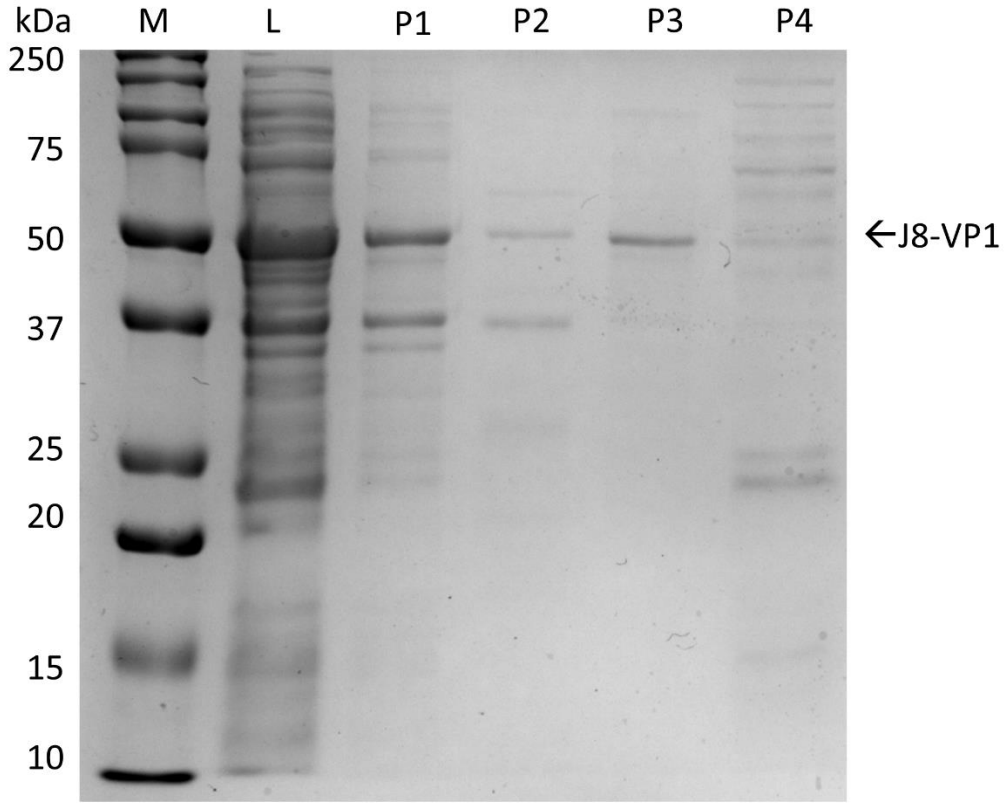

Figure A4-4 SDS-PAGE analysis of Figure A3-3. (M) marker, (L) crude lysate, (P1-P4) according to chromatogram in Figure A3-3.

9.2 Appendix Chapter 5

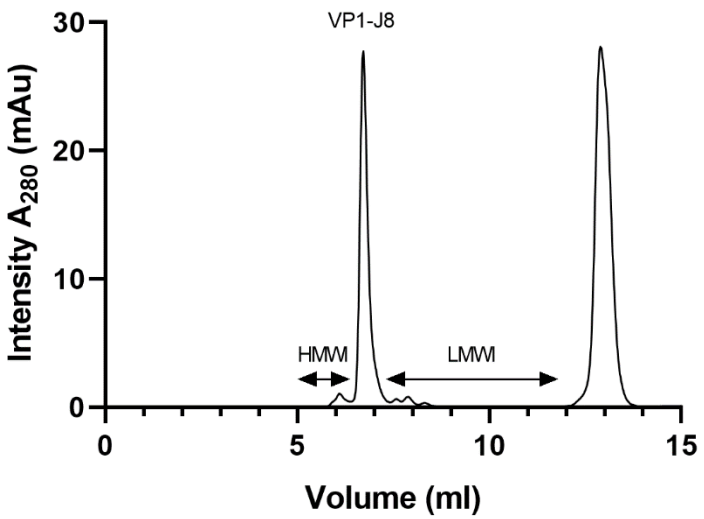

Figure A5-1 HPLC-SEC (TSK3000) chromatogram of sample purified by pathway B (PEG precipitation, Capto™ MMC and Capto™ Q) as an example to clarify the measured impurity parameters HMWI and LMWI. The salt peak, mostly caused by oxidised DTT, is excluded from the calculation.

Protocol LC-ESI-MS/MS

Provided gel bands were digested with trypsin using the in-gel digest method as follows:

1. Gel bands were destained by incubating in 50 mM NH_4HCO_3 for 5 minutes, then sonicating them with 50 mM NH_4HCO_3 in 30% ACN for 15 minutes. Destaining solution was removed from the gel bands by pulse centrifugation.

2. ACN was added to each tube containing the gel band samples and incubated for 15 minutes. All liquid was removed from the gel bands by pulse centrifugation. The gel pieces were further dried down by vacuum centrifugation for 10 minutes.

3. In-gel reduction was performed by adding 10 mM DTT in 100 mM NH_4HCO_3 to the gel pieces and incubating the samples for 45 minutes at 56 °C. All liquid was removed from the gel pieces by pulse centrifugation.

4. In-gel alkylation was performed by adding 55 mM IAA in 100 mM NH_4HCO_3 to the gel pieces and incubating the samples for 30 minutes in darkness at ambient temperature. All liquid was removed from the gel pieces by pulse centrifugation.

5. Gel pieces underwent subsequent incubations in 5 mM NH_4HCO_3 for 10 minutes and in ACN for 15 minutes with all liquid removed by pulse centrifugation in between each incubation. Gel pieces were then dried by vacuum centrifugation for 10 minutes.

6. Gel pieces were treated with trypsin (100 ng μL^{-1}) and incubated overnight at 37 °C.

7. Peptides were extracted by subsequent 15-minute incubations in 50% ACN/1% FA and 100% ACN. All peptide-containing liquid was removed from the gel pieces by pulse centrifugation and dried to approximately 1 μL by vacuum centrifugation.

8. Dried peptides were reconstituted in 3% ACN/0.1% FA for LC-MS/MS analysis.

Note: All samples (gels, digests, etc.) not consumed in the analysis were stored at the APC for 12 months and then discarded.

Data acquisition

Liquid chromatography – electrospray ionisation tandem mass spectrometry

Nano-LC−ESI-MS/MS was performed on an Ultimate 3000 RSLC system (Thermo-Fisher Scientific) coupled to a LTQ Orbitrap XL ETD mass spectrometer (Thermo-Fisher Scientific). The peptide sample was pre-concentrated onto a C18 trapping column (Acclaim PepMap100 C18 75 μm × 20 mm, Thermo-Fisher Scientific) at a

flow rate of 5 µL min^{-1} in 2% (v/v) ACN 0.1% (v/v) FA for 10 minutes. Peptide separation was performed using a 75 µm ID C18 column (Acclaim PepMap100 C18 75 µm × 15 cm, Thermo-Fisher Scientific) at a flow rate of 0.3 µL min^{-1} using a linear gradient from 5 to 45% B (A: 5% (v/v) ACN 0.1% (v/v) FA, B: 80% (v/v) ACN 0.1% (v/v) FA) over 38 minutes, followed by a 2-minute wash with 90% B, and a 15-minute equilibration with

5%. MS scans were acquired in the mass range of 300 to 2000 m/z at a resolution of 60 000 in FT mode. The 10 most intense precursor ions selected for isolation and were subjected to CID fragmentation using a dynamic exclusion of 5 seconds. Dynamic exclusion criteria included a minimum relative signal intensity of 1000, and ≥2+ charge state. An isolation width of 3.0 m/z was used with a normalized collision energy of 35.

Data analysis

Raw MS/MS data were searched against the target sequence of the recombinant protein and *Escherichia coli* entries present in the Swiss-Prot database in Proteome Discoverer (v2.4, Thermo Fisher scientific). Search parameters were specified as follows: tryptic peptides with a maximum of 2 missed cleavages were allowed, peptide mass tolerance of 20 ppm, fragment mass tolerance of 0.8 Da, cysteine carbamidomethylation set as fixed modification, and methionine oxidation, protein N-terminus acetylation, and deamidation of glutamine and asparagine set as variable modifications. The lists of identified proteins from samples 3, 4, 5, and 6 are as shown in the excel spreadsheets.

9.3 Appendix Chapter 6

9.3.1 Appendix A6-1:

Derivation formula 16

$$\Delta C(k,B) = \frac{c^0_{non-binding} + c^0_{binding} * B}{c^0_{non-binding} + c^0_{binding}} * 100$$

$$B = \frac{\left(\frac{\Delta C}{100} * \left(c^0_{non-binding} + c^0_{binding}\right)\right) - c^0_{non-binding}}{c^0_{binding}}$$

$$B * c^0_{binding} = \left(\frac{\Delta C}{100} * \left(c^0_{non-binding} + c^0_{binding}\right)\right) - c^0_{non-binding}$$

$$B * \left(c^0_{binding} + c^0_{non-binding} - c^0_{non-binding}\right) = \left(\frac{\Delta C}{100} * \left(c^0_{non-binding} + c^0_{binding}\right)\right) - c^0_{non-binding}$$

$$B * \left(c^0_{binding} + c^0_{non-binding}\right) - B * c^0_{non-binding} = \left(\frac{\Delta C}{100} * \left(c^0_{non-binding} + c^0_{binding}\right)\right) - c^0_{non-binding}$$

$$B - B\left(\frac{c^0_{non-binding}}{c^0_{binding} + c^0_{non-binding}}\right) = \frac{\Delta C}{100} - \frac{c^0_{non-binding}}{c^0_{non-binding} + c^0_{binding}}$$

$$B = \frac{\frac{\Delta C}{100} - \frac{c^0_{non-binding}}{c^0_{non-binding} + c^0_{binding}}}{1 - \frac{c^0_{non-binding}}{c^0_{non-binding} + c^0_{binding}}}$$

9.3.2 Appendix A6-2

Can be downloaded at: https://ars.els-cdn.com/content/image/1-s2.0-S0021967322000826-mmc2.zip

9.3.3 Appendix A6-3

Can be downloaded at: https://ars.els-cdn.com/content/image/1-s2.0-S0021967322000826-mmc3.zip

9.4 Appendix Chapter 7

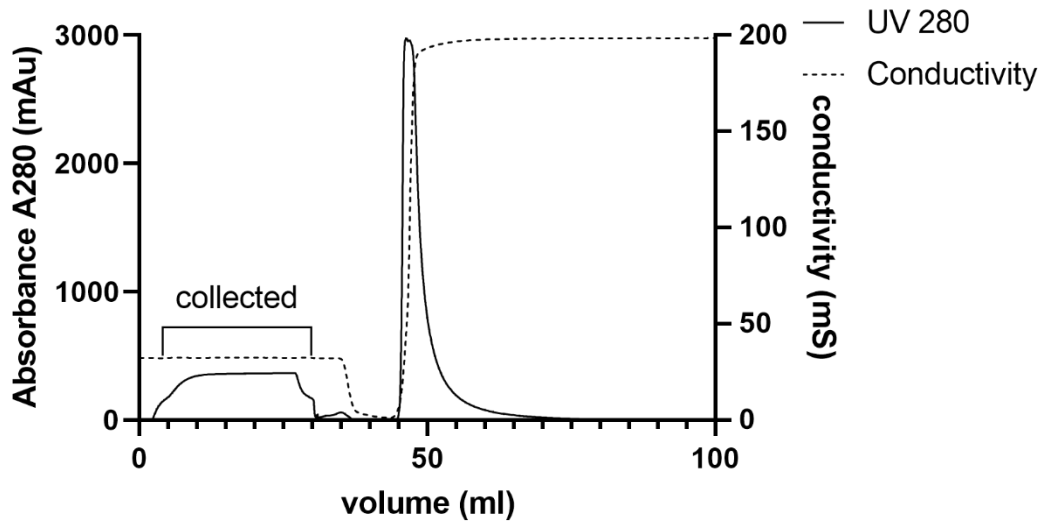

Figure A7-1 Chromatogram of the flow through step on Capto™ Q, showing UV 280 nm absorbance and conductivity. The product flow-through is collected as highlighted.

Figure A7-2 Set-up of the continuous process consisting of a flow through step (left), a PCC step (middle) and an in-line assembly step (right). The unit operations were coupled using 50 ml stirred tank vessels, and 3 Äkta systems were used to implement the process. A schematic process diagram can be found in Figure 7-1.